

**Photomorphological and Photochemical Effects of  
UV-B Radiation on *Brassica napus* (L.) and *Arabidopsis thaliana* (L.)  
Heynh: Morphological, Cellular and Structural Biological Changes.**

**by Michael Ian Wilson**

**A thesis  
presented to the University of Waterloo  
in fulfillment of the  
thesis requirement for the degree of  
DOCTOR OF PHILOSOPHY  
in  
BIOLOGY  
Waterloo, Ontario, Canada, 1998**

**© Michael Ian Wilson 1998**



National Library  
of Canada

Acquisitions and  
Bibliographic Services

395 Wellington Street  
Ottawa ON K1A 0N4  
Canada

Bibliothèque nationale  
du Canada

Acquisitions et  
services bibliographiques

395, rue Wellington  
Ottawa ON K1A 0N4  
Canada

*Your file Votre référence*

*Our file Notre référence*

The author has granted a non-exclusive licence allowing the National Library of Canada to reproduce, loan, distribute or sell copies of this thesis in microform, paper or electronic formats.

The author retains ownership of the copyright in this thesis. Neither the thesis nor substantial extracts from it may be printed or otherwise reproduced without the author's permission.

L'auteur a accordé une licence non exclusive permettant à la Bibliothèque nationale du Canada de reproduire, prêter, distribuer ou vendre des copies de cette thèse sous la forme de microfiche/film, de reproduction sur papier ou sur format électronique.

L'auteur conserve la propriété du droit d'auteur qui protège cette thèse. Ni la thèse ni des extraits substantiels de celle-ci ne doivent être imprimés ou autrement reproduits sans son autorisation.

0-612-38282-6

**The University of Waterloo requires the signatures of all persons using or photocopying this thesis. Please sign below, and give address and date.**

## ABSTRACT

Reductions in plant growth and morphology are some of the most widely reported effects of solar UV-B on plants. A key goal of this thesis was to investigate the nature of the UV-B photoreceptor(s) that trigger these changes. Cotyledon curling in *B. napus* and *Arabidopsis* was found to be a UV-B specific response. Mediation of this morphological change by a signal-transduction pathway was investigated. The morphology of UV-B-irradiated phytochrome and cryptochrome photoreceptor mutants of *Arabidopsis* was found to be similar to wild-type plants, indicating that these photoreceptors do not mediate the changes. A photosynthesis mutant of *Arabidopsis* with an apparent lesion in the photosystem I reaction center was isolated, and found to also undergo cotyledon curling in the presence of UV-B. Hence, UV-B effects on photosynthesis are not the basis of cotyledon curling. To examine the absorbance characteristics of the photoreceptor. The first action spectrum for morphological changes triggered by UV-B in light-grown *Brassica napus* (L.), upward cotyledon curling, is reported. In the course of the study dry weight accumulation and carotenoid concentration were found to be physiological parameters most highly sensitive to UV-B. Photosynthetic efficiency was found to change 24 h after a brief exposure to UV-B indicating that other processes may be regulated by the UV-B photoreceptor(s). Some of these represent acclimation, while others represent stress. Characterization of UV-B-induced changes in epidermal cells from cotyledons of *B. napus* was carried out since this is a likely site of UV-B photoreception. Investigation of their protein composition and secondary metabolism is reported. The profiles of soluble proteins changed after a brief exposure to UV-B. The concentration of sinapoylmalate and sinapoylglucose were shown to accumulate in response to UV-B. The photocross-linking of plant proteins by UV-B, as well as an analysis of the basis of such photochemical events is reported.



I would like to thank Dr. Sibdas Ghosh for being such a great collaborator. I would like to thank the following people for the help and resources they provided to this project. Dale Weber, Barb Moffatt, Marilyn Griffith, Carol Peterson, Xiao-Dong Huang, Karen Gerhardt, Bill Taylor, Nick Taylor, Jim Britton, Brendan McConkey, Ken Wilson. Special thanks to Lynn Hoyles.

I would like to thank all of the following people for their encouragement and comments about this work Dana Simmonds, Doug Ormrod, Dennis McCormac, Bill Diehl-Jones, Craig Mandato, Sue Moore, and Sudhakar Babu.

I would like to give special thanks to my committee members Drs. Dutch Dumbroff, Jim Lepock and John Thompson, Giles Lajoie and Doug Bruce for the insights that they have given me.

Finally, no words adequately express my gratitude to Professor Bruce Greenberg. I have been greatly influenced by him regarding the value of a relaxed and open laboratory atmosphere. He has provided me with many memorable milestones and continues to be a great inspiration to me personally and professionally.

**I would like to dedicate this thesis to my Mother**

**Rosemary,**

**To the memory of my Father**

**John**

**and to my daughter**

**Kyla**

## TABLE OF CONTENTS

1. Introduction	
1.1 A prelude to plants	1
1.2 A brief history of ultraviolet radiation	2
1.3 Variations in solar UV-B radiation at the Earth's surface	4
1.4 Effects of solar UV-B on plant growth and metabolism	6
1.5 Detrimental photochemical effects of UV-B radiation	11
1.6 Photoregulation of plant cells by UV-B photoreceptors	14
1.7 Rationale and Objectives	18
2. UV-B-induced Morphological Changes in <i>Arabidopsis thaliana</i> (L.) Heynh	22
2.1 Introduction	
2.2 Materials and Methods	
2.2.1 Wavelength-dependant changes in <i>Arabidopsis</i> cotyledons	
2.2.1.1 Plant growth and lighting conditions	25
2.2.1.2 Monochromatic UV-B exposures	25
2.2.1.3 Scanning electron microscopy	27
2.2.1.4 Quantitative plant growth measurements	28
2.2.1.5 Chlorophyll <sub>a</sub> fluorescence	28
2.2.1.6 Pigment analyses	29
2.2.2 UV-B exposure of <i>Arabidopsis</i> photomorphological mutants	
2.2.2.1 Plant growth and lighting conditions	29
2.2.3 Isolation of a UV-B-resistant photosynthesis mutant of <i>Arabidopsis</i>	
2.2.3.1 Mutagenesis and Growth Conditions	30
2.2.3.2 Identification of UV-B-resistant mutant	32
2.2.3.3 Room temperature and 77K chlorophyll <sub>a</sub> fluorescence	33
2.3 Results	
2.3.1 Wavelength-dependant changes in <i>Arabidopsis</i> cotyledons	
2.3.1.1 Changes in cotyledon morphology and growth	34
2.3.1.2 The effect of UV-B on cotyledon photosynthesis	41
2.3.1.3 The accumulation of UV-screening pigments	43
2.3.2 The effect of UV-B on <i>Arabidopsis</i> photomorphological mutants	43
2.3.3 Genetic analysis of a UV-B-resistant photosynthesis mutant of <i>Arabidopsis</i>	45
2.4 Discussion	
2.4.1 Wavelength-dependant changes in <i>Arabidopsis</i> cotyledons	51
2.4.2 The isolation of a photosynthetic mutant resistant to UV-B	57
3. The Photobiological Basis of UV-B-induced Cotyledon Curling in <i>Brassica napus</i> L.	
3.1 Introduction	58
3.2 Materials and Methods	
3.2.1 The action spectrum for curling of <i>B. napus</i> cotyledons	60
3.2.2 Effects of chemical agents on UV-B-induced cotyledon curling	62
3.3 Results	
3.3.1 The action spectrum for curling of <i>B. napus</i> cotyledons	63
3.3.2 Effects of chemical agents on UV-B-induced cotyledon curling	66
3.4 Discussion	71

4.	Acclimation of Epidermal Cells to UV-B	
4.1	Introduction	81
4.2	Materials and Methods	
4.2.1	Growth and treatment conditions	84
4.2.2	Isolation of epidermal protoplasts	85
4.2.3	Extraction and analysis of epidermal protoplast proteins	86
4.2.4	Extraction and isolation of UV-B-absorbing compounds	88
4.2.5	Mass spectrometry analysis of UV-B absorbing compounds from <i>B. napus</i>	89
4.2.6	X-ray crystallographic analysis of isolated UV-B absorbing compounds	91
4.3	Results	
4.3.1	Epidermal protoplast isolation	92
4.3.2	Epidermal cell proteins	94
4.3.3	Purification and identification of UV-absorbing compounds from cotyledons	98
4.3.4	Accumulation of UV-absorbing compounds in UV-exposed cotyledons	105
4.4	Discussion	110
5.	UV-B-induced Photocrosslinking of Rubisco Subunits	
5.1	Introduction	117
5.2	Materials and Methods	
5.2.1	Growth and lighting conditions	120
5.2.2	Protein and immunoblot analysis	123
5.2.3	Two-dimensional electrophoresis	124
5.2.4	Partial proteolytic digests	124
5.2.5	Purification of rubisco holoenzyme from leaves of <i>B. napus</i> L.	125
5.2.6	<i>In vitro</i> experiments with rubisco	127
5.2.7	Analysis of amino acid sequences and structures of rubisco from dicots and cyanobacteria	128
5.2.8	Proteolytic digestion and separation of peptide fragments from UV-B-irradiated spinach rubisco	130
5.3	Results	
5.3.1	Initial identification of a UV-B-induced product of rubisco	131
5.3.2	Two-dimensional PAGE Analysis	133
5.3.3	Partial proteolytic digest Analysis	133
5.3.4	Induction of a UV-B-induced rubisco in other plant species	136
5.3.5	<i>In vitro</i> formation of the rubisco photoproduct and identification of SSU as a substituent	140
5.3.6	Accumulation of the rubisco photoproduct during UV-B irradiation	143
5.3.7	The mechanism of photoproduct formation: effects of free radical scavengers	143
5.3.8	Location of UV-B intersubunit cross-link	146
5.4	Discussion	155
6.	Literature cited	168

## LIST OF TABLES

<b>Table 2.1</b>	Room temperature chlorophyll <sub>a</sub> fluorescence induction measurements.	42
<b>Table 2.2</b>	Photosynthesis and UV-B-absorbing pigment concentrations.	42
<b>Table 2.3</b>	Genetic analysis of Yg mutant.	47
<b>Table 2.4</b>	Analysis of F <sub>v</sub> /F <sub>M</sub> of Yg mutants.	47
<b>Table 3.1</b>	Some effects of biochemicals on cotyledon curling in <i>Brassica napus</i> .	68
<b>Table 4.1</b>	Crystallographic data for the structure of l-sinapoylglucose.	106

## LIST OF ILLUSTRATIONS

Figure 1.1	Solar spectrum.	5
Figure 2.1	Lighting spectrum used for mutant study.	31
Figure 2.2	UV-B-irradiated <i>Arabidopsis</i> .	35
Figure 2.3	SEM cross-sections of UV-irradiated <i>Arabidopsis</i> .	36
Figure 2.4	SEM of epidermis of UV-irradiated <i>Arabidopsis</i> .	38
Figure 2.5	Effect of UV on growth of <i>Arabidopsis</i> .	39
Figure 2.6	Effect of UV on <i>Arabidopsis</i> at different developmental stages.	40
Figure 2.7	Hypocotyl elongation in photomorphogenic mutants.	44
Figure 2.8	Phenotypes of photosynthesis mutant of <i>Arabidopsis</i> .	46
Figure 2.9	77K chlorophyll fluorescence of <i>Yg</i> mutant.	49
Figure 2.10	Cotyledon curling of the <i>Yg</i> photosynthesis mutant.	50
Figure 3.1	Fluence-response curves for cotyledon curling.	64
Figure 3.2	Action spectrum for cotyledon curling in <i>Brassica napus</i> L.	65
Figure 3.3	H <sub>2</sub> O <sub>2</sub> -induced cotyledon curling in <i>B. napus</i> .	70
Figure 4.1	The adaxial epidermis of cotyledons.	83
Figure 4.2	Fluorescence of cotyledon cross-sections.	93
Figure 4.3	1-D PAGE of epidermal and mesophyll protoplast proteins.	95
Figure 4.4	2-D PAGE of epidermal and mesophyll protoplast proteins	96
Figure 4.5	Accumulation of chalcone synthase in epidermal cells.	97
Figure 4.6	UV-B-absorbing compounds in cotyledons.	100
Figure 4.7	HPLC of compounds from whole cotyledon extracts.	101
Figure 4.8	HPLC of UV-absorbing compounds from <i>Arabidopsis</i> mutants.	102
Figure 4.9	Electrospray ionization mass spectrometry of compound 2	103
Figure 4.10	X-ray crystal structure of compound 1.	107
Figure 4.11	Accumulation of sinapate esters after UV-B exposure.	108
Figure 4.12	Comparison <i>B. napus</i> compounds to its parent species.	109
Figure 4.13	The sinapate biosynthetic pathway of <i>B. napus</i> .	113
Figure 5.1	Spectrum of lighting used for rubisco study.	122
Figure 5.2	1-D PAGE and western of UV-B-irradiated <i>B. napus</i> .	132
Figure 5.3	2-D PAGE and western of <i>B. napus</i> leaf protein extracts.	134

Figure 5.4	Partial proteolytic digest of rubisco photoproduct.	135
Figure 5.5	Presence of photoproduct in other species.	137
Figure 5.6	Formation of the photoproduct in <i>Synechococcus</i> .	138
Figure 5.7	<i>In vitro</i> formation of the <i>B. napus</i> rubisco photoproduct.	139
Figure 5.8	Formation of photoproduct from of urea-denatured rubisco.	141
Figure 5.9	Identification of SSU in the rubisco photoproduct.	141
Figure 5.10	Accumulation of photoproduct during UV-B irradiation.	142
Figure 5.11	Effect of antioxidants on formation of photoproduct.	144
Figure 5.12	Effect of D <sub>2</sub> O on photoproduct formation.	144
Figure 5.13	Comparison of LSU amino acid sequences.	146
Figure 5.14	Comparison of SSU amino acid sequences.	148
Figure 5.15	View of rubisco crystal structure.	149
Figure 5.16	View of proposed photocross-link site in rubisco.	150
Figure 5.17	Proteolytic cleavage of spinach rubisco and photoproduct.	152
Figure 5.18	Irradiated spinach rubisco used for digest and peptide digest.	153
Figure 5.19	Photooxygenation of tryptophan residues.	159

## 1. INTRODUCTION

### 1.1 A Prelude to Land Plants

The story of life's emergence onto the land is, in part, about its struggles with solar ultraviolet (UV) radiation. A struggle that continues today. Life very likely evolved in the oceans, protected from exposure to the full spectrum of solar radiation, which includes UV-C (190-290 nm), UV-B (290-320 nm), UV-A (320-400 nm) radiation, and visible light or photosynthetically active radiation (PAR; 400-700 nm), (Henderson, 1977; Walker, 1980; Cleaves and Miller, 1998). UV-C and UV-B radiation cause photochemical damage of DNA (Quaite et al, 1992), proteins (Wilson et al, 1995; Andley et al, 1997) and membranes (Mendez and Penner, 1998). Life in its earliest photosynthetic forms would have had to develop mechanisms to protect against and repair damage of DNA, proteins and membranes by solar UV radiation, since it was dependant on sunlight (Rambler and Margulis, 1980). This probably continued until the first photosynthetic organisms, which utilized hydrogen sulfide ( $H_2S$ ), were replaced by those that could utilize water ( $H_2O$ ) and produced oxygen (see Clayton, 1980). Following this, the concentration of oxygen in the atmosphere increased as oxygen-evolving photosynthetic organisms proliferated. Eventually a stratospheric ozone layer was generated high in the atmosphere by the interaction of short wavelength solar UV with molecular oxygen (Rowland, 1991). The resulting ozone now absorbed solar UV-C and some UV-B. However, much of the UV-B remained. Thus, to spread onto the land, plants would still require protection and repair systems.

DNA repair in living organisms may have evolved very early. One of the DNA repair mechanisms, DNA photolyase (Sancar, 1994), is an example of the elegance of nature. The energy of the blue/UV-A wavelengths in sunlight is used to repair the damage of DNA induced by the UV-B in sunlight. Once shielded by the stratospheric ozone layer, plants would have less



DNA damage from UV-C, and these enzymes could be adapted for other uses. For instance, it has recently been demonstrated that there is homology between DNA photolyase from archbacteria, eubacteria, animals and plants (Tako et al, 1989; Yasui et al, 1994), and the blue light photoreceptor (cryptochrome) of plants (Ahmad and Cashmore, 1996). It has also been revealed that this protein family has members in both plants and animals that regulate the circadian rhythms of these organisms (Miyamoto and Sancar, 1998). One wonders whether the system of circadian rhythms evolved before or after the shielding of UV-C from sunlight. Certainly it is possible that before the stratospheric ozone layer was in place, early life forms minimized exposure to sunlight, and would have had a good reason to evolve a system for anticipating the beginning and end of each day. It is likely that the land plants that evolved later carried with them the genetic legacy of the ancestral struggles with solar UV, and that today they could be used to ameliorate the effects of UV-B.

## **1.2 A Brief History of Ultraviolet Radiation.**

Solar ultraviolet (UV) radiation was first observed in 1801 by J.W. Ritter who was investigating the potential of different parts of the solar spectrum for blackening silver chloride (Jagger, 1967). He found the effect of the dark region beyond the violet (380 nm) part of the spectrum was more effective than any of the visible wavelengths. Measurements of the solar UV spectrum at increasingly shorter wavelengths were made, and in 1879 a limit of 295.5 nm was reported. By relating the shortest detectable wavelength to the solar zenith angle it was postulated that the atmosphere absorbs the wavelengths shorter than 295.5 nm. For example when the sun is directly overhead shorter wavelengths can be measured than when it is closer to the horizon (Toussey, 1966). Two years later, it was proposed that atmospheric ozone was absorbing the solar

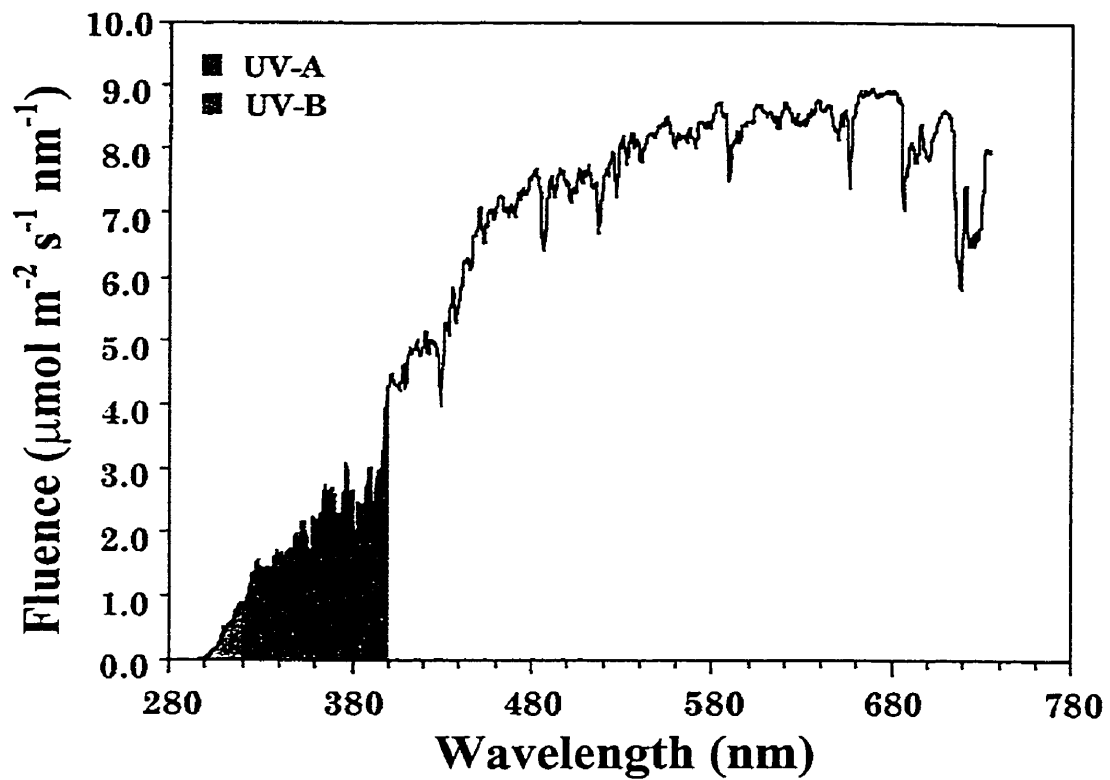
UV. This was based on the similarity between the abrupt termination of the solar spectrum and the absorption spectrum of ozone ( $O_3$ ), which had been measured in the laboratory. With more accurate measures of atmospheric attenuation spectra, it was found that they agreed exactly with the absorption of  $O_3$ . These findings accounted for the discrepancy between measurements of solar radiation at the Earth's surface, and the solar spectrum predicted by Max Planck's theory of black body radiation, which predicted wavelengths as short as 200 nm are emitted by the sun. Throughout the 20<sup>th</sup> century the fluctuations of the atmospheric ozone were explored by such pioneers as Dobson who made portable spectrophotometers for daily monitoring of the ozone layer in remote locations (Griggs, 1966; Toussey, 1966).

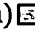

Researchers began laboratory experiments many years ago to explore the biological and photochemical effects of UV radiation. Carbon-arc lamps were used initially as UV sources (see Sage, 1992). In 1887, the discovery that a glass filter would only transmit radiation from a carbon-arc lamp above 320 nm led to the development of UV filters and provided a means to study the effects of different UV wavelengths. As a result, in 1904, it was shown that bacteria were killed 10-12 times more effectively by carbon-arc radiation between 200-290 nm than radiation at wavelengths longer than 295 nm. This line of investigation culminated when Gates reported in 1928, that the effectiveness (or action) spectrum for killing bacteria corresponded more closely to the absorption of the nucleic acids - cytosine, thymine and uracil, than to the aromatic amino acids tryptophan, tyrosine and phenylalanine (Gates, 1928). Later, similar conclusions were made for induction of mutations (Hollaender and Emmons, 1941) and retardation of cell division (Giese, 1966). However, not all UV effects were found to result from nucleic acid absorbance, especially at wavelengths greater than 290 nm where aromatic amino acids absorb more strongly than DNA. For instance, immobilization of ciliary activity of protozoa

by UV corresponds to protein absorption (Giese, 1961). Thus depending on the UV wavelength present in a light source, different biological effects can be anticipated. However, much research was focused on the bacterial effects of UV-C radiation. The killing of bacteria was of great interest to those trying to prevent the spread of disease. The discovery of mercury vapor fluorescence with a peak at 254 nm in 1905, led to the invention of mercury arc UV lamps. These lamps were found to be germicidal by targeting bacterial DNA and were eventually used during World War II for sterilization of medical equipment (Jagger, 1967).

### **1.3 Variations in Solar UV-B Radiation at the Earth's Surface**

Sunlight is attenuated as it passes through the atmosphere due to the absorbance of atomic and molecular species. The most significant atmospheric absorber of UV-C and UV-B radiation is stratospheric O<sub>3</sub>, which is itself the product of solar UV-C absorbance by O<sub>2</sub> (Rowland, 1991). Other molecules, such as O<sub>2</sub>, N<sub>2</sub> and water, also contribute to atmospheric absorbance of UV-B. This effectively limits solar spectrum to wavelengths longer than 290 nm (Fig. 1) (Toussey, 1966). The density of O<sub>3</sub> in the stratosphere overhead is a fundamental determinant of the amount of UV-B reaching the ground. The thickness of the ozone layer is greatest in polar regions during Winter and becomes thinner during Summer. Temperate regions experience a more moderate seasonal variation. In equatorial regions, between 20°N and 20°S, the ozone layer is thinnest and there is almost no seasonal variation (Frederick et al, 1989; Madronich et al, 1995). The amount of UV-B in sunlight is also increase with altitude.



**Figure 1.1.** Spectral distribution of sunlight between 280 and 740 nm, measured at 42°N 81°W on July 13, 1994. The UV-B (290-320 nm) , and UV-A (320-400 nm)  spectral regions are indicated.

The combination of latitude and altitude results in a gradient of solar UV-B intensity from high altitude in equatorial regions to sea level in subarctic regions (Caldwell et al, 1980a; Caldwell et al, 1980b); Sullivan et al, 1990; Madronich et al, 1995). Solar UV-B is attenuated greatly by cloud cover such that geoclimatic variations at the same altitude and latitude (wet versus dry) will result in very different seasonal exposures to UV-B radiation (Seckmeyer et al, 1994; Madronich et al, 1995). It is also attenuated throughout the day depending on the solar zenith angle. At low angles sunlight travels further through the atmosphere and solar UV-B is attenuated to a greater extent.

In temperate latitudes, the molar ratio of PAR:UV-A:UV-B at the surface of the earth is approximately 100:10:0.5 (Krizek et al, 1997). The photon fluence rate (or photon flux) of PAR in sunlight is about 2000-3000  $\mu\text{mol m}^{-2} \text{s}^{-1}$  on a cloudless day at temperate latitudes (this is equivalent to 500-750  $\text{W m}^{-2}$ ). However, the content of UV-B is highly variable. For example, on a clear day in summer the UV-B:visible ratio at latitudes and elevations corresponding to London, England, is only about 0.2 % of visible on a photon basis. While closer to the equator or at higher elevations the UV-B level is as much as 1.5 % of visible (Caldwell et al, 1980; Caldwell 1981; Gerstle et al, 1986; Frederick et al, 1991). Furthermore, the intensity of UV-B in temperate latitudes varies between sunrise and noon much more so than other regions of the solar spectrum (Frederick et al, 1989; Madronich et al, 1995).

#### **1.4 Effects of Solar UV-B on Plant Growth and Metabolism**

Although UV has historically been associated with biological damage, it has also been recently established that current levels of solar UV-B modulate plant growth in the absence of damage and in ways which may have ecological significance (Caldwell et al, 1989). This

realization is emerging from field experiments that compared plants grown in full sunlight to those that were grown under filters which absorbed the UV-B component of sunlight. There have been two types of filter systems used. One which uses ozone filled cuvettes to absorb the UV-B (Tevini et al, 1990) and another which uses thin plastic which has an absorbance close to that of ozone (Ballare et al, 1996; Mark and Tevini, 1996; Krizek et al, 1997). As well, to understand the effects of UV-B on plants under highly controlled conditions, artificial lighting under field and laboratory conditions has been employed (see references in Tevini and Teramura, 1989; Caldwell et al, 1995). While this approach may result in spectral outputs that do not precisely mimic sunlight, it has nevertheless provided insight into the effects of UV-B radiation on plants.

Leaf morphology undergoes a number of changes that can reduce the penetration of UV-B to chloroplasts. For example, the chlorophyll becomes redistributed within the leaf, such that concentrations increase in the lower spongy mesophyll and decrease in the upper palisade layers (Day and Vogelmann, 1995). Another common change in leaf morphology in response to UV-B is an increase in leaf thickness which also has the effect of reducing exposure of underlying photosynthetic cells (Cen and Bornman, 1993; Day and Vogelmann, 1995). Many plants increase the thickness of their cuticular wax layer in response to UV-B (Steinmuller and Tevini, 1985; Tevini and Steinmuller, 1987). This presumably increases absorbance or reflection of UV-B. In general, the growth responses of plants to supplemental UV-B also varies greatly between species (Tevini et al, 1983; Barnes et al, 1990; Sullivan et al, 1990).

Ambient solar UV-B diminishes biomass accumulation, yet, has no effect on net carbon assimilation rates (Krizek et al, 1997). The steadfastness of the net assimilation rates in the face of reductions in plant biomass indicates that modulation of plant growth by solar UV-B is not a result of inhibited photosynthesis (Krizek et al, 1998, Krizek et al, 1997; Nogues et al, 1998).

Rather, UV-B may be morphogenically effecting cell expansion or division (Staxen et al, 1993; Logemann et al, 1995; Krizek et al, 1997; Nogues et al, 1998). Nonetheless, the photosynthetic apparatus is of particular interest since UV-B directly affects the turnover of D1 PSII reaction centre protein and inhibits PSII (Greenberg et al, 1989). Thus, protection against UV-B is an important response.

The effects of UV-B can be beneficial to plant growth. Diminished leaf area and number of stomata resulting from exposure to UV-B reduces water loss and increases water-use efficiency. This would be beneficial to plants which are subject to drought (Sullivan and Teramura, 1989; Nogues et al, 1998). Additionally, some of the changes in leaf biochemistry resulting from ambient UV-B, such as increased accumulation of secondary compounds such as flavonoids, reduce attack by herbivorous insects (Ballare et al, 1996). UV-B radiation also increases plant resistance to heat stress by an unknown mechanism (Mark and Tevini, 1996; Jenkins et al, 1997).

Ambient solar UV-B affects a number of enzyme activities in plants. Both catalase and ascorbate peroxidase activities are at higher levels when plants are grown under full sunlight (Mazza et al, 1998). Moreover, decreases in biomass and grain yield of barley are greater in a catalase-deficient mutant than wild-type plants grown under full sunlight. This indicates that solar UV-B increases oxidative stress in plants (Mazza et al, 1998). These effects of sunlight on active oxygen scavenging enzymes under field conditions are similar to those reported for laboratory experiments with *Arabidopsis* (Rao et al, 1996).

One of the common responses of plants to UV-B is alteration in leaf transmittance properties, which results in attenuation of UV-B in the epidermis before it can reach the photosynthetic mesophyll tissue in the interior of the leaf (Caldwell, 1981; Day and Vogelmann, 1995). This has been observed in numerous plant species. However, the concentration of UV-B-

absorbing pigments varies between species (Day et al, 1994). For example, the UV-B component of sunlight produced no significant changes in cucumber leaves (Krizek et al, 1997), although barley did increase UV-B-absorbing pigments (Mazza et al, 1998). As well, the leaves of *Brassica napus* increase UV-absorbing epidermal flavonoids in response to UV-B, and they seem to protect photosystem II (Tevini et al, 1991; Wilson and Greenberg, 1993a; Wilson et al, 1998). There is a great variety in the types of UV-B-absorbing compounds plants produce and the way in which they are distributed in leaves (Caldwell et al, 1980a; Day et al, 1994; Wilson et al, 1998). The most common components are flavonoids and sinapates (Bharti and Khurana, 1997).

Flavonoids are a group of secondary metabolites with 15 carbon backbones comprised of a 2-phenyl-1-benzopyran-4-one ring system that absorb strongly between 280 and 340 nm (Strack, 1997). They are localized in the vacuoles of epidermal cells (Schmelzer et al, 1988) and thus they provide a UV-B screen for underlying tissues (Cen and Bornman, 1993; Day and Vogelmann, 1995). They are effective in preventing UV-B damage of DNA (Stapleton and Walbot, 1994) and the photosynthetic apparatus (Tevini et al, 1991; Wilson and Greenberg, 1993a; Day and Vogelmann, 1995; Rao and Ormrod, 1995b; Reuber et al, 1996). Although plants synthesize many flavonoids at basal levels, only particular compounds accumulate during exposure to UV-B indicating that this response to UV-B is highly regulated (Wilson et al, 1998).

Many of the changes described above are a result of alterations in gene expression. UV-B induces increased expression of flavonoid biosynthetic enzymes in plants (Kruezaler et al, 1983; Beggs and Wellmann, 1985; Dangi et al, 1987; Schmelzer et al. 1988; Hahlbrock and Scheel, 1989; Kubasek et al, 1992; Ensminger, 1993). The best characterized gene for an enzyme in the flavonoid biosynthetic pathway is the gene for chalcone synthase (CHS), which is present as a multigene family (Koes et al, 1989; Wingender et al, 1989). CHS catalyzes the committal step in



flavonoid biosynthesis (Hahlbrock 1981; Harborne 1988). For the plant species that have been examined to date, the majority of CHS gene transcription in response to UV-B occurs in epidermal cells of leaves, where the flavonoids are ultimately localized (Hradina et al, 1982; Beerhues et al, 1988; Jahnen and Hahlbrock, 1988; Schmelzer et al, 1988). However, this pattern may differ in other species (Day et al, 1994). Analysis of the CHS gene promoter revealed DNA segments 5' to the transcription start site (*cis*-elements) that are required for UV-B induction of gene expression (Schulze-Lefert et al, 1989; Wingender et al, 1990; Batschauer et al, 1991; Kaiser et al, 1995; Fuglevand et al, 1996; Hartmann et al, 1998). As well, transcription factors that bind to CHS promoter regions have been characterized (Staiger et al, 1989; Weisshaar et al, 1991; Kircher et al, 1998). Activation of CHS gene expression by UV-B involves a signal transduction pathway that includes elevation of cytosolic calcium levels and protein phosphorylation (Frohnmeier et al, 1994; Christie and Jenkins, 1996; Fuglevand et al, 1996). Expression of other genes in the flavonoid pathway that are known to be activated by UV-B include phenylalanine ammonia lyase, 4-coumarate:CoA ligase, chalcone flavone isomerase and dihydroflavonol-4-reductase (Douglas et al, 1987; Kuhn et al, 1987; van Tunen et al, 1988; Beld et al, 1989; Douglas et al, 1991).

The expression of a number of genes encoding photosynthetic proteins is reduced after UV-B exposure, such as PSII light-harvesting proteins and the D1 PSII reaction center protein (Jordan et al, 1991), the carbon fixation enzyme ribulose-1,5-bisphosphate carboxylase oxygenase (rubisco; E.C. 4.1.1.39) (Jordan et al, 1992). Other genes are also induced, such as those encoding catalase, guaiacol peroxidase and ascorbate peroxidase (Rao et al, 1996; Boldt and Scandalios, 1997; Polidoros and Scandalios, 1997), cell cycle proteins (histones and cyclin kinase) (Logemann et al, 1995) and pathogen defense proteins (Wingender et al, 1989; Margis-Pinheiro et al, 1993). There are a number of examples of genes which are regulated by UV as

well as fungal elicitors (Kuhn et al, 1987; Gregersen et al, 1994; Logemann et al, 1995). Taken together it is likely that plants have photoreceptors for UV-B radiation that trigger a number of complex changes in gene expression *via* signal-transduction pathways.

### **1.5 Detrimental Photochemical Effects of UV-B Radiation**

UV-B can also produce direct photochemical damage of many key biological molecules. The first report of the damage of plants by solar radiation (possibly the UV component) was by Darwin in the following passage from his lucid monograph “The Power of Movement In Plants” (1880):

“...The leaflets and cotyledons of some plants are known to be injured by too much light; and when the sun shines brightly on them, they move upwards or downwards, or twist laterally, so that they direct their edges towards the light, and thus escape being injured.”

UV-B is a high-energy non-ionizing radiation that is readily absorbed by aromatic compounds such as DNA, aromatic amino acid residues in proteins and many natural products of plants. UV-B induced damage to plants depends on a few basic photochemical processes (Foote 1979; Larson and Barenbaum 1988; Foote 1991). There are essentially two ways light can promote damage to a biological system: photomodification and photosensitization. Photomodification of proteins, most commonly an oxidation reaction, results in alteration of sidechains that can change its biological activity (Bhatnagar, 1984; Zhang et al, 1991; Huang et al, 1993; Borkman and McLaughlin, 1995; Dean et al, 1997). For instance, tryptophan of lens proteins is readily photooxidized to N-formylkynurenine by UV-B radiation (Pirie, 1971). Another common photoreaction is photoisomerization about the carbon-carbon double bond. This occurs in the chromophore for the red light photoreceptor of plants, phytochrome, and in the metabolites of the

phenylpropanoid pathway such as cinnamic acid (Yamamoto and Towers, 1985; Mavandad et al, 1990; Quail, 1997).

Photosensitization reactions usually proceed via the formation of highly reactive singlet-state oxygen (Foote, 1968; Krinsky, 1979; Foote, 1991). This process begins with the molecule absorbing a photon, which elevates electrons to an excited singlet-state. From there the molecule can be transformed by intersystem crossing to the excited triplet-state, where it can react with ground triplet-state oxygen to form excited singlet-state oxygen. Singlet-state oxygen can attack almost any biomolecule to form an organic peroxide, potentially disrupting biological function. For example, lipid hydroperoxides, which result from such reactions, greatly inhibit membrane fluidity and function (Krinsky, 1979; Thompson, 1984; Gallo et al, 1989; Girotti, 1990; Kochevar, 1990).

The above photochemical reactions can have direct effects on plant growth and morphology. For instance, proteins generally become oxidized when plants are exposed to UV-B (Levine et al, 1990; Landry et al, 1995; Rao et al, 1996). Proteins may be even more vulnerable to damage if they are associated with additional chromophores that absorb UV-B, such as the PS II reaction center protein D1. These proteins degrade more rapidly when irradiated with UV-B (Greenberg et al, 1987; Friso et al, 1994; Joshi et al, 1994; Jansen et al, 1996; Vass et al, 1996; Jansen et al, 1998).

Photosensitization reactions which generate oxidants, occur in UV-B irradiated plants. In response, plants increase the levels of antioxidants and antioxidant enzymes (Landry et al, 1995; Rao and Ormrod, 1995b; Rao et al, 1996; Boldt and Scandalios, 1997; Polidoros and Scandalios, 1997; Mazza et al, 1998). The level of oxidative stress resulting from the UV-B in sunlight is sufficient to reduce biomass accumulation. For instance a line of barley which is deficient in

catalase has a third less biomass when grown in full spectrum sunlight compared to those grown with solar UV-B screened out (Mazza et al, 1998).

Plant membranes also become oxidized when plants are exposed to UV-B (Kramer et al, 1991; Landry et al, 1995), possibly due to photosensitization by the tryptophan residues of membrane proteins and other membrane bound chromophores (Kochevar, 1990) or by hydrogen peroxide generated during UV-B irradiation (Rao et al, 1996; Allan and Fluhr, 1997). In addition, plants irradiated with UV-C increase expression of several plant defensive genes that are normally activated by jasmonic acid which is derived from linolenic acid of membranes through the octadecanoid pathway (Conconi et al, 1996). Pathogen-related proteins have also been shown to accumulate in response to UV-B *via* a hydrogen peroxide mediated signal-transduction pathway (Green and Fluhr, 1995; Allan and Fluhr, 1997).

DNA in plants undergoes direct photooxidation when exposed to solar UV-B, forming both cyclobutane pyrimidine dimers and 6,4-photoproducts (Takayanagi et al, 1994; Britt, 1995; Ballare et al, 1996; Nakajima et al, 1998; Szwarcberg-Bracchitta et al, 1998). Plants that are grown in full sunlight, however, appear to be tolerant of DNA damage (Takayanagi et al, 1994; Ballare et al, 1996). Increases in the number of cyclobutane-pyrimidine dimers (CPD) formed was not proportional to the amount of solar UV-B, and in fact accumulation of CPDs became saturated at lower UV-B levels than are present in full sunlight. This indicates that the mechanisms for protection of DNA from damage and repair of CPDs were effective in full sunlight (Ballare et al, 1996). The level of CPD repair is likely to be critical, since plants which lack CPD repair are sensitive to ambient UV-B (Hidema et al, 1997). Hence there are a number of ways that photochemical reactions resulting from UV-B irradiation can have a direct impact on plant growth.

## 1.6 Photoregulation of Plant Cells by UV-B Photoreceptors

A great number of plant movements are stimulated by light. For example, after emergence, the cotyledons of *B. napus* seedlings, like many others, rise and stand vertically up at night, to angle of at least 60°, and relax back to horizontal position by morning (Darwin, 1880). Such plasticity of form in plants is made even more apparent by the bending of plant stems and leaf organs toward or away from light (phototropism). This was of particular interest to Darwin:

“The extreme sensitiveness of some seedlings to light...is highly remarkable. The cotyledons of *Phalaris* become curved towards a distant lamp, which emitted so little light, that a pencil held vertically close to the plants, did not cast any shadow which the eye could perceive on a white card.” (Darwin, 1880).

Darwin was further struck by the fact,

“...that with some seedling plants the uppermost part alone is sensitive to light, and transmits an influence to the lower part causing it to bend. If therefore the upper part be wholly protected from light, the lower part may be exposed for hours to it, and yet it does not become in the least bent, although this would have occurred quickly if the upper part had been excited.” (Darwin, 1880)

In essence, plants have evolved a tremendous capacity to regulate cell growth and development in response to a variety of environmental stimuli. When light is the stimulus, the process is referred to as photomorphogenesis (Kendrick and Kronenberg, 1994). In many cases the regulation is coordinated, resulting in differential cell growth within an organ, for example, as in the case of phototropic bending of a stem. Investigation of these phenomena in plants over the last century has revealed that many other aspects of plant development and cellular metabolism are regulated by light. In each case, absorption of light by a particular photoreceptor initiates the

response. Three general classes of photoreceptors have been identified in plants: phytochrome, a blue light/UV-A photoreceptor (cryptochrome) and UV-B photoreceptor(s) (see references in Holmes, 1991; Kendrick and Kronenberg, 1994). Homologues of cryptochrome have recently been identified in mammals and now form part of a photolyase/cryptochrome family of proteins (Ahmad and Cashmore, 1993; Lin et al, 1995; Ahmad and Cashmore, 1996; Hsu et al, 1996; Todo et al, 1996; Ahmad et al, 1998; Miyamoto and Sancar, 1998)

Considerably more is known about phytochrome and cryptochrome than the UV-B photoreceptor(s) (Sage, 1992; Ahmad and Cashmore, 1996; Fankhauser and Chory, 1997). Much of the information about phytochrome and UV-A/blue light detection was derived first from studies on specific, readily-quantifiable photomorphogenic responses (Sage, 1992; Kendrick and Kronenberg, 1994). Responses that have been used to characterize phytochrome include induction of seed germination, flowering, leaf expansion (see Sage, 1992 and references therein), and gene expression (see Furuya, 1993). Under field conditions phytochrome regulates these processes (Ballare et al, 1991c; Smith et al, 1997a) and others such as shoot:root ratio (Britz, 1990), and neighbor proximity sensing (Kasperbauer, 1987; Ballare et al, 1994), which affect the ecology of plant communities. Processes triggered by UV-A/blue light include phototropism, and regulation of growth and development (Gaba and Black, 1987; Holmes, 1991; Liscum et al, 1992; Ahmad and Cashmore, 1993).

These photoreceptors have also been characterized biochemically (Mohr 1986; Baskin and Iino 1987; Vierstra and Quail 1986; Briggs and Short 1991; Warpeha et al. 1992). Finally, through the study of genetic mutants the genes have been cloned for both the phytochrome (see references in Furuya, 1993) and the cryptochrome photoreceptor families (Ahmad and Cashmore, 1996;

Ahmad et al, 1998). Each of these gene families has been found to have homologues in other groups of organisms. Phytochrome has been found to be a member of a family of light-regulated histidine kinases, which are part of two-component photosensory systems in cyanobacteria and eubacteria (Hughes et al, 1997; Yeh et al, 1997). These proteins mediate red/far-red reversible phosphorylation of small response proteins which transmit the light signal (Quail, 1997). Cryptochrome is a part of a highly conserved DNA photolyase/blue-light photoreceptor family of proteins implicated as the circadian clock photoreceptor in plants (Ahmad et al, 1998) and animals (Zhao and Sancar, 1997; Miyamoto and Sancar, 1998).

While much is known about these two groups of photosensory systems, the characterization of UV-B photoreceptors is still at a very early stage. The recent concern about thinning of the stratospheric ozone layer has focused some attention on the potential impact on plant productivity the of increased solar UV-B radiation (290-320 nm) which may result (Madronich et al, 1995). Thus, there is interest in determining how plants detect UV-B and trigger the protection mechanisms mentioned above (see section 1.5).

For life under the sun, plants require DNA repair enzymes (Jiang et al, 1997), antioxidant and free radical scavenging enzymes (Rao and Ormrod, 1995b; Boldt and Scandalios, 1997; Mazza et al, 1998), mechanisms for repair of membrane damage (Kramer et al, 1991; Arami et al, 1997), protein damage (Andley and Clark, 1989a; Caldwell, 1993; Rao, et al, 1996), and screening pigments (Caldwell et al, 1995). Because of biogeoclimatic and seasonal fluctuations in the level of solar UV-B, it is likely that plants regulate these mechanisms (Caldwell et al, 1980a; Sullivan et al, 1990). It has been shown that plants have developed a means for sensing and responding to UV-B (Hashimoto et al, 1984; Ensminger, 1993; Wilson and Greenberg, 1993b; Ballare et al, 1995a; Fagerberg and Bornman, 1997).

UV-B radiation could trigger these changes in plants in a number of ways. In all cases, however, the initial step involves photochemical modification of a biomolecule(s). To date, a number of UV-B chromophores and photoreceptors have been proposed - including DNA (Quaite et al, 1992; Wellmann et al, 1984), protein chromophore complexes (Brodhun and D-P, 1993), the phytohormone indole-3-acetic acid (Ray and Curry, 1958; Bhatnagar, 1984; Braun and Tevini, 1993), photosynthetic pigments (Greenberg et al, 1989; Fagerberg and Bornman, 1997), and metabolites of the phenylpropanoid biosynthetic pathway (Yamamoto and Towers, 1985). One of the best-characterized UV-B photoreceptors is one of the accessory photoreceptors of DNA photolyase which is a tryptophan residue of the protein (Kim et al, 1992). This residue acts as an accessory chromophore in addition to the BL chromophore, which both directly donates an electron to a cyclobutane pyrimidine dimer reducing it to two thymidine bases and thus repairing the damaged DNA. The diversity in plant responses indicated that there will also be many ways to acclimate to UV-B. However, the basis of UV-B-sensing may also be similar to red light- and blue light/UV-A-sensing, in that once an efficient photoreceptor is evolved, it is conserved (Quail, 1997; Yeh et al, 1997; Pepper, 1998; Ahmad and Cashmore, 1996; Miyamoto and Sancar, 1998). There are many examples of responses to UV-B, yet identification of the UV-B photoreceptor(s) continues to elude us.



## 1.7 Rationale and Objectives

The goals of this investigation were to characterize the photoreceptors that plants use to detect UV-B radiation, to study photomorphogenic and biochemical responses of plants that occur during acclimation to UV-B, and to isolate mutants that display tolerance to UV-B radiation. Overall the thesis progresses from studies of UV-B effects on whole organs to effects on cells and then to effects on proteins.

From the foregoing discussion it is clear that plants can detect UV-B and that this process triggers a range of cellular changes. The most extensive work on UV-B photoreception and signal-transduction, so far, has been the UV-B induction of flavonoid accumulation and in particular the upregulation of the flavonoid enzyme chalcone synthase gene expression (Martin, 1993; Weisshaar et al, 1991). The approach used has been to characterize the response, UV-B-induced accumulation of flavonoids, then to begin at the level of gene expression to identify transcription factors and the signal-transduction pathway that triggers them. Recently progress has been made identifying transcription factors and some of the proteins in the signal-transduction pathway (Christie and Jenkins, 1996; Hartmann et al, 1998; Kircher et al, 1998). This could be described as a molecular biological approach. Alternatively, a photobiological approach can be used. Both of the other known plant photoreceptors, phytochrome (RL/FR) and cryptochrome (BL/UV-A) were identified after careful photobiological characterization of the photoreceptors associated with light responses (Sage, 1992; Ahmad and Cashmore, 1996; Fankhauser and Chory, 1997). Ultimately the isolation and cloning of genes encoding these photoreceptors was accomplished by analyzing plants carrying genetic mutations which disrupted normal photomorphogenesis. This is the approach adopted by this study, principally because of

the success of this approach for other photoreceptors, and also since the aim of the study was to investigate UV-B induced morphological changes for which no genes have been identified.

The emphasis of the first half of the study is on the changes in cotyledon morphology after exposure of seedlings to UV-B. These responses are particularly interesting for a number of reasons. As mentioned above, the most widely reported changes in plants grown in the presence of UV-B are reductions in the size of leaves, stems and biomass (Caldwell et al, 1995; Ballare et al, 1996). To date there have been some studies carried out to investigate the basis of morphological changes resulting from exposure to UV-B (Curry et al, 1956; Hashimoto et al, 1984; Lecari et al, 1990; Ballare et al, 1991b; Ballare et al, 1991a; Goto et al, 1993; Ballare et al, 1995a; Ballare et al. 1995b; Ros and Tevini, 1995; Wheeler et al, 1997). The aim was to determine the presence and characteristics of the UV-B photoreceptor and signal-transduction system involved in UV-B-induced morphological changes. The work progresses from ultrastructural and physiological studies of morphological changes, to construction of an action spectrum for the cotyledon curling response in order to characterize the photoreceptor and finally, to biochemical studies to investigate whether signal-transductions are associated with the response.

Cotyledons were chosen for this study for a number of reasons. Previous work has shown the upward curling of *Brassica napus* cotyledons has the characteristics of a UV-B-specific photomorphological response and is suitable for more detailed photobiological analysis of photoreceptor involved (Wilson and Greenberg, 1993b). This particular organ has a much simpler tissue organization than leaves making interpretation of results more straightforward. Moreover, the study of cotyledon growth has an important advantage over leaves since growth is due almost completely to cell expansion whereas in leaves growth is also due to cell division. Cotyledons are

almost fully formed during embryogenesis (Dhillon and Miksche, 1983; Gendreau et al, 1997). Hence interpretation of results can focus on the effects of UV-B on cell expansion. The study of cotyledons also fulfills another aim of this work, which is to study the process of plant acclimation to UV-B. In the field, seedlings are first exposed to sunlight during early stages of development. Hence, the process of acclimation to solar UV-B may be quite active.

Two species of plants from the family Brassicaceae were used in this study, *Arabidopsis thaliana* L. (Columbia ecotype), and *Brassica napus* L. cv. Topas. The first, *Arabidopsis*, has been exceptionally well characterized genetically. It was selected principally because a number of photomorphogenic mutants of this species have been well characterized and were available for testing of hypotheses about UV-B responses in plants (Chory et al, 1995). In addition, its diploid genome is ideally suited for the generation and screening of populations of mutagenized seedlings to identify genes that affect the capacity of these plants to respond to UV-B (Meyerowitz and Somerville, 1994; Pyke, 1994). Since this is the only member of this genus, it is referred to as *Arabidopsis*. *B. napus* was selected for this study because it is an important crop plant and it has been used as a model system for studying the plant responses to UV-B (Fagerberg and Bornman, 1997; Greenberg et al, 1997; Wilson et al, 1998). In addition, a number of techniques used in this study, such as isolation of epidermal protoplasts, could not be carried out using *Arabidopsis* because of its small size, making the use of a larger species such as *B. napus* advantageous.

The middle section of the thesis describes the isolation and characterization of epidermal protoplasts from the upper surface of *B. napus* cotyledons. An understanding of the responses of these cells to UV-B is central to the question of what protective mechanisms plants have evolved to cope with solar UV-B, since these cells are unshielded and directly exposed to sunlight. Epidermal cells in general are not well characterized and they have been isolated from only a few

species (Schulz and Weissenbock, 1986; Weissenbock et al, 1986; Dietz et al, 1992). They are known to be the main site for accumulation of UV-B absorbing flavonoids in leaves in response to UV-B radiation (Beerhues et al, 1988; Schmelzer et al, 1988; Cen et al, 1993; Ålenius et al, 1995; Greenberg et al, 1997). The exact nature of UV-B-absorbing compounds in the epidermis of cotyledons, however, has not been determined. Hence, to characterize the role of these cells during acclimation to UV-B, epidermal protoplasts were isolated and their UV-B-absorbing compounds analyzed.

During the course of these studies the photomodification of a chloroplast protein, ribulose-1,5-bisphosphate carboxylase oxygenase (rubisco; E.C. 4.1.1.39), *in vivo* by UV-B was observed. Crosslinking of proteins *in vivo* by UV-B has been reported to occur in the lens of mammals in association with cataract formation (Andley and Clark, 1989a; Andley et al, 1997). This was the first observation of protein crosslinking by UV-B in plants, and similar reactions may be involved in cellular responses to UV-B (Schieven et al, 1994). Thus, an investigation was carried out and is reported in the last section of this thesis.

## **2. UV-B-INDUCED MORPHOLOGICAL CHANGES IN *Arabidopsis thaliana* (L.) Heynh.**

### **2.1 INTRODUCTION**

There is a dramatic increase in solar irradiance from short-wave UV-B (290-305 nm) to long-wave UV-B (305-320 nm) (Madronich et al, 1995). Long-wave UV-B is 10-20 times more abundant than short-wave UV-B during maximum summer irradiance in temperate northern and southern latitudes. Depletion of stratospheric ozone, however, will disproportionately increase short-wavelength UV-B because ozone absorbance increases through the UV-B region as the wavelength drops (Caldwell et al, 1989; Kerr and McElroy, 1993; Madronich et al, 1995). This is of concern, in that short-wave UV-B radiation is more damaging than long-wave UV-B to many essential biological molecules in plants. The molecular targets include DNA, proteins, lipids and phytohormones (Ray and Curry, 1958; Greenberg et al, 1989; Quaitte et al, 1992; Landry et al, 1995; Ros and Tevini, 1995; Wilson et al, 1995).

Plants respond to current levels of solar UV-B. The morphology and physiology of seedlings grown in sunlight differ from those grown under optical filters which shield plants from UV-B radiation (Tevini et al, 1990; Ballare et al, 1996; Mark and Tevini, 1996; Krizek et al, 1997). In addition, many species grown in presence of supplemental UV-B under growth chamber, greenhouse and field conditions exhibit marked differences from plants grown without UV-B. These include, inhibition of hypocotyl elongation, delayed emergence of seedlings, reduced shoot height, changes in distribution of dry weight, decreased leaf area, increased leaf thickness, tillering and number of leaves, increased UV-B-absorbing compounds in leaves, and upward curling of cotyledons (Tevini et al, 1983; Steinmetz and Wellmann, 1986; Barnes et al, 1990; Sullivan et al, 1990; Cen and Bornman, 1993; Caldwell et al, 1995; Wilson and Greenberg, 1993a; Wilson and Greenberg, 1993b; Ballare et al, 1996). It appears that UV-B can reduce total

biomass accumulation, not through damage to photosynthesis, but instead by reducing the leaf area (Nogues et al, 1998). The decrease in leaf area is a result of decreased cell number and epidermal cell expansion. In this way ambient solar UV-B may limit the productivity of crops by inducing cellular changes that alter plant morphology.

Seedlings likely acclimate to daily cycles of UV-B as they emerge from the soil, and at later stages in development, plants acclimate to seasonal increases in UV-B (Frederick, 1990). However, relatively little is known about the processes by which young seedlings acclimate to current levels of UV-B. Cotyledons must carry out photosynthesis, and supply the seedling with nutrients during the initial stages of growth and development. In this regard, the responses of cotyledons may be quite different from leaves of mature plants, since cotyledons are primary photosynthetic organs for only a relatively short period of time after which they senesce.

To study how cotyledons acclimate to UV-B radiation, the effectiveness of various wavelengths of UV to initiating changes in the growth, morphology and physiology of *Arabidopsis* seedlings was investigated. In particular, the objective was to determine if different responses triggered by UV-B could be separated based on wavelength. Previous studies using etiolated seedlings of sorghum and tomato indicate some biochemical and morphological changes resulting from exposure to UV-B can be separated on the basis of wavelength dependence (Hashimoto et al, 1984; Ensminger, 1993; Ballare et al, 1995a). Indeed, a great deal continues to be discovered about photoreceptors in general using this approach (Ballare et al, 1991c; Sage, 1992).

One of the obstacles to studying the UV-B photoreceptors that trigger morphological responses is that a number of other photoreceptors are also affected by UV-B. In particular, phytochrome and the BL/UV-A cryptochrome photoreceptor system(s) absorb UV-B to a small

extent. Specific questions about the mechanistic details of how plants detect and respond to UV-B radiation can be addressed by the use of photomorphogenic mutants. Strains of *Arabidopsis*, which carry genetic mutations in components of known photoreceptor systems (phytochrome and cryptochrome) that render them non-functional, can be used to determine the role of these receptors in UV-B responses.

The isolation of photomorphological mutants has been invaluable for gaining a better understanding of the mechanism of light-regulated development in plants. Such mutants have led to the discovery of completely new aspects of photomorphogenesis. For example, analysis of the *det2* mutant of *Arabidopsis*, in which normal light-regulated de-etiolation occurs in the dark, revealed for the first time the role of steroids in plant development (Li et al, 1996). A similar approach can be used to investigate plant responses to UV-B. A number of mutants have already been identified which are more susceptible to damage by UV-B because of defects in DNA repair enzymes (Britt et al, 1993; Jenkins et al, 1995; Landry et al, 1997). Also a number of mutants which have defects in biosynthetic enzymes have been used to test the effectiveness of secondary metabolites (e.g. flavonoids) as UV-B-screening compounds (Li et al, 1993; Landry et al, 1995; Rao and Ormrod, 1995a; Rao and Ormrod, 1995b; Rao and Ormrod, 1995c; Rao et al, 1996). Also, photosynthesis mutants can be isolated to determine how this light driven process affects acclimation to UV-B. Mutants can be selected which exhibit increased resistance to the damaging effects of UV-B, and which grow better than wild-type plants under UV-B. The reduction of leaf area is one of the most commonly reported changes in growth when plants are exposed to UV-B (Barnes et al, 1990; Wilson and Greenberg, 1993a; Caldwell et al, 1995; Ballare et al, 1996; Mark and Tevini, 1996). Hence, leaf area may be a particularly interesting parameter to use as a measure of plant resistance to UV-B and as a phenotype marker for UV-B effects.

In this chapter, wavelength-dependent responses of *Arabidopsis* to UV-B were investigated. The results from this study indicate that these responses can be studied using 4-day old seedlings *Arabidopsis* grown under normal indoor lighting. Cotyledons display a number of separate wavelength-dependent UV responses affecting growth, morphology, phenylpropanoid metabolism and physiology.

## **2.2 MATERIALS AND METHODS**

### **2.2.1 Wavelength-dependant changes in *Arabidopsis***

#### **2.2.1.1 Plant Growth and Lighting Conditions**

*Arabidopsis thaliana* ecotype Columbia seeds (gift of Dr. B. A. Moffatt) were germinated in moist non-sterile Pro-mix soil mixture (Premier Brands, Rivière-du-Loup, Canada). Plants were grown for 4-10 days at 21°C under 100  $\mu\text{mol m}^{-2} \text{s}^{-1}$  PAR from cool white fluorescent lamps (F40T12CW; General Electric Co., Wilmington, MA) using a 16 h light/8 h dark photoperiod. Lamps were screened with a polyester film (0.08 mm Mylar D) (Johnson Industrial Plastics, Mississauga, ON) to shield out any extraneous UV-B or UV-C from the fluorescent lamps (Learn et al, 1993).

#### **2.2.1.2 Monochromatic UV-B Exposures**

Seedlings were exposed to monochromatic UV-B (10 nm bandwidth) from a water-cooled 150 W xenon arc lamp (Photon Technology Inc., South Brunswick, NJ) for 100 minutes and then incubated under continuous PAR for 24 h. The control sample was exposed to PAR for 100 minutes. A water filter with quartz windows was used to attenuate the infrared radiation from the xenon lamp. A specific UV spectral region was then isolated with an interference filter



covering the optical entrance to the exposure chamber. The interference filters used had 10 nm bandwidths and had peak transmittance at 270 nm, 280 nm, 290 nm, 300 nm, 313 nm and 320 nm (Oriel, Stratford, CT). After the interference filter, the radiation was focused with an f 1.7 quartz condenser lens, diffused through a quartz diffuser, and reflected with an aluminum mirror (Oriel, Stratford, CT), such that a beam of uniform fluence rate was vertically incident on the seedlings. The irradiance ( $\mu\text{W cm}^{-2}$ ) at the level of the cotyledons was measured using a calibrated radiometer (Photodyne, Hollandschdiep, Netherlands). This measurement was converted to the fluence rate of the UV radiation ( $\mu\text{mol m}^{-2} \text{s}^{-1}$ ) based on the sensitivity of the radiometer at the wavelength of interest. Seedlings was exposed to  $2.5 \pm 0.4 \mu\text{mol m}^{-2} \text{s}^{-1}$  for 100 min ( $\sim 15 \text{ mmol m}^{-2}$ ) at  $21^\circ\text{C}$  and either sampled immediately or incubated under continuous PAR ( $\sim 100 \mu\text{mol m}^{-2} \text{s}^{-1}$ ) for 24 h at  $21^\circ\text{C}$  and then sampled. The PAR used was from cool white fluorescence lamps filtered through polyester film (0.08 mm) to remove radiation below 320 nm (Johnson Industrial Plastics, Missasauga, ON). The biologically effective UV-B doses given in the 100 minute UV exposure period for each wavelength used (calculated from Caldwell's generalized damage weighting function normalized to 300 nm; Caldwell, 1971) were 320 nm,  $0 \text{ kJ m}^{-2}$ ; 313 nm,  $0.8 \text{ kJ m}^{-2}$ ; 300 nm,  $6.5 \text{ kJ m}^{-2}$ ; 290 nm,  $11.9 \text{ kJ m}^{-2}$ ; 280 nm,  $30.7 \text{ kJ m}^{-2}$ ; 270 nm,  $56.7 \text{ kJ m}^{-2}$ .

### **2.2.1.3 Scanning Electron Microscopy**

Seedlings were prepared for SEM using the following protocol adapted from standard procedures (O'Brien and McCully, 1969). The upper shoot of approximately 20 seedlings from each UV-B and control treatment was detached and immediately fixed in a solution of 1.5% glutaraldehyde in 25 mM sodium phosphate buffer (pH 6.8) for 1h, followed by 3% glutaraldehyde in 25 mM sodium phosphate buffer (pH 6.8) for 12 h at room temperature. The specimens were given 3 changes of 25 mM sodium phosphate buffer (pH 6.8) over 12 h at 0°C and then dehydrated to absolute ethanol using five 15-min steps of 25%, 50%, 75%, 95% and 100% ethanol. The fixed specimens were stored at -20°C until required. Freeze-fracturing of cotyledons was carried out after specimens were infiltrated a cryoprotectant. This was done by rehydrating the specimens to 25 mM sodium phosphate buffer (pH 6.8) by reversing the dehydration process, then taking the specimens to 30% glycerol using 10% increments in three 15-min steps. The specimens were then frozen in liquid nitrogen and the cotyledons fractured transversely approximately midway along their length using a razor blade pre-cooled in liquid nitrogen. After fracturing specimens were thawed to room temperature, taken to 25 mM sodium phosphate buffer by lowering the glycerol concentration in 10% increments and dehydrated to absolute ethanol as described above. Specimens were critical point dried, mounted and sputter-coated with gold. The specimens were viewed and photographed using a 15 kV scanning electron microscope (Hitachi S-570, San Jose, CA). Between 10 and 15 specimens from two separate experiments were viewed for each treatment. The pictures shown here are of representative cotyledons.

#### 2.2.1.4 Quantitative Plant Growth Measurements

For each sample, the cotyledons from 40 seedlings were detached from the shoot apex. The total cotyledon area of individual seedlings was measured by analyzing video images of the cotyledons viewed under a 40X magnification (Olympus IMT, Tokyo, Japan) and captured with a monochrome CCD camera (Cohu, San Diego, CA) for computer analysis (NIH Image, Bethesda, MD). Each image contained a standard scale for calibrating them measurement of area. Fresh weights were measured immediately with an analytical balance (Sartorius). Samples were then dried for 72 h at 70°C, cooled in a desiccator and dry weights measured using a microbalance (Cahn C31, Cerritos, CA). Seedlings older than 5 days had true leaves that were included in the measurements of fresh and dry weights. Each experiment was repeated and data analyzed using analysis of variance (ANOVA) (Systat). Where appropriate results were pooled and significant differences ( $p < 0.05$ ) assigned using Tukey's test (Sokal and Rolfe, 1991).

#### 2.2.1.5 Chlorophyll a Fluorescence

Room temperature chlorophyll<sub>a</sub> fluorescence of cotyledons from individual seedlings was measured *in situ* using a pulse amplitude modulated (PAM) fluorometer (Walz, Effeltrich, Germany). Seedlings were dark-adapted for 30 min before fluorescence measurements were made. The initial fluorescence ( $F_0$ ), maximum fluorescence ( $F_M$ ) and the ratio of  $F_v/F_M$ , where  $F_v = F_M - F_0$ , were used as a measure of maximal PSII activity (Schreiber, 1983).

### **2.2.1.6 Pigment Analyses**

Photosynthetic pigments (chlorophyll<sub>a</sub> and carotenoids) were extracted from 5 mg of cotyledon tissue for 14 h at 4°C into 80% acetone and quantified spectrophotometrically (Lichtenthaler, 1987). UV-B-absorbing pigments were extracted from 5 mg of cotyledon tissue using acidified methanol (70:29:1, MeOH:H<sub>2</sub>O:HCl) for 24 h at 4°C and the extracts were scanned with a UV/Visible spectrophotometer (absorbances at 280, 300 and 325 nm were recorded).

## **2.2.2 Exposure of *Arabidopsis* photomorphological mutants to UV-B.**

### **2.2.2.1 Plant Growth and Lighting Conditions**

Seeds of the following mutants of *Arabidopsis* were obtained from the *Arabidopsis* Centres in Ohio and Nottingham (*Arabidopsis* Biological Resource Center, Ohio State University, Columbus, OH; Nottingham *Arabidopsis* Stock Centre, University of Nottingham, Nottingham, UK): phytochrome mutants *phyB9*, *phyA211*, and cryptochrome mutant *hy4-1*. The mutants *phyB9*, *phyA211* and *hy4-1* have non-functional phytochrome B, phytochrome A and cryptochrome photoreceptors respectively, and are derived from the Columbia ecotype.

Seeds were germinated in moist non-sterile Pro-mix soil mixture (Premier Brands, Rivière-du-Loup, Canada) at 21°C. Lighting conditions were used for seedling germination which allowed the observation of UV-B-specific effects in the seedlings. Thus, the only PAR provided came from the UV fluorescent lamps. Plants were exposed to PAR plus UV-A and UV-B or PAR plus UV-A. UV-B fluorescent lamps were either shielded by cellulose acetate (0.13 mm) for the PAR plus UV-A plus UV-B treatment, or cellulose acetate and mylar (0.08 mm) for the PAR plus UV-A treatment. Under the UV-B treatment conditions, the total radiation measured between

280-780 nm ( $7.0 \mu\text{mol m}^{-2} \text{s}^{-1}$ ) was comprised of  $1.2 \mu\text{mol m}^{-2} \text{s}^{-1}$  UV-B,  $4.1 \mu\text{mol m}^{-2} \text{s}^{-1}$  of UV-A,  $0.8 \mu\text{mol m}^{-2} \text{s}^{-1}$  BL,  $0.2 \mu\text{mol m}^{-2} \text{s}^{-1}$  RL,  $0.6 \mu\text{mol m}^{-2} \text{s}^{-1}$  FR (Fig. 2.1). The control plants were exposed to UV-B ( $0.1 \mu\text{mol m}^{-2} \text{s}^{-1}$ ) and UV-A ( $3.4 \mu\text{mol m}^{-2} \text{s}^{-1}$ ). The BL, RL and FR were the same under control and treatment conditions. Phytochrome is a key photoreceptor during seedling development that also absorbs UV radiation. The photostationary state calculation for native oat phytochrome (124 kDa) under these lighting conditions, based on data from Lagarias *et al* (personal communication), was 0.64 for control conditions and 0.68 for UV-B conditions, respectively, compared to 0.62 for full midday sunlight. In terms of the amount of biologically effective UV-B radiation (weighted by Caldwell's generalized damage action spectra normalized to 300 nm) treated plants received  $14.6 \text{ kJ m}^{-2} \text{ d}^{-1}$  UV-B<sub>BE</sub> and control plants received  $0.02 \text{ kJ m}^{-2} \text{ d}^{-1}$  UV-B<sub>BE</sub> (Caldwell et al, 1986). Plants were grown under the above conditions for 14 d. The hypocotyl height was then measured.

### **2.2.3 Isolation of a UV-B-resistant photosynthesis mutant of *Arabidopsis*.**

#### **2.2.3.1 Mutagenesis and Growth Conditions**

*Arabidopsis thaliana* L. ecotype Columbia seeds were germinated in moist non-sterile Pro-mix soil mixture (Premier Brands, Rivière-du-Loup, Canada). Plants were grown to seed as described in above (section 2.2.1.1). After flowering and seed set, plants were dried, and the seeds were collected and stored in glass vials. The mutagenesis was carried out as follows. Approximately 100,000 seeds of *Arabidopsis* ecotype Columbia (2.0 g) were added to 100 mL of 0.3% (v/v) ethylmethanesulfonate (EMS) for 2 h with occasional stirring. The EMS solution was discarded and seeds were rinsed 10 times with deionized water over a 2 h period.

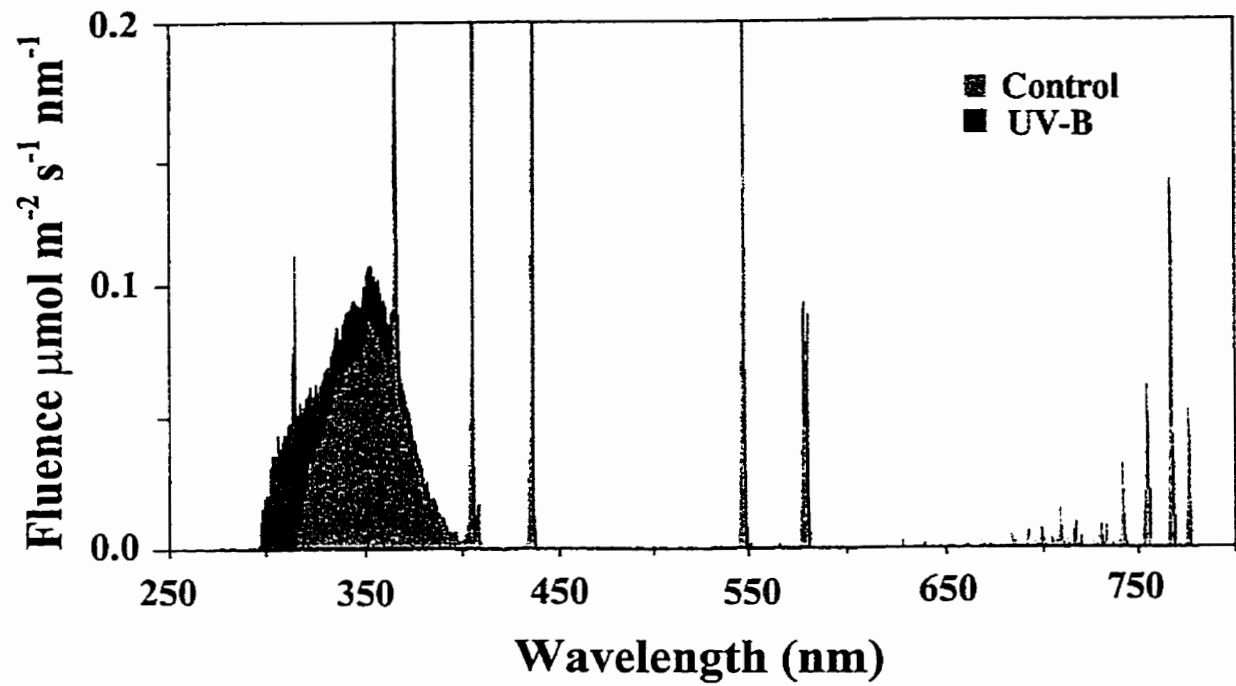


**Figure 2.1.** The spectral distribution of the lighting used for experiments with photomorphogenic mutants. The radiation from UV mercury-arc lamps was filtered through mylar D film for control conditions (■), and through cellulose acetate film for the UV-B treatment (▣) (see section 2.2.2.1 for descriptions of the artificial light sources).

These seeds are the first generation mutant seeds (M1), which are expected to carry heterozygous mutations (Meyerowitz and Somerville, 1994). Only mutations in dominant genes would be expected to produce measurable phenotypes in this generation. Seeds were then added to 700 mL 0.1% agar and ~5000 seeds per tray distributed by pipette onto 20-53 x 27 cm trays containing moistened Pro-mix soil mixture. Plants were grown in a greenhouse growth chamber under  $\sim 250 \mu\text{mol m}^{-2} \text{s}^{-1}$  PAR and sprayed with water daily. Lamps were screened with a polyester film (0.08 mm Mylar D) to shield out any extraneous UV-B or UV-C from the fluorescent lamps. Plants were allowed to self-fertilize and produce second generation mutant (M2) seeds. In this generation mutant plants are expected to be heterozygous and homozygous and hence mutations in recessive or dominant genes with measurable phenotypes would be evident when the M2 seeds are grown. Seeds were allowed to dry on the plants and the seeds from each tray used to make separate pools of M2 seeds.

#### **2.2.3.2 The identification of UV-B-resistant mutants.**

Approximately 5000 seeds from each M2 pool was grown for 1 week under  $100 \mu\text{mol m}^{-2} \text{s}^{-1}$  in trays (53 x 27 cm) containing Pro-mix soil (Premier Brands, Rivère-du-Loup, Canada) along with two 6" pots of wild-type seeds ( $\sim 100$  seeds per pot). At this point  $2 \mu\text{mol m}^{-2} \text{s}^{-1}$  of supplemental UV-B and  $5 \mu\text{mol m}^{-2} \text{s}^{-1}$  UV-A from 4-FS40 UV lamps (National Biological Co., Twinsburg, Ohio) was added to the lighting for all of the mutant seedlings and one tray of wild-type seedlings (positive control plants). One tray of wild-type seedlings was left under PAR plus UV-A conditions (negative control plants). All mutant plants and the positive control wild-type plants were screened with cellulose acetate (0.13 mm) to shield extraneous UV-C from the UV lamps. The negative control wild-type plants were screened with mylar D (0.13 mm) which

absorbs both the UV-B and UV-C (see Fig 5.1). After 3 weeks, plants were scored in two ways. A mutant was scored as being sensitive to UV-B if its growth was inhibited relative to the positive control wild-type seedlings grown under UV-B, or scored as tolerant to UV-B if growth was similar to the negative control wild-type seedlings grown under UV-A plus PAR.

### 2.2.3.3 Room temperature and 77K chlorophyll<sub>a</sub> fluorescence.

To investigate whether differences in photosynthesis were present in selected mutants both room temperature and 77K chlorophyll<sub>a</sub> fluorescence was measured with a spectrofluorometer (Photon Technology International, South Brunswick, NJ) using 450 nm  $\lambda_{ex}$  and 695 nm  $\lambda_{em}$  (5 nm slit widths). For room temperature measurements individual 4-d old seedlings, which had been grown in individual cells (2 x 2 cm) under conditions described above, were dark-adapted for 30 min then positioned in the sample holder. The mechanical shutter used gave an intensity rise time of 2 ms to a maximum of 40  $\mu\text{mol m}^{-2} \text{s}^{-1}$ , and data was collected at a rate of 500 points  $\text{s}^{-1}$  for 20s.  $F_O$  was measured as the chlorophyll fluorescence after 2 ms,  $F_M$  was measured as the maximum observed fluorescence during the measurement.  $F_V/F_M$  was calculated as  $(F_M - F_O)/F_M$ .

For measurement of fluorescence at 77K, an individual 3 d old seedling was removed from the soil, adhered to a sample support rod using silicone grease such that the cotyledons were parallel to the probe surface. They were then placed into liquid nitrogen (77K) and then into a liquid N<sub>2</sub>-cooled glass cuvette. Fluorescence of the sample was measured from 650 nm to 800 nm with 450 nm excitation light ( $\sim 40 \mu\text{mol m}^{-2} \text{s}^{-1}$ ) perpendicular to the sample rod using a spectrofluorometer with slitwidths set at 5 nm (Photon Technology International, South Brunswick, NJ). Fluorescence emission was collected from 650 nm and 800 nm.



## **2.3 RESULTS**

### **2.3.1 Wavelength-dependent changes in *Arabidopsis* cotyledons**

#### **2.3.1.1 Changes in cotyledon morphology and growth**

It has been shown that when *Arabidopsis* seedlings are grown under a light source containing UV-B, seedlings are morphologically and biochemically distinct from seedlings grown in PAR light alone (Li et al, 1993). However, the dependence of these changes on wavelength has not been studied. There are a number of photomorphogenic responses in plants that involve a variety of photoreceptors including phytochrome, cryptochrome and the UV-B photoreceptor(s). For example, the inhibition of hypocotyl elongation in cucumber seedlings involves phytochrome (Yanovsky et al, 1995), cryptochrome (Attridge et al, 1984; Ahmad et al, 1995) and the UV-B photoreceptor(s) (Ballare et al, 1991a). To minimize the interactions between photoreceptors during the treatments in this study, relatively short exposures to monochromatic UV radiation were given without a background of PAR, followed by an incubation period in PAR without UV-B. The effects of phytochrome and cryptochrome should be saturated in each case by the PAR incubation which contains red and blue light. Hence, UV-specific effects more easily identified.

Initially, 4-day old seedlings grown under PAR were exposed to 100 minutes of 290 nm UV-B and then incubated in continuous PAR for 24 h. After the 24 h incubation period, UV-B-exposed cotyledons were curled upward, had a glazed appearance and were smaller than control seedlings (Fig. 2.2). An examination of the cotyledons using SEM revealed that a number of changes were dependent on UV wavelength (Fig. 2.3). A 100 minute exposure to 290 nm radiation was the most effective wavelength for initiating cotyledon curling of the wavelengths tested (Fig. 2.3).

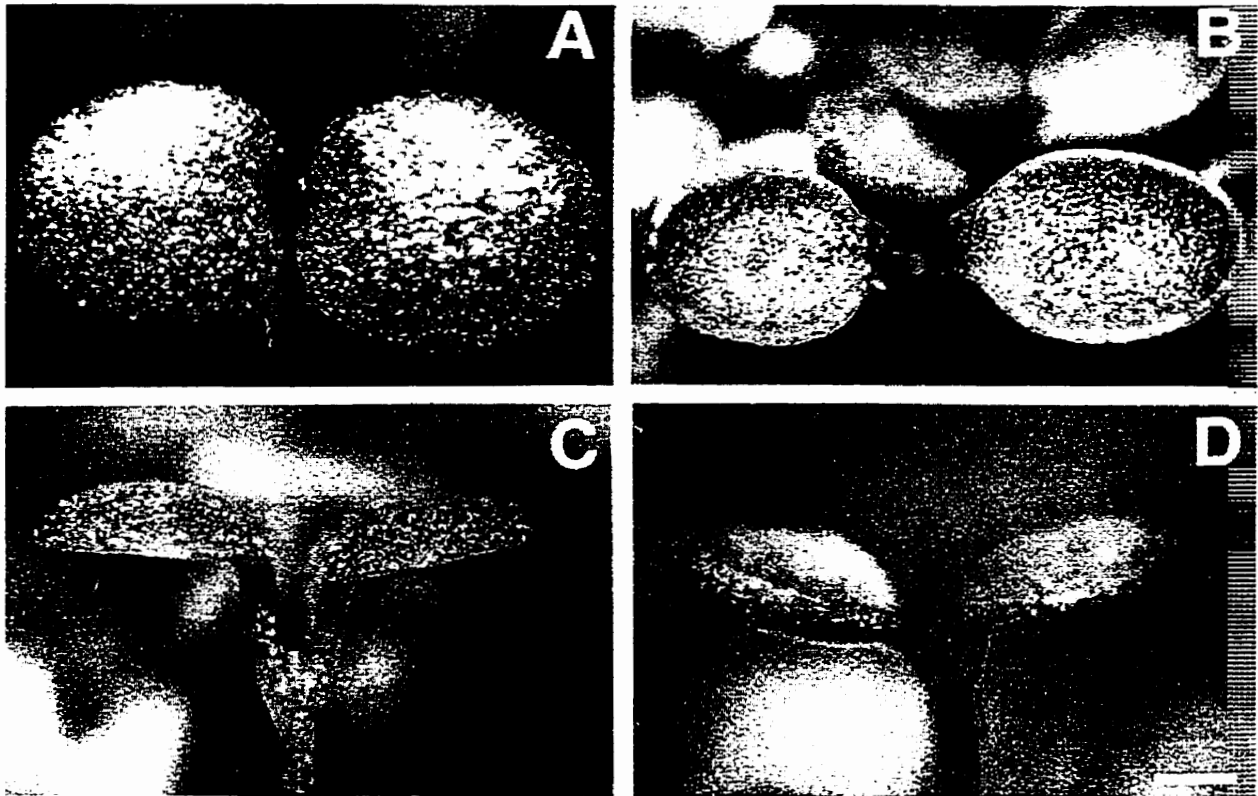


**Figure 2.2.** Top and side views of curled cotyledons from 5-d-old *Arabidopsis* seedlings after exposure to either white light (A, B), or  $15 \text{ mmol m}^{-2} 290 \text{ nm}$  radiation (C, D), followed by a 24 h incubation in visible light in all cases. Plants were viewed with a dissecting microscope. The scale bar =  $400 \mu\text{m}$ .

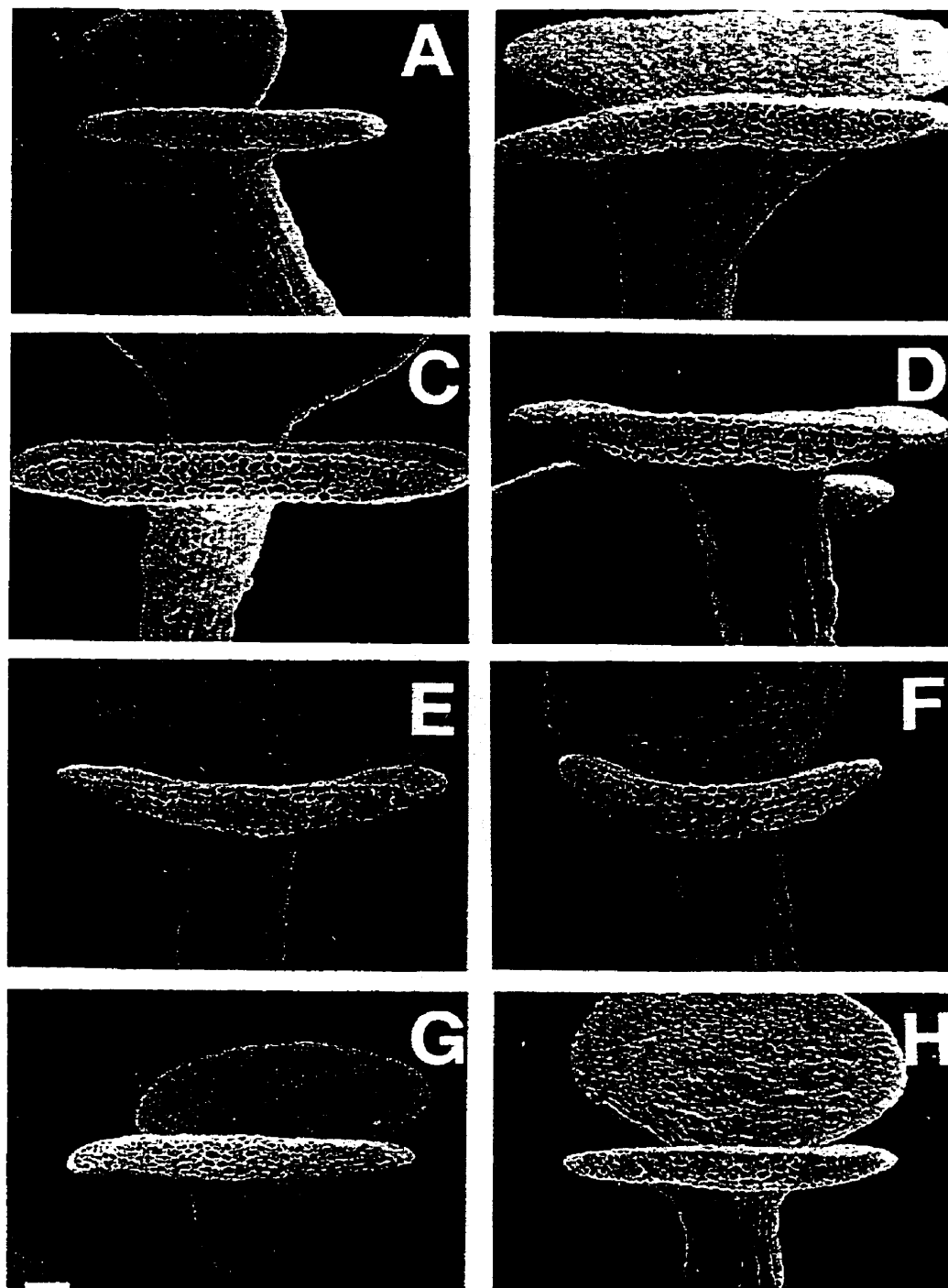


**Figure 2.3.** SEM of transverse freeze-fracture cross sections of 3-day old *Arabidopsis* cotyledons before and after exposure to monochromatic UV radiation followed by 24 h incubation in visible light. Seedlings that received only PAR are shown before (A) and after the 24 h incubation period (B). The wavelengths used for exposures were 320 nm (C), 313 nm (D), 300 nm (E), 290 nm (F), 280 nm (G) and 270 nm (H). The scale bar = 100  $\mu$ m.

Cotyledons were smaller than controls if seedlings were exposed to radiation < 320 nm. The upper epidermis of curled cotyledons (those exposed to 290 nm, 300 nm and 313 nm) appeared quite turgid indicating that the curling phenomenon was not a result of epidermal collapse (Figs. 2.4). This was further supported by the observation that curling was not observed in cotyledons exposed to 280 nm and 270 nm radiation, and in these plants the upper epidermis had collapsed (Figs. 2.4).

Changes in cotyledon growth were quantified by measuring cotyledon area, fresh weight and dry weight. During the 24 h incubation period the cotyledon area, fresh weight and dry weight of control seedlings increased approximately two fold (Fig. 2.5). The two longest wavelengths used (320 and 313 nm) had very little effect on increases in cotyledon area or fresh weight. However, exposure to wavelengths less than 313 nm significantly diminished cotyledon expansion and wavelengths less than 290 nm completely inhibited expansion (Fig. 2.5A). Similarly, fresh weight accumulation was modestly inhibited at short UV-B wavelengths, and fully inhibited by UV-C wavelengths (<290 nm) (Fig. 2.5B). Cotyledon dry weight accumulation, however, was inhibited to a similar degree at all UV wavelengths examined (Fig. 2.5C).

To determine if the effects induced by short-wave UV-B are observed at later stages of cotyledon expansion, 4-10 day old seedlings were exposed to a 100 min pulse of 290 nm radiation. Fresh and dry weight accumulation was measured after a subsequent 24 h exposure to PAR. In each case the accumulation of fresh weight and dry weight was inhibited by short-wave UV-B radiation (Fig. 2.6).

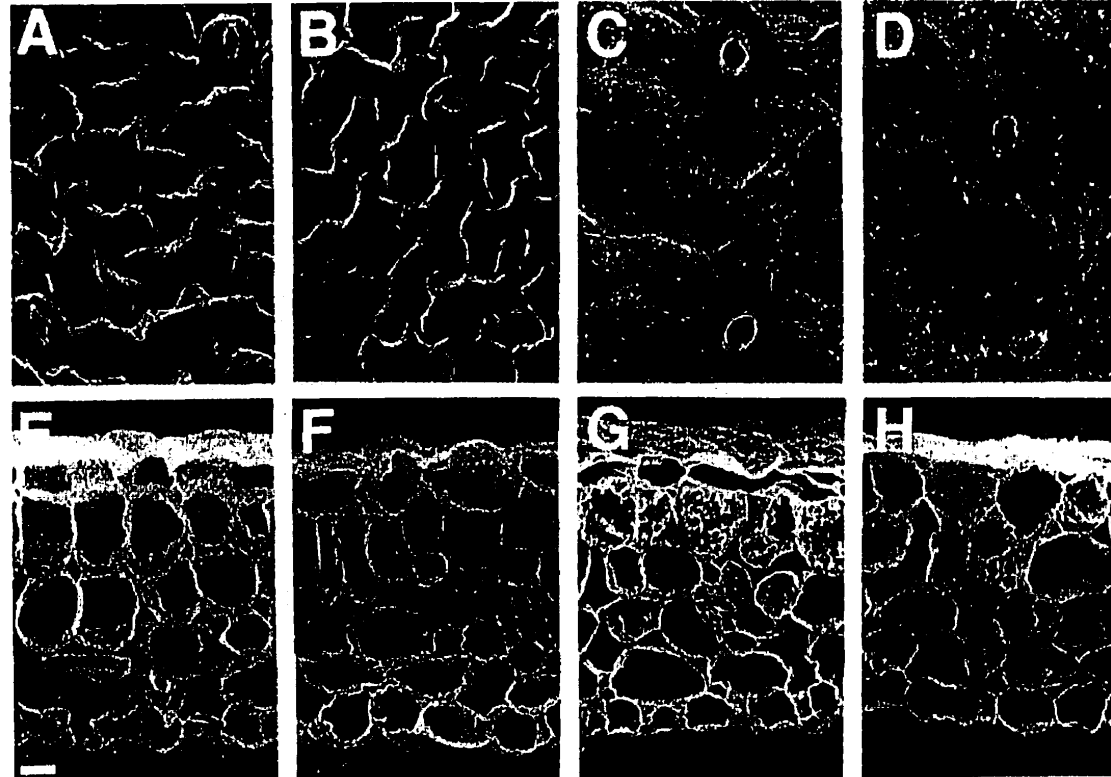


**Figure 2.4.** SEM of adaxial epidermal surface (A-D) and freeze fracture cross-section of cotyledons (E-H) from 3-day old *Arabidopsis* seedlings exposed to PAR and UV as in Fig. 2.3. Showing collapse of epidermal cells after exposure to short wavelength UV. The exposures shown are the PAR control (A, E), 290 nm (B, D), 280 nm (C, G) and 270 nm (D-H). The scale bar = 16  $\mu$ m.

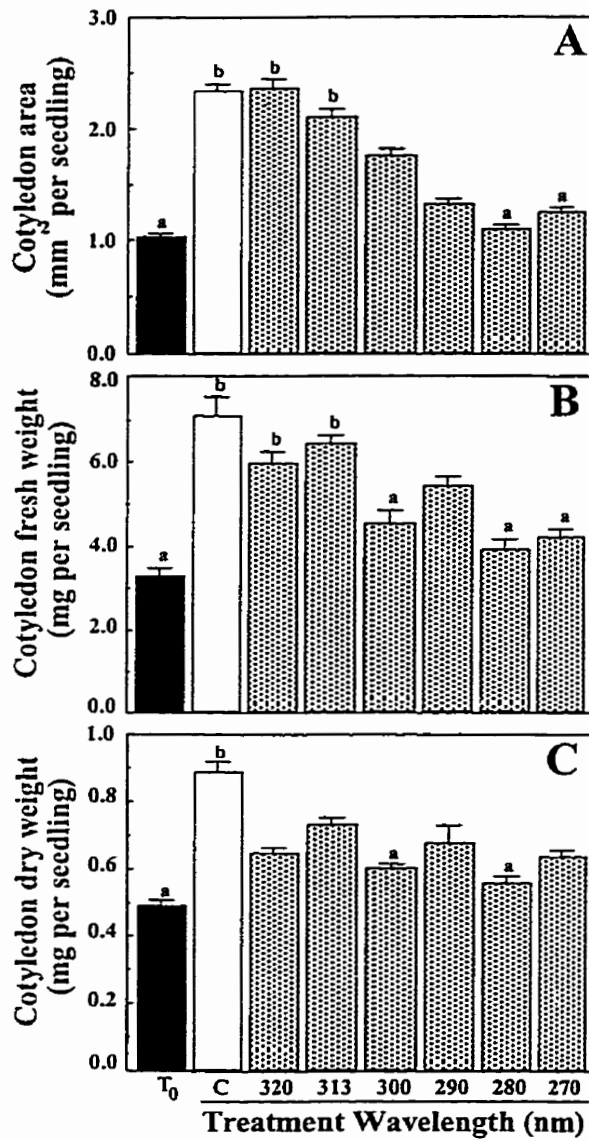


**Figure 2.5.** Growth of *Arabidopsis* cotyledons during 24 h incubation period after exposure to UV radiation ( $15 \text{ mmol m}^{-2}$ ). The area, A, fresh weight, B, and dry weight, C, of cotyledons from 4-day old seedlings were measured just before treatment ( $T_0$ ) and after exposure to a PAR control treatment (C) or particular wavelengths of UV followed by a 24 h incubation period for each treatment. Error bars represent the SE ( $n=40$ ). Within each graph, treatments that do not differ significantly ( $p<0.05$ ) from controls are labeled with the same letters.

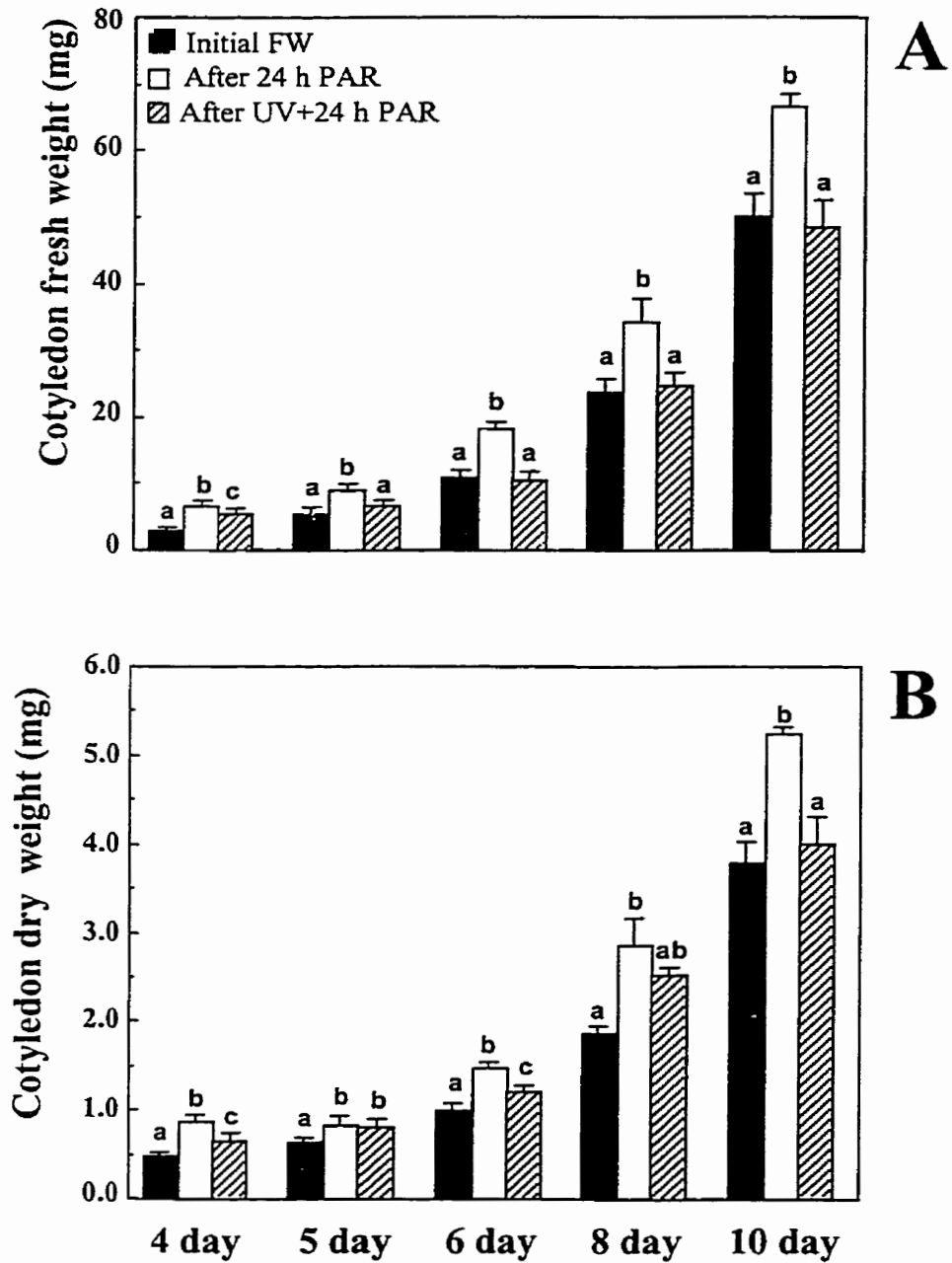


**Figure 2.6.** The effect of UV radiation on *Arabidopsis* cotyledons at different developmental stages. Growth of shoots from 4-10 day old seedlings after exposure to 290 nm radiation ( $15 \text{ mmol m}^{-2}$ ) and incubation for 24 h in PAR. Error bars represent the SE ( $n=40$ ). Within each graph, treatments that do not differ significantly ( $p<0.05$ ) are labeled with the same letters.

### 2.3.1.2 The effect of UV-B on cotyledon photosynthesis.

The physiological effects of UV-B radiation have been studied extensively. It has been shown that photosynthesis is sensitive to UV-B under many conditions (Bornman, 1989; Jansen et al, 1996). Chlorophyll<sub>a</sub> fluorescence induction was used to measure photosynthetic function in the cotyledons immediately after exposure to UV-B, and again at the end of the 24 h incubation period in PAR. In each case, there was a trend of decreasing  $F_v/F_M$  ratio as seedlings were exposed to shorter wavelengths (Table 2.1). The decreases were significant for 280 and 270 nm immediately after a 100 min UV exposure at any wavelength. However, after 24 h incubation cotyledons exposed to 290 nm radiation also had significantly lower  $F_v/F_M$  ratios than untreated seedlings.

To further characterize the impact of UV on photosynthetic capacity of *Arabidopsis* cotyledons photosynthetic pigments (chlorophyll and carotenoids) were analyzed. There were no significant changes immediately after any of the 100 min UV exposures. After the 24 h incubation in PAR, carotenoid and xanthophyll pigments were diminished at wavelengths less than 313 nm (Table 2.2). Chlorophyll concentrations showed a similar trend of decreasing at shorter UV wavelengths, however, decreases were only significant in seedlings exposed to UV-C wavelengths.



**Table 2.1.** Room temperature chlorophyll<sub>a</sub> fluorescence induction measurements (Fv/Fm) of 4 d old *A. thaliana* cotyledons taken immediately after exposure to UV-B treatment, or after 24 h incubation in WL following exposure to UV-B treatment.

	Control	320 nm	313 nm	300 nm	290 nm	280 nm	270 nm
0 h	.720 (0.03)	.686 (0.03)	.676 (0.03)	.699 (0.02)	.686 (0.02)	.583* (0.06)	.621*
24	.722 (0.02)	.719 (0.02)	.686 (0.05)	.711 (0.03)	.649 (0.04)	.402* (0.19)	.481*

The means of readings from 20 plants from two experiments are shown with the SE in brackets. Asterisks indicate difference from control is significant ( $p < 0.05$ ).

**Table 2.2.** Photosynthesis and UV-B-absorbing pigment concentrations in cotyledons from 4 d old *A. thaliana* sampled immediately after 24 h incubation in WL following exposure to UV-B treatment.

	Control	320 nm	313 nm	300 nm	290 nm	280 nm	270 nm
Chl a+b mg g <sup>-1</sup>	1.92 (0.07)	1.83 (0.12)	1.77 (0.12)	1.53 (0.08)	1.45 (0.11)	1.31* (0.01)	1.36* (0.03)
Chl a/b	3.05 (0.15)	2.99 (0.02)	2.89 (0.06)	2.77 (0.05)	2.63* (0.11)	2.68 (0.01)	2.74 (0.02)
C+X µg mg <sup>-1</sup>	306 (15)	298 (18)	288 (12)	234* (4.7)	231* (7.9)	212* (1.7)	218* (11)
A300 mg <sup>-1</sup>	82.0 (5.5)	79.2 (1.4)	88.5 (8.9)	129* (8.5)	105 (11)	117 (7.7)	109 (2.2)
A325/280	1.84 (0.06)	1.69 (0.09)	1.83 (0.04)	2.00 (0.02)	1.89 (0.08)	1.33* (0.01)	1.55 (0.05)

The means of readings from 20 plants are shown with the SE in brackets. Asterisks indicate difference from control is significant ( $p < 0.05$ ).

### **2.3.1.3 The accumulation of UV-screening pigments.**

*Arabidopsis* produces a variety of UV-B-absorbing compounds that include flavonoids and hydroxycinnamates. Some of these pigments accumulate in response to UV-B irradiation (Li et al, 1993; Lois, 1994; Landry et al, 1995). The peak effectiveness for induction of UV-B-absorbing compounds in 4-day old cotyledons was at 300 nm (Table 2.2). This corresponds to the peak in action spectra for induction of flavonoids in other plant species (Hashimoto et al, 1991; Ensminger, 1993). Hence, acclimation responses occurred in *Arabidopsis* cotyledons at wavelengths where UV-B effects on cellular expansion and photosynthesis were also apparent. In addition, some qualitative differences measured as a decrease in the A325/A280 ratio in UV-absorbance spectra of extracts from seedlings exposed to 280 nm radiation were observed. This indicates that specific UV-B-absorbing compounds were accumulating in response to only a 60 min exposure to UV-B.

### **2.3.2 The effect of UV-B on *Arabidopsis* photomorphological mutants**

One of the most widely reported responses of plants to UV-B radiation is the inhibition of hypocotyl elongation (Barnes et al, 1990). The identity of the photoreceptor(s) involved has not been established. A number of mutants lacking either phytochrome or cryptochrome were investigated to determine if these photoreceptors are required for this response. After germination for 7 days under control lighting which contained ten times less UV-B than treatment conditions, wild-type seedlings had elongated hypocotyls with an average length of 10.5 mm and expanded green cotyledons (Fig. 2.7). Seedlings germinated under UV-B treatment conditions, exhibited upward cotyledon curling, reduction of hypocotyl length (57%) and visibly diminished cotyledon expansion.

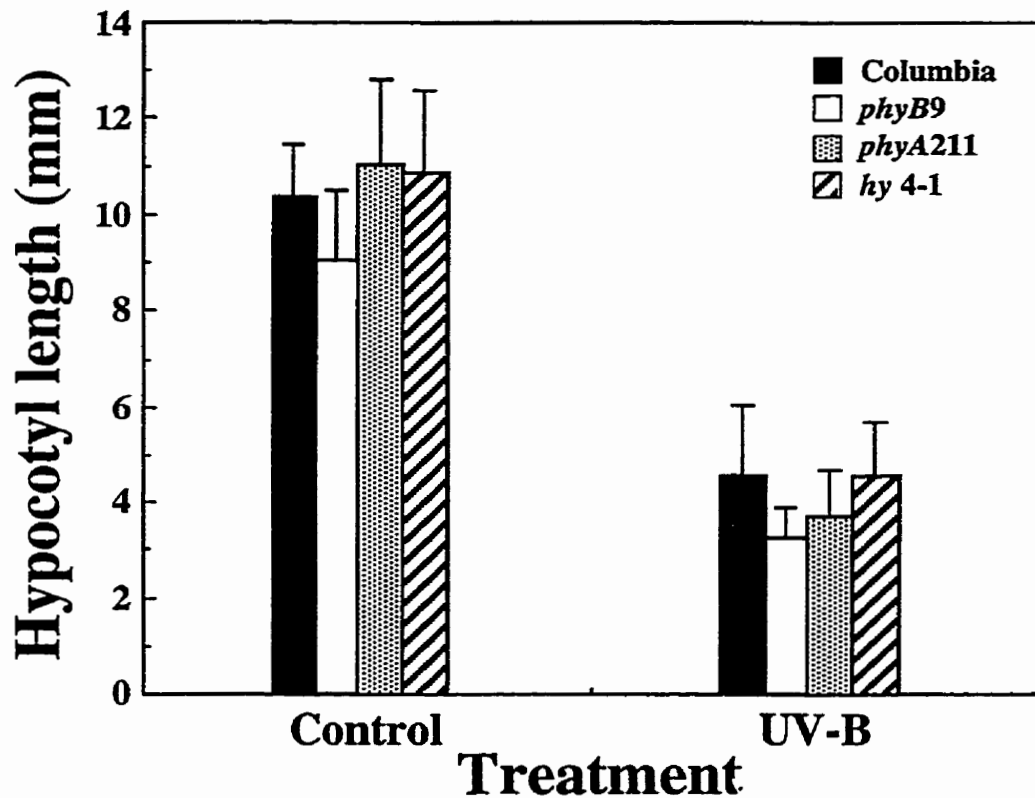


**Figure 2.7.** The effect of UV-B radiation on hypocotyl elongation of *Arabidopsis* photomorphology mutants. Plants that lack functional phytochrome B (*phyB9*), phytochrome A (*phyA211*) and cryptochrome (*hy4-1*) were compared to wild-type *Arabidopsis* (Columbia) after growth under continuous UV-B ( $14.6 \text{ kJ m}^{-2} \text{ d}^{-1} \text{ UV-B}_{\text{BE}}$ ) or control ( $0.02 \text{ kJ m}^{-2} \text{ d}^{-1} \text{ UV-B}_{\text{BE}}$ ) conditions for 14 days (see Fig. 2.1 for spectral distribution). Bars represent the mean of each treatment. Error bars represent the SE (n=40).

All of the mutants tested showed a similar pattern of growth inhibition of both hypocotyl and cotyledons. The three mutant lines also showed cotyledon curling in response to UV-B (data not shown). Thus, mutants lacking functional phytochrome A or B, or cryptochrome photoreceptors, exhibited normal responses to UV-B. This indicates there is a UV-B-specific photoreceptor that can operate independently of phytochrome A and B and cryptochrome photoreceptors.

### 2.3.3 Genetic analysis of a UV-B-resistant photosynthesis mutant of *Arabidopsis*

A population of mutant seedlings was generated using EMS. One mutant did not exhibit inhibited growth under UV-B, and was considered UV-B-tolerant. This mutant, which had pale green tissue throughout (Yg, yellow-green) and large flat leaves was analyzed further. The Yg mutant was transplanted into a separate pot, a mylar cone placed over it to shield the flowers from extraneous pollen, the plant was allowed to self-pollinate and set seeds. All the seeds were collected and pooled. A sample of the population (91 seeds) was sown in 6" pots and germinated for 2 weeks. Three tissue colour phenotypes were evident: wild-type green, yellow-green, and albino (Fig. 2.8).

A hypothesis was made that the yellow-green plants were heterozygotes and the albino a homozygous recessive. A  $\chi^2$  test showed the expected phenotypic ratio of 1:2:1 for green:yellow-green:albino was significant (Table 2.3). The presence of three phenotypes indicates this is not simply a case of a recessive gene mutation. It is a case of incomplete dominance such that a single copy of the gene does not provide sufficient levels of expression to produce a wild-type phenotype.  $F_M$  was diminished by almost half in the heterozygote mutant (Yg/+) compared to the wild-type, and by almost 90% in the albino (Yg/Yg) compared to the wild type (Table 2.4).

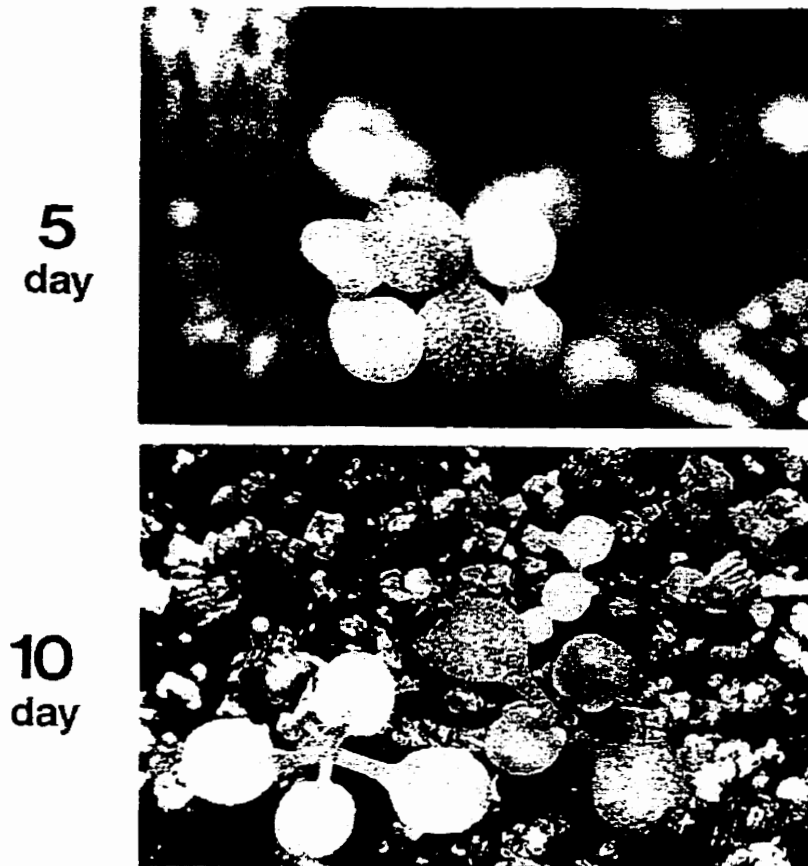


**Figure 2.8.** The phenotypes of the *Yg* chlorophyll mutants and wild-type *Arabidopsis* after 5 and 10 days growth under  $\sim 250 \mu\text{mol m}^{-2} \text{s}^{-1}$  PAR. From left to right the genotypes are heterozygous *Yg/+*, wild-type and homozygous albino. The scale bar represents 1 mm.

**Table 2.3.** Genetic analysis of seeds from a self-fertilized yellow-green mutant of *Arabidopsis*. Progeny in the subsequent generation were scored using phenotypic colour. The hypothesis tested was that a single gene mutation gives rise to an incomplete dominance phenotype that affects chlorophyll concentration. The expected phenotypic ratio for wild-type:yellow-green:albino is 1:2:1.

Cross	Generation	Total	Wild-type (%)	Yellow-green (%)	Albino (%)	$\chi^2$
<i>Yg/+</i> x <i>Yg/+</i>	F1	91	25	44	31	1.6

$\chi^2$  value indicates the observed deviation from the predicted segregation ratios. A value of <5.99 is acceptable ( $p > 0.05$ ).

**Table 2.4.** Room temperature chlorophyll<sub>a</sub> fluorescence induction measurements ( $F_v/F_M$ ) of cotyledons from 4-day old wild-type and yellow-green mutants. Measurements were taken after 30 minutes incubation in the dark.

	Control	Wild-type	Yellow-green	Albino
$F_v/F_M$	0.677 (2.1)	0.652 (2.2)	0.733 (4.4)	0.568 (11.9)

The means of readings from 3 plants are shown with % SE in brackets.

However,  $F_v/F_M$  was slightly higher (12%) in the heterozygote, and only slightly lower (13%) in the albino homozygote. 77K fluorescence spectra were collected to determine if one of the two photosystems is affected by the mutation. The spectra were very distinctive for each of the genotypes (Fig. 2.9). The peak at 680 nm, which originates from PSII, was present at very similar levels in all three genotypes. The peak at 730 nm, thought to originate from a light-harvesting chlorophyll of PSI, was present at approximately half the level observed in the wild-type, and completely absent in the albino mutant (McCormac et al., 1994). This indicates that PSI was selectively affected due to the mutation. More detailed analysis of this mutant is required to confirm the nature of the defect in PS I. This should include further spectroscopic measurements and analysis of the thylakoid proteins.

The identification of a photosynthesis mutant presents an opportunity to test whether the UV-B-induced curling described above (section 2.3.1.1) requires photosynthesis. When 4 d-old heterozygotes or albino homozygotes (*Yg/Yg*) are exposed to UV-B the cotyledons curled upwards (Fig. 2.10) to a level comparable to the controls (see Fig. 2.3E). This indicates that the mechanism of UV-B-induced curling does not act through photosynthesis and does not require photosynthetic activity. Because the phytochrome A and B, and cryptochrome mutants also exhibit normal curling, it can be concluded that this response likely requires only a UV-B photoreceptor.

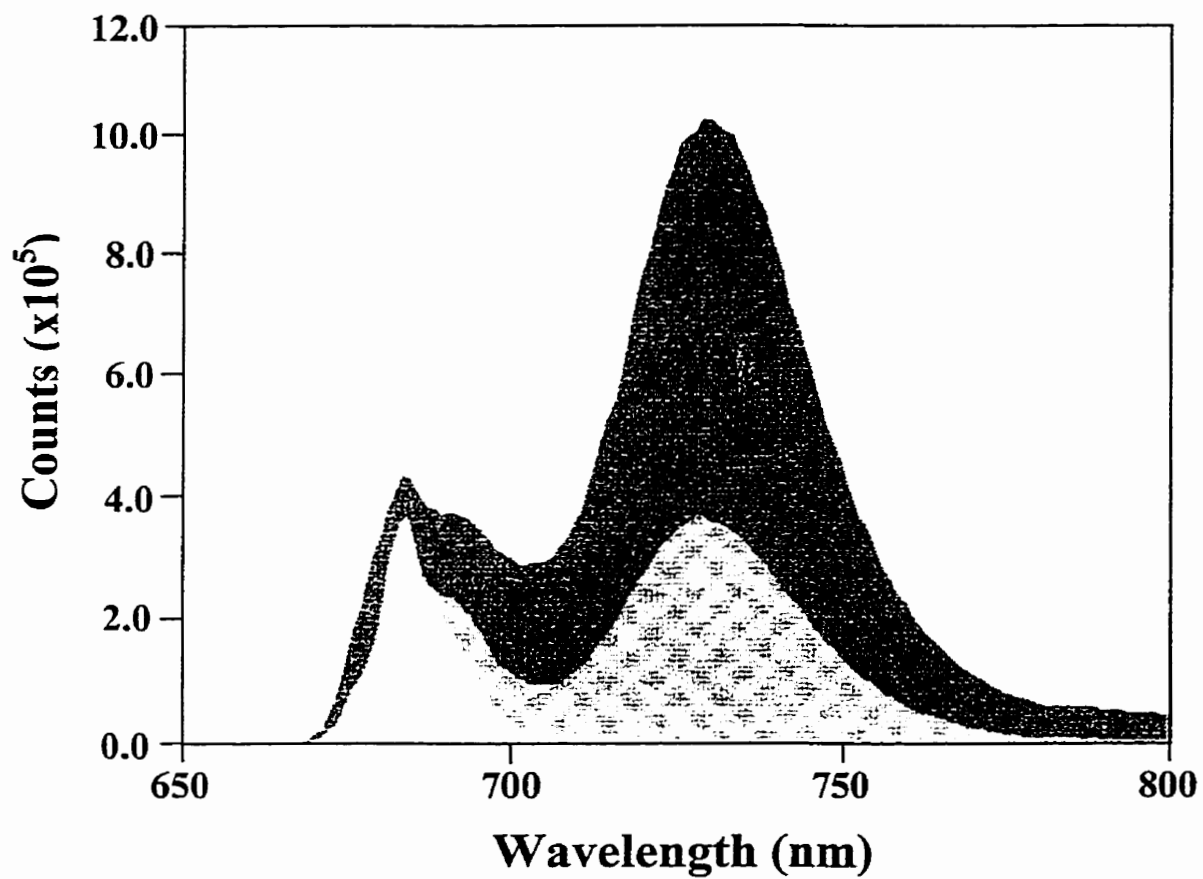


**Figure 2.9.** 77K chlorophyll fluorescence of wild-type *Arabidopsis* (▨), heterozygous *Yg* photosynthesis mutant (▩), and homozygous *Yg* mutant (▭). Fluorescence emissions were recorded as a function of wavelength between 650 and 800 nm using 450 nm  $\lambda_{ex}$  ( $\sim 40 \mu\text{mol m}^{-2}$ ).



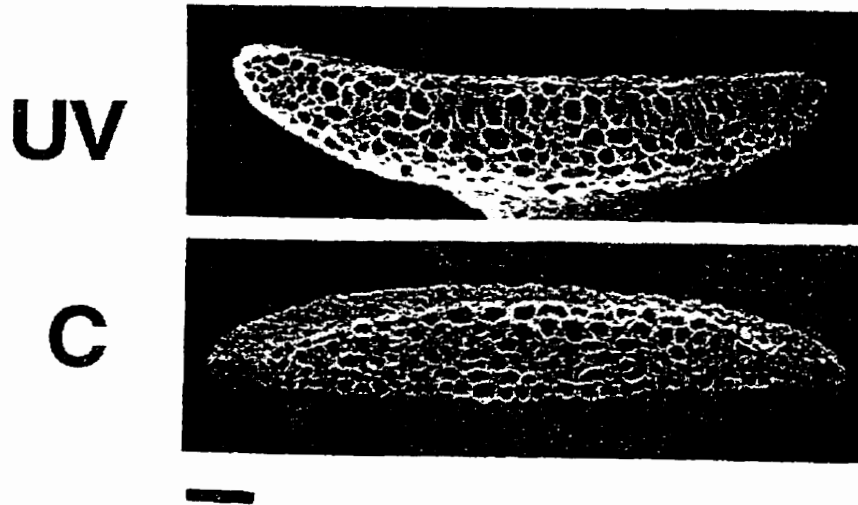


**Figure 2.10.** SEM of freeze-fractured cross-sections of 4-day old cotyledons from a homozygous *Yg* photosynthesis mutant of *Arabidopsis*. The morphology is of cotyledons is shown 24 h after 100 min exposure of the cotyledon to UV-B radiation (UV) or control lighting (C). The bar represents 0.1 mm.

## 2.4. DISCUSSION

### 2.4.1. Wavelength-dependant changes in *Arabidopsis* cotyledons

The effectiveness of specific UV-B wavelengths for inducing a number of morphological and biochemical changes in plants is of particular interest since seasonal and anthropogenic increases in UV radiation incident on the biosphere occur at the shortest UV wavelengths (Caldwell et al, 1989). This study was carried out to determine whether physiological and morphological changes observed in *Arabidopsis* seedlings could be separated on the basis of wavelength. A number of responses to UV-B were observed and almost all were wavelength-dependent. Those associated with development or acclimation had peaks at ~300 nm, and those associated with stress, increased significantly at wavelengths less than 290 nm. Short-wave UV-B radiation has striking effects on *Arabidopsis*. A relatively short exposure to 290 nm UV-B resulted in development of changes in cotyledon growth and morphology, including maximal upward curling. This UV-B-induced curling of cotyledons has been observed previously in *Arabidopsis*, *Brassica napus* and cotton (Ambler et al, 1975; Li et al, 1993; Wilson and Greenberg, 1993a; Landry et al, 1995), and presents an opportunity to study the mechanism by which UV-B affects plant cell growth and organ development. Moreover, the response is photomorphogenic in nature (Wilson and Greenberg, 1993b), which might allow characterization of the UV-B-photoreceptor(s). It is worthwhile considering the potential mechanism(s) behind this UV-induced change in morphology based on current knowledge of cotyledon growth.

The curling response may result from differential inhibition of cell expansion on the upper and lower epidermal layers. While a great deal is known about cell division and growth during expansion of true leaves in *Arabidopsis*, little is know about these changes in rapidly expanding cotyledons. During germination of *Arabidopsis*, cell division takes place early in

development of cotyledons and it is primarily associated with differentiation of stomatal guard cells (Wei et al, 1994). Expansion of epidermal pavement cells is quite dramatic in *Arabidopsis* cotyledons during the first five days of germination (Wei et al, 1994). Multiple replications of DNA by endoreduplication (endomitosis) occur in hypocotyl cells and may be related to the expansion of cells during elongation (Gendreau et al, 1997). A similar process may occur during cotyledon cell expansion. Leaf epidermal cells in a number of species, including *Arabidopsis*, are known to have high ploidy numbers (4n-32n), allowing these cells to attain a larger size (Melaragno et al, 1993). These cells are not multi-nucleated. Because the cell cycle can be delayed or arrested by UV-B radiation in plant cells, UV-B could conceivably affect the rates of endomitosis in epidermal cells and hence cell expansion (Logemann et al, 1995). One consequence of this would be to force the upper epidermal cells to maintain a smaller size and thus result in upward curling. Inhibited replication may occur directly as a result of UV-B-induced DNA damage, which must be repaired before chromosomal replication can occur, or indirectly as a result of UV-B-induced disruption of protein function.

It is also possible that there is a UV-B photoreceptor(s) that triggers the inhibition of cell growth. Evidence is accumulating that the UV-B photoreceptor(s) can trigger the production of active oxygen species, such as H<sub>2</sub>O<sub>2</sub>, which can act as a signal transduction molecules in plants and animals (Green and Fluhr, 1995; Horvath and Chua, 1996; Levine et al, 1996; Allan and Fluhr, 1997; Chamnongpol et al, 1998). In particular, the activity of an active oxygen-producing enzyme, NADPH-oxidase, and the concentration of H<sub>2</sub>O<sub>2</sub> have been reported to increase in *Arabidopsis* and tobacco, respectively, after exposure to UV-B (Rao et al, 1996; Allan and Fluhr, 1997). Increased cellular H<sub>2</sub>O<sub>2</sub> triggered by UV-B may inhibit DNA replication and hence endoreduplication, thus inhibiting cotyledon expansion. For instance, DNA replication in

mammalian cells undergoes long term arrest (>15 days) when exposed to H<sub>2</sub>O<sub>2</sub> (Chen et al, 1998). Indeed, recently it was found as part of this thesis research that externally applied H<sub>2</sub>O<sub>2</sub> induces cotyledon curling (see section 3.3.2).

The collapse of the upper epidermis of cotyledons exposed to UV-C wavelengths is similar to an effect of growth under continuous UV-B radiation for 10 days reported for cucumber (Tevini et al, 1983). The 280 nm and 270 nm wavelengths also correspond to the maximal effectiveness in the action spectra for inhibition of photosystem II (Table 2.1). As well, UV-C radiation is approximately 6 times more effective than 290 nm radiation in causing DNA damage in plants (Quaite et al, 1992). Damage to DNA has been shown to trigger programmed cell death in animal cells (Godar, 1996). While other forms of damage are also occurring simultaneously, it is possible that the collapsed epidermal cell layer observed after UV-C irradiation, is in part, a result of apoptosis, possibly through increased DNA damage, elevated cytosolic H<sub>2</sub>O<sub>2</sub>, or both (Conconi et al, 1996; Levine et al, 1996). Thus, where cotyledon curling occurs there may be a signal preventing cell expansion, but where epidermal collapse is observed there may be irreversible cellular damage. However, both processes may be triggered by active oxygen and/or DNA damage, with different targets dominating depending on the amount of UV radiation.

UV-B morphological responses like cotyledon curling do not seem to be dependent on the phytochrome or cryptochrome photoreceptors. The marked inhibition of hypocotyl elongation by UV-B was used as a marker to evaluate the role of plant photoreceptors and the phytohormone ethylene in UV-B photoreception and signal-transduction. Inhibition of hypocotyl elongation under UV-B was not affected in the phytochrome mutants *phyB9*, *phyA211*, and the

cryptochrome photoreceptor mutant *hy4-1*. Thus, inhibition of hypocotyl elongation and/or cotyledon curling by UV-B may not involve these photoreceptors.

Cotyledon curling could potentially result from an inhibition of photosynthesis by UV-B. However,  $F_v/F_M$  (maximal PSII activities) ratios were only significantly affected by UV-C and at these wavelengths curling was not observed. Moreover, the photosynthetic mutant of *Arabidopsis*, which lacks a functional PSI, still displayed cotyledon curling in response to UV-B (section 2.3.3). The general decrease in total Chl concentration and  $Chl_{a,b}$  ratios may be a result of molecular changes in thylakoid composition induced by UV-B. Reorganization of thylakoid membranes into shade-type morphology has been shown to occur within 30 minutes of exposure to UV-B (Fagerberg and Bornman, 1997). In particular, loss of PSII is possible, since UV-B promotes D1 and D2 degradation and has been shown to inhibit *psbA* gene expression potentially delaying replacement of the damaged PSII (Greenberg et al, 1989; Jordan et al, 1991; Jansen et al, 1996). This would lower chlorophyll concentration and change the chlorophyll ratios. Carotenoids and xanthophylls were affected by longer wavelengths of UV-B than chlorophyll. Hence, these compounds may be important indicators of UV-B-induced damage in photosynthetic membranes (Pfundel et al, 1992; Fagerberg and Bornman, 1997). As well, carotenoids may be consumed while protecting the plant by scavenging free radical molecules (Middleton and Teramura, 1993).

The inhibition of DW accumulation by all UV wavelengths was striking, since the amount of radiation used at 313 nm and 320 nm was 7-10 times less than is found in sunlight on clear summer days at temperate latitudes (Madronich et al, 1995). Decreases in accumulated DW likely represent a diminished  $CO_2$  assimilation. However, it is clear from this study that inhibition of PSII photosynthetic efficiency was not the mechanism through which long-wavelength UV-B

was acting. Lack of significant decreases in  $F_v/F_m$  during UV-B-induced loss of CO<sub>2</sub> assimilation has also been reported for mature pea leaves (Nogues and Baker, 1995).

The efficiency of photosynthesis makes it unlikely that loss of CO<sub>2</sub>-fixation would result from damage to photosynthetic reaction centers by solar UV-B. The capacity for increasing photosynthetic efficiency is evident from studies of photosynthetic *aurea* mutants of tobacco and other species, which are deficient in light harvesting protein II (LHCII), have 40-70% less chlorophyll per reaction center and a two-fold higher Chla/b ratio. However, these mutants have maximal photosynthesis rates that are 2-3 times higher than wild-type plants under high light conditions. Another key step in CO<sub>2</sub> assimilation is the incorporation of CO<sub>2</sub> into ribulose-1,5-bisphosphate, which is catalyzed by the chloroplast enzyme ribulose-1,5-bisphosphate carboxylase oxygenase (rubisco; E.C. 4.1.1.39). Although rubisco is considered to be a relatively inefficient enzyme because oxygen is able to compete with CO<sub>2</sub> for reaction with the substrate, chloroplasts appear to have a great capacity for carbon fixation (Andrews and Lorimer, 1987). This is evident from the observation that the concentration of rubisco in transgenic plants can be reduced to 40% of that in wild-type without observable changes in growth or CO<sub>2</sub>-fixation. Moreover, UV-B irradiation of rosette leaves of *Arabidopsis* ecotype Landsberg *erecta* did not have significant impact on rubisco activity or activation state (Rao and Ormrod, 1995a). Interestingly, although the levels of UV-B used by Rao and Ormrod were similar to those used in this study, there was no effect on dry weight accumulation in the leaves. This may indicate that carbohydrate metabolism in cotyledons is more sensitive to UV-B than leaves. Inhibition of dry weight accumulation has been reported to occur in cotyledons of other species exposed to UV-B (Takeuchi et al, 1989; Mark and Tevini, 1996). Moreover, it has been observed that rubisco from

several plant species is covalently crosslinked *in vivo* by exposure to UV-B (Wilson et al, 1995 and Chapter 5).

The total fluence of radiation used in this study at each wavelength ( $15 \text{ mmol m}^{-2}$ ) was very similar to maximum summer levels measured in temperate climates between 300-305 nm, and is less than that found between 310-315 nm (Kerr and McElroy, 1993). The sensitivity of dry weight accumulation and cotyledon expansion to the levels of 300 nm radiation used in this study may be particularly relevant since these levels of UV-B are already found at temperate latitudes and thus will increase with loss of ozone (Madronich et al, 1995). The wavelength dependence of plant responses to UV-B is especially relevant to experimental lighting conditions. The spectral distribution of sunlight is very difficult to simulate in the laboratory. In particular, the short-wave UV-B, which can have striking effects on plants, is often exaggerated in UV fluorescent lamps relative to sunlight.

The sensitivity of *Arabidopsis* to UV-B between 290-300 nm indicates that particular attention should be given to the amounts of radiation at these wavelengths used in experiments. The use of generalized plant action spectra for weighting spectral distributions is an essential tool for comparing differences in effectiveness of particular wavelengths. However, as has been pointed out previously, action spectra should be constructed for studying specific responses since most responses have different photoreceptors or absorbing chromophores (Caldwell, 1971). Extrapolation must be done with care as most action spectra have a minimum of a 10 nm bandwidth at any given wavelengths. It is nonetheless clear that the wavelength dependence of UV-B responses in plants must be considered when trying to interpret the environmental relevance of UV-B effects.

#### **2.4.2 The isolation of a photosynthetic mutant resistant to UV-B.**

The efficiency of photosynthesis is very apparent from the ability of chlorophyll deficient mutants to carry out carbon fixation at rates comparable to wild-type plants (Edwards et al, 1993). This capacity to maintain the high quantum yield of photosynthesis when chlorophyll concentrations are more than 50% lower may be a distinct advantage in the presence of UV-B. The carrier molecules of the photosynthetic electron transport chain can act as strong UV-B photosensitizers (Greenberg et al, 1989; Asada, 1993). In particular, plastoquinones can donate energy or electrons from a photo-excited triplet state to oxygen, producing singlet oxygen or superoxides, respectively. Indeed, UV-B irradiation appears to increase the concentration of superoxide in chloroplasts of *Arabidopsis* seedlings to the extent that the enzyme activities and metabolite concentrations of the ascorbate-glutathione cycle are significantly increased (Rao and Ormrod, 1995b).

Chlorophyll may also enter an excited triplet state and donate either energy or an electron to oxygen producing singlet oxygen or superoxide. Thus, diminished chlorophyll in the *yg* heterozygote may lower the potential of these targets of UV-B to produce singlet oxygen and/or superoxide. Indeed, one of the responses of UV-B irradiated wild-type plants is to down-regulate the expression of both of the main chlorophyll binding proteins LHCII and D1 and D2 (Jordan et al, 1991). Thus it is interesting that the *Yg* heterozygote was selected as a UV-B-resistant mutant.



### 3. THE PHOTOBIOLOGICAL BASIS OF UV-B-INDUCED COTYLEDON CURLING IN *Brassica napus* L.

#### 3.1 INTRODUCTION

There are a number of changes in plant growth resulting from exposure to UV-B. Plant height and leaf area are often affected in mature plants (Barnes et al, 1990; Sullivan et al, 1990). In younger plants, hypocotyl elongation is inhibited by UV-B (Steinmetz and Wellmann, 1986; Ballare et al, 1991a; Hodick and Kutschera, 1992). Other morphological responses to UV-B include coiling of etiolated sorghum internodes (Hashimoto et al, 1984; Hada et al, 1996), upward curling of *B. napus* cotyledons (Wilson and Greenberg, 1993b) and phototropic curvature in alfalfa (Baskin and Iino, 1987). In each case, the changes in photomorphogenic processes are initiated by UV-B absorbing chromophores.

A central question in photobiology is how absorbance of photons by a photoreceptor is translated into a biochemical or morphological change. This requires determining the identity of the primary photoreceptor for a given photobiological response. One way of obtaining information about the photoreceptor is to generate an action spectrum of the response (Hader and Tevini, 1987; Fankhauser and Chory, 1997). If a response is readily quantified and obeys the Bunsen-Roscoe law of reciprocity for photobiological responses, the action spectrum can be constructed (Coohill, 1989; Coohill, 1992). The law of reciprocity simply means that for each wavelength tested the extent of the response is proportional to the number of photons received by the photoreceptor, independent of how the photon rate or exposure time are varied (Hader and Tevini, 1987). Using this approach an approximation of the absorbance spectra of the photoreceptor can be made.

Action spectra have been constructed for UV-B inhibition of hypocotyl elongation (Steinmetz and Wellmann, 1986; Goto et al, 1993; Ballare et al, 1995a), coiling of sorghum internodes (Hashimoto et al, 1984; Hada et al, 1996), phototropism of alfalfa seedlings (Baskin and Iino, 1987), production of flavonoids (Wellmann et al, 1984; Beggs and Wellmann, 1985) and a variety of other UV-B responses in plants (see Ensminger, 1993 and references therein). Some of these responses have narrow developmental windows in which they are active. The induction of chalcone synthase gene expression by UV radiation in young *Arabidopsis* seedlings occurs only during some stages of germination (Kubasek et al, 1992). An example of a morphogenic response to UV that occurs in young seedlings is the upward curling of *B. napus* cotyledons (Wilson and Greenberg, 1993b). This response has been shown to obey the Bunsen-Roscoe law of reciprocity and can be quantified (Wilson and Greenberg, 1993b). Furthermore, cotyledon curling can be studied using light-grown seedlings, whereas many other studies require etiolated seedlings. Thus, it was of interest to construct an action spectrum for this response in order to understand the nature of the UV-B photoreceptor involved.

The expression of some genes are regulated by UV-B, for example chalcone synthase (EC 5.5.1.6; CHS) (Schulze-Lefert et al, 1989). The photoreceptors which initiate these changes act through signal-transduction pathways (Harter et al, 1994; Christie and Jenkins, 1996; Fuglevand et al, 1996; Allan and Fluhr, 1997). UV-B also triggers an increase in the production of active oxygen which may also act as a signaling mechanism within cells (Levine et al, 1994; Rao et al, 1996; Shirasu et al, 1996; Allan and Fluhr, 1997). The question of whether UV-B photoreceptors that trigger changes in morphology also act through signal-transduction pathways has only recently been addressed. The inhibition of hypocotyl elongation in cucumber seedlings does not occur if the cotyledon is shielded from the UV-B radiation (Ballare et al, 1991a).

Moreover, the application of phenylacetic acid or potassium iodide to tomato seedlings prevents inhibition of hypocotyl elongation by UV-B (Ballare et al, 1995a). The cotyledon curling response of UV-B irradiated *B. napus* is well suited for testing the effectiveness of compounds known to effect signal-transduction pathways. Using such an approach may lead to a better understanding of the mechanism underlying cotyledon curling. Thus, in this chapter an action spectrum for cotyledon curling was constructed to probe the nature of the chromophore. Additionally, modulators of signal-transduction were used to assess if a known signal-transduction pathway was involved.

## **3.2 MATERIALS AND METHODS**

### **3.2.1 Action spectrum for curling of *B. napus* cotyledons**

All experiments and data analyses were carried out as described in Wilson and Greenberg (1993) with the exception that the source of the monochromatic radiation was changed. Briefly, the following conditions were used. Seeds of *Brassica napus* cv Topas were planted in pots containing Pro-Mix potting media (Premier Brands, Rivière-du-Loup, Quebec) approximately 30 seeds per pot. They were germinated for at 22°C under 80  $\mu\text{mol m}^{-2} \text{s}^{-1}$  PAR from cool white fluorescent lamps (F40T12CW; General Electric Co., Wilmington, MA) using a 16 h light/8 h dark photoperiod in an environmentally controlled growth chamber. Lamps were screened with a polyester film (0.08 mm Mylar D) (Johnson Industrial Plastics, Missauga, ON) to shield out any extraneous UV-B or UV-C from the lamps. After 4 days seedlings were thinned by hand to 9 plants of similar cotyledon size and height and grown for another 24 h under the same conditions. After this period, individual pots of seedlings were exposed to monochromatic UV radiation (10 nm half-power bandwidth) for varying amounts of time. The apparatus used is

essentially as described in section 2.2.1, with the following changes. A mercury arc lamp (100W, Photon Technology Inc., South Brunswick, NJ) was used as the radiation source, and the radiation was passed directly through a monochromator (1200 gratings per mm; Photon Technology Inc., South Brunswick, NJ) with slitwidths set at 10 nm, and then into the exposure chamber (section 2.2.1). The fluence at the height of the cotyledons was set at the beginning of each exposure to be  $2.5 \mu\text{mol m}^{-2} \text{ s}^{-1}$  by adjusting the optical length from the lamp and the current flow through the arc lamp. The fluence was measured at the beginning and end of each exposure using a planar radiometer (Photodyne, Hollandschdiep, Netherlands). The spectral photon distributions and fluence rates of all light sources were measured using a calibrated spectroradiometer integrated continuously over the bandwidth of interest using a diode array detector (Oriel Inc., Stamford, Connecticut) (Greenberg et al, 1996). The seedlings were shielded from extraneous light during the exposure. Exposures were carried out from seconds to hours depending on the fluence required.

Immediately after the exposure the pot of seedlings was placed in a growth chamber at  $22^{\circ}\text{C}$  under  $80 \mu\text{mol m}^{-2} \text{ s}^{-1}$  PAR from cool white fluorescent lamps, for 24 hours. At the end of that period seedlings were removed and measurements made of the curling angle of cotyledons as described in Wilson and Greenberg (1993). Briefly, this involved taking three measurements of each cotyledon using vernier calipers in order to calculate the angle between the main vein and the edge of the cotyledon relative to a horizontal line through the main vein. The angle calculated was referred to as a curling angle for which negative angles indicate downward angled cotyledons and positive angles indicate upward angled cotyledons. This measurement was only carried out using the uppermost cotyledon of the pair. Data were collected for nine individual seedlings in each pot and each experiment was repeated at least once. The data were pooled from each

experiment and the mean values calculated. These values were plotted on semi-logarithmic axes. The relative effectiveness for three curling response levels (0°, 10° and 20°) was calculated as the reciprocal of the fluence required to elicit each of the response levels. The fluence value was obtained from the least squares regression between the points which span that range of the data. The fluence was then normalized to the wavelength with the smallest effective fluence. These values were plotted as a function of wavelength to give the action spectra (Coohill, 1989).

### 3.2.2 Effects of chemical agents on UV-B-induced cotyledon curling

The effect of each of the following compounds on cotyledon was assayed using the procedure described above (section 2.2.1.2). *cis*-4-cyclohexene-1,2-dicarboximide (CHDC), phenylacetic acid (PAA), indole-3-acetic acid (IAA), calcium ionophore A23187, N-(6-aminohexyl)-5-chloro-1-naphthalenesulfonamide (W-7), trifluoperazine (TFP), 8-(N,N-diethylamino)-octyl-3,4,5-trimethoxybenzoate-HCl (TMB-8), calcium and potassium channels blocker nifedipine (1,4-dihydropyridine-type), imidazole, hydrogen peroxide, ascorbate, glutathione ( $\gamma$ -glutamyl-cysteinyl-glycine ; reduced), L-cysteine, L-cystine, N-acetylcysteine and taxol (Sigma Chemical Co, St. Louis, MI). The concentrations used are indicated in Table 3.1. Each assay was carried out using an exposure of 60 minutes to  $2.5 \mu\text{mol m}^{-2} \text{s}^{-1}$  of 290 nm radiation followed by 24 h incubation in  $80 \mu\text{mol m}^{-2} \text{s}^{-1}$  PAR. Compounds were dissolved in water, the adjusted to pH 5.5 with 10 mM HCl. Triton X-100 (Sigma Chemical Co, St. Louis, MI) was added to a final concentration of 0.01%. The solutions were applied to the upper surface of the cotyledons 1 hour before exposure to UV-B. No measurement of cellular uptake efficiencies were made. Each assay was carried out with a pot of 9 treated seedlings and a pot of control seedlings which received an application of 0.01% triton X-100 pH 5.5 and were not exposed to

UV-B. Measurement of cotyledon curling was done as described above (section 2.2.4). Each assay was carried out twice. All compounds tested were obtained from Sigma Chemical Co (St. Louis, MI) with the exception of *cis*-4-cyclohexene-1,2-dicarboximide (CHDC) which was a gift from Dr. J.D. Bewley.

### 3.3 RESULTS

#### 3.3.1 Action spectrum for curling of *B. napus* cotyledons

The cotyledon curling response of *B. napus* cv Topas to UV radiation varied with wavelength in the UV bandwidth. The unexposed cotyledons had an average curling angle of  $-23.9^\circ$  ( $\pm 5.4^\circ$ ), where negative angles signify downward curling. Each UV-B wavelength tested was effective for inducing the cotyledon curling response, with the exception of 310 nm (Fig. 3.1). There was a measurable threshold for initiation of cotyledon curling for 280 to 305 nm, in that the low fluences used did not result in increased curling angles. In each case, the maximum curling response was reached within an order of magnitude of the threshold fluence level. The curling response became saturated and curling declined at higher fluences as previously observed (Wilson and Greenberg, 1993b) (data not shown). This aspect of the action spectra was not investigated further in this study.

The rise in the fluence-response curve was used in the calculation of the action spectrum (Fig. 3.2). The amount of radiation at each wavelength that is required for cotyledons to reach a curling angle of  $0^\circ$ ,  $10^\circ$  or  $20^\circ$  was calculated.

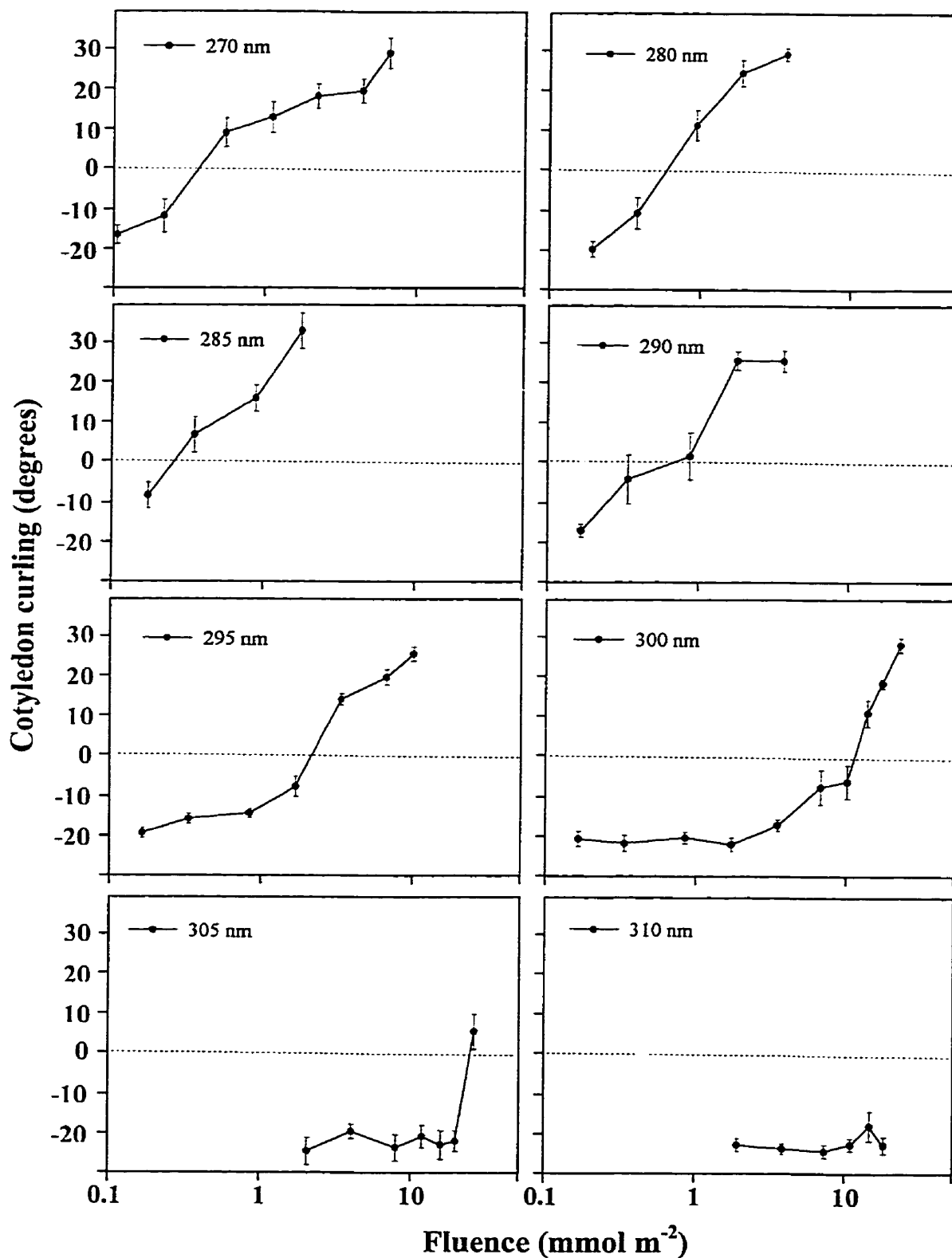
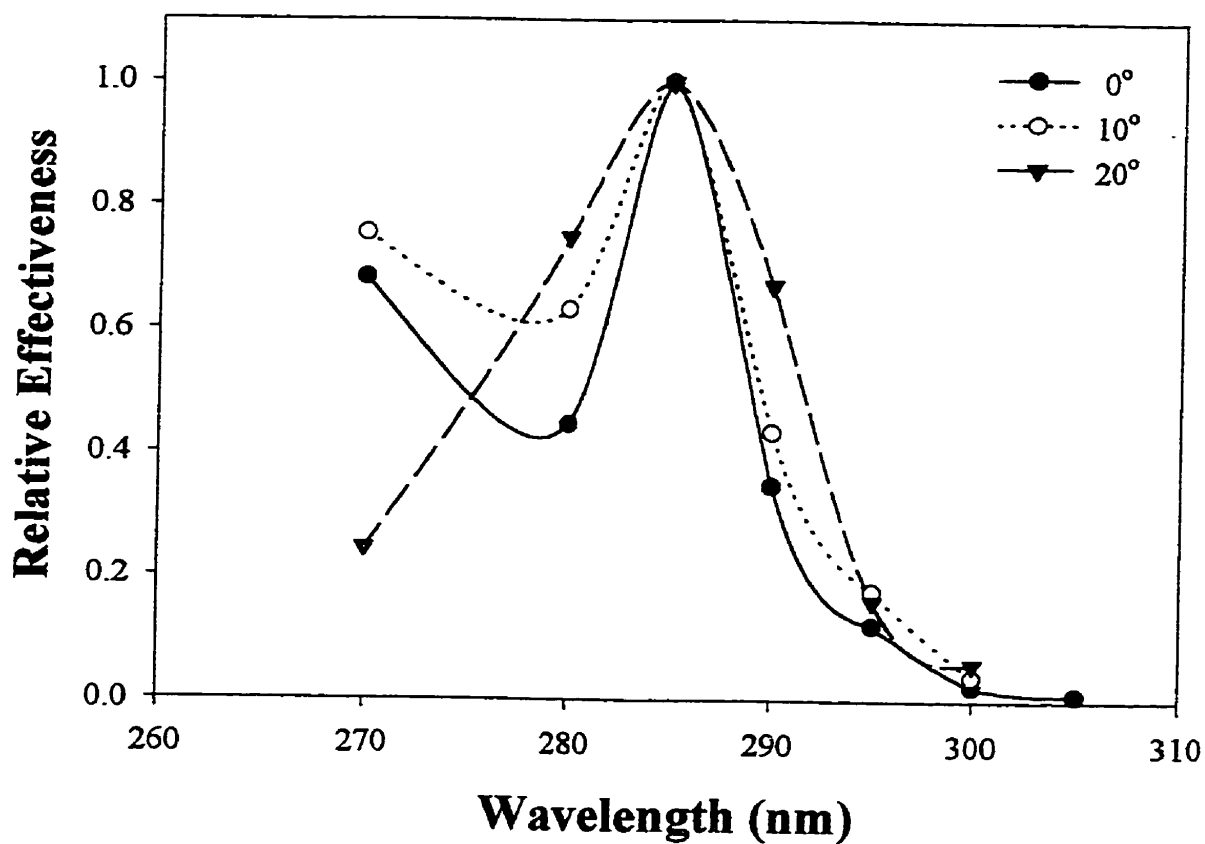


Figure 3.1. Fluence-response curves for cotyledon curling response of *B. napus* L. cv Topas. Error bars show SE (n=18).



**Figure 3.2.** The UV action spectra for cotyledon curling response of *B. napus* L. cv. Topas. Ordinate gives the reciprocal of the photon fluence required to give a curling response of 0° (●), 10° (○) and 20° (▼), normalized to the peak effectiveness, which was 285 nm in each case.



Each group of fluence values was normalized relative to the most effective wavelength, and the values were expressed as reciprocals. This gave the peak wavelength for curling to 0°, 10° and 20° was a value of 1.0 in all cases. The threshold fluences for each curling angle were lowest for 285 nm. The fluences of 285 nm radiation which cotyledons required to reach 0°, 10° or 20° were 0.2, 0.4 and 0.7 mmol m<sup>-2</sup>, respectively. As the wavelength increased the effectiveness decreased rapidly, for example, 10 times more 295 nm radiation was required for cotyledons to reach a 0° curling than 285 nm radiation. The effectiveness also decreases between 285 and 280 nm and then rises from 280 to 270 nm in the case of 0° and 10° spectra. However, 270 nm radiation was much less effective for producing 20° curling than for 0° or 10° curling. Also, the action spectrum for 20° curling is broader, in general than, for 0° or 10°. The peak of the action spectra, at 285 nm, is suggestive of the absorption spectrum of tryptophan residues in proteins (Kirschenbaum, 1972). The increase in the effectiveness at 270 nm suggests that DNA may also act as a photoreceptor for curling in the UV-C. However, the predominant photoreceptor for curling is clearly not DNA since the effectiveness at 270 nm would be expected to be substantially higher than the effectiveness at 285 nm based on absorbance of DNA and the action spectrum for DNA damage in plants (Quaite et al, 1992).

### **3.3.2 Some effects of chemical agents on UV-B-induced cotyledon curling**

The compounds used could be placed in five categories based on their mode of action: cell growth effectors, signal-transduction effectors, antioxidants, reductants/oxidants and targeted effectors. Some compounds like phenylacetic acid and quercetin could be placed in more than one category. Growth effectors tested were the auxin hormones phenylacetic acid (PAA) and indole-3-acetic acid (IAA), and *cis*-4-cyclohexene-1,2-dicarboximide (CHDC), which inhibits

phytochrome-induced hypocotyl elongation and cotyledon expansion (Stewart and Bewley, 1990). Many of the signal-transduction effectors used targeted components of the calcium signaling pathways. These included the calcium ionophore A23187, calmodulin antagonists N-(6-aminohexyl)-5-chloro-1-naphthalenesulfonamide (W-7) and trifluoperazine (TFP), the permeable calcium chelator, 8-(N,N-diethylamino)-octyl-3,4,5-trimethoxybenzoate-HCl (TMB-8), and the L-type calcium and potassium channels blocker nifedipine (1,4-dihydropyridine-type). In addition, imidazole, which activates phosphodiesterases, was used to determine if signaling *via* cyclic mononucleotides (cNMP) cAMP or cGMP was involved.

Hydrogen peroxide which can act as either a signaling molecule or an oxidant, was also tested for initiation of curling (Alvarez et al, 1998). Because of the potential for UV-B to generate oxidants within the cell (Rao et al, 1996; Allan and Fluhr, 1997; Masaki and Sakurai, 1997; Brenneisen et al, 1998) antioxidants were applied to cotyledons. These antioxidants used were ascorbate (Conklin et al, 1996) and glutathione ( $\gamma$ -glutamyl-cysteinyl-glycine) (reduced) (Rao and Ormrod, 1995b). The reductants L-cysteine, L-cystine, and N-acetylcysteine were also used to determine if oxidation of sulfhydryls might be involved in signal transduction as is the case with some receptor tyrosine kinases (Knebel et al, 1996). Finally, since UV-B effects assembly of microtubules (Zamansky et al, 1991), taxol was applied to cotyledons to stabilize polymerized microtubules in case the UV-B effect involves changes in the cytoskeletal organization..

After the incubation period, the control plants had cotyledons which curled downward ( $-13^\circ$ ) with PAR exposure and upwards ( $24^\circ$ ) with UV-B exposure. The effects of the above compounds are listed in Table 3.1. Of the growth effectors, the auxins PAA and IAA had the most dramatic effects on cotyledon curling. Application to the upper epidermis enhanced downward curling with or without exposure to UV-B relative to controls.

**Table 3.1.** Some effects of compounds that affect growth, signal-transduction and redox status on cotyledon curling in *Brassica napus*.

<u>Type</u>	<u>Compound</u>	<u>Concentration</u>	<u>Curling Angle (degrees)</u>		<u>Effect</u>
			<u>PAR</u>	<u>UV-B</u>	
	Control		-13.2 ● 2.3	24.5± 2.8	
Growth	IAA	6 μM	Epinasty	Epinasty	-
Effectors	PAA	10 mM	-26.2 ± 1.6	-16.3 ± 3.3	-
	CHDC	10 mM	-12.5 ± 4.0	-13.0 ± 2.2	-
Ca <sup>2+</sup> -chelator	TMB-8	10 μM	-14.5 ± 2.4	23.5 ± 2.1	None
Ca <sup>2+</sup> -channel	Nifedipine	10 μM	-0.5 ± 4.1	28.3 ± 3.1	+
Ca <sup>2+</sup> ionophore	A23187	10 μM	12.5 ± 1.8	6.9 ± 6.8	+ -
Calmodulin	W7	10 μM	13.4 ± 5.2	-9.32 ± 4.0	- +
antagonists	TFP	10 mM	27.4 ± 2.9	18.9 ± 7.1	+
cAMP	Imidazole	10 mM	-23.8 ± 2.1	-14.1 ± 4.4	-
	H <sub>2</sub> O <sub>2</sub>	88 mM	29.9 ± 3.9	N.D.	+
Free radical	Ascorbate	50 mM	3.8 ± 5.1	12.1 ± 5.0	●
Scavengers	GSH	10 mM	-4.3 ± 4.2	26.7 ± 3.5	None
Reductants	L-cysteine	50 mM	-15.2 ± 2.3	26.2 ± 3.0	None
	L-cystine	1 mM	-11.3 ± 8.0	15.3 ± 7.6	None
Microtubule	Taxol	10 μM	-19.9 ± 1.9	25.0 ± 3.1	None

IAA-treated cotyledons became extremely rolled under (epinasty) in both cases by the end of the incubation period. This indicates, importantly, that even after UV-B irradiation, the upper epidermis of the cotyledon has a large capacity to expand. The CHDC pre-treatment blocked the UV-B-induced curling but did not affect the unexposed controls. This compound increases auxin regulated cell expansion and blocks phytochrome regulated growth responses. Since it was shown that phytochrome A and B are not involved in cotyledon curling (ref. section 2.3.2), it is assumed to be related to its auxin effect. CHDC may potentially be compensating for a loss of IAA by increasing the sensitivity of the tissue to IAA.

Of the calcium effectors, the ionophore A23187 and the two calmodulin antagonists W7 and TFP, induced upward curling in the control plants to a greater extent than in the UV-B exposed plants. UV-B was less effective in inhibiting TFP-induced curling. The calcium and potassium channel-blocker nifedipine only increased upward curling in PAR. These results may indicate that a signal-transduction pathway involving intracellular calcium may play a role in cotyledon curling. The phosphodiesterase activator imidazole also promoted downward curling in both UV-B and PAR. Hence, calcium and cyclic nucleotides have roles in the transduction pathway for cotyledon curling.

Hydrogen peroxide induced cotyledon curling in the absence of UV-B (Table 3.1 and Fig. 3.3A). It was effective at 88 mM and could not be blocked by 10 mM imidazole or 500 mM NAC. However, 10 mM PAA did prevent H<sub>2</sub>O<sub>2</sub>-induced curling. UV-B absorbing compounds increased 30% (per mg tissue fresh weight) above control levels after exposure to 290 nm radiation. However, H<sub>2</sub>O<sub>2</sub> treatments did not result in higher levels of UV-B-absorbing compounds (Fig. 3.3 B).

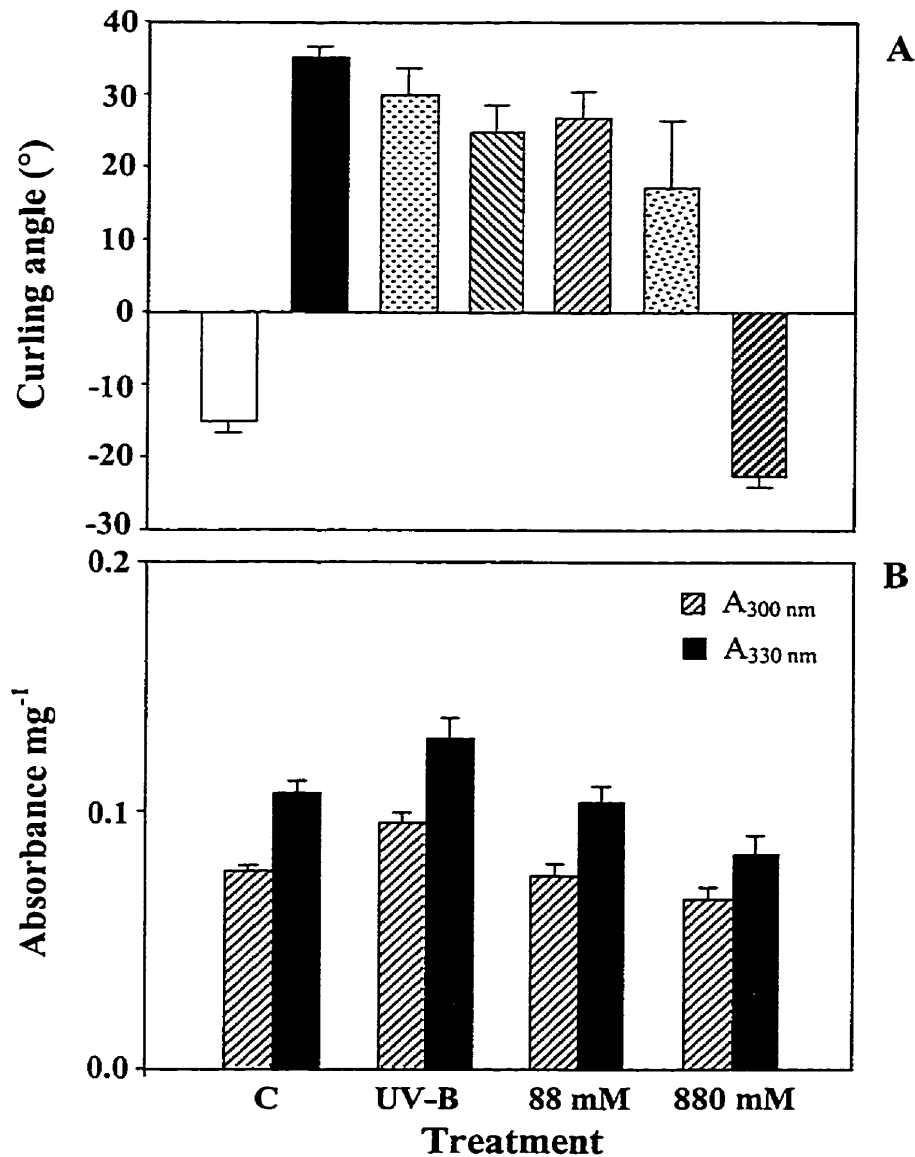


**Figure 3.3.** A, the degree of cotyledon curling after treatment of intact *B. napus* cotyledons with H<sub>2</sub>O<sub>2</sub>. The cotyledon curling angle of control plants (□) was compared to cotyledons treated with 0.88 M H<sub>2</sub>O<sub>2</sub> (■), 88 mM H<sub>2</sub>O<sub>2</sub> (▨), and 10 mmol m<sup>-2</sup> of 290 nm radiation (▩). The effects of the curling inhibitor imidazole (10mM) (▧), and also the free radical scavenger NAC (0.5 M) (▦) on H<sub>2</sub>O<sub>2</sub>-induced curling were tested. To determine if cotyledon expansion is irreversibly effected by H<sub>2</sub>O<sub>2</sub>, PAA (10 mM) was applied to the cotyledons after H<sub>2</sub>O<sub>2</sub> treatment (▨). B, the effect of H<sub>2</sub>O<sub>2</sub> on the accumulation of UV-B-absorbing compounds in cotyledons of *B. napus*. UV-absorbing compounds were extracted into 80% MeOH from untreated cotyledons (C), cotyledons exposed to 10 mmol m<sup>-2</sup> 290 nm radiation (UV-B), treated with 88 mM H<sub>2</sub>O<sub>2</sub> or 880 mM H<sub>2</sub>O<sub>2</sub>. Concentrations expressed as absorbance mg<sup>-1</sup> tissue fresh weight. Error bars indicate the SE (n=20).

During this same time cotyledons had curled. Cotyledons treated with 880 mM H<sub>2</sub>O<sub>2</sub> had slightly lower levels of UV-B-absorbing compounds and were also curled at the end of the incubation period. Hence, H<sub>2</sub>O<sub>2</sub> may act as a signaling molecule that is specific for morphological responses to UV-B. The data imply that IAA can overcome the affect of UV-B and be acting as a UV-B photoreceptor, also that signal-transduction may involve calcium, cNMP and active oxygen.

The antioxidants ascorbate and glutathione, promoted a slight increase in the curling angle of control plants, but only ascorbate inhibited UV-B-induced curling. Since ascorbate affected both control and UV-B treated cotyledons it may have a non-specific effect on cotyledon curling. None of the reductants or taxol showed any effects on cotyledon curling.

#### 3.4. DISCUSSION

In this chapter the UV-B-specific cotyledon curling response was employed to probe the UV-B photoreceptor and signal-transduction pathway. The action spectrum showed a single peak at 285 nm with a rise at 270 nm. Application of biochemical effectors indicated that a signal-transduction pathway may be present. In particular, effectors of calcium and cyclic nucleotide metabolism, as well as H<sub>2</sub>O<sub>2</sub> were all shown to affect curling. The application of auxins showed that UV-B exposure did not damage the capacity of cotyledons to expand. It is also clear that cotyledons are very responsive to IAA, raising the possibility that photodestruction of endogenous cotyledon IAA may be involved in the UV-B response.

In general, two types of plant responses to UV-B have been studied using action spectroscopy, those that result in increases in the amount of UV-B absorbing compounds like flavonoids, and those that result in morphological changes. The action spectra for those which

initiate accumulation of flavonoids or anthocyanins, have peaks between 290 and 300 nm (Ensminger, 1993). The action spectra for UV-B induced morphological changes have generally have broad plateaus which slope up toward 260 nm, implicating DNA damage as a basis for the change (Ensminger, 1993). There is one notable exception is the base curvature in oat seedlings, where the action spectra had no indication of DNA effects and had a peak at 295 nm (Curry et al, 1956).

The action spectrum for cotyledon curling has a number of characteristics shared by other photomorphological responses. The rise from 300 nm found here for curling was also observed for base curvature of oat seedlings (Curry et al, 1956), growth inhibition in cress seedlings (Steinmetz and Wellmann, 1986), sorghum stem coiling (Hashimoto et al, 1984), and inhibition of hypocotyl elongation in tomato (Ballare et al, 1995a). Action spectra for these responses either drop off after a peak near 290 nm (Curry et al, 1956), or they continue to rise past 290 nm but along a gentler slope (Hashimoto et al, 1984; Steinmetz and Wellmann, 1986). Nonetheless, the action spectrum for cotyledon curling is characteristic of UV-B photomorphological responses and is likely triggered by a photoreceptor common to other UV-B responses.

There was a small rise at 270 nm for 0° and 10° curling, which was not present for 20° curling. The peak absorbance of DNA (260 nm) is very near 270 nm. Perhaps at the higher fluences of 270 nm required for 20° curling, DNA was damaged to such an extent that cotyledon growth was inhibited (Fig. 2.3 and 2.4 section 2.3.1.1), resulting in a loss of curling at 270 nm.

When analyzing the action spectra of cotyledon curling the absorbance of epidermal compounds that might shield the photoreceptor should be considered. The epidermal transmittance properties of greater than 40 species have been measured in the 280-300 nm

spectral region *in situ*, using fibre optic spectroscopy (Day et al, 1994). In general, the epidermal transmittance rises only 10% from 280 to 300 nm and plateaus at 300 nm. The decrease in epidermal transmittance from 285 to 280 nm is likely to be no more than 5%. This would not account for the 25-60% drop in effectiveness observed for cotyledon curling over this interval. Nor does it account for the large drop in curling from 285 to 300 nm. Therefore, the action spectrum shape should be primarily due to the photoreceptor.

The stem-coiling response of etiolated sorghum seedlings exposed to UV-B (Hashimoto et al, 1991) has an action spectrum similar to cotyledon curling inasmuch as 285 nm is more effective than 290 nm in both cases. However, the stem-coiling action spectra does not have a well defined peak at 285 nm and the effectiveness of 270 nm was almost twice as effective as 285 nm in the case of stem-coiling (Hashimoto et al, 1991). Increasing effectiveness in this region indicates the response results from DNA damage. A fundamental difference between the experiments is that etiolated seedlings were used here to study stem-coiling, whereas light-grown seedlings were used here to study cotyledon curling. It is quite likely that light-grown seedlings have much better protection against DNA damage than cotyledons. For instance, accumulation of UV-B-absorbing compounds is light dependent and hence, light-grown cotyledons will have a generally higher level of UV-shielding than etiolated seedlings. It is also known that expression of DNA repair enzymes, like DNA photolyase, are up-regulated by light (Ahmad et al, 1997). Thus, the action spectra for these two responses can be assumed to be very similar if green cotyledons are considered to be less sensitive to DNA damage. Perhaps the peak at 285 nm for cotyledon curling is masked in etiolated sorghum by a higher level of DNA damage.

The photoreceptor at 285 nm is very similar to other UV-B responses. Action spectra for the induction of phenylpropanoid accumulation or expression of phenylpropanoid enzymes



such as chalcone synthase invariably have a peak effectiveness is between 290 and 300 nm with 280 nm being less effective (Ensminger, 1993). This is also observed in *Arabidopsis* as shown above (section 2.3.1.3). The wavelengths used in these studies were such that a peak at 285 nm could have been missed.

The location of a single peak at 285 nm in the action spectra for cotyledon is suggestive of an indole type of photoreceptor (Hader and Tevini, 1987). Two possibilities photoreceptors of this type are the plant growth hormone, IAA Ros and Tevini, 1995), and tryptophan residues of protein (MacLaren and Waldt, 1952; Kim et al, 1992). In the case of IAA its action has been proposed to result from irreversible photodestruction and formation of a biologically active product (Ros and Tevini, 1995).

Proteins can undergo a number of changes resulting from UV-B radiation which might give rise to a transducible signal. In all cases the UV-B photoreceptor in protein is assumed to be a tryptophan residue since other residues do not absorb wavelengths >290 nm (McLaren and Shugar, 1964). The strongest evidence for the role of tryptophans as UV-B photoreceptors is that one of the tryptophans in DNA photolyase (W277) has been shown to act as the UV-B photoreceptor at the active site of DNA photolyase (Kim et al, 1992). It carries out photosensitized repair of cyclobutane thymidine dimers. This is an example of how proteins can act directly as UV-B photoreceptors without being irreversibly damaged. There are also numerous examples of how proteins can be irreversibly photomodified by UV-B through irreversible photooxidation of tryptophan residues (Pirie, 1971; Tallmadge and Borkman, 1990; Borkman and McLaughlin, 1995; Wilson et al, 1995; Andley et al, 1997). Finally, it has been found that irradiation of proteins with UV-B results in generation of active oxygen species such as H<sub>2</sub>O<sub>2</sub> (Andley and Clark, 1989a). This can give rise to general lipid and/or protein oxidation

(Kochevar, 1990; Landry et al, 1995). Further, the active oxygen species generated by UV-B irradiation appear to mediate a number of UV-B responses in animals and plants (Schieven et al, 1994; Adler et al, 1995; Green and Fluhr, 1995; Allan and Fluhr, 1997; Bender et al, 1997; Huang et al, 1996; Shimmura et al, 1996; Huang et al, 1997; Brenneisen et al, 1998). Hence, UV-B-irradiation of proteins can give rise to a number of potential signals which could be transduced. Whether any of these pathways regulate cotyledon morphology remains to be determined.

The pretreatment of cotyledons with the growth-promoting hormone IAA (6  $\mu$ M) demonstrated that the upper epidermis of UV-B-treated cotyledons still has a great capacity to expand. The epinasty (extremem downward curling) induced by IAA has been reported to occur in tobacco leaves (Keller and Van Volkenburg, 1997). Cotyledons may be especially sensitive to IAA since they are in a stage of rapid cell expansion. This raises the question of whether photodestruction of endogenous IAA could form the basis of UV-B-induced growth inhibition. IAA is pleiotropic and has many effects on cells. The role of IAA during cell expansion is not yet well defined and but appears to involve regulation of membrane channels, vesicle trafficking, plasma membrane H<sup>+</sup>-ATPase and regulation of gene expression (Rayle and Cleland, 1992; Bowler and Chua, 1994; Sembdner et al, 1994; Llic et al, 1996; Millner, 1995; Leyser, 1998). Much of this may be mediated by IAA-binding receptors (Millner et al, 1994; Millner, 1995; Kim et al, 1997; Ulmasov et al, 1997). The role of IAA as photoreceptor for growth inhibition has been argued on the basis of the UV action spectra for the base curvature of oat seedlings (Ray and Curry, 1958). However, that action spectra has a peak at 295 nm followed by a drop to 285 nm, which is more characteristic of protein absorbance. This does not coincide with the peak absorbance for IAA which is 285 nm. A second line of evidence comes from the observation that a naturally occurring photooxidation product of IAA, 3-methyleneoxindole (3-MO), also acts as a

growth inhibitor (Bhatnagar, 1984; Ros and Tevini, 1995). The experiments implicating 3-MO were carried out *in vitro* using continuous UV-B irradiation and the response was found to be reversible after irradiation (Ros and Tevini, 1995). Furthermore, *in vivo* levels of 3-MO were not reported. The conditions under which cotyledon curling occurs are quite different. Cotyledon curling is induced by exposure to UV during a short interval followed by an incubation period. The upward curling only begins to develop after 12 h and then does so rapidly over a period of 2-4 h (Wilson and Greenberg, 1993b). If 3-MO was the active agent in cotyledon curling, it would have to be stable, or form a stable inhibitory complex with a target protein during the 12h before curling develops. It is clear from the action spectra that IAA is a likely target of UV-B. However, detailed analysis of cotyledon growth and tissue concentrations of IAA and metabolites such as 3-MO is needed before a role for IAA as the UV-B photoreceptor for cotyledon curling can be established.

Application of another auxin that occurs naturally, phenylacetic acid (PAA) (10 mM) to cotyledons promotes downward curling to a small extent and is able to block UV-B-induced cotyledon curling. The manner in which PAA promotes growth is quite distinct from IAA. Endogenous PAA is found at several times greater concentrations than IAA in plants (Wightman and Lighty, 1982), and it affects growth at concentrations three orders of magnitude greater than IAA (Vierstra and Poff, 1981). It has two potential modes of action: inhibition of carrier-mediated efflux of IAA (Johnson and Morris, 1987), and formation of adducts with photoreactive flavins (Vierstra and Poff, 1981). Both of these properties could result in blocking cotyledon curling. By inhibiting polar transport of IAA in the tissues treated by PAA, IAA would accumulate and promote growth. However, PAA cannot replace IAA since they have different modes of action. For instance, many steps in IAA action are mediated by IAA-binding proteins or IAA receptors,

which are unlikely to bind PAA . Therefore, if photodestruction of IAA is the cause of upward cotyledon curling, it is not clear why PAA-treated cotyledons did not curl upward when exposed to UV-B. The loss of IAA or formation of a growth inhibiting photoproduct of IAA should be the same, in the presence or absence of PAA.

Another chemical inhibitor of cell expansion, *cis*-4-cyclohexene-1,2-dicarboximide (CHDC), also blocked cotyledon curling (Stewart and Bewley, 1990). This compound inhibits plant growth which is developmentally regulated by phytochrome, but promotes IAA-induced cell-expansion. In the context of cotyledon curling, CHDC could be promoting IAA-induced cotyledon expansion, although it does not affect unexposed control seedlings.

There are a number of signal-transduction molecules associated with changes in gene expression induced by UV-B. These include changes in cytosolic calcium concentrations (Christie and Jenkins, 1996), phosphorylation of proteins (Harter et al, 1994; Christie and Jenkins, 1996), and concentrations of active oxygen (Rao et al, 1996; Allan and Fluhr, 1997). Some UV responses also share common signaling pathways with other environmental stresses and stimuli such as heat (Jenkins et al, 1997), fungal and bacterial elicitors, and wounding (Wingender et al, 1989; Logemann et al, 1995). Moreover, UV-A, BL and phytochrome signaling pathways modulate UV-B regulation of CHS gene expression (Fuglevand et al, 1996). Hence, it was of interest to investigate whether signal transduction molecules mediate the induction of cotyledon curling.

Calcium has been widely studied as a second messenger molecule in plants (Tretyn et al, 1992). A number of compounds that interfere with calcium signaling were found to affect curling. The curling response initiated by UV-B was almost completely blocked by pre-treatment with the calcium ionophore A23187 or the calmodulin antagonist W7. In the first case, A23187

would be expected to lower intracellular calcium concentrations by making the plasma membrane leaky to calcium. In the second case, W7 would be expected to block activity of enzymes that are responsive to elevated intracellular calcium. The results presented here indicate that signaling by elevation of intracellular calcium is required for normal cotyledon expansion, and for development of cotyledon curling after UV irradiation. The induction of CHS gene expression by UV-B also appears to involve calcium signaling (Christie and Jenkins, 1996).

The first intracellular second messenger molecule identified in a signal-transduction pathway was cAMP (reviewed in Ashcroft, 1997). Activation of phosphodiesterase leads to lower cytosolic levels of cAMP, which reduces the activity of a number of cAMP-dependent kinases (Mons et al, 1998). Although the presence of cAMP in plants has been implied experimentally (Assmann, 1995), it is only recently that the presence of adenylate cyclase in plants has been confirmed (Ichikawa et al, 1997). Pre-treatment of cotyledons with imidazole, which activates adenosine 3',5'-cyclic monophosphate (cAMP) phosphodiesterase, resulted in inhibition of cotyledon curling initiated by UV-B. Furthermore, cAMP signaling has been implicated in initiation of plant cell division by IAA (Ichikawa et al, 1997), and therefore could potentially play a role in growth inhibition triggered by UV-B. This would be particularly interesting if in fact IAA was acting as the UV-B photoreceptor for inhibition of cell division by UV-B and cotyledon curling (Nogues et al, 1998).

The application of H<sub>2</sub>O<sub>2</sub> to cotyledons resulted in cotyledon curling to the same levels as those induced by 290 nm UV-B. Even at the high concentrations used, no visible tissue damage was observed. This observation raises the possibility H<sub>2</sub>O<sub>2</sub> is a second messenger triggered by UV-B that mediates cotyledon curling. However, pre-treatment of cotyledons with the free radical scavenger, ascorbate, had only a very small effect on UV-B-induced curling. The

treatment of cotyledons with  $H_2O_2$  did not seem to damage the capacity of cells to undergo expansion. This was demonstrated by the restoration of the cotyledon curling to control levels by pre-treatment of cotyledons with PAA. Thus, both UV-B and  $H_2O_2$  are causing cotyledon curling by a mechanism that does not cause irreversible cell damage. A number of responses initiated in animal cells by exogenous  $H_2O_2$  are inhibited by application of N-acetylcysteine (NAC), which scavenges peroxides (Adler et al, 1995; Quillet-Mary et al, 1997). There was only a small inhibition of  $H_2O_2$ -induced cotyledon curling by NAC, and this was difficult to quantify because of the variability of the response to these treatments. It may be that a more sensitive assay is required for a more detailed analysis of the signal-transduction pathways involved in UV-B-induced cotyledon curling.

Another response of cotyledons to UV-B, an increase in the level of UV-B-absorbing compounds, was unaffected by treatment of cotyledons with  $H_2O_2$ . The concentration of  $H_2O_2$  used was sufficient to induce curling. The measurements of UV-B-absorbing compounds indicate sustained changes in the cotyledons, since they were made 24 h after treatment. This indicates that, not only do photoreceptors differ for growth and phenylpropanoid responses to UV-B, but that the signal transduction pathway may also be different for these two UV-B responses.

The possible involvement of  $H_2O_2$  in UV-B-induced cotyledon curling may be significant for understanding the growth inhibition response of plants exposed to UV-B. UV-B-induced active oxygen production in plant cells has been described recently (Allan and Fluhr, 1997; Rao et al, 1996). There is also an increasing number of examples of signal-transduction by  $H_2O_2$  in plants (Low and Merida, 1996; Wojtaszek, 1997; Alvarez et al, 1998). Thus,  $H_2O_2$  may play an important role in growth inhibition in plants exposed to UV-B radiation.

The identity of the indole-like photoreceptor remains unresolved. It may be that UV-B irradiation of plants proteins results in the generation of sufficient amounts of H<sub>2</sub>O<sub>2</sub> to trigger morphological changes, or that UV-B maybe degrading or modifying IAA which then disrupts cell expansion. In either case, Ca<sup>2+</sup> and cAMP maybe involved subsequent steps. Initially, quantification of H<sub>2</sub>O<sub>2</sub>, IAA and photodegradation products of IAA may give a clearer indication. Investigation of signal transduction pathways, such as the activation of tyrosine kinase or phosphatase activities may help to distinguish between the affects of H<sub>2</sub>O<sub>2</sub> and IAA (Chen et al, 1996; Dai et al, 1995). Finally, a sensitive *in vivo* assay for induction of H<sub>2</sub>O<sub>2</sub>- or IAA-responsive genes by UV-B may give some direct evidence. For example, one of the glutathione-S-transferase genes in *Arabidopsis* is specifically inducible by H<sub>2</sub>O<sub>2</sub> and could be used as a reporter gene for increased levels of H<sub>2</sub>O<sub>2</sub> *in vivo* (Chen et al, 1996). A better understanding of the process of cell expansion in cotyledons may also lead to a means to assay the effect of UV-B on cell growth and a more precise description of the properties of the UV-B photoreceptor.

## 4. ACCLIMATION OF EPIDERMAL CELLS TO UV-B

### 4.1 INTRODUCTION

Plants adjust a variety of physiological processes to acclimate to changing environmental stress factors such as light, temperature and moisture (Taiz and Zeigler, 1995). Ambient solar UV-B (290-320 nm) is one such factor that can cause stress (Caldwell et al, 1995). Plants have likely evolved many acclimation mechanisms that minimize biological effects of solar UV-B. Of these, UV-B absorbing compounds such as flavonoids are important for providing screening protection to the mesophyll (Tevini et al, 1991; Wilson and Greenberg, 1993a; Wilson et al, 1998).

Plants can acclimate to ambient UV-B in ways that are not clearly related to mitigating the damaging effects of UV-B. For example, ultrastructural changes in chloroplasts resembling a transition to a shade-tolerant state were observed in *B. napus* when grown under low levels of UV-B (Fagerberg and Bornman, 1997). This may be a result of an increased rate of degradation of the D1-D2 proteins which form the core of PS II reaction center (Greenberg et al, 1989; Jansen et al, 1996; Jansen et al, 1998). Such changes in PS II may affect the size of the plastoquinone pool which can result in changes in gene expression (Huner et al, 1998). In this way the D1-D2 proteins may be acting as sensitive UV-B photoreceptors that trigger acclimation of the photosynthetic apparatus.

The process of acclimation to UV-B may be significant shortly after shoot emergence from the soil (Ballare et al, 1995b; Ballare et al, 1996). Crops grown at temperate latitudes, where growing seasons begin late in the Spring, are exposed to the high levels of UV-B already present in solar radiation when germination begins (Madronich et al, 1995; Ballare et al, 1996). Young field-grown alfalfa and *Datura* express enzymes in their cotyledons which specifically repair UV-



B-induced DNA lesions (Takayanagi et al, 1994; Ballare et al, 1996). Nonetheless, very little is known about how cotyledons acclimate to UV-B. However, they undergo morphological changes in response to UV-B (see Chapters 2 and 3). A number of striking changes have been observed in the upper epidermis and the adjacent cuticle of cotyledons of plants grown under lighting that contains UV-B are compared to those grown under PAR (photosynthetically active radiation) alone. These include changes in number of stomata, collapse of epidermal cells (see Fig. 2.34 and 2.4), increased cuticular wax layers and changes in wax composition (Tevini et al, 1983; Steinmuller and Tevini, 1985). The process of acclimation of epidermal cells to UV-B is likely to be important in cotyledons, since dicots are dependent on this organ during initial growth stages for biosynthesis of metabolites. However, the protection mechanism could be quite different from leaves, since cotyledons senesce early in plant growth. That is, cotyledon acclimation to UV-B is likely to be rapid, and transient since it is only required for relatively short periods of time.

Epidermal cells of the upper surface of cotyledons most likely play a particularly important role in acclimation to UV-B since they are the first line of defence. Thus, the approach chosen was to isolate and characterize these cells with respect to changes resulting from UV-B exposure. The cotyledon epidermal tissue layer is made up of guard cells and pavement cells (Fig. 4.1). Guard cells have been the subject of many studies, however, little is known about the pavement cells, which make up the majority of the epidermal surface. They have only been the subject of a few studies in leaves of dicots (pea) and monocots (rye and barley) (Weissenbock et al, 1986; Schulz and Weissenbock, 1986; Dietz et al, 1992). In order to understand the impact of UV-B during early stages of growth in *B. napus* better, changes in protein composition and secondary metabolites in pavement cells of the upper epidermis were investigated within 12 h of exposure to UV-B radiation.

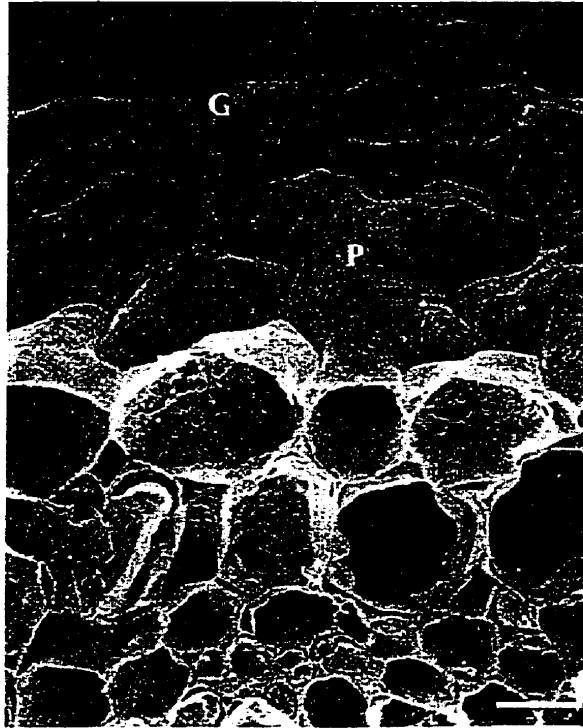


**Figure 4.1.** The adaxial epidermal surface of 5-day old *B. napus* cotyledon viewed using SEM. The cotyledon was cryoprotected and freeze-fractured under liquid nitrogen. The scale bar represents 20  $\mu\text{m}$ . Guard cells and pavement cells are indicated.

To do this, plants were exposed to UV-B and then adaxial epidermal protoplasts were isolated. Using this approach it was found that the protein composition of protoplasts from UV-B treated plants differed from untreated plants and that specific UV-B-absorbing compounds accumulated in protoplasts from UV-B treated plants.

## 4.2 Materials and Methods

### 4.2.1 Growth and Treatment Conditions

Seeds of *Brassica napus* cv Topas and cv Corvette, *Brassica campestris* cv Shogoin, and *Brassica oleracea* cv Copenhagen were planted in individual pots containing Pro-Mix potting media (Premier Brands, Rivière-du-Loup, Quebec). Plants were grown for 5 days at 22°C under 80  $\mu\text{mol m}^{-2} \text{s}^{-1}$  PAR from cool white fluorescent lamps (F48T12CW; General Electric Co., Wilmington, MA) using a 16 h light/8 h dark photoperiod. Lamps were screened with a polyester film (0.08 mm Mylar D) (Johnson Industrial Plastics, Missauga, ON) to shield out any extraneous UV-B or UV-C from the fluorescent lamps. UV radiation from FS40 UV lamps (National Biological Co., Twinsburg, Ohio) were added to the light source and the plants were subsequently grown for 12 h under PAR (80  $\mu\text{mol m}^{-2} \text{s}^{-1}$ ) either plus UV-A, or plus UV-B and UV-A. UV irradiation conditions were created by screening plants with either cellulose acetate (0.13 mm) for the PAR plus UV-B (1.6  $\mu\text{mol m}^{-2} \text{s}^{-1}$ ) and UV-A (2.4  $\mu\text{mol m}^{-2} \text{s}^{-1}$ ) treatment, or with mylar D for the PAR plus UV-A treatment (1.6  $\mu\text{mol m}^{-2} \text{s}^{-1}$ ). The UV-B exposure is the equivalent of 11.7  $\text{kJ m}^{-2} \text{d}^{-1}$  UV-B<sub>BE</sub> normalized to 300 nm (Caldwell, 1971). After the UV exposures, plants were grown for 12 h under PAR alone and analysed. Seeds of wild-type *Arabidopsis thaliana* (L.) Heynh (ecotype Ler) and the mutants *sng-1* and *fah-1* were also grown under control conditions for 7 days. All experiments were carried out a minimum of two times.

The spectral photon distributions and fluence rates of all light sources were measured using a calibrated spectroradiometer (Oriel Inc., Stamford, CT) and are identical to those previously reported (Greenberg et al, 1996).

#### **4.2.2 Isolation of Epidermal Protoplasts**

The upper surface of cotyledons was sectioned paradermally using a razor blade. Sections were immediately placed in filter-sterilized (0.2  $\mu\text{m}$  syringe filter, Nalgene, Rochester, NY) resuspension buffer (10 mM MES-KOH, pH 5.5; 2 mM  $\text{CaCl}_2$ ; 0.42 M D-mannitol) in a 55 x 12 petri dish. The procedure used for the release and isolation of epidermal protoplasts was adapted from Weissenbock et al (1986) with modifications. Once sufficient tissue had been collected to fill the dish, the resuspension buffer was replaced with a cell wall digestion buffer (10 mM MES-KOH, pH 5.5; 2 mM  $\text{CaCl}_2$ ; 1.7% Cellulysin w/v; 0.03% pectolyase w/v; 0.42 M D-mannitol) and incubated at room temperature for 1 hour. The partially digested tissue was transferred to 1 mL of resuspension buffer in an eppendorf tube and centrifuged at room temperature for 1 minute. All centrifugations were performed at 82 x g. The mesophyll protoplasts and tissue debris pelleted while the epidermal protoplasts floated. The upper 800  $\mu\text{L}$  of the mixture was transferred with a wide bore plastic pipette into a new tube. The centrifugation was repeated up to 6 times until the pelleted mesophyll cells could no longer be seen by eye. To concentrate and wash the protoplasts, 500  $\mu\text{L}$  of the mixture was transferred to 700  $\mu\text{L}$  of pelleting buffer (10 mM MES-KOH, pH 5.5; 2 mM  $\text{CaCl}_2$ ; 0.42 M betaine) and the mixture was centrifuged. This was repeated twice and the final pellet was resuspended in 200  $\mu\text{L}$  of resuspension buffer. Part of the second mesophyll protoplast pellet was retained and washed similarly. The complete isolation procedure was carried out over a two hour period with tissue

from approximately 50 cotyledons. Protoplast concentrations were determined using a Fuchs Rosenthal hemocytometer (200  $\mu\text{m}$  deep). Protoplast integrity and viability were assessed by light microscopy using uptake of neutral red and the presence of active transvacuolar streaming.

#### **4.2.3 Extraction and Analysis of Epidermal Protoplast Proteins**

All isolation buffers used to isolate protoplasts for protein extraction were prepared with the addition of chloramphenicol (300  $\mu\text{g ml}^{-1}$ ) and cycloheximide (300  $\mu\text{g ml}^{-1}$ ) to prevent protein synthesis during cell isolation. Approximately  $4 \times 10^4$  protoplasts were collected as described above. Cells were lysed in 200  $\mu\text{L}$  lysis buffer (50 mM Tris-HCl, pH 8.0; 0.08% SDS w/v; 15 mM DTT; 2 mM PMSF; 10  $\mu\text{M}$  leupeptin; 50  $\mu\text{g ml}^{-1}$  chymostatin; 100  $\mu\text{g ml}^{-1}$  pepstatin), then heated for 20 minutes at 70°C and cooled to room temperature. After centrifugation (14000 x g, 30 min), an aliquot (2  $\mu\text{L}$ ) was taken to measure protein concentration using a densitometric spot assay (Ghosh et al, 1988). The remaining extract was used for either SDS PAGE (Laemmli, 1970; Wilson et al, 1995) or 2D PAGE analysis (O'Farrell, 1975; Wilson et al, 1995).

Proteins were prepared for SDS-PAGE by diluting an aliquots of each protein extract (2:1) in SDS sample buffer (30% glycerol w/v; 9% SDS w/v; 120 mM Tris-HCl, pH 6.6; 15% 2-mercaptoethanol w/v) and then heating at 90°C for 2 min. Proteins were separated by SDS-PAGE (12% acrylamide w/v) in the buffer system of Laemmli (1970). Separated proteins were visualized using Coomassie brilliant blue R staining or silver staining.

To each sample aliquot (100  $\mu\text{L}$ ) used for 2D-PAGE was added 160 mg solid urea (9 M), 16 mg solid CHAPS (8% w/v; 3-[(3-chloamidopropyl)dimethylammonio]-1-propane-sulfonate), ampholines (40% w/v, pH 3-10, Pharmacia Biotech AB, Uppsala, Sweden) to a final concentration of 5% (w/v), and 10  $\mu\text{L}$  of freshly made 150 mM DTT. The mixture was vortexed

at room temperature until the urea was dissolved. An aliquot of each sample (50  $\mu$ L) was loaded onto a polyacrylamide tube gel (1.5 x 160 mm; 4% acrylamide:bis-acrylamide [30%/1% w/v]). Tube gels were loaded into a electrophoresis unit (Protean II, BioRad, Hercules, CA) with the samples at the basic (cathode) end of the unit, and IEF was carried out at 20°C for 20 h using 800V (16000 V-h) according to the manufacturer's protocol with the following changes. The anode buffer was 150 mM phosphoric acid (pH 2), and the cathode buffer was 50 mM NaOH (pH 12). Since the pH gradient that develops using this method of IEF is non-uniform, the pH of tube gel slices was not measured (Freiburghaus, 1994). It was assumed that each end of the tube gel was in equilibrium with either the cathode or the anode buffers after electrophoresis. Also, since proteins were well resolved without a pre-focusing of the ampholines, this step was omitted.

Tube gels were frozen at -20°C until used for SDS PAGE. After thawing at room temperature, tube gels were gently removed from the glass tubes using air pressure and transferred into petri dishes containing SDS sample buffer (Laemmli, 1970), and equilibrated for 15 minutes at room temperature. Tube gels were then placed in the sample well of 15% acrylamide:bis-acrylamide (30%/1% w/v) SDS-PAGE gels (10 x 10 cm). The proteins were electrophoresed 4h at 30 mA constant current. The gels were silver-stained (Rabilloud et al, 1988), and scanned with a computerized scanning densitometer to evaluate spot intensity and location (Molecular Dynamics, Sunnyvale, CA). Measurement of protein concentrations in protein extracts was carried out as described previously using a densitometric dot assay with 2 repeats of each measurement of each 2  $\mu$ L aliquot (Ghosh et al, 1988).

For immunological western blot analysis, immediately after SDS PAGE, proteins in each gel were electroblotted onto 0.2 micron nitrocellulose membrane (Biorad) using 16 mM glycine; 25 mM Tris-HCl, pH 8.7; 0.02% SDS w/v; 20% methanol as the transfer buffer. Electrophoretic transfer was

carried out for 2 h at 300 mA constant current using a Mini Protean II apparatus (Biorad) following the manufacturer's protocol. Transfer of proteins was checked by silver-staining gels after the transfer procedure using the procedure of Rabilloud et al (1988). Protein blots were blocked with 1% milk powder in Tris-buffered saline (25 mM Tris-HCl, pH 7.6; 140 mM NaCl) and incubated with a 1:3000 dilution of a rabbit antiserum raised against chalcone synthase from peanut. Antibody binding was visualized using goat anti-rabbit immunoglobulin G secondary antibody conjugated to alkaline phosphatase according to manufacturer's protocol (Biorad). The colour reaction was carried out using blue tetrazolium and 5-bromo-4-chloro-3-indonyl phosphate. The relative molecular weight of the bands which appeared were estimated from migration distances of pre-stained standards had been run on the gel (Biorad).

#### **4.2.4 Extraction and Isolation of UV-B-absorbing Compounds**

Protoplasts were isolated as described above (section 4.2.2) and extracted with 80% methanol. As well, intact cotyledons were extracted. Samples from control and UV-B-treated seedlings described above (section 4.2.1), were removed with a cork borer which produced disks of approximately 0.38 cm<sup>2</sup>. The samples were weighed and extracted with 80% MeOH for 48 h at 4°C. Absorbance of extracts at 300 and 330 nm were measured using a spectrophotometer (Beckman Lambda 3). Samples of each extract were analyzed using reverse phase HPLC (Shimadzu, Columbia, MD) following protocols described in Wilson *et al* (1998). Briefly, aliquots (100 µL) were applied to Hypersil ODS C18 column (4.6 x 250) (Supelco, Bellefonte, PA) and gradient of 8-50% acetonitrile:water (pH 3.0; 0.01 % phosphoric acid w/v) was used to elute the column at 1 mL min<sup>-1</sup> over a period of 50 minutes. Between runs, the column was washed with 100% acetonitrile for 5 minutes and then equilibrated at 8% acetonitrile for five

minutes. The elution profile was monitored at 320 nm and the UV-absorbance spectra (250-400 nm) of individual compounds were collected with a diode array detector (Shimadzu, Columbia, MD) and used for sample identification (Wilson *et al*, 1998). Samples that were to be compared were run in the same batch of samples using the same separation method and injection volume (100  $\mu$ L) for each extract. Shoots from *Arabidopsis* plants were also extracted and analysed with the same protocol described in this section.

To identify compounds in extracts, a number of known flavonoid and hydroxycinnamic acid compounds were run as standards using the same sample volumes and elution conditions. Their UV spectrum and elution time were recorded for comparison to compounds in extracts. These included the flavonols kaempferol, quercetin, narigenin, and hydroxycinnamic acids ferulate, sinapate and coumarate (Sigma Chemical Co, St. Louis, MI).

An estimate of the concentration of compounds that were putatively identified as derivatives of sinapic acid was made using HPLC-diode array analysis. Standards of sinapic acid (Aldrich, Milwaukee, WI) were made up in 80% methanol over a range of 1  $\mu$ M-10 mM. The area under the elution peak for each standard was analyzed and used to calculate a least squares regression for the standard concentration curve. The concentration of purified compounds was then estimated from the area under the elution peak. Samples which were not being prepared for quantitative analysis were given an additional extraction with an equal volume of chloroform to improve the quality of separation during HPLC.

#### **4.2.5 Mass spectrometric analysis of UV-B absorbing compounds from *B. napus*.**

The five most abundant UV-absorbing (320 nm) compounds in *B. napus* cotyledon tissue, were collected and pooled for further analysis. They were collected from *B. napus* cv. Corvette



because it accumulates these compounds to much higher levels than cv. Topas (Wilson, 1996). Plants were grown under the same control conditions as described in section 3.2.1. After 5 d of growth, cotyledons (40 g) were excised and extracted into 500 mL of 80% MeOH in the dark for 48 h at 4°C. An equal volume of chloroform was added to remove non-polar compounds such as chlorophyll, the mixture shaken by hand for 5 minutes and allowed to partition at 4°C for 1 hour. The aqueous layer (~350 mL) was removed with a pipette and transferred into a 600 mL beaker. The beaker was placed in a vacuum chamber the volume was reduced to approximately 10 mL. This concentrated extract was applied to a Hypersil ODS C18 column (4.6 x 250) (Supelco, Bellefonte, PA) RP-HPLC column in 400 µL aliquots and separated using a gradient that was optimized for quick separation of the five predominant compounds. The gradient consisted of increasing acetonitrile concentration from 10-40% in the presence of water (pH 3.0; 0.04 % phosphoric acid w/v) over the period of 30 minutes with a wash and equilibration cycle between runs as described above in section 3.2.4. The elution of compounds was monitored at 320 nm and five peaks were collected individually into separate glass vials (5 ml). The purity of the compounds was assessed by confirming the retention times coincided with those of the corresponding peak in tissue extracts using the same RP-HPLC method.

Electrospray ionization mass spectroscopy (ESI-MS) of HPLC purified compounds from cotyledons was carried out on a triple-quadrupole instrument (Micromass, Manchester, UK) (Wilson *et al*, 1998). Samples were dissolved in 20% acetonitrile (pH 3.0, 0.04 % phosphoric acid w/v) when injected into the mass spectrophotometer. Both negative mode (with the addition of NH<sub>3</sub> to the sample to remove H<sup>+</sup>) which separates negative ions, and positive mode, which separates positive ions were used. The five most abundant HPLC peaks were tentatively identified as sinapate derivatives. Thus, the parent compound, sinapic acid, was also included for

comparison to the putative sinapoyl derivatives. The masses of dominant ions were compared to the expected mass of potential UV-B absorbing sinapoyl esters from *Brassica* species, those being sinapoylglucose, sinapoylmalate, sinapoylcholine and disinapoylglucose (Linscheid et al, 1980).

#### **4.2.6 X-ray crystallographic analysis of isolated UV-B-absorbing compounds.**

To identify the dominant UV-B-absorbing compounds definitively crystallization trials were carried out with 4 compounds isolated by RP-HPLC as described in section 3.2.5. Pooled fractions for each compound were dried down under vacuum at room temperature, then redissolved in 100  $\mu$ L deionized water (pH 5.0) plus 400  $\mu$ L 80 % MeOH, and transferred into 2 mL glass vials. Vials were placed in a refrigerated dessicator at 4°C in order that slow evaporation of MeOH could take place and the concentration of the compounds could gradually approach saturation. Crystals formed for compound 1 and were prepared for X-ray crystallographic analysis. Crystals were pipetted from the mother liquor onto a clean glass slide and the liquor evaporated slowly. A single piece approximately 1 x 0.3 x 0.03 mm was mounted with epoxy on the end of the glass fibre ~0.1 mm dia., which was attached to a crystal mounting stub. Collection of X-ray diffraction data from this crystal was carried out at the Department of Chemistry X-ray Facility at McMaster University (Hamilton, ON) by Dr. J. F. Britten using a Siemens Molybdenum rotating-anode generator with a P4 diffractometer and a SMART CCD detector.

## 4.3 RESULTS

### 4.3.1 Epidermal protoplast isolation

When cotyledons of 5-d old *B. napus* seedlings are exposed to UV they undergo a number of changes which potentially lead to acclimation (see Chapter 2). Epidermal cells on the upper surface of cotyledons of course receive the greatest UV-B exposure. To examine the effects of UV-B on epidermal cells, and how they might contribute to rapid acclimation of cotyledons to UV-B, a procedure for examining and isolating epidermal protoplasts from *B. napus* was developed.

Initially, epidermal cells were examined *in situ*. When 5-day old *B. napus* cotyledons are sectioned transversely and viewed using fluorescence microscopy ( $\lambda_{ex}=365$  nm), the upper epidermal layer is easily distinguished by the greatly reduced red chlorophyll fluorescence and blueish fluorescence of vacuolar compounds (Fig. 4.2). When a strip of cotyledon tissue was incubated in 0.01%  $NH_4OH$  (Strack, 1977), the alkalization of vacuolar compounds in epidermal cells results in a strong green fluorescence in contrast to the red chlorophyll fluorescence of the mesophyll layer (Fig. 4.2). These observations were used to distinguish between epidermal and mesophyll protoplasts during isolation.

Protoplasts were isolated from *B. napus* cotyledons and separated into epidermal and mesophyll cell fractions. The epidermal protoplast preparation very homogenous fraction, judging from microscopic examination (Fig. 4.2B). However, the epidermal cells contaminated the mesophyll protoplasts (Fig. 4.2C). This was likely due to the similar densities of mesophyll protoplasts and a subpopulation of epidermal protoplasts which leads to co-sedimentation. The epidermal cells from the upper surface of *B. napus* cotyledons contain chloroplasts, albeit, far fewer than mesophyll cells.

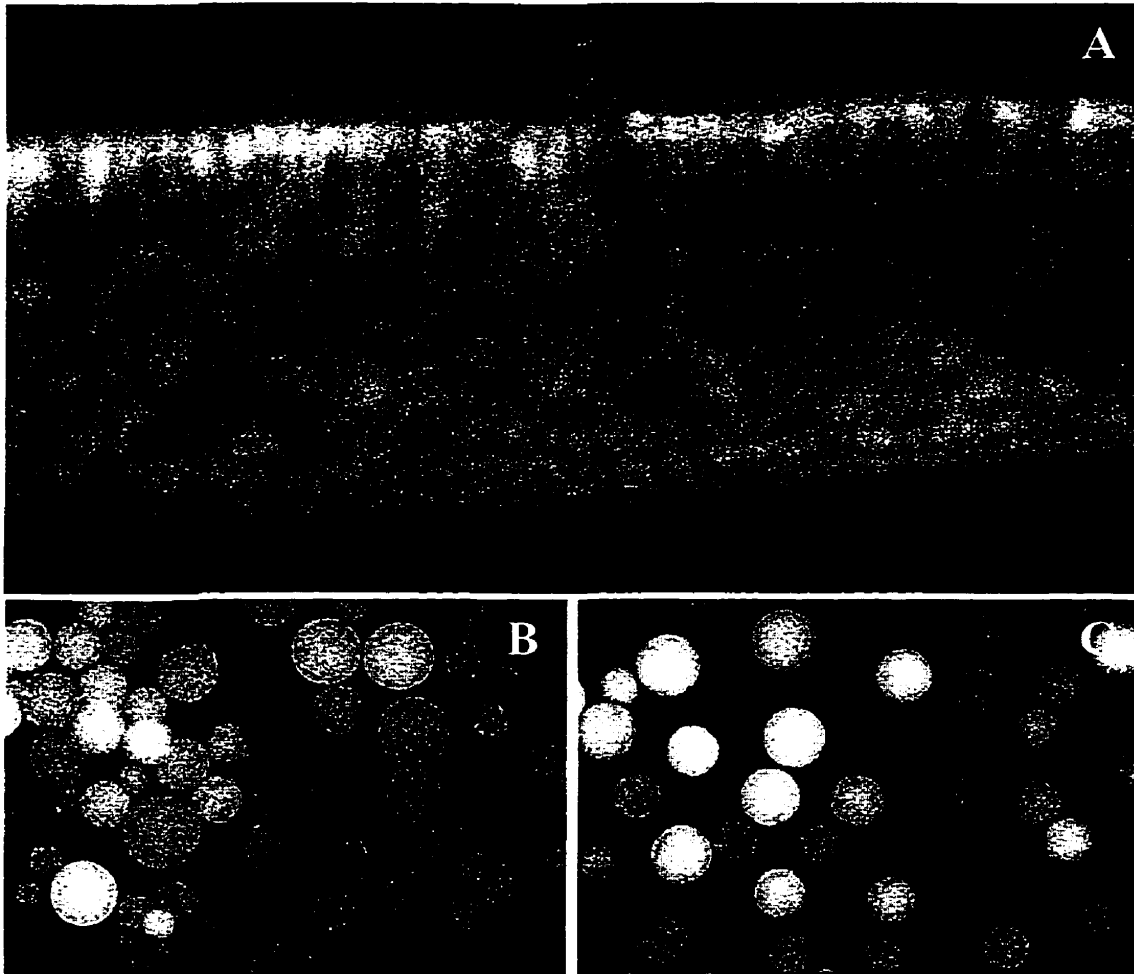


**Figure 4.2.** Isolation of protoplasts from the upper epidermis of 5 day old *Brassica napus* cotyledons. A, Transverse section of cotyledon; B, Epidermal protoplasts and C, mesophyll protoplasts. Tissue and protoplasts were treated with 0.01%  $\text{NH}_4\text{OH}$  before viewing at 100X magnification using a fluorescence microscope,  $\lambda_{\text{ex}}=365$  nm (Zeiss, Axiophot).

They were observed as red spots under fluorescence microscopy ( $\lambda_{ex}=440$  nm) (Fig. 4.2B). The chloroplasts were in the cytoplasm of the epidermal protoplasts, and were generally half the size of mesophyll chloroplasts. The functional integrity of the epidermal protoplasts was evaluated by observing their ability to take up neutral red dye into the vacuole and the observation of active transvacuolar cytoplasmic streaming, both are processes which require active cellular metabolism (data not shown). It can be concluded from these observations that a nearly pure preparation of intact functional epidermal cells from *B. napus* cotyledons was achieved.

#### 4.3.2 Epidermal cell proteins

With a rapid procedure for isolating intact epidermal protoplasts, the effect of UV-B on these cells could be examined. The *B. napus* cv Topas, were exposed to UV-B, after which epidermal cells were isolated and analyzed. Many of the proteins present in mesophyll cells were also found at low levels in epidermal cells. For instance, ribulose-1,5-bisphosphate carboxylase/oxygenase was present among the proteins, because the epidermal cells have chloroplasts. Other polypeptide bands were unique to epidermal cells. A good example is a band at 33 kDa, which is only present in epidermal cells (Fig. 4.3).

Two-dimensional PAGE revealed a number of changes in response to UV-B. In one case, the appearance of additional proteins at 66 kDa corresponds to isoforms of photocross-linked subunits of rubisco (66 kDa) (Fig. 4.4A and 4.4B). This photoproduct has been observed in leaves exposed to UV-B (Wilson et al, 1995).

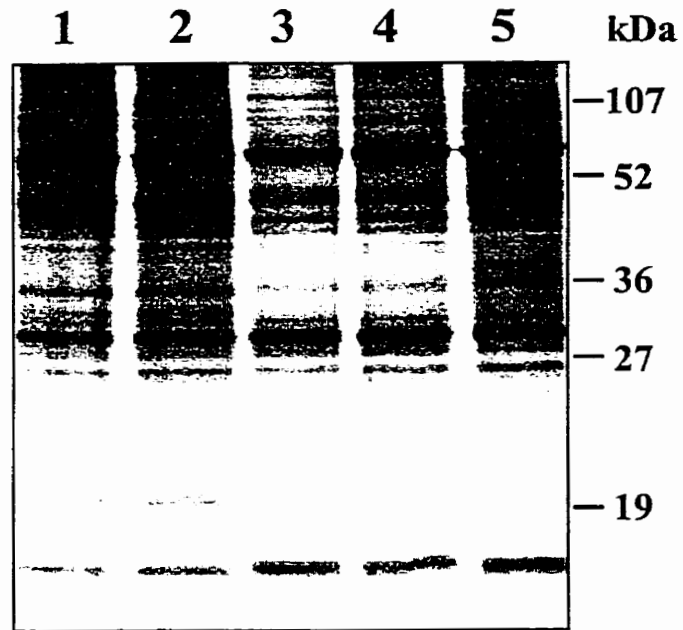


**Figure 4.3.** Profiles of soluble epidermal protoplast proteins extracted from control or UV-B-treated cotyledons and separated using SDS PAGE (20  $\mu$ g per lane). Lane 1, control epidermal cells, 2, UV-B-treated epidermal cells, 3, control mesophyll cells, 4, UV-B-treated mesophyll cells, 5, whole cotyledon. Gels were silver-stained to visualize proteins. Positions of molecule weight markers are shown.

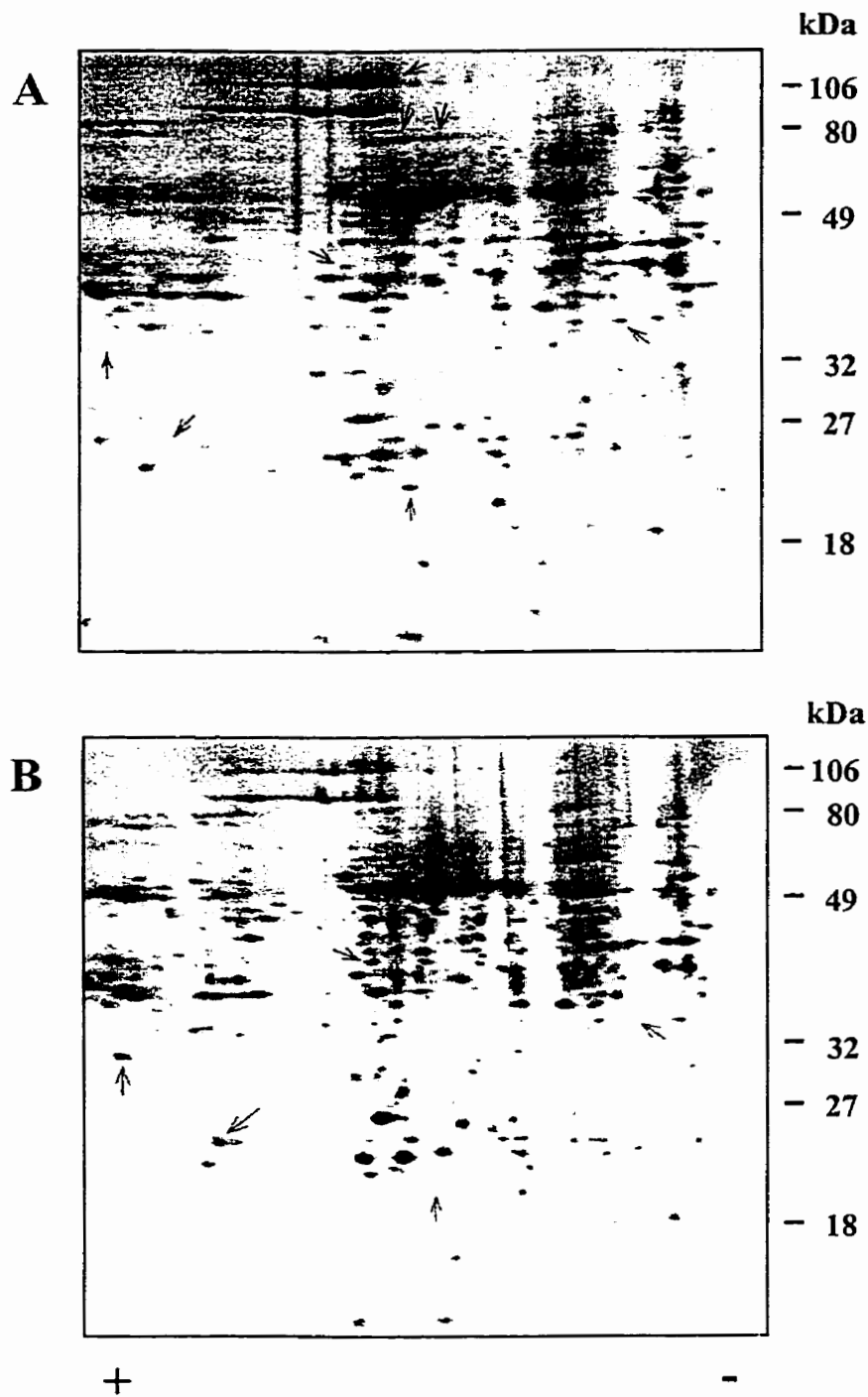


**Figure 4.4.** Profile of proteins extracted from epidermal protoplasts from UV-B-treated (A), or control (B). Protein samples (50  $\mu\text{g}$ ) were resolved in the horizontal dimension by IEF in a gradient from pH 5 to 10 and in the vertical dimension by gradient SDS-PAGE (10-15% acrylamide w/v). Gels were silver-stained to visualize proteins. Arrows indicate proteins that changed abundance in plants treated with UV-B. Positions of molecular weight markers are shown.

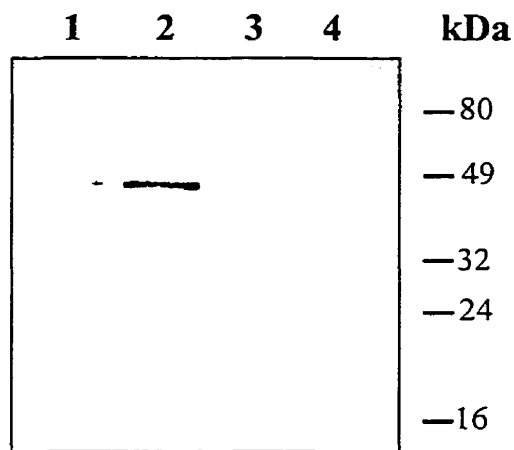


**Figure 4.5.** Western blot of proteins extracted from epidermal protoplasts isolated from control or UV-B-treated cotyledons (5  $\mu$ g per lane). Lane 1, control epidermal cells, lane 2, UV-B-treated epidermal cells, lane 3, control mesophyll cells, lane 4, UV-B-treated mesophyll cells. After separating the proteins using SDS PAGE (15% acrylamide w/w), (see Fig. 4.3), proteins were transferred to nitrocellulose proteins probed with anti-chalcone synthase immune serum (1:10000). Positions of pre-stained molecular weight markers are shown.



The abundance of at least two other proteins increased, and three other proteins almost completely disappeared from the silver-stained gel. A group of high molecular weight proteins (~80-100 kDa) also increased in UV-B treated cells. The epidermal cells are responding to UV-B at the protein level. One well-studied response to UV-B is increased expression of the flavonoid biosynthesis enzyme chalcone synthase (43 kDa) (Schmelzer et al, 1988; Fuglevand et al, 1996). Epidermal flavonoids are important UV-B absorbing compounds that provide screening protection to the mesophyll (Cen and Bornman, 1993; Wilson and Greenberg, 1993a; Ålenius et al, 1995; Wilson et al, 1998). Interestingly, only a modest accumulation of CHS in epidermal cells from UV-B-treated cotyledons was detected using CHS antiserum (Fig. 4.5). Although enzyme activity was not measured, this raises questions about production of UV-absorbing flavonoids in these cells.

#### **4.3.3 Purification and identification of UV-absorbing compounds from cotyledons**

Plants commonly acclimate to UV-B radiation by producing vacuolar UV-B-screening compounds, such as flavonoids or hydroxycinnamic acids (Li et al, 1993; Wilson and Greenberg, 1993a; Landry et al, 1995; Ålenius et al, 1995; Wilson et al, 1998). Because there was only a modest increase in the amount of CHS, cotyledon epidermal cells were analyzed for both hydroxycinnamic acids and flavonoids.

Initially, the extent to which UV-B-absorbing compounds accumulate in the cotyledons of 5 d-old seedlings was examined. Samples of cotyledon tissue from UV-B-treated and control seedlings were extracted to isolate the UV-absorbing compounds. Extracts from UV-B-treated cotyledons had an absorbance at 300 and 330 nm that was 36% greater than control cells ( $p < 0.02$ ) (Fig. 4.6). The extracts from the cotyledon cells were separated using reverse phase HPLC. Five

compounds dominated each extract and they were increased in UV-B-exposed plants (Fig. 4.7). Each of these five compounds were abundant in the epidermal cell fraction, thus they could act as screens protecting the mesophyll. A number of approaches were used to identify the five compounds that increased in response to UV-B. The UV absorbance spectra were compared to known compounds and found to have very similar spectra to sinapic acid and the flavonol kaempferol (data not shown). Specifically, compounds 1, 2, 4 and 5 (see Fig. 4.7) were likely sinapic acid esters. Compound 3 was likely a kaempferol derivative (Wilson et al, 1998). These compounds were less polar than sinapic acid (longer retention time on reverse phase HPLC column), implying that a functional group has been esterified to sinapic acid. There are a number of such compounds which have been identified in members of the Brassica family, including *B. napus* (Linscheid et al, 1980; Vogt et al, 1993).

The next approach was to compare the *B. napus* UV-B-absorbing compounds to those previously identified in *Arabidopsis*. Both of these species have similar sinapic acid ester metabolism pathways during early stages of growth (Chapple et al, 1992; Vogt et al, 1993). Two *Arabidopsis* sinapic acid biosynthesis mutants have been identified that lack sinapoyl malate (*sng1*) (Chapple et al, 1992; Lorenzen et al, 1996). Sinapoylmalate does not accumulate in *sng1*, due to loss of sinapoylglucose:malate transferase activity (Chapple et al, 1992; Lorenzen et al, 1996). By comparing extracts of *B. napus* cotyledons to extracts from wild-type *Arabidopsis* (Ler) and *sng1* and it was possible to identify compounds with identical retention times and UV-absorbance spectra (Fig. 4.8). Compound 1 from *B. napus* was identified as sinapoylglucose.

The identity of compound 2 as sinapoylmalate was confirmed using ESI-MS, which gave the expected mass of 339 (Fig. 4.9).

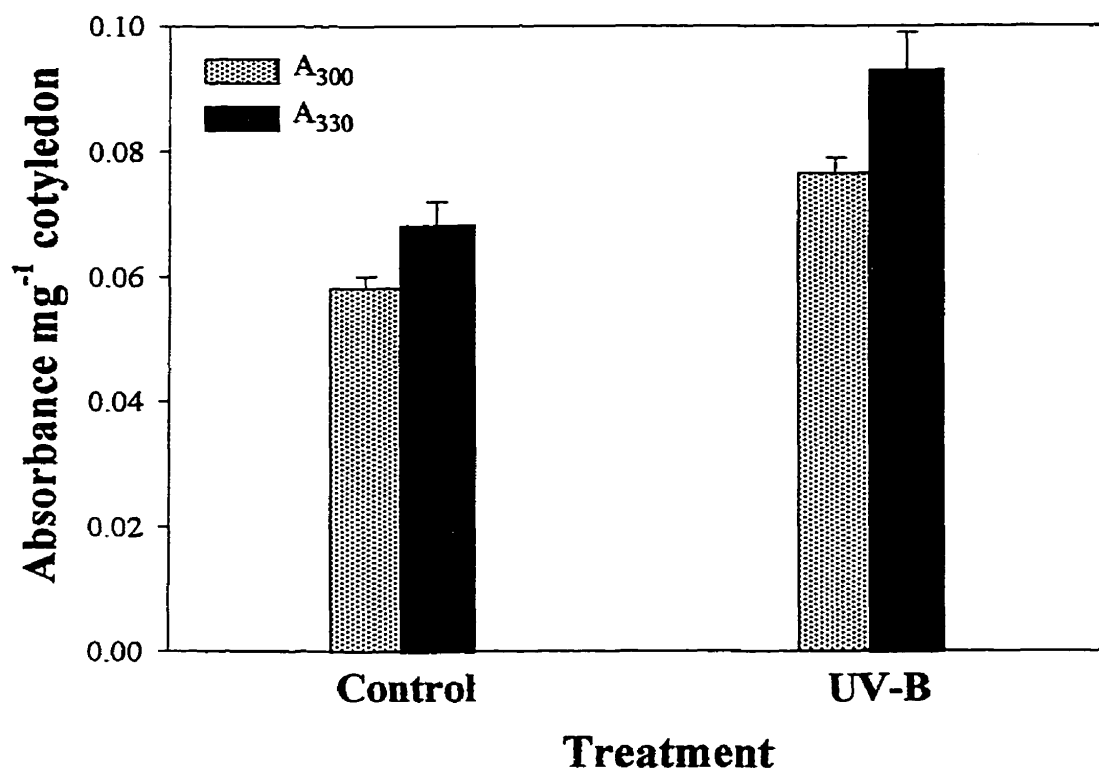


**Figure 4.6.** Accumulation of UV-B-absorbing compounds in 5-day old *B. napus* seedlings exposed to UV-B ( $15 \text{ mmol m}^{-2}$ ) after 24 h incubation in visible light. The mean absorbance at 300 nm (▨) and 330 nm (■) of methanol (80%) extracts of cotyledons expressed on a fresh weight basis is shown. Error bars indicate standard error for four experiments (n=20).

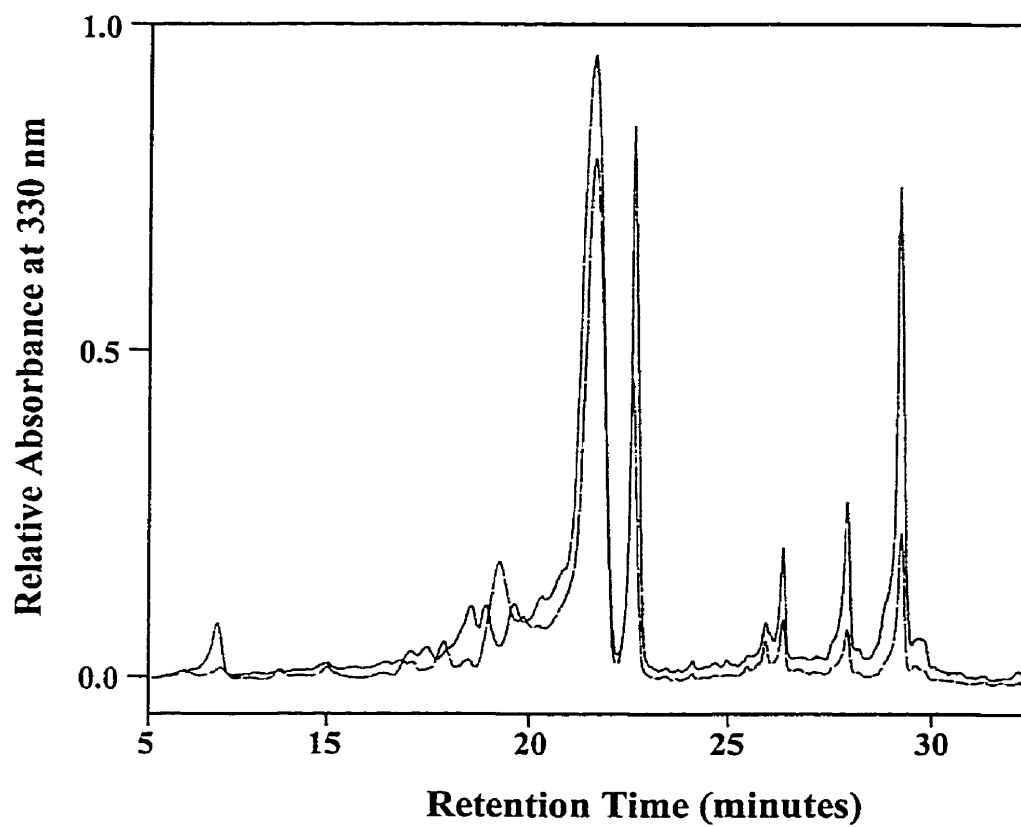


**Figure 4.7.** Reverse phase-HPLC separation of total cotyledon 80% methanol extracts from control seedlings (---) and seedlings treated with  $15 \text{ mmol m}^{-2}$  290 nm radiation (—). For HPLC conditions see section 4.2.4. Elution of compounds from the column was monitored by absorbance at 330 nm. In each case the upper peak is from the UV-B-treated cotyledon extract. The weight of the tissue sample is the same in both cases (11 mg). The total absorbances at 330 nm before separation were 86.6 (control) and 118.9 (UV-B)  $\mu\text{g}^{-1}$  fresh weight, respectively.

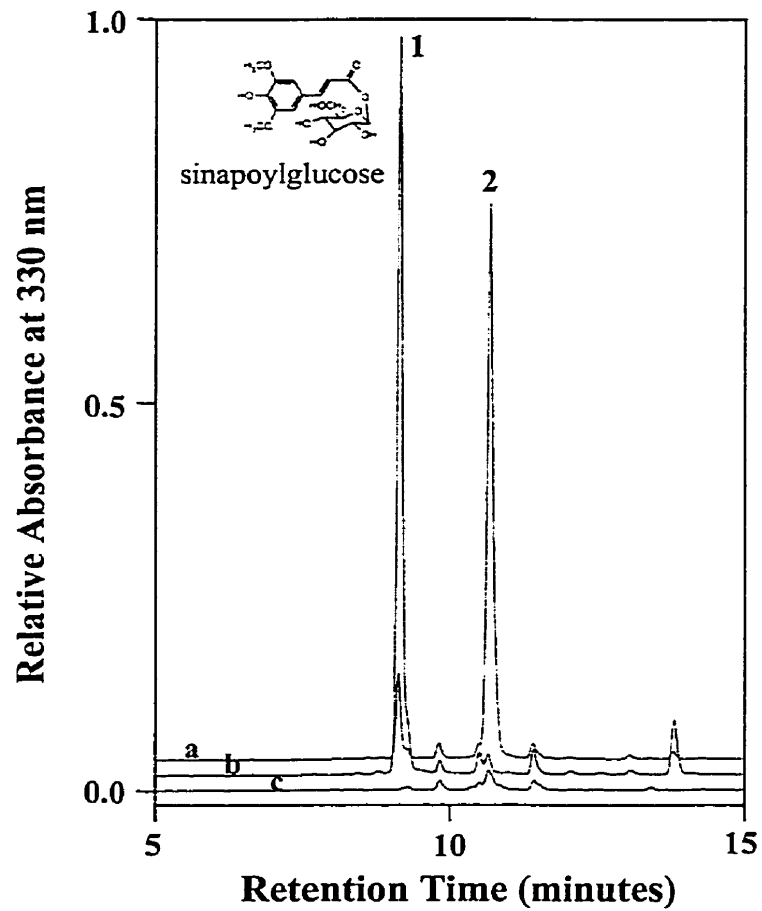


**Figure 4.8.** Reverse phase HPLC separation of MeOH (80%) extracts of whole *B. napus* cotyledon (a), wild-type *Arabidopsis* (b), and the *Arabidopsis* mutant *sng1* (c), which does not make sinapoylglucose. Peaks corresponding to compounds 1 and 2 from *B. napus* are labelled as in Fig. 4.7. Compounds were detected during elution by measuring absorbance at 330 nm.

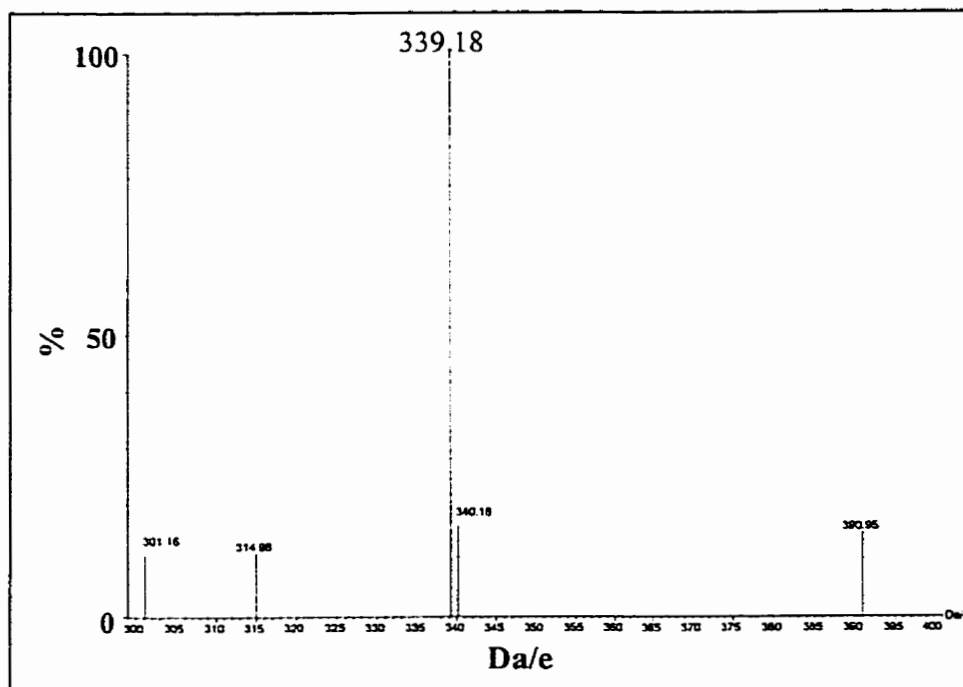


**Figure 4.9.** Electrospray ionization mass spectrum of reverse phase HPLC-purified compound 2 from *B. napus* cotyledons. The dominant peak at 339.18 corresponds to the mass of sinapoylmalate.

It is possible that phosphoric acid in the solutions was interfering with the ionizations. This problem may be remedied by substituting trifluoroacetic acid for phosphoric acid in the HPLC elution buffer, since this volatile acid could be removed by drying pooled samples down under vacuum. However, this was not performed in this study.

Crystallization was attempted to identify the remaining sinapates. After 48 h under crystallization conditions compound 1 had formed clusters of thin transparent plates. These plates appeared to be crystalline because they were able to polarize light when placed between two polarizing filters and viewed under a microscope. The solvents for the other compounds evaporated to dryness without visible evidence of crystal formation. Compound 5, which eluted from the RP HPLC column under the most non-polar conditions, partitioned into amber-coloured oil-like droplets that were dispersed throughout the solution within 24 h of evaporation and remained in this state until evaporation to dryness. The compounds were redissolved in a number of different solvents and slowly evaporated at 4°C and room temperature, without successful crystallization. The solvents used were: water, 20% MeOH, EtOH, 80% EtOH, and 20% EtOH. In each case the solvent was allowed to fully evaporate and then redissolved in another solvent. The starting volume was reduced to 200  $\mu$ L using 80% MeOH. During this trial, compound 5 yielded octahedral crystals. However, crystallographic analysis revealed these crystals to be an unidentified inorganic salt (data not shown).

The blade-like crystals from compound 1 were used for crystallographic analysis. They ranged in size up to 1 mm long and 0.3 mm wide, with a thickness as much as 0.03 mm. The identity of compound 1 was found to be sinapoylglucose (Fig. 4.10, Table 4.1) as suggested based on comparison to *Arabidopsis* pigments (Fig. 4.8). This is the first structure of a sinapic acid glycosyl ester to be solved by X-ray crystallography. Only the structure of the parent compound,

sinapic acid (Allen et al. 1991), can be found in the Cambridge Structural Database for small molecules (Cambridge Crystallographic Data Centre, Cambridge, UK).

To summarize, compound 1 has been identified by X-ray crystallography as 1-sinapoylglucose, compound 2 has been identified as 1-sinapoylmalate by ESI-MS. As well, it was possible to identify compound 3 as a kaempferol derivative based on previous work (Wilson et al, 1998).

#### **4.3.4 Distribution of UV-absorbing compounds in cotyledons and induction by UV-B.**

Sinapoylmalate (compound 2) and sinapoylglucose (compound 1) were the main UV-B-absorbing compounds in epidermal protoplasts from *B. napus* cotyledons (Fig. 4.11). These two sinapates also accumulated to a greater degree in UV-B-exposed cotyledons, increasing more than the other peaks combined. Compounds 3, 4 and 5 also accumulated due to UV-B, but to a lesser degree. *In toto*, these 5 compounds would appear to account for the majority of the vacuolar UV-B-screening capacity in *B. napus* cotyledons. The other compounds present in the extracts, including the kaempferol glycosides, were enriched compared to whole cotyledon tissue but were still present in small amounts relative to the sinapates. Comparison of epidermal protoplasts to mesophyll protoplasts was difficult since the mesophyll preparation contained epidermal cells. Nonetheless, extracts of the mesophyll preparations contained similar profiles of sinapic acid compounds, however, at much lower concentrations.



**Table 4.1.** Crystallographic data and refinement parameters for solution of structure of  
1-sinapoylglucose.

<b>Crystal Data</b>	
$C_{17}H_{22}O_{10}$	Mo $K\alpha$
$M_r = 386.3$	$\lambda = 0.71073 \text{ \AA}$
Orthorhombic	Cell parameters from 50 reflections
$P2_12_12_1$	$\theta = 27^\circ$
$a = 4.8530 \text{ \AA}$	$\mu = 0.12 \text{ mm}^{-1}$
$b = 27.1763 \text{ \AA}$	$T = 300 \text{ K}$
$c = 15.7593 \text{ \AA}$	Plate $1.0 \times 0.3 \times 0.01 \text{ mm}$
$\alpha = 90^\circ$	Colourless
$\beta = 90^\circ$	
$\gamma = 90^\circ$	
Volume = $2078.444 \text{ \AA}^3$	
$Z = 2$	
$D_x = 1.407 \text{ mg m}^{-3}$	
$D_m$ not measured	
<b>Data Collection</b>	
Siemens P4 diffractometer	$R_{int} = 0.1573$
$\omega/2\theta$ scans	$\theta_{max} = 53.11^\circ$
Absorption correction: none	$h = -5 \rightarrow 6$
17472 measured reflections	$k = -19 \rightarrow 19$
4282 independent reflections	$l = -34 \rightarrow 34$
1308 reflections with $I > 2\sigma(I)$	3 standard reflections frequency: 120 min
	Intensity decay: none
<b>Refinement</b>	
Refinement on $F^2$	
$R(F) = 0.1198$	$\Delta\rho_{max} = 0.66 \text{ e \AA}^{-3}$
$WR(F^2) = 0.3516$	$\Delta\rho_{min} = -0.55 \text{ e \AA}^{-3}$
$S = 1.003$	Extinction correction: none
4282 reflections	Scattering factors from International
113 parameters	Tables for X-ray Crystallography (Vol. IV)
H atoms not refined	
$w = 1/[\sigma^2(F_o^2) + (0.1939P)^2 + 3.61P]$	
where $P = (F_o^2 + 2F_c^2) / 3$	

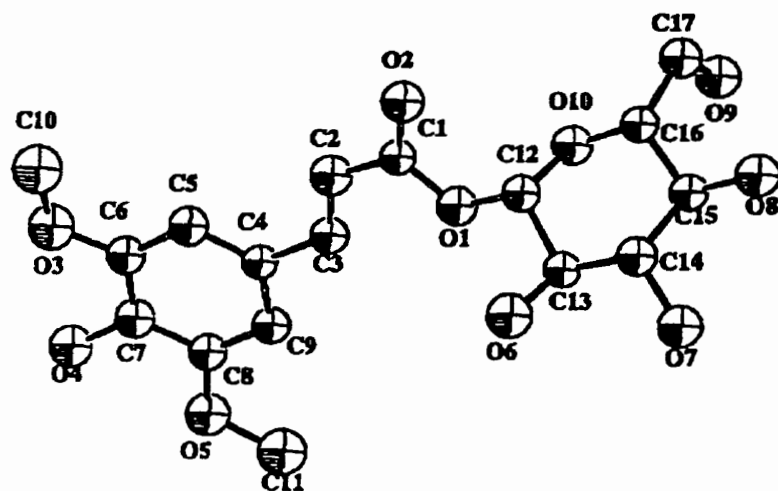


**Figure 4.10.** The crystal structure of 1-sinapoylglucose (compound 1) isolated from *B. napus* cotyledons. Displacement ellipsoids are shown at the 50% probability level. Hydrogens are not shown.

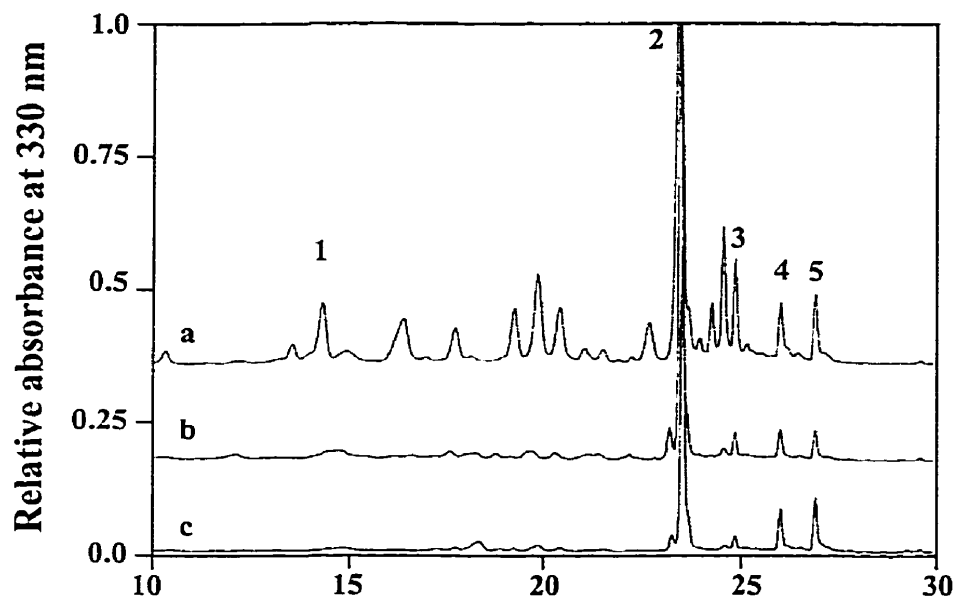


**Figure 4.11.** Separation of UV-B-absorbing compounds from epidermal protoplasts (a), mesophyll protoplasts (b) and cotyledon total extracts (c), using RP-HPLC (absorbance at 330 nm shown).

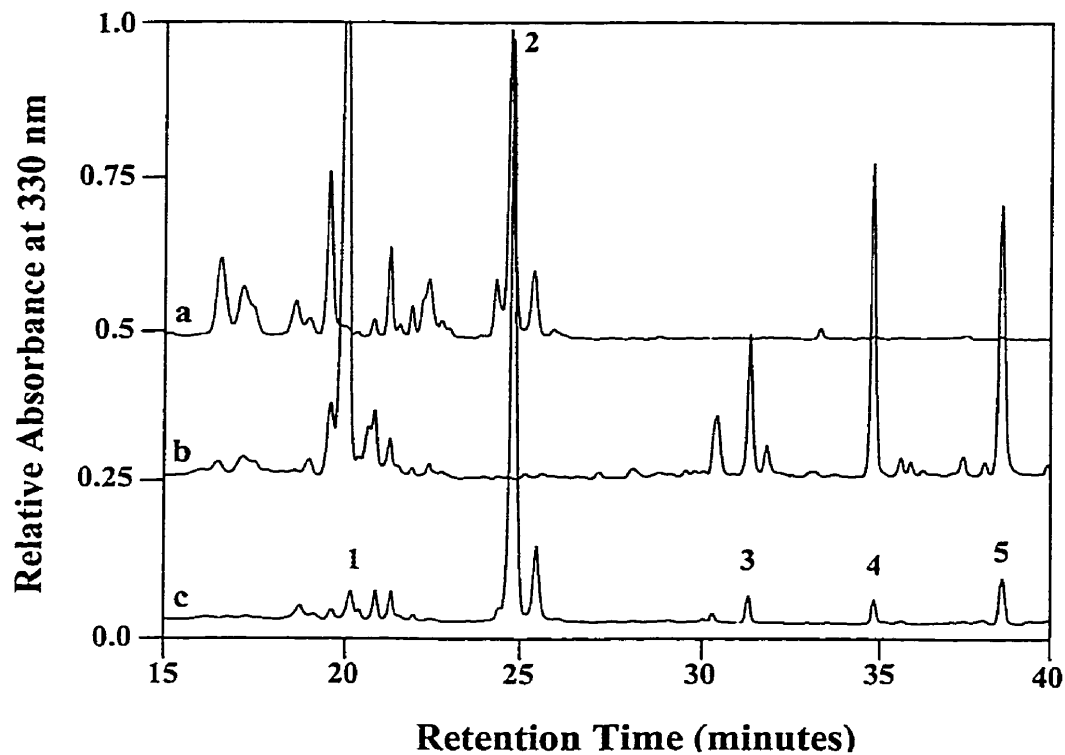


**Figure 4.12.** Comparison of compounds from cotyledons of *B. napus* (c) and its parent species *B. campestris* (a), and *B. oleracea* (b). UV-absorbing compounds from cotyledons were extracted into 80% MeOH and separated using RP-HPLC. Elution of compounds was monitored using absorbance at 330 nm. Compounds are labelled as in Fig. 4.7.

Since *B. napus* is an amphidiploid hybrid of *B. campestris* (*B. rapa*) and *B. oleracea*, it was of interest to determine if these compounds are also produced by both of its parent species. Sinapoylmalate was completely absent from *B. oleracea*, which contained sinapoylglucose along with compounds 3, 4 and 5 (Fig. 4.12), whereas, *B. campestris* appeared to accumulate only sinapoylmalate. Thus, *B. napus* has the biosynthetic pathways from both parental lines.

#### 4.4 DISCUSSION

The contribution that epidermal cells make to the acclimation of cotyledons to UV-B has been investigated by utilizing a rapid procedure for isolating these cells from the upper epidermis of cotyledons after they were exposed to UV-B radiation. Examination of proteins in the epidermal protoplasts revealed changes in the abundance of at least six proteins after irradiation of cotyledons with UV-B. Two 66 kDa protein isoforms, which were present 12 h after UV-B irradiation are photocross-linked heterodimers of the rubisco large and small subunits (Wilson et al, 1995). There was also a modest increase in the abundance of the flavonoid biosynthesis enzyme, CHS. An increase in UV-B-absorbing compounds was one of the early events during acclimation of cotyledons to UV-B. There was a 30% increase in the total UV-B absorbance after a 12 h UV-B irradiation of cotyledons. Unlike leaves, however, the compounds that accumulate in cotyledons are predominately sinapic acid esters, rather than flavonoids. Sinapoylglucose and sinapoylmalate were identified as two of the key absorbing sinapoyl esters in *B. napus* cotyledons.

The protoplasts isolated had active transvacuolar cytoplasmic streaming and took up neutral red dye into their vacuoles, indicating the presence of a membrane potential and functional integrity. The epidermal cell isolation procedure also allowed the observation of the

presence of chloroplasts in these cells. This was reflected in the protein profiles, which contained rubisco. Chloroplasts have been reported in epidermal cells from spinach, *Arabidopsis* and tobacco (Rose et al, 1975; Rother et al, 1988; Vorst et al, 1993; Winter et al, 1994). As well, the smaller size of epidermal chloroplasts compared to mesophyll chloroplasts observed in this study is consistent with previous reports of epidermal chloroplasts from spinach (Lawrence and Possingham, 1986). The presence of chloroplasts in the epidermal cells raises questions about the nature of the thylakoid membranes in these organelles, and whether they can adapt to UV-B so that the photosynthetic apparatus is not excessively damaged. Since the epidermal cells do not benefit from the UV-B-screening they provide to the mesophyll, the sustained effects of UV-B on proteins of these cells may have important ramifications for cell viability.

The presence of an acclimation process affecting soluble proteins in epidermal cells was apparent from 2D PAGE analysis. At least three proteins decreased and three increased in abundance during the 12 h period after UV-B irradiation. The function of these proteins should provide clues to the cellular processes affected by UV-B and the nature of changes, which might minimize damage in epidermal cells. The elevated accumulation of CHS in epidermal cells of cotyledons exposed to UV-B indicates that, like epidermal cells in leaves, they are able to up regulate in biosynthesis of flavonoids in response to UV-B to some extent (Schmelzer et al, 1988; Wilson et al, 1998). However, the modest increase in abundance of CHS in the epidermal protoplasts from UV-B irradiated cotyledons implies there are other screening mechanisms. The presence of CHS in control seedlings may indicate that CHS is at least partially induced in PAR by phytochrome as is the case for another member of the mustard family, *Sinapis alba* (Batschauer et al, 1991). It also implies there are other screening mechanisms.

Phenylpropanoids are very important compounds since they can act as optical screens for UV-B as well as antioxidants (Castelluccio et al, 1995; Takahama and Oniki, 1997). The dominant phenylpropanoids in seeds and cotyledons of the Brassica family are sinapates (Strack et al, 1978; Linscheid et al, 1980). They are synthesized from phenylalanine which originates from the shikimic acid pathway (Fig. 4.13). Sinapic acid esters are excellent screens against solar UV-B since they all have one strong absorbance maximum at 330 nm which decreases to a minimum at 260 nm (Sheahan, 1996). They also have an extinction coefficient in the UV-B range similar to flavonoids (Sheahan, 1996). Sinapoylglucose and sinapoylmalate are the most abundant UV-B-absorbing compounds in *B. napus* cotyledons. Along with two unidentified sinapic acid esters, they increase approximately 30 % during a 24 h acclimation to UV-B.

Sinapic acid esters are already present in cotyledons because they play an important role as a carrier of storage metabolites in *Brassica napus* during seed formation and germination (Strack et al, 1978; Vogt et al, 1993). Conjugation of sinapic acid with choline provides a storage pool for choline in seeds. The choline that is released during germination as precursors for lipid biosynthesis. Vacuolar enzymes transfer glucose to the free sinapic acid, which can subsequently be exchanged for malate (Strack, 1982; Sharma and Strack, 1985). There are a number of other sinapoyl esters in the mustard family, some of which have been identified (Linscheid et al, 1980). These versatile secondary metabolites are also precursors for extracellular guaiacyl-syringyl lignin. Thus, the seed sinapates might serendipitously be stored in vacuoles of epidermal cells during seed germination where they can subsequently be used as a UV-B screen. It would be interesting to determine if there is actually new sinapate ester synthesis during UV-B acclimation or simply less degradation.

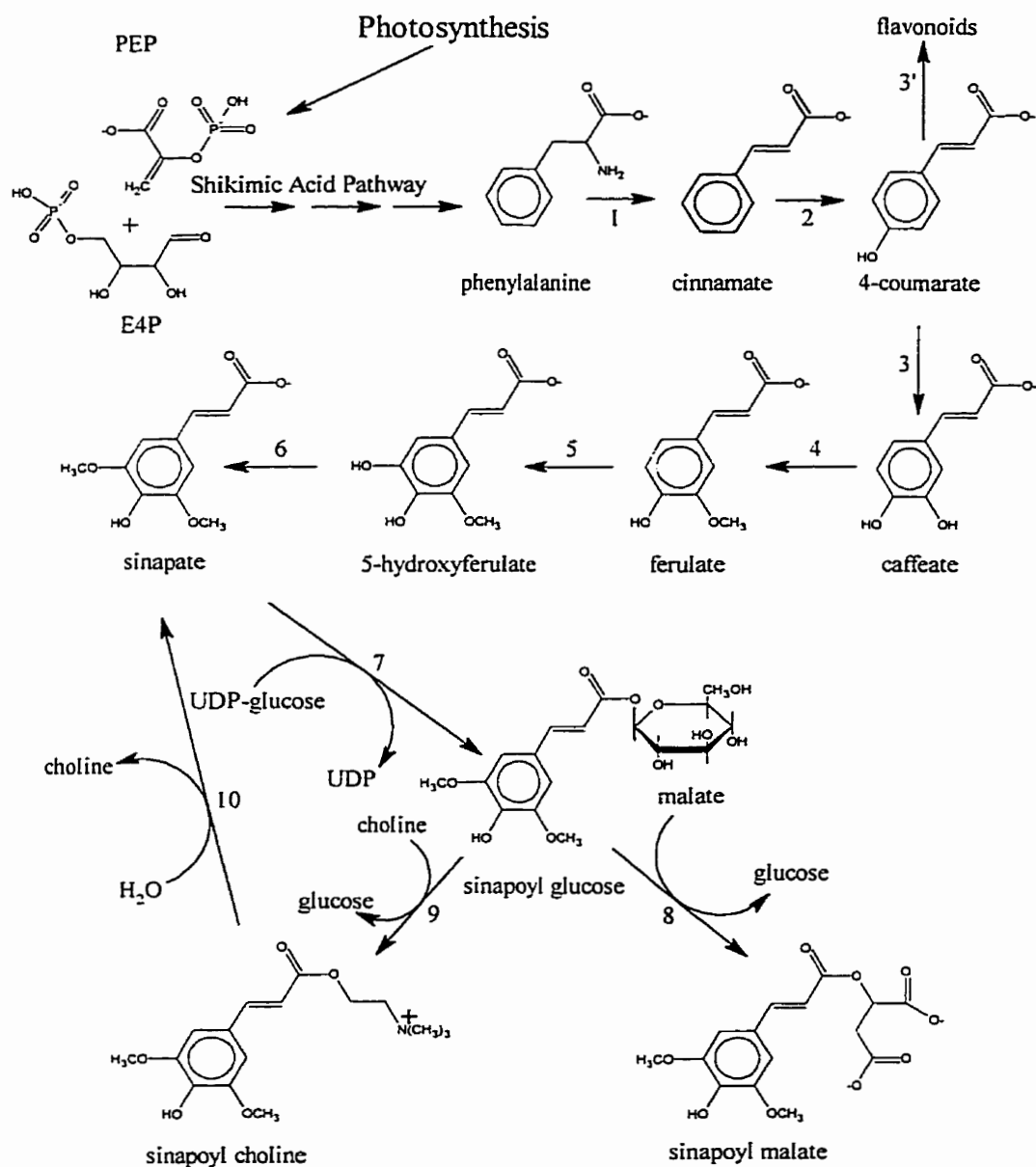


**Figure 4.14.** The biosynthetic pathway leading to sinapic acid esters. PEP, phosphoenolpyruvate; E4P, erythrose-4-phosphate; 1, phenylalanine ammonia lyase; 2, cinnamate-4-hydroxylase; 3, 4-coumarate-3-hydroxylase; 3', 4-coumarate-CoA ligase; 4, caffeate *O*-methyltransferase; 5, ferulate 5-hydroxylase; 6, 5-hydroxyferulate *O*-methyltransferase; 7, UDP-glucose:sinapoyl transferase; 8, sinapoylglucose:malate sinapoyltransferase; sinapoylglucose:choline sinapoyl transferase; 10, sinapoylcholine esterase.



If sinapate biosynthesis is modest during exposure to UV-B, this would imply, when the seed is formed, the initial capacity to protect against UV-B has also been stored as sinapoylcholine. Such a scenario would allow seedlings to acclimate rapidly if UV-B irradiation is high during germination.

Because sinapic acid esters seem to play an important role during acclimation to UV-B in *B. napus* cotyledons, it was important to determine how common these sinapoyl esters were in other members of the Brassica family. Cotyledons of *B. napus* contain two unidentified sinapic acid esters that are not found *Arabidopsis*. In addition, sinapoylmalate was not detected in *B. oleracea*, and sinapoylglucose along with two other unidentified sinapic acid esters were not detected in *B. campestris*. The absence of sinapoylmalate in *B. oleracea* indicates that sinapoylglucose:malate sinapoyltransferase (SMT) may not be present in these cotyledons (Strack, 1982). These species may present a unique opportunity to study the evolution of a biosynthetic pathway for secondary metabolites. It is interesting to consider that *B. napus* is able to utilize sinapate esters from both parental lines, and whether this might provide additional tolerance to UV-B compared to the two parent species. How wide spread these differences are among other *Brassica* cultivars and other developmental stages is not known. It should be cautioned, however, that only one developmental stage has been sampled in this study, other stages might have different patterns of biosynthesis.

The persistence of high levels of sinapate metabolism in mature leaves of *Arabidopsis* may be due to the lower capacity for flavonoid biosynthesis in these plants. Hence, both sinapate and flavonoid biosynthesis may be required to produce sufficient concentrations of UV-B screening compounds in *Arabidopsis* (Landry et al, 1995; Sheahan, 1996). Certainly the different developmental patterns of phenylpropanoid metabolism in these two species is worth considering.

The accumulation of sinapic acid esters in cotyledons is in contrast to the accumulation of flavonoids in leaves of *B. napus* (Wilson and Greenberg, 1993a; Wilson et al, 1998). Although CHS, accumulates to a modest degree under UV-B, and there is some increase in flavonoids in cotyledons, the sinapic acid esters are apparently utilized to a greater degree. This is likely a result of the importance of sinapic acid metabolism during germination and its UV-B-screening properties, which make biosynthesis of flavonoids unnecessary. In leaves, flavonoids could provide a more diverse set of biological functions. For instance flavonoids can act as pro-oxidant allelochemicals against phytophagous species of insects, as antioxidants within plant cells and/or antifungal phytoalexins (Dixon et al, 1996; Yamasaki et al, 1997). This is also reflected by the complex regulation of CHS genes. In particular, CHS in cotyledons of alfalfa is rapidly induced by wounding but not by UV-B (McKhann and Hirsch, 1994). Moreover, leaves are much longer-lived than cotyledons and therefore must have more stable protection mechanisms. However, the selection of flavonoids over sinapates in leaves is not due to stronger absorbance, as they both have very similar extinction coefficients between 290 and 320 nm (Sheahan, 1996).

Another consequence of UV-B irradiation is an increase in the concentrations of cellular hydrogen peroxide (Rao et al, 1996) by the action of UV-B-absorbing photosensitizers such as tryptophan (Andley and Clark, 1989a). As well as acting as a UV-B screening compound, sinapic acid esters may play a role in cellular antioxidant metabolism. Vacuolar hydroxycinnamic acids act as substrates for vacuolar ascorbate peroxidases (Takahama and Oniki, 1997). Hence, accumulation of these compounds could also increase the capacity of the vacuole to metabolize hydrogen peroxide. Such a hydrogen peroxide scavenging system might explain how epidermal cells, which are unshielded, can survive solar UV-B. In epidermal cells of leaves, flavonoids play a similar role as antioxidants (Castelluccio et al, 1995; Rao et al, 1996).

The epidermal cells of *B. napus* cotyledons play an active role in protection of this vital organ from UV-B during the early stages of plant development. The UV-B-absorbing compounds in cotyledons, which are predominately sinapoyl esters, are distinct from the flavonoids found in leaves. The epidermal cells of cotyledons respond to UV-B irradiation not only by accumulating these compounds, but also by changing the abundance of particular proteins. Hence, the complexity of plant acclimation to solar UV-B is readily studied in epidermal cells and further investigation may lead a better understanding of the mechanisms that minimize damaging effects of solar UV-B.

## 5. UV-B-INDUCED PHOTOCROSSLINKING OF RUBISCO SUBUNITS

### 5.1 INTRODUCTION

Decreases in the concentration of ozone in the stratosphere are resulting in higher levels of UV-B (290-320 nm) reaching the Earth's surface (Kerr and McElroy, 1993; Madroinch et al, 1995; Coldiron, 1996; Moseley and Mackie, 1997). The increases in UV-B will be disproportionately greater for wavelengths shorter than 300 nm. This is due to the absorption spectra of the stratospheric ozone layer (Caldwell et al, 1989). In animals, proteins in the lens of the eye, or in exposed skin are particularly vulnerable (Andley and Clark, 1989; Devary et al, 1993; Stuart and Doughty, 1996; Gilchrest et al, 1996). For example, cross-linking of lens proteins ( $\alpha$ -crystallins) resulting from UV-B-irradiation can give rise to cataract formation (Schauerte and Gafni, 1995). Also, skin exposed to solar UV-B radiation undergoes premature aging as a result of changes in proteins and DNA (Fisher et al, 1996; Huang et al, 1997; Scharffetter-Kochanek et al, 1997).

Analysis of UV-B photomodified proteins has been carried out for only a hand full cases (Pigault and Gerard, 1984, Pigault and Gerard, 1989). One example, the crystallin family of proteins ( $\alpha$ ,  $\beta$ ,  $\gamma$ ) from mammalian lens have been studied in relation to cataract formation (Tallmadge and Borkman, 1990; Hott and Borkman, 1992; Taylor, 1994; Schauerte and Gafni, 1995; Andley et al, 1997). The crystallins, are small proteins (20-22 kDa) which form large complexes (>800 kDa) in the lens. They are present at concentrations up to 35% (~500 mg mL<sup>-1</sup>) by weight (Chiesa et al, 1990; Delaye and Tardieu, 1983). The ordered arrangement and solubility of these proteins is largely responsible for the transparency of the lens (Delaye and Tardieu, 1983; Rao et al, 1995). Photocrosslinking of these proteins occurs during UV-B-irradiation and results in turbidity of the lens (Li et al, 1990). The  $\alpha$ -crystallin complex has a chaperone function required for maintaining

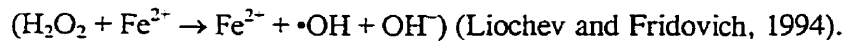
solubility of other crystallins, which is disrupted by UV-B radiation (Borkman and McLaughlin, 1995; Lee et al, 1997).

There are no equivalent studies of plant proteins, even though plants are exposed to higher doses of solar UV-B. There is evidence, that the carbon fixing enzyme of chloroplasts, ribulose-1,5-bisphosphate carboxylase oxygenase (rubisco; E.C. 4.1.1.39) is affected by UV-B. A decrease in rubisco specific activity occurs when plants are grown under UV-B (Vu et al, 1984). Losses of total rubisco activity also result from UV-B irradiation. This may be due to degradation of the enzyme or reduced transcription of the genes encoding rubisco, rather than photomodification of the enzyme (Strid et al, 1990; Caldwell, 1993; He et al, 1993; Jordan et al, 1993). To date, only the inhibition of  $K^+$ -ATPase activity in *Canthareus roseus* cells (Imbrie and Murphy, 1984) and disruption of the structural proteins of microtubules in plants (Zaremba et al, 1984; Staxen et al, 1993) have been shown to be a direct effect of UV-B irradiation.

Plants, because of their sessile nature, are exposed to solar UV-B to a much greater extent than animals. They must also balance shielding of solar radiation against the requirement for light-harvesting in order to maintain their photosynthetic metabolism. Hence, plants receive relatively high daily doses of solar UV-B radiation. Proteins in plants become oxidized when exposed to UV-B radiation *in vivo* as judged from the increased numbers of carbonyl groups present in proteins after irradiation (Levine et al, 1990; Landry et al, 1995; Rao et al, 1996). Carbonyls may result from oxygenation of tryptophan, histidine, arginine, lysine and proline (Amici et al, 1989). For example, glutamyl semialdehyde is a product of arginine oxidation (Climent and Levine, 1991).

There is a distinct lack of information about the photomodifications of plant proteins by UV-B. Furthermore, evidence for direct effects of UV-B on proteins continues to increase for animal systems (Devary et al, 1993; Schauerte and Gafni, 1995; Vile et al, 1995; Bender et al,

1997). A direct effect would involve the absorbance of UV-B by a tryptophan residue, followed by chemical reaction of the tryptophan to produce a modified residue (eg. oxygenation) (Foote, 1984). An indirect modification of proteins by UV-B occurs when the chemical modification occurs on an amino acid residue other than tryptophan. That is, tryptophan can act as a photosensitizer, once in an excited triplet state after absorbing a UV-B photon, it can pass an electron to oxygen producing oxygen free radicals such as  $\bullet\text{O}_2^-$ , which can dismutate to yield  $\text{H}_2\text{O}_2$  (Pigault and Gerard, 1989; Halliwell, 1992; Foote, 1991). The  $\text{H}_2\text{O}_2$  can then diffuse to other locations in the protein and react with other residues in the presence of iron (Andley and Clark, 1989b; Guptasarma et al, 1992; Shimmura et al, 1996; Smith et al, 1997b; Brenneisen et al, 1998). The reactivity of  $\text{H}_2\text{O}_2$  depends on the presence of  $\text{Fe}^{2+}$  for the formation of the hydroxyl radical,  $\bullet\text{OH}$ , which occurs via a Fenton-like reaction:



In this study, the effects of UV-B on rubisco were examined at the molecular level both *in vivo* and *in vitro*. Rubisco is a 550 kDa enzyme complex consisting of four catalytic homodimers of large subunit (LSU) (i.e. a total of eight LSUs), and capped at either end by eight small subunits (SSU) (Knight et al, 1990). Rubisco accumulates in chloroplasts to very high concentrations ( $\sim 250 \text{ mg mL}^{-1}$ ) similar to the levels of crystallins in the lens (Lawlor, 1987; Winter et al, 1994). It was found that a specific  $\sim 66 \text{ kDa}$  variant of rubisco subunits is formed *in vivo* via intersubunit photocross-linking in a number of species after exposure to UV-B. The same photocross-linked heterodimer also forms after UV-B irradiation of partially purified rubisco *in vitro*. Hence, further investigation of the mechanism of photocross-link formation was carried out, including identification of a putative site of cross-linking.

## 5.2 MATERIALS AND METHODS

### 5.2.1 Growth and Lighting Conditions

Seeds of *Brassica napus* L. cv Topas (canola), *Pisum sativum* L. cv Trapper, and *Lycopersicon esculentum* cv Sub-arctic Maxi were germinated for 21 days in Pro-Mix potting media (Premier Brands) in growth chambers at a temperature of 22°C. Plants were grown under visible light with a 16h light:8h dark photoperiod. Photosynthetically active radiation (400-700 nm, PAR) at the soil surface ( $70 \mu\text{mol m}^{-2} \text{s}^{-1}$ ) was generated with cool white fluorescent lamps (F48T12CW; General Electric Co., Wilmington, MA) filtered through clear polyester film (0.08 mm; Johnson Industrial Plastics, Missasauga, ON) to screen out extraneous UV-B and UV-C radiation (<310 nm). After 21 days, plants were treated for up to 32 h with continuous visible light plus either UV-A (320–400 nm) for control conditions or UV-A plus UV-B (290–400 nm) for UV-B conditions. During the treatment period visible light ( $70 \mu\text{mol m}^{-2} \text{s}^{-1}$ ) plus UV-B ( $1 \mu\text{mol m}^{-2} \text{s}^{-1}$ ) was generated with the addition of UV-B fluorescent lamps (FS40 for UV-B, National Biological Co.) filtered through 0.08 mm cellulose diacetate to screen out UV-C (<290 nm). Visible light plus UV-A ( $0.5 \mu\text{mol m}^{-2} \text{s}^{-1}$ ) was generated by filtering radiation from the UV-B lamps through 0.08 mm polyester film which has a 310 nm transmittance cut-off.

The spectral photon distributions and fluence rates of all light sources were measured at the level of the leaves using a calibrated spectroradiometer (Optronic Model 752, Orlando, FL, USA or Instaspec II, Oriel, Stratford, CT) (at 1 nm intervals and a 1 nm bandwidth) or with a radiometer (Photodyne Technologies, Canoga Park CA) and interference filters (10 nm half-power bandwidth) to isolate individual bandwidths (Fig. 5.1). The fluence of PAR was also measured using a calibrated quantum sensor (LiCor, Lincoln, NB). The biologically effective dose of UV-B used in the *in vivo* plant experiments was equivalent to  $300 \text{ mW m}^{-2} \text{ UV-B}_{\text{BE}}$  for treated plants and  $10 \text{ mW m}^{-2} \text{ UV-B}_{\text{BE}}$

for control plants using Caldwell's general plant damage action spectra normalized at 300 nm (Caldwell, 1971).

A culture of *Synechococcus leopoliensis* PCC 6301 (UTCC 102) was obtained from University of Toronto Culture Collection (UTCC, University of Toronto, Toronto, ON) and inoculated into a sterile 2L flask containing 1L of sterilized BG11 media (NaNO<sub>3</sub>, 17.65 mM; K<sub>2</sub>HPO<sub>4</sub>·3H<sub>2</sub>O, 0.18 mM; MgSO<sub>4</sub>·7H<sub>2</sub>O, 0.30 mM; CaCl<sub>2</sub>·2H<sub>2</sub>O, 0.25 mM; Citric acid, 0.03 mM; ferric ammonium citrate, 0.03 mM; Na<sub>2</sub>EDTA 0.003 mM; Na<sub>2</sub>CO<sub>3</sub>, 0.19 mM); trace metal mix (H<sub>3</sub>BO<sub>3</sub>, 2.86 g L<sup>-1</sup>; MnCl<sub>2</sub>·4H<sub>2</sub>O, 1.81 g L<sup>-1</sup>; ZnSO<sub>4</sub>·7H<sub>2</sub>O, 0.222 g L<sup>-1</sup>; Na<sub>2</sub>MoO<sub>4</sub>·2H<sub>2</sub>O, 0.390 g L<sup>-1</sup>; CuSO<sub>4</sub>·5H<sub>2</sub>O, 0.079 g L<sup>-1</sup>; Co(NO<sub>3</sub>)<sub>2</sub>·6H<sub>2</sub>O, 0.049 g L<sup>-1</sup>); deionized water; pH 7.4 (UTCC, Toronto, ON). The culture was maintained under low light (~20 μmol m<sup>-2</sup> s<sup>-1</sup> PAR) and bubbled with air containing 1% CO<sub>2</sub> which had been passed through a sterilizing air filter. Subculturing was done once a month or as required. To expose cells to UV-B radiation, a sample of cells (1 mL) were transferred to a quartz cuvette and placed in the sample holder of a spectrofluorometer (Photon Technology International, South Brunswick, NJ). Radiation from a mercury arc lamp (100 W) was passed through a monochromator (Photon Technology International, South Brunswick, NJ) set at 300 nm wavelength with a 10 nm slitwidth and focused on the cuvette using a fused silica condenser lens (f 1.7, Oriel, Stratford, CT). UV-B radiation impinging on the cuvette was measured using both a spectroradiometer with integrating sphere (InstaspecII, Oriel, Stratford, CT) and a radiometer (Photodyne Technologies, Canoga Park CA). The cells were exposed to ~20 μmol m<sup>-2</sup> s<sup>-1</sup> 300 nm radiation (10 nm bandwidth) for 10 min. This very high fluence was used to ensure that proteins were thoroughly exposed to UV-B.



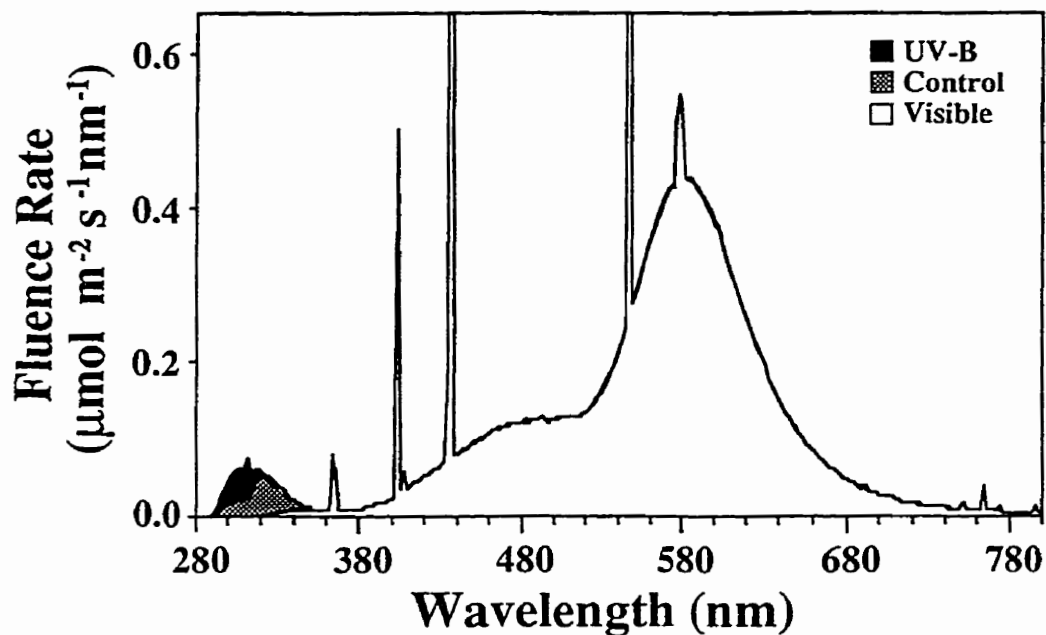


**Figure 5.1.** Spectral output of lamps used for growth of *B. napus* seedlings. Visible light alone ( $\square$ ) was used for germination and growth of plants. The control light source used during the treatment period contained visible plus UV-A ( $\blacksquare$ ). The spectral distribution used for treatment contained of visible plus UV-A and UV-B ( $\blacksquare$ ). Photosynthetically active radiation (400-700 nm, PAR) at the cotyledon surface was  $70 \mu\text{mol m}^{-2} \text{s}^{-1}$ . During the treatment period  $1 \mu\text{mol m}^{-2} \text{s}^{-1}$  UV-B plus UV-A ( $\lambda > 290 \text{ nm}$ ) was added to treatment conditions, and  $0.5 \mu\text{mol m}^{-2} \text{s}^{-1}$  UV-A ( $\lambda > 310 \text{ nm}$ ) was added to control lighting. See section 4.2.1 for details on lighting used.

### 5.2.2 Protein and Immunoblot Analysis

Leaf disks (2 x 0.4 cm<sup>2</sup>) were taken from first fully expanded leaves of individual plants at various times during the treatment period (0', 30', 1h, 2h, 4h, 8h, 12h, 16h, 32h), immediately frozen in liquid N<sub>2</sub> and then stored at -70°C for subsequent protein analysis. Frozen leaf disks were homogenized in protein extraction buffer (50 mM Tris:HCl, pH 8.0; 0.5 mM EDTA; 2 mM DTT, 2 mM PMSF; 10 µM leupeptin; 1 mM *p*-aminobenzamidine; 1% PVPP; 0.02% sodium azide) at 4°C. After centrifugation (14000 x g, 30 min) the concentration of soluble proteins in the supernatant was determined (Ghosh et al, 1989). Proteins were then prepared for either SDS-PAGE or IEF. Aliquots of protein extracts were diluted (2:1) in SDS sample buffer (30% glycerol w/v; 9% SDS w/v; 120 mM Tris-HCl, pH 6.6; 15% 2-mercaptoethanol w/v) and heated at 90°C for 2 min. Proteins were separated by SDS-PAGE (12% acrylamide w/v) in the buffer system of Laemmli (1970). Separated proteins were visualized using Coomassie brilliant blue R staining or silver staining.

For immunological analysis, proteins were electroblotted onto 0.2 micron nitrocellulose membrane (Biorad) using 16 mM glycine; 25 mM Tris-HCl, pH 8.7; 0.02% SDS w/v; 20% methanol as the transfer buffer. Electrophoretic transfer was carried out for 2 h at 300 mA constant current using a Mini Protean II apparatus (Biorad) following the manufacturer's protocol. Transfer of proteins was checked by silver-staining gels after the transfer procedure using the procedure of Rabilloud et al (1988). Protein blots were blocked with 1% milk powder in Tris-buffered saline (25 mM Tris-HCl, pH 7.6; 140 mM NaCl) and incubated with a 1:3000 dilution of a rabbit antiserum raised against rubisco (holoenzyme) purified from *Euglena gracilis* (Gift of Professor M. Edelman, Weitzmann Institute, Rehovot, Israel). Antibody binding was visualized using goat anti-rabbit immunoglobulin G secondary antibody conjugated to alkaline phosphatase according to manufacture's protocol (Biorad). The colour reaction was carried out using blue tetrazolium and

5-bromo-4-chloro-3-indonyl phosphate. The relative molecular weight of the bands which appeared were estimated from migration distances of pre-stained standards had been run on the gel (Biorad). Other anti-rubisco antibodies used were raised against corn, peanut and spinach (gifts from Dr. E.B. Dumbroff; Ghosh et al, 1989), and *Synechococcus* (gift of Dr. F.M. Tabita, Ohio State University).

### **5.2.3 Two-dimensional Electrophoresis**

Protein samples from plants treated for 12 h were separated by two-dimensional gel electrophoresis as described in section 3.2.3. (O'Farrell, 1975). Briefly, aliquots of proteins (50 µg) were prepared for IEF by addition of 9.5 M urea, 10% sucrose, 8% CHAPS, 5% ampholines (pH 3-10), 15 mM DTT and loaded onto tube gels. The IEF tube gels were electrophoresed for 16000 V-h. The proteins in each tube gel were separated in the second dimension by equilibrating each tube gel with SDS sample buffer and placing it on a 1.5 mm thick 10-15% SDS gels with 5% stacking gel. The proteins were electrophoresed for 4 h at 100 V constant voltage. Proteins were visualized by silver staining, or electroblotted for immunodetection using rabbit antisera raised against spinach LSU.

### **5.2.4 Partial proteolytic digests**

Partial proteolysis gels were made by co-electrophoresis of individual proteins with measured amounts of papain (EC 3.4.22.2; Sigma Chemical Co, St. Louis, MI) as described by Cleveland et al (1977) with modifications (Marder et al, 1986). Soluble proteins samples from UV-B-treated plants were loaded onto SDS gels in duplicate, after electrophoresis half the gel was stained with Coomassie blue and the other half was transferred to nitrocellulose for immunodetection using anti-rubisco antibodies as described in section 4.2.2. Bands corresponding to large subunit of

rubisco and a higher molecular weight variant were located on the stained gel using the immunoblot as a reference, those parts of the gel were then excised separately. Each gel slice was immersed in equilibration buffer (0.5 M Tris-HCl, pH 6.6; 0.8% SDS w/v; 10% glycerol; 1% 2-mercaptoethanol; 1 mM EDTA) for 15 min then placed in wells of an SDS gradient gel (15-20% acrylamide w/v; 10 cm x 10 cm x 1.5 mm). The gel was placed in an electrophoresis unit, covered with upper reservoir buffer and then covered with equilibration buffer (10  $\mu$ L). An overlay buffer (10 $\mu$ L) containing various concentrations of papain (0-25 ng mL<sup>-1</sup>) was added to each well. The protein mixture was electrophoresed for 1.5 h at 100V, the electrophoresis was stopped for 30 min to allow proteolysis to occur and electrophoresed for 3 h at 100V. Proteins were transferred to nitrocellulose and proteolytic fragments of rubisco subunits immunodetected with rabbit antisera raised against rubisco (holoenzyme) from *Euglena gracilis*.

#### **5.2.5 Partial Purification of rubisco holoenzyme from leaves of *B. napus* L.**

Rubisco holoenzyme was purified from leaves of *B. napus* cv Topas using a rapid purification method adapted from Salvucci et al (1986). Forty grams of leaves from three week-old plants grown in Pro-Mix potting media (Premier Brands) in growth chambers at a temperature of 22°C under 100  $\mu$ mol m<sup>-2</sup> s<sup>-1</sup> PAR with a 16 h L/8 h D photoperiod, were harvested into a chilled 500 mL Waring blender (Waring, New Hartford, CT). 200 mL of homogenization buffer chilled on ice (0.33 M sorbitol, 10 mM PP<sub>i</sub>, 5 mM MgCl<sub>2</sub> and 4 mM ascorbate adjusted to pH 6.5 with HCl before chilling) was added and the mixture homogenized two times for 30s at 4°C. The homogenate was kept on ice during all steps. The resulting brei was filtered through two layers of Miracloth (Calbiochem, San Diego, CA) to remove unhomogenized tissue and cellular debris, and the filtrate distributed into six 50 mL tubes and centrifuged at 4000 rpm (1930 g) in a Sorvall SS-34 (Sorvall,

Newtown, CT) rotor for total elapsed time of 1 min to pellet chloroplasts. Mitochondria and other smaller organelles would not be expected to pellet under these conditions. Supernatants were discarded and pellets gently resuspended in 20 mL resuspension buffer (0.33 M sorbitol, 50 mM Hepes pH 7.6 at 22°C, 2 mM CaCl<sub>2</sub>, 2 mM MnCl<sub>2</sub>, 5 mM EDTA, and distributed into four 50 mL tubes and centrifuged at 2000 rpm (482 g) for 1 min to form a pellet enriched with intact chloroplasts. The supernatants were discarded and each pellet gently resuspended in 10 mL of lysis buffer (5 mM Tricine-NaOH pH 8.0, 4 mM 2-mercaptoethanol). The solutions of lysed chloroplasts, were combined into two 50 mL tubes and centrifuged at 4250 rpm (2000 g) for 4 min. The greenish supernatant was then transferred to ultracentrifugation tubes and clarified by ultracentrifugation at 24000 rpm (40000 g) for 20 min in a 60 Ti rotor (Beckman, Mississauga, ON). At this stage the supernatant contains soluble chloroplast proteins in their native state.

Purification of rubisco holoenzyme from this mixture was accomplished by taking advantage of its large size (~550 kDa). In chloroplasts the only other soluble protein complex of a similar size is the chaperonin complex (~720 kDa), hence an ultrafiltration filter with a cut off of 300 kDa was used to separate rubisco from the majority of other soluble chloroplast proteins. Approximately 80 mL of clarified supernatant was placed into a 150 mL Omegacell (Filtron Technology Corp., Northborough, MA) with a 300 kDa cutoff filter which had been equilibrated with distilled water and filtration buffer (50 mM Tricine-NaOH pH 8.0, 150 mM NaCl). The supernatant was concentrated under pressure to 10 mL, and washed twice by adding 50 mL of filtration buffer and concentrating to 10 mL. At this point the rubisco was >95% pure judging from Coomassie-stained SDS PAGE of preparations.

### 5.2.6 *In vitro* Exposure of Rubisco to UV-B.

A series of *in vitro* experiments were carried out using rubisco holoenzyme either purified from *B. napus* as described above, or lyophilized rubisco from spinach (Sigma Chemical Co, St. Louis, MI). In each case, rubisco was resuspended in filtration buffer to a concentration of 1 mg mL<sup>-1</sup> (Ghosh et al, 1988). Initially, exposures were carried out in a sealed 1 mL quartz cuvette and irradiated with 290 nm radiation (2.5 μmol m<sup>-2</sup> s<sup>-1</sup>) from a xenon arc lamp (150 W) which had been passed through a 290 nm interference filter (10 nm half-power bandwidth). Irradiation was for 100 min equivalent to a fluence of 15 mmol m<sup>-2</sup>.

Purified rubisco from *B. napus* was irradiated and compared to protein extracts from UV-B irradiated leaves. The affects of a number of free radical scavengers on rubisco photomodification were tested. The chemicals used were: ascorbate (10 mM), reduced glutathione (10 mM), quercetin (10 μM), propylgallate (10 mM) and β-carotene (saturated solution). Each chemical was added as 10 μL of a 100X stock solution (or a saturated solution in the case of β-carotene) to purified *B. napus* rubisco. To test whether the photoproduct could be formed when *B. napus* rubisco holoenzyme was denatured, urea and CHAPS detergent were added as solids to final concentrations of 4 M and 0.8%, respectively, before irradiation. In other experiments, lyophilized spinach rubisco (Sigma Chemical Co, St. Louis, MI) was reconstituted with D<sub>2</sub>O which increases the rate of reactions involving singlet oxygen by reducing the rate of solvent quenching (Andley and Clark, 1989b).

### 5.2.7 Analysis of amino acid sequences and structures of rubisco from dicots and cyanobacteria.

The availability of both sequence and structural information for rubisco from a number of species was exploited for the purpose of deducing likely sites for the formation of an intersubunit cross-link. The environments around tryptophan residues at the interface between large and small subunits were examined. The species used for comparison were canola, spinach, tobacco, pea and *Synechococcus*. With the exception of *Synechococcus*, all of these species were shown in this study to form the photocross-linked heterodimer *in vivo*.

Amino acid sequences were obtained from NIH GenBank database (National Center for Biotechnology Information, National Library of Medicine, Bethesda, MD). In each case the primary literature reference is given and the accession number for the GenBank database. The following sequences were used for large subunit: spinach (Zurawski et al, 1981; 132051); tobacco (Shinozaki and Sugiura, 1982; 132057); pea (Zurawski et al, 1986; 132009); *Synechococcus leopoliensis* PCC 6301 (UTCC 102), (Reichelt and Delaney, 1983; 132053). Unfortunately no sequence was deposited in the database for canola LSU. However the sequence for one of the genetic parents of canola, *Brassica oleracea*, is available (Manhart, 1992; 1346967). The sequences used for the small subunit comparison were: canola (Baszczyński et al, 1988; 17855); spinach (Knight et al, 1990; 132157); tobacco (Mazur and Chui, 1985; 132160); pea (Fluhr et al, 1986; 132106); *Synechococcus leopoliensis* PCC 6301 (UTCC 102) (Shinozaki and Sugiura, 1983; 132158). The amino acid sequence of LSU is highly conserved across species and between higher and lower plants. Hence the use of the *B. oleracea* sequence, while viewed with caution, should be a very close representation of the *B. napus* sequence. Sequences were aligned for each subunit with the CLUSTALW multiple sequence alignment algorithm (Thompson et al, 1994),

using default settings for alignment parameters. The sequences from the following species of algae were also used for comparison: *Pseudopedinella elastica* (2894825); *Pelagomonas calceolata* (2894823); halophyte algae, *Pleurochrysis carterae* (730478); red algae, *Porphyridium aerugineum* (730479); red algae, *Porphyra purpurea* (1710043); *Odontella sinensis*, (1352822); *Cyanidium caldarium* (585792); red algae, *Antithamnion sp.*, (132134); brown algae, *Pilayella littoralis*, (132152); chromophyte, *Heterosigma akashiwo*, (132149); *Ralstonia eutropha* (132131) (GenBank).

Since tryptophan residues in these proteins are assumed to be the primary photoreceptor for the intermolecular photocrosslinking reaction, the molecular environments around tryptophans were examined. The X-ray crystallographic structures of rubisco holoenzyme from a number of species including spinach, tobacco and *Synechococcus leopoliensis* PCC 6301 (UTCC 102), have been solved to high resolution. Since the UV-B-cross-linked heterodimeric form of spinach rubisco has been shown in this study to form *in vitro*, a spinach structure was chosen for analysis which is in an activated form and contains the substrate analogue 2-carboxyarabinitol-1,5-bisphosphate (CAB) bound in the active site (Shibata, et al 1996; PDB 1BUR). Subsequent experiments with *Synechococcus* described below indicated its structure should be included in the analysis. A structure of *Synechococcus* rubisco also in the activated form with CAP bound in the active site was chosen (Newman and Gutteridge, 1993; PDB 1RBL). Atomic coordinates for these proteins were obtained from PDB (Protein Data Base, Brookhaven National Laboratory Box 5000, Upton, NY) database via the Entrez server system at NIH (<http://www.ncbi.nlm.nih.gov/Entrez>). Structures around each tryptophan were visualized for examination and presentation using the RasMol molecular visualization program (version 2.6) written by Roger Sayle (Glaxo Research and Development, Greenford, Middlesex, U.K.). All



measurements of distances between atoms are based on the atomic coordinates provided by PDB. Hydrogen bond distances are defined as 2.2-3.5 Å between donor and acceptor atoms (Jeffrey and Saenger, 1991). In all cases, the activated form of the enzyme was used for comparison. However, no appreciable differences were observed between activated and inactivated forms in the environments around tryptophans.

#### **5.2.8 Proteolytic digestion and separation of peptide fragments from UV-B-irradiated spinach rubisco.**

To maximize the success of this approach, large amounts of UV-B-cross-linked heterodimers were required. Spinach rubisco holoenzyme (Sigma Chemical Co, St. Louis, MI) was dissolved in 50 mM  $\text{NH}_4\text{CO}_3$  (pH 7.5), at a concentration of 1 mg  $\text{mL}^{-1}$  and placed on ice. For each exposure a fresh preparation was made and 800  $\mu\text{L}$  was pipetted into a quartz cuvette which was placed in the sample holder of a spectrofluorometer (Photon Technology International, South Brunswick, NJ), and irradiated with 20  $\mu\text{mol m}^{-2} \text{s}^{-1}$  300 nm radiation (10 nm half-power bandwidth) for 30 min at room temperature. The radiation source was a 100 W mercury arc lamp, the output of which was passed through a monochromator with 10 nm slit widths and focused by a quartz condenser lens (f 1.7) onto the quartz cuvette. The output and spectra of the radiation were measured using a spectroradiometer (Oriel Instruments, Stratford, CT). In addition, a radiometer (Photodyne Technologies, Canoga Park CA) was calibrated against the spectroradiometer to measure the exposure levels during experiments. After exposure, samples were placed on ice and DTT and  $\text{CaCl}_2$  and added to final concentrations of 15 mM and 2 mM respectively. Clostripain (EC 3.4.22.8) (Sigma Chemical Co, St. Louis, MI), which had been dissolved (1 mg  $\text{mL}^{-1}$ ) in  $\text{NH}_4\text{CO}_3$  (pH 7.5), 15mM DTT, 2 mM  $\text{CaCl}_2$  and activated overnight at

4°C was added to both native and UV-B-crosslinked rubisco at 1:50 (w/w). The mixtures were incubated for 4 h at 37°C. Aliquots (100 µL) were transferred to an eppendorf tube (1.5 mL) at 1 h, 2 h and 4 h after the start of the incubation. To each of these samples was immediately added 50 µL 3X SDS sample buffer (0.5 M Tris-HCl, pH 6.6; 10% glycerol v/v; 10% SDS w/v; 5% 2-mercaptoethanol w/v; 0.05% bromophenol blue w/v). Samples were then heated to 90°C for 2 min and stored at -20°C for later analysis. The partial proteolytic digests were separated using Tricine SDS PAGE (Schagger and von Jagow, 1987). Broad range molecular weight markers (BioRad, Hercules, CA) which were included in each gel include aprotinin (7 kDa).

## 5.3 RESULTS

### 5.3.1 Initial identification of a UV-B-induced product of rubisco.

When *B. napus* plants were grown in PAR for 21 d and then given supplemental UV-B a novel soluble protein appeared in leaf protein extracts. It had an apparent molecular weight of 66 kDa and was detected after a 4 h exposure to UV-B (Fig. 5.2A). The amount of this protein increased over the remainder of the 16 h exposure to UV-B.

Antisera were used in an attempt to identify this 66 kDa protein product. Since rubisco enzyme activity and concentration are diminished when plants are grown under UV-B radiation (Vu et al, 1984; Jordan et al, 1993), antisera raised against rubisco were used. Immunoblots of soluble leaf proteins from UV-B-treated plants exhibited a protein band, approximately 66 kDa, which immunoreacted with antibodies raised against spinach rubisco LSU (Fig. 5.2B).

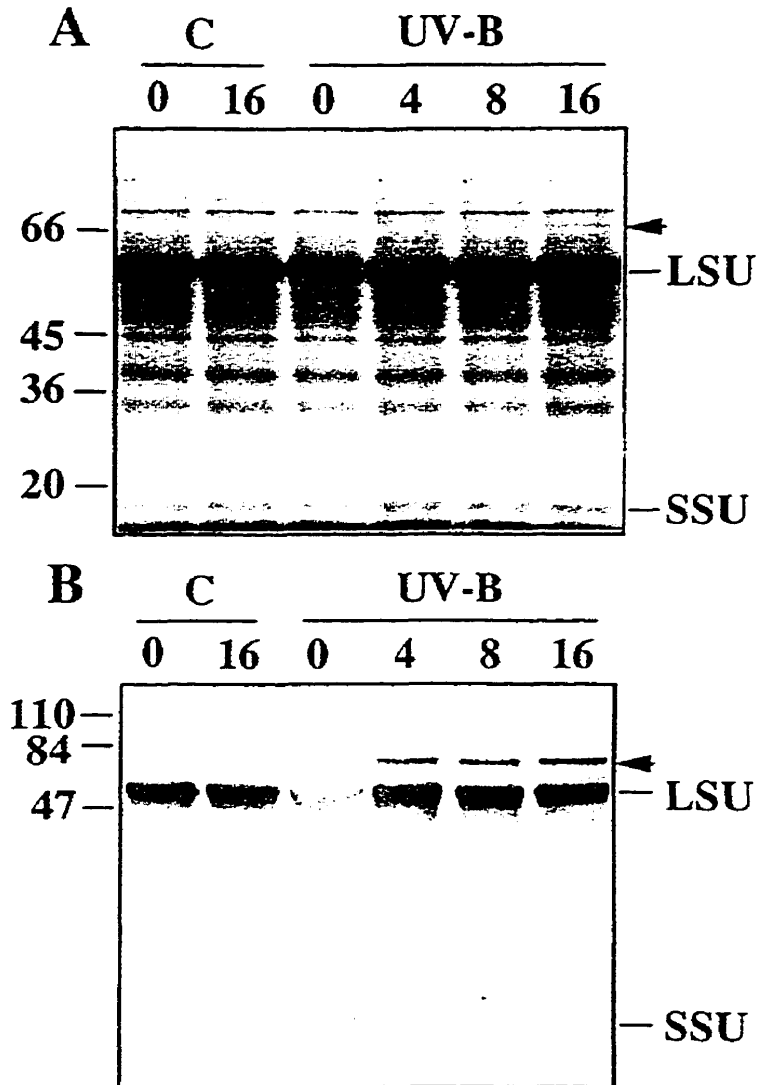


**Figure 5.2.** The effect of UV-B on soluble leaf proteins from *B. napus* grown 21 d without UV and then treated for 16 h with UV-A plus visible (Control) or UV-B and UV-A plus visible (UV-B). A and B, SDS-PAGE and immunoblot analysis of protein samples. Lanes 1-4, samples taken from plants under control conditions after 0, 4, 8 and 16 h respectively; Lanes 5-8, samples taken from UV-B-treated plants after 0, 4, 8 and 16 h respectively. A, Coomassie blue-stained SDS-PAGE gel (12 % acrylamide w/v) of protein samples (15  $\mu$ g). B, immunoblot of protein samples (2  $\mu$ g). Positions of a protein which accumulates during the treatment and the molecular weight standards (kDa) are indicated.

### **5.3.2 Two-dimensional PAGE Analysis**

It has been shown that the subunits of rubisco can be separated into several isoforms each with a slightly different pI, related in some instances to the oxidation state of free cysteines in the molecule (Huner et al, 1981; Robbins and Vaughn, 1983). To identify the 66 kDa UV-B-induced protein, soluble leaf protein samples were separated using 2-D gel electrophoresis. In silver-stained gels of control samples the major isozymes of rubisco LSU and SSU were observed (Fig. 5.3A) (Robbins and Vaughn, 1983).

The isoforms of rubisco were also identified on the immunoblot of the control sample using anti-rubisco immune serum (Fig. 5.3B). The leaf proteins from UV-B-treated plants contained a number of additional protein spots at about 66 kDa each having pIs corresponding to the isoforms of the LSU proteins. These 66 kDa products were detected in silver-stained gels and immunoblots (Fig. 5.3C and 5.3D). This is evidence that the 66 kDa product is a modified form of rubisco containing LSU.

### **5.3.3 Partial Proteolytic Digest Analysis**

Partial proteolytic fragmentation patterns of the unmodified LSU of rubisco and the high molecular weight variant were compared, in an effort to determine whether the 66 kDa protein is a high molecular variant of LSU. Digestion of LSU with the protease papain gave a pattern of peptide fragments characteristic of rubisco (Fig. 5.4) (Bottomley, 1982). Seven of the fragments from LSU were detected with anti-rubisco immune serum. All five proteolytic fragments from the 66 kDa protein matched those derived from the LSU, including one fragment that co-migrated with the LSU.

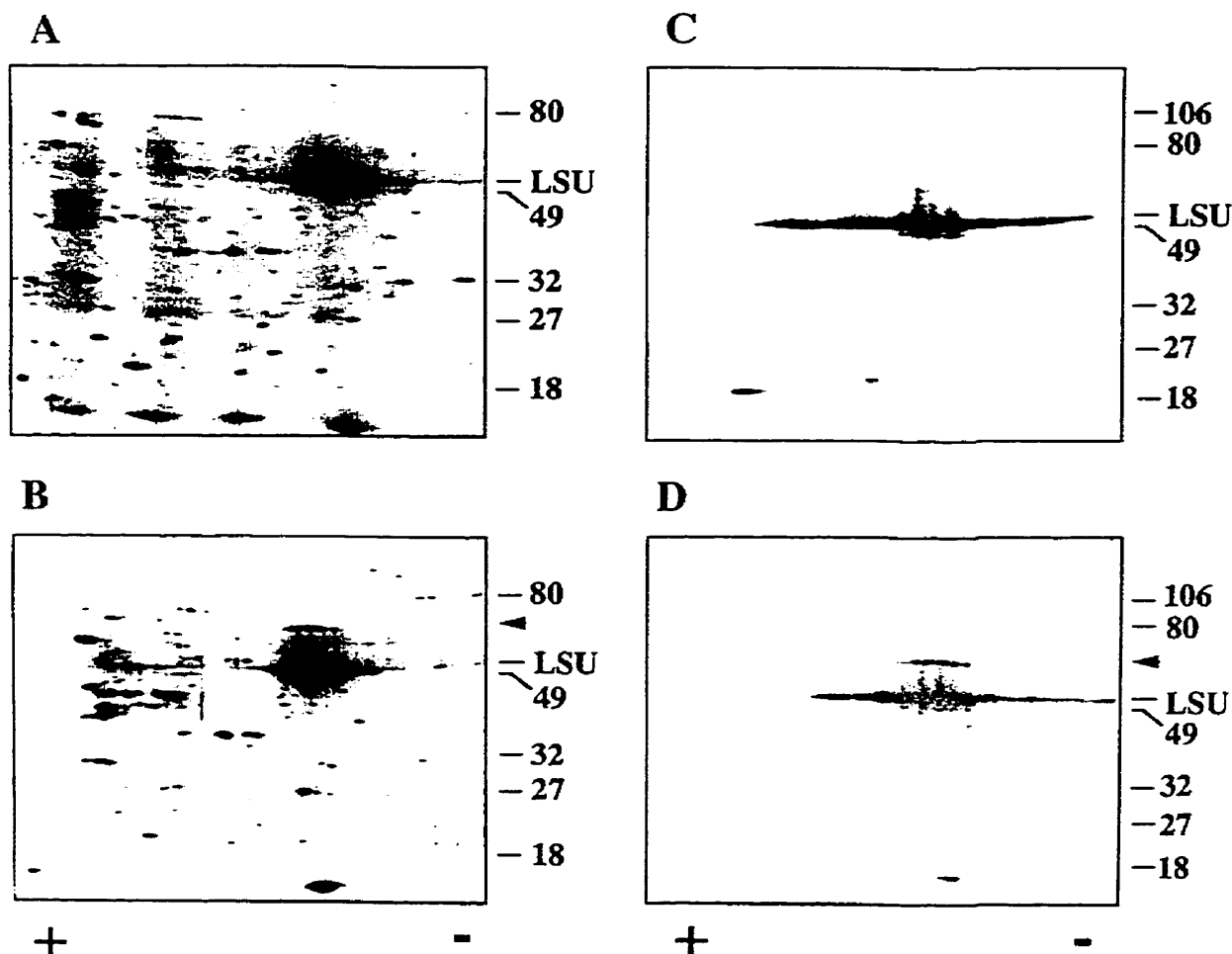


**Figure 5.3.** Two-dimensional PAGE and immunoblot analyses of soluble leaf proteins from control and UV-B-treated *B. napus*. Protein samples (20  $\mu$ g) were resolved in the horizontal dimension by IEF in a gradient from pH 5 to 10 and in the vertical dimension by gradient SDS-PAGE (10-15% acrylamide w/v). A and C, silver-stained gels of soluble leaf proteins from control and UV-B-treated *B. napus* respectively. Positions of molecular weight markers are shown. C and D, protein immunoblots of duplicate soluble leaf protein samples separated by two-dimensional PAGE corresponding to silver-stained gels in A and B respectively. Immunoblots were probed with anti-rubisco holoenzyme immune serum. Positions of prestained molecular weight markers are shown. Arrows indicate protein which accumulates during UV-B treatment.

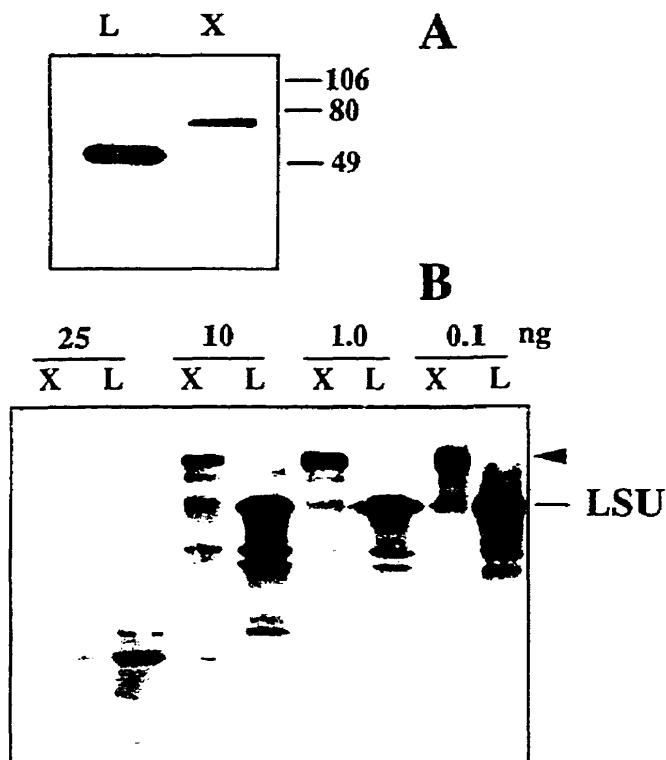


**Figure 5.4.** Comparison of peptide maps of LSU and a 65 kDa soluble leaf protein which accumulates when *B. napus* is irradiated with UV-B radiation. Excised gel slices containing either LSU or the 65 kDa protein were placed into wells of an SDS gel (10-15% acrylamide w/v), electrophoresed with various amounts of added papain, partially digested *in situ* and electrophoresis of the resulting fragments completed. Peptide maps were visualized by immunoblotting of proteins and probing with anti-rubisco holoenzyme immune serum. A, LSU and 65 kDa proteins from excised gel slices separated by SDS-PAGE in the absence of papain. B, LSU and 65 kDa proteins from excised gel slices after digestion with various amounts of papain.

Thus, the 65 kDa protein is a high molecular weight variant of LSU that is induced by UV-B radiation. The apparent molecular weight is highly suggestive of a cross-linking between a LSU and a SSU to form a heterodimer.

#### **5.3.4 Induction of a UV-B-induced rubisco in other plant species.**

To determine how widespread this phenomenon is, a number of other species were given the same UV-B treatment and analysed. Pea and tomato were tested for the induction of the 66 kDa variant of rubisco in the presence of UV-B. The high molecular weight protein was generated in each of these species (Fig. 5.5). This indicates that production of the high molecular weight variant may be common in dicots.

To investigate whether the structural determinants for photocross-linking of rubisco subunits were evolutionarily conserved, the cyanobacteria *Synechococcus* was exposed to UV-B. Irradiation of *Synechococcus* PC6301 cells with high doses of 300 nm radiation ( $\sim 20 \mu\text{mol m}^{-2} \text{s}^{-1}$ ) did not result in formation of a photoproduct which could be detected by antisera raised against rubisco from corn, *Euglena*, maize, peanut or *Synechococcus* (Fig. 5.6). A much higher molecular weight product ( $\sim 110$  kDa) does appear which may correspond to a LSU dimer. Thus, there are sufficient differences between the *Synechococcus* and higher plant rubisco, that the 66 kDa photoproduct does not form.

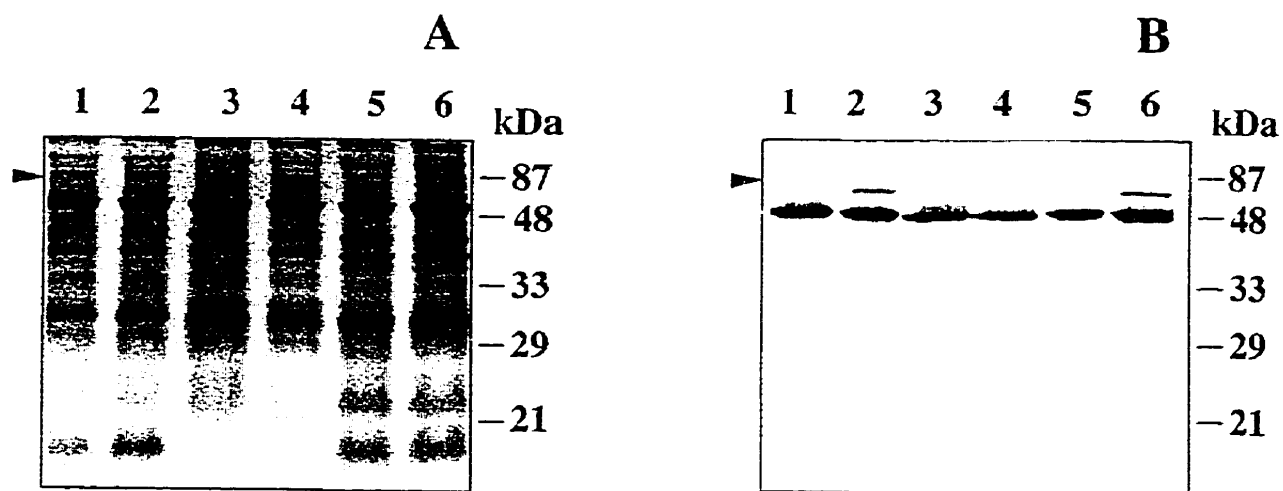


**Figure 5.5.** Presence of the rubisco photoproduct in other species. Comparison of LSU from *B. napus* (lanes 1 and 2), tomato (lanes 3 and 4), and pea (lanes 5 and 6). Plants were exposed to control lighting (lanes 1,3 and 5) or UV-B lighting conditions (lanes 2, 4 and 6) for 4 h. Immunoblot of soluble leaf proteins samples (2  $\mu$ g) separated by SDS-PAGE (12 % acrylamide w/v) were probed with anti-rubisco holoenzyme immune serum. Positions of molecular weight markers are shown.



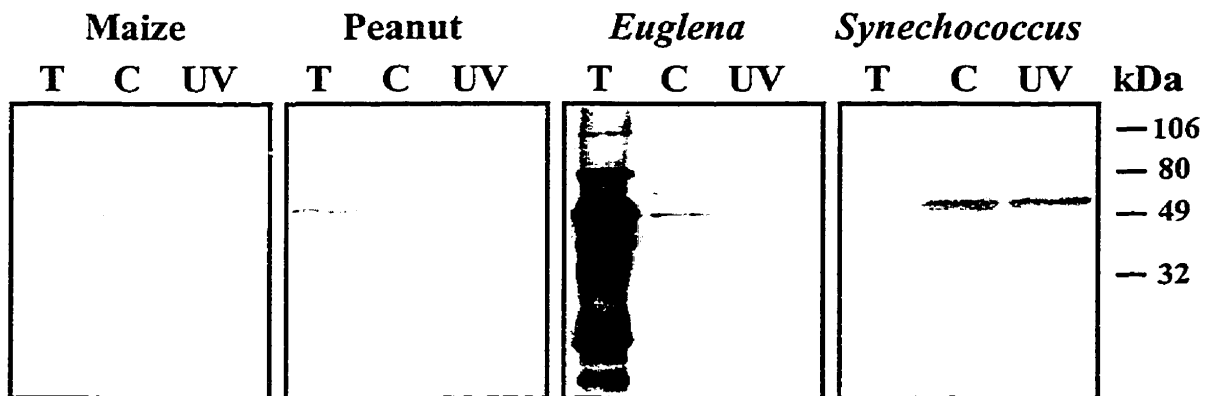


**Figure 5.6.** Formation of the rubisco photoproduct in UV-B-irradiated *Synechococcus*. Cultured *Synechococcus* was irradiated with 300 nm UV-B ( $20 \mu\text{mol m}^{-2} \text{s}^{-1}$  for 10 min). Soluble proteins were extracted from the samples of unirradiated *Synechococcus* (C), irradiated *Synechococcus* (UV) and from 5-day old UV-B-irradiated *B. napus* cv Topas (T) (see section 5.2.1 for growth conditions). Proteins were separated by SDS PAGE (15% acrylamide w/w), and transferred to nitrocellulose for immunoblotting. The samples were probed with anti-rubisco immune serum raised against maize holoenzyme, peanut LSU and SSU, *Euglena* holoenzyme or *Synechococcus* holoenzyme. Molecular weight markers are indicated.

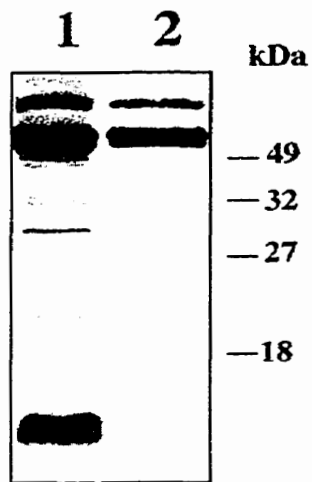


**Figure 5.7.** Comparison of the 66 kDa rubisco photoproduct that forms in UV-B exposed *B. napus* to the photoproduct formed during *in vitro* UV-B irradiation of purified *B. napus* rubisco using immunoblotting. Protein samples were separated using SDS-PAGE (15% acrylamide, w/w), proteins transferred to nitrocellulose and probed with anti-rubisco holoenzyme immune serum. Lane 1, soluble leaf proteins from UV-B-treated *B. napus*; lane 2, purified rubisco from *B. napus* from untreated plants after irradiation with UV-B ( $15 \text{ mmol m}^{-2}$  290 nm radiation). The position of pre-stained molecular weight markers on immunoblot are shown.

### 5.3.5 *In vitro* formation of the rubisco photoproduct and identification of SSU as a substituent.

There are a number of possible mechanisms by which such a cross-link may arise *in vivo*. Within chloroplasts there are many molecules that could absorb UV-B and act as photosensitizers to give rise to oxidation reactions with result in covalent cross-linking between rubisco subunits. One way to determine whether molecules other than rubisco subunits are required for *in vivo* cross-linking to take place is to irradiate purified rubisco holoenzyme *in vitro* with 290 nm radiation. It was found that photoproduct formation occurred *in vitro* (Fig. 5.7).

The photoproduct formed from purified rubisco *in vitro* co-migrates on SDS-PAGE gels with that found in protein extracts from irradiated leaves of *B. napus*. To confirm that the photomodification requires that subunits be assembled into the holoenzyme, purified rubisco was denatured with urea (4M) and then irradiated (Fig. 5.8).

Identification of the SSU as part of the photoproduct was made using immunodetection with antisera raised against SSU. A distinct band corresponding to the photoproduct was detected on anti-SSU Western blots in addition to the SSU (Fig 5.9). The formation of a rubisco photoproduct comprised of both LSU and SSU has also been reported for spinach rubisco (Gerhardt, 1996). The availability of an *in vitro* experimental system should allow the identification of the cross-linked residues and the nature of the chemical mechanism to be determined. It is likely that at least one tryptophan residue at the interface between SSU and LSU is initiating the formation of a covalent cross-link between the two chains.

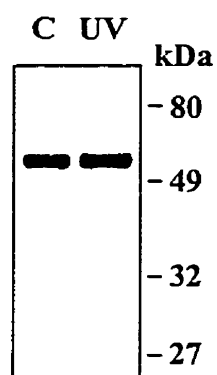


**Figure 5.8.** Purified *B. napus* rubisco was denatured in urea (4M) and CHAPS detergent (0.8%) for 1 hour before irradiation with  $15 \text{ mmol m}^{-2}$  290 nm radiation. Samples ( $5 \mu\text{g}$ ) of UV-B irradiated rubisco and controls were separated using SDS PAGE (15% acrylamide w/w) and transferred to nitrocellulose. The blots were probed with anti-rubisco holoenzyme immune serum. The positions of pre-stained molecular weight markers are shown.

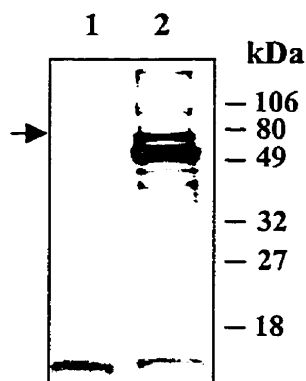


**Figure 5.9.** The presence of the rubisco small subunit (SSU) in the *B. napus* rubisco photoproduct was investigated. Purified *B. napus* rubisco was irradiated with  $15 \text{ mmol m}^{-2}$  290 nm radiation and transferred to nitrocellulose for Western blot analysis. Blots were probed with either anti-SSU immune serum (lane 1), or anti-rubisco holoenzyme immune serum (lane 2). The positions of pre-stained molecular weight markers are shown. The arrow indicates the position of a band that cross-reacts with the anti-SSU immune serum.

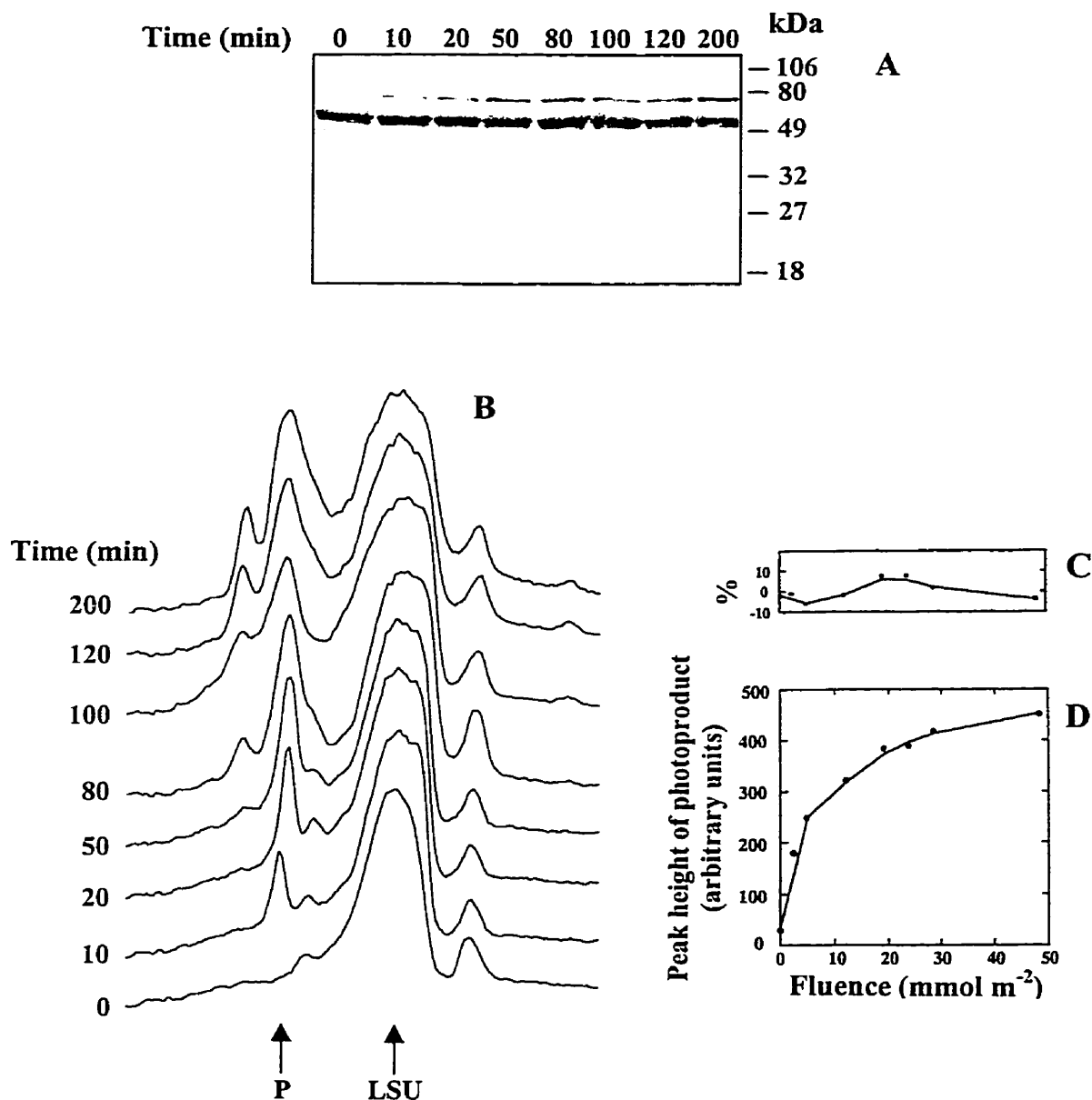


**Figure 5.10.** The accumulation of photoproduct during irradiation of purified *B. napus* rubisco ( $1 \text{ mg mL}^{-1}$ ) with 290 nm radiation ( $4 \mu\text{mol m}^{-2} \text{ s}^{-1}$ ). Samples taken at various time points during the irradiation were separated using SDS PAGE (15% acrylamide, w/w), and transferred to nitrocellulose for Western blot analysis. Blots were probed with anti-rubisco holoenzyme immune serum (A). The western blot was scanned with a densitometer (B). The peaks corresponding to LSU and the photoproduct (P) are indicated by arrows. The percent difference of each LSU peak from the mean LSU peak height (mean =  $1138 \pm 57$ ) was calculated and as a measure of the lane to lane variation in staining (C). Peak heights of the photoproduct were measured and plotted as a function of fluence for each time point (D).

### 5.3.6 Accumulation of the rubisco photoproduct during UV-B irradiation.

When purified rubisco is exposed to  $4 \mu\text{mol m}^{-2} \text{s}^{-1}$  290 nm radiation the photoproduct continued to accumulate over a period of 200 min period (Fig. 5.10A). Formation of the photoproduct was measured by scanning western blots with a densitometer (Fig. 5.10B). Peak heights of LSU and the photoproduct measured and plotted as a function of fluence indicated that formation of the photoproduct began to saturate after  $30 \text{ mmol m}^{-2}$  290 nm radiation (Fig. 5.10C and D). This shows also that a large fraction of rubisco can be photomodified in 200 minutes with significant loss of the 55 kDa LSU band.

### 5.3.7 The mechanism of photoproduct formation - effects of free radical scavengers.

One question to ask about the nature of the photochemical mechanism is whether singlet oxygen or oxygen free radicals take part in the formation of the cross-link. This is a possibility since tryptophan in an excited state can transfer an electron or energy to oxygen.

Ascorbate (10 mM) (Fig. 11A),  $\beta$ -carotene (11B), propylgallate (Fig. 11C), and the flavonol quercetin (10 mM) (Fig. 11D), are all efficient scavengers of oxygen free radicals and were effective at preventing formation of the rubisco photoproduct. This indicates that one of the essential steps in the chemical mechanism involves formation of oxygen free radicals.

Oxygen may also act through a singlet oxygen intermediate. One test for the involvement of singlet oxygen is to monitor the rate of photoproduct formation when the lyophilized rubisco is resuspended in  $\text{D}_2\text{O}$  (Fig. 5.12). In an aqueous environment, water molecules rapidly quench oxygen in an excited singlet state. When water is replaced by  $\text{D}_2\text{O}$ , the rate of quenching is reduced approximately 10 fold, hence, a reaction that requires singlet oxygen will be enhanced in  $\text{D}_2\text{O}$ .

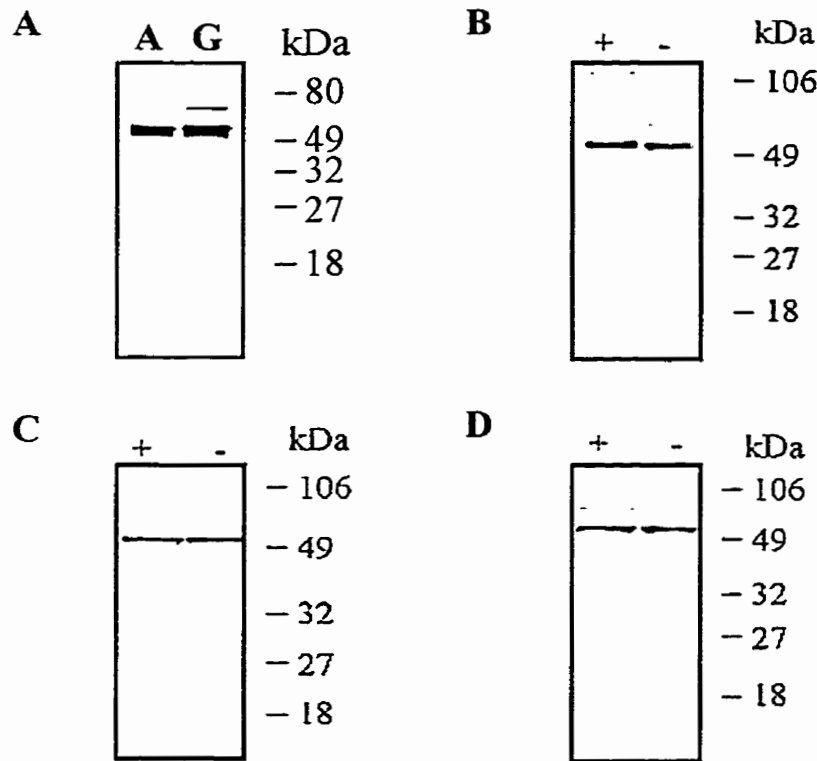


**Figure 5.11.** The effects of free radical scavengers on formation of *B. napus* rubisco photoproduct *in vitro*. Purified rubisco ( $1 \text{ mg mL}^{-1}$ ) was treated with  $15 \text{ mmol m}^{-2}$  290 nm radiation after addition of free radical scavengers. A, 10 mM L-ascorbate (A) or 10 mM reduced glutathione. B,  $\beta$ -carotene (saturated). C, quercetin 10  $\mu\text{M}$  or D, propylgallate (10 mM). The rubisco was denatured and proteins separated using SDS PAGE (15% acrylamide w/w). Proteins were immunoblotted and probed using anti-rubisco (*Euglena*) holoenzyme immune serum. Molecular weight markers are shown.

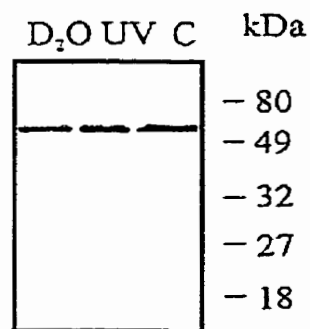


**Figure 5.12.** The effect of D<sub>2</sub>O on formaton of the rubisco photoproduct. Lyophilized spinach rubisco was reconstituted in either D<sub>2</sub>O or water and irradiated with  $15 \text{ mmol m}^{-2}$  290 nm radiation, D<sub>2</sub>O and UV respectively. An untreated sample in water is shown in lane C. Proteins were separated using SDS PAGE and immunoblotted using anti-rubisco holoenzyme (*Euglena*) immune serum.

When rubisco was resuspended in D<sub>2</sub>O there was no appreciable increase in the formation of the photoproduct (Fig. 5.12). This indicates either that singlet oxygen is not involved with the cross-linking mechanism or that the reactions are taking place in a hydrophobic environment within the protein.

### **5.3.8 Location of UV-B inter-subunit cross-link**

Tryptophan is most likely chromophore for the UV-B effects observed. Analysis of rubisco LSU and SSU amino acid sequences (Fig. 5.13 and 5.14), and crystal structures (Fig. 5.15 and 5.16), indicates a likelihood that the linkage between large and small subunits could occur between R194L and W4S (given as residue, position, subunit). This is based on location of residues at the interface between subunits, and their proximity to each other. On this basis a strategy was devised to isolate a proteolytic fragment from the heterodimer that encompasses the two cross-linked peptides, one from each subunit. The approach selected was to compare partial proteolytic digests of native spinach rubisco with UV-B-irradiated holoenzyme containing cross-linked heterodimers. The appearance of novel peptide fragments in the latter could represent cross-linked fragments. Proteolysis was carried out under non-denaturing conditions using the thiol protease clostripain that cleaves specifically at the C-terminal side of arginine residues. This cleavage site is relatively infrequent in most proteins. Clostripain digestion should result in larger proteolytic fragments than those produced by other proteases such as trypsin, which cut at a number of different sites. The peptides that result will be of sufficiently large size to be separated using Tricine-SDS PAGE that can resolve peptides as small as 1 kDa in size. The use of arginine by clostripain has another important consequence.



		1			
B. oleracea	MSPQTETKAS	VGFKAGVKEY	KLNYTPEYE	TKDTDILAAF	RVTPQPGVPP
Spinach	MSPQTETKAS	VEFKAGVKDY	KLTYTPEYE	TLDTDILAAF	RVSPQPGVPP
Tobacco	MSPQTETKAS	VGFKAGVKEY	KLTYTPEYQ	TKDTDILAAF	RVTPQPGVPP
Pea	MSPQTETKAK	VGFKAGVKDY	KLTYTTPDYQ	TKDTDILAAF	RVTPQPGVPP
Synechococcus	<u>...</u> MPKTQSA	AGYKAGVKDY	KLTYTTPDYT	PKDTDLLAAF	PVSPQPGVPA
		51			
B. oleracea	EEAGAAVAE	SSTGTWTTVW	TDGLTSLDRY	KGRCYHIEPV	PGEETQFIAIY
Spinach	EEAGAAVAE	SSTGTWTTVW	TDGLTNLDRY	KGRCYHIEPV	AGEENQYICY
Tobacco	EEAGAAVAE	SSTGTWTTVW	TDGLTSLDRY	KGRCYRIERV	VGEKDQYIAY
Pea	EEAGAAVAE	SSTGTWTTVW	TDGLTSLDRY	KGRCYEIEPV	PGEDNQFIAIY
Synechococcus	DEAGAAIAE	SSTGTWTTVW	TDLLTDMDRY	KGKCYHIEPV	QGEENSYFAF
		101			
B. oleracea	VAYPLDLFEE	GSVTNMFTSI	VGNVFGFKAL	AALRLEDLRI	PPAYTKTFQG
Spinach	VAYPLDLFEE	GSVTNMFTSI	VGNVFGFKAL	RALRLEDLRI	PVAYVKTFQG
Tobacco	VAYPLDLFEE	GSVTNMFTSI	VGNVFGFKAL	RALRLEDLRI	PPAYVKTFQG
Pea	VAYPLDLFEE	GSVTNMFTSI	VGNVFGFKAL	RALRLEDLRI	PYAYVKTFQG
Synechococcus	IAYPLDLFEE	GSVTNILTISI	VGNVFGFKAI	RSLRLEDIRF	PVALVKTFQG
		151		194	
B. oleracea	PPHGIQVERD	KLNKYGRPLL	GCTIKPKLGL	SAKNYGRAVY	ECLRGGLDFT
Spinach	PPHGIQVERD	KLNKYGRPLL	GCTIKPKLGL	SAKNYGRAVY	ECLRGGLDFT
Tobacco	PPHGIQVERD	KLNKYGRPLL	GCTIKPKLGL	SAKNYGRAVY	ECLRGGLDFT
Pea	PPHGIQVERD	KLNKYGRPLL	GCTIKPKLGL	SAKNYGRAVY	ECLRGGLDFT
Synechococcus	PPHGIQVERD	LLNKYGRPML	GCTIKPKLGL	SAKNYGRAVY	ECLRGGLDFT
		201		227	
B. oleracea	KDDENVNSQP	FMRWRDRFLF	CAEAIYKSQA	ETGEIKGHYL	NATAGTCEEM
Spinach	KDDENVNSQP	FMRWRDRFLF	CAEALYKAQA	ETGEIKGHYL	NATAGTCEEM
Tobacco	KDDENVNSQP	FMRWRDRFLF	CAEALYKAQA	ETGEIKGHYL	NATAGTCEEM
Pea	KDDENVNSQP	FMRWRDRFLF	CAEAIYKSQA	ETGEIKGHYL	NATAGTCEEM
Synechococcus	KDDENINSQP	FQRWRDRFLF	VADAIHKSQA	ETGEIKGHYL	NVTAPTCEEM
		251			
B. oleracea	MKRAIFAREL	GVPIVMHDYL	TGGFTANTSL	AHYCRDNGLL	LHIHRAMHAV
Spinach	MKRAVFAREL	GVPIVMHDYL	TGGFTANTTL	SHYCRDNGLL	LHIHRAMHAV
Tobacco	IKRAVFAREL	GVPIVMHDYL	TGGFTANTSL	AHYCRDNGLL	LHIHRAMHAV
Pea	LKRAVFAREL	GVPIVMHDYL	TGGFTANTTL	SHYCRDNGLL	LHIHRAMHAV
Synechococcus	MKRAEFAKEL	GMPIIMHDFL	TAGFTANTTL	AKWCRDNGLL	LHIHRAMHAV

**Figure 5.13.** Comparison of amino acid sequences of the ribulose-1,5-bisphosphate oxygenase/carboxylase LSU from canola (*Brassica napus* L.), spinach (*Spinacea oleracea* L), tobacco (*Nicotiana tobacum* L.), pea (*Pisum sativum* L.) and *Synechococcus leopoliensis* PCC 6301 (UTCC 102) (cyanobacteria). Tryptophan and arginine residues are highlighted. Tryptophan residue positions which differ among higher plants and cyanobacteria are underlined. Residues referred to in the text are numbered.

	301					
B. oleracea	IDRQKNHGMH	FRVLAKALRL	SGGDHVHAGT	VVGKLEGDRE	STLGFVDLLR	
Spinach	IDRQKNHGMH	FRVLAKALRL	SGGDHIHSGT	VVGKLEGERD	ITLGFVDLLR	
Tobacco	IDRQKNHGIH	FRVLAKALRM	SGGDHIHSGT	VVGKLEGERD	ITLGFVDLLR	
Pea	IDRQKNHGMH	FRVLAKALRL	SGGDHIHAGT	VVGKLEGERE	ITLGFVDLLR	
Synechococcus	IDRQRNHGIH	FRVLAKCLRL	SGGDHLHSGT	VVGKLEGDKA	STLGFVDLMR	
	351					
B. oleracea	DDYVEKDRSR	GIFFTQDWVS	LPGVLPVASG	GIHVWHMPAL	TEIFGDDSVL	
Spinach	DDYTEKDRSR	GIYFTQSWVS	TPGVLPVASG	GIHVWHMPAL	TEIFGDDSVL	
Tobacco	DDFVEQDRSR	GIYFTQDWVS	LPGVLPVASG	GIHVWHMPAL	TEIFGDDSVL	
Pea	DDYIKKDRSR	GIYFTQDWVS	LPGVIPVASG	GIHVWHMPAL	TEIFGDDSVL	
Synechococcus	EDHIERDRSR	GVFFTQDWAS	MPGVLPVASG	GIHVWHMPAL	VEIFGDDSVL	
	401					
B. oleracea	QFGGGTLGHP	WGNAPGAVAN	RVALEACVQA	RNEGRDLAVE	GNEIIREACK	
Spinach	QFGGGTLGHP	WGNAPGAVAN	RVALEACVQA	RNEGRDLARE	GNTIIREATK	
Tobacco	QFGGGTLGHP	WGNAPGAVAN	RVALEACVKA	RNEGRDLAQE	GNEIIREACK	
Pea	QFGGGTLGHP	WGNAPGAVAN	RVALEACVQA	RNEGRDLARE	GNAIIREACK	
Synechococcus	QFGGGTLGHP	WGNAPGATAN	RVALEACVQA	RNEGRDLYRE	GGDILREAGK	
	451					
B. oleracea	WSPELAAACE	VWKEITFNFP	TIDKLDGQD			
Spinach	WSPELAAACE	VWKEIKFEFP	AMDTV....			
Tobacco	WSPELAAACE	VWKEIVNFA	AVDVLDK..			
Pea	WSPELAAACE	VWKEIKFEFP	AMDTL....			
Synechococcus	WSPELAAALD	LWKEIKFEFE	TMDKL....			

Figure 5.13. Continued.

Canola	...MASSMLS	SAAVVTSPAQ	ATMVAPFTGL	KSSSAFPVTR	KANNDITSIV
Spinach	.....	.....	.....	.....	.....
Tobacco	.MASSVLSSA	AVATRSNVAQ	ANMVAPFTGL	KSAASFPVSR	KQNLDITSIA
Pea	MASMISSAV	TTVSRASTVQ	SAAVAPFGGL	KSMTGFPVK.	KVNTDITSIT
Synechococcus	.....	.....	.....	.....	.....
		1 4			38
Canola	SNGGRVSCMK	VWPPVGKKKF	ETLSYLPDLT	EVELGKEVDY	LLRNKWIPCV
Spinach	.....MQ	VWPPPLGLKKF	ETLSYLPPLT	TEQLLAEVNY	LLVKGWIPPL
Tobacco	SNGGRVQCMQ	VWPPINKKKY	ETLSYLPDLS	QEQLLSEVEY	LLKNGWVPCL
Pea	SNGGRVKCMQ	VWPPIGKKKF	ETLSYLPPLT	RDQLLKEVEY	LLRKGWVPCL
Synechococcus	.....MS	MKTLPKERRF	ETFSYLPPLS	DRQIAAQIEY	MIEQGFHPLI
			67		
Canola	EFELEHGFVY	REHGSTPGYY	DGRYWTMWKL	PLFGCTDSAQ	VLKEVQECKT
Spinach	EFEVKDGFVY	REHDKSPGY	DGRYWTMWKL	PMFGGTDPAQ	VVNEVEEVKK
Tobacco	EFETEHEGFVY	RENNKSPGY	DGRYWTMWKL	PMFGCTDATQ	VLAEEVEAKK
Pea	EFELEKGFVY	REHNKSPGY	DGRYWTMWKL	PMFGTTDASQ	VLKELDEVVA
Synechococcus	EFNEHS....	.....NP...	EEFYWTMWKL	PLFDCKSPQQ	VLDEVRECRS
Canola	EYPNAFIRII	GFDNNRQVQC	ISFIAKPPS	FTGA	
Spinach	APPDAFVRFI	GFNDKREVQC	ISFIAKPKG	Y...	
Tobacco	AYPQAWIRII	GFDNVRQVQC	ISFIAKPEG	Y...	
Pea	AYPQAFVRII	GFDNVRQVQC	ISFIAHTPES	Y...	
Synechococcus	EYGDCYIRVA	GFDNIKQCQT	VSFIVHRPGR	Y...	

**Figure 5.14.** Comparison of amino acid sequences of the ribulose-1,5-bisphosphate oxygenase/carboxylase SSU from canola (*Brassica napus* L.), spinach (*Spinacea oleracea* L), tobacco (*Nicotiana tobacum* L.), pea (*Pisum sativum* L.) and *Synechococcus leopoliensis* PCC 6301 (UTCC 102) (cyanobacteria). Tryptophan and arginine residues are highlighted. W4 and W38, which are conserved among higher plants, are absent in cyanobacteria. Residues referred to in the text are numbered as well as the first residue for each protein. Transit peptide sequences are also included for some of the canola, tobacco and pea.

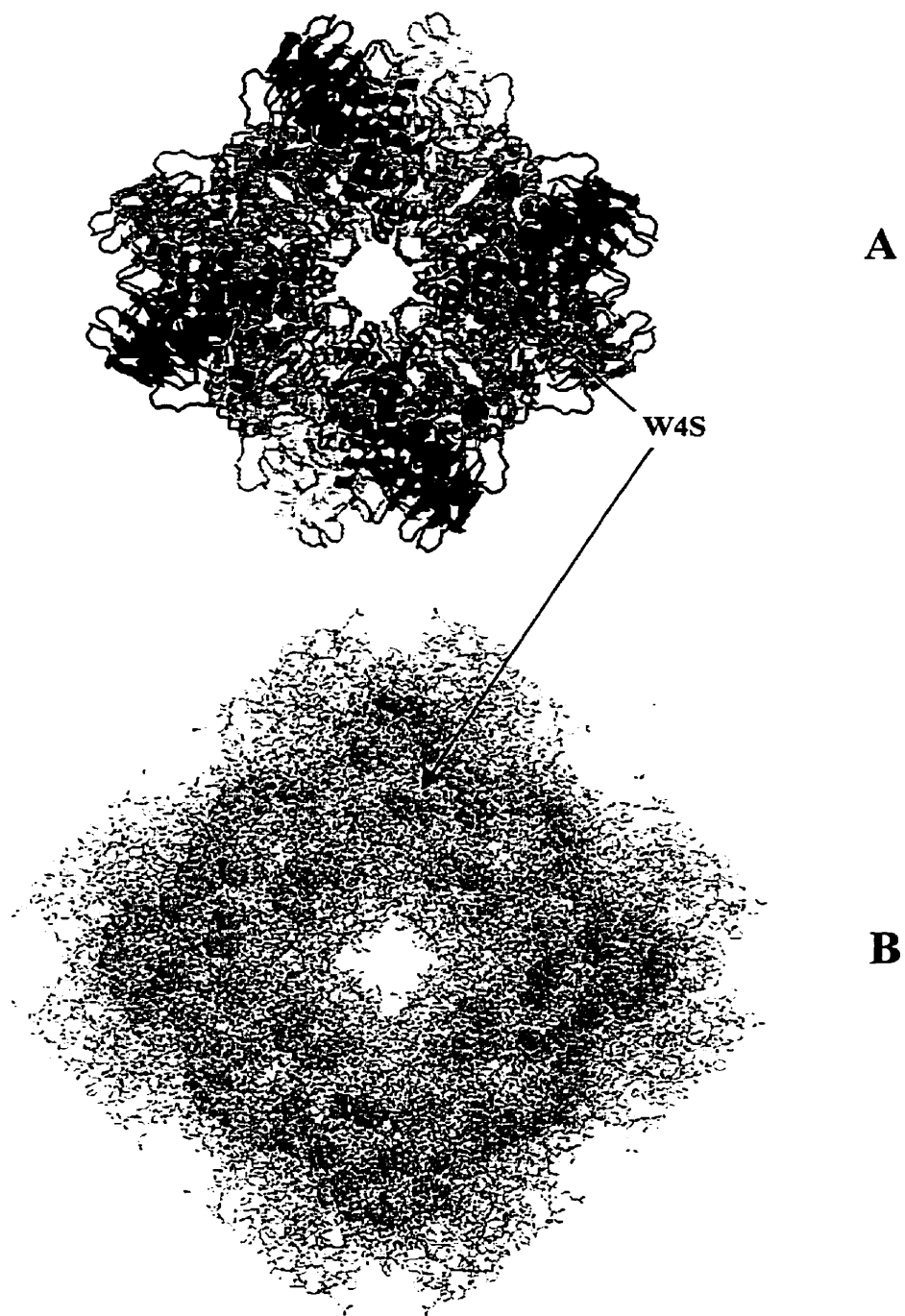
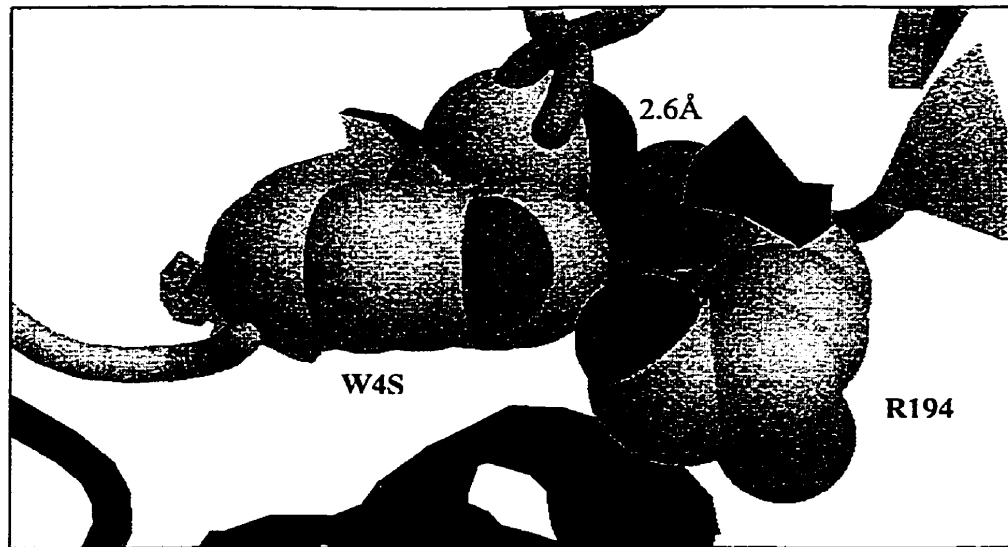
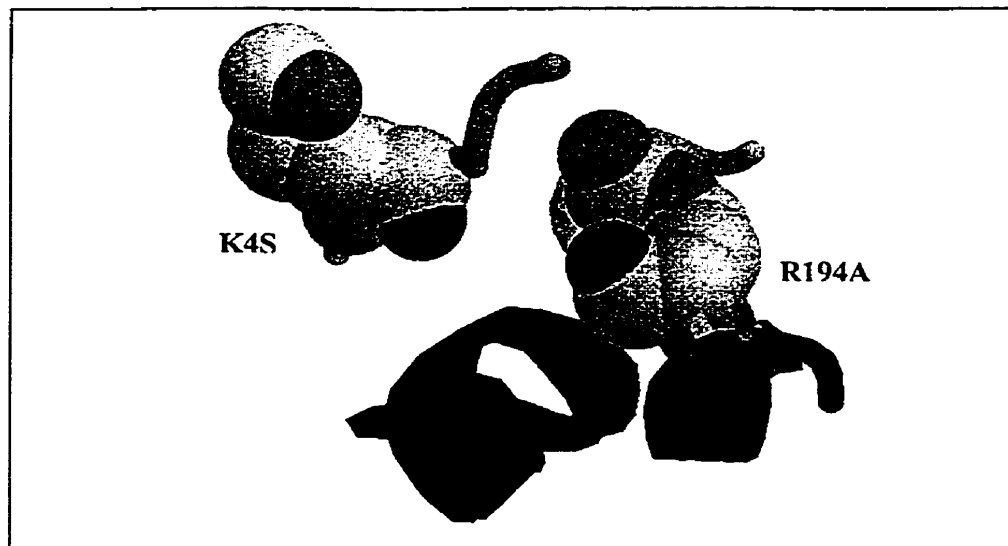


**Figure 5.15.** Structure of spinach rubisco. A top view of the rubisco holoenzyme (A) shown in a ribbon representation. Four small subunits (SSU) are coloured green and eight large subunits (LSU) coloured alternately. The arrow indicates the location of W4S in one of the SSU which is shown as a space-filling representation. The location of other tryptophans in rubisco is shown in (B).



A



B

**Figure 5.16.** Comparison of potential photocrosslinking site in spinach rubisco (A) to the same position in *Synechococcus rubisco* (B). The hydrogen bond (2.6 Å) between R194L and the backbone carbonyl of W4S in spinach rubisco is shown in (A).

The formation of a photocross-link involving an arginine, would result in loss of particular cleavage site. Analysis of the LSU and SSU sequences reveals that approximately 29 fragments should result from complete proteolysis of LSU by clostripain (Fig. 5.17), ranging in size from 261 to 6332 Da. Five fragments should result from digestion of the SSU ranging from 996 to 6208 Da. Fragments smaller than 200 Da are not taken into consideration, since they cannot be resolved with the methods used here. Crosslinking between W4S and R194L would have two consequences for a clostripain digestion of rubisco. First, an arginine cleavage site at R194L would be lost due to the crosslinking. This is taken into account by adding the fragments adjacent R194L together. In a crosslinked LSU, this will give an LSU fragment of ~3023 Da. Second, if R194L is crosslinked to the SSU fragment containing W4S the fragment will now be ~9232 Da. Hence, if the cross-link forms between residues W4S and R194L, digestion of UV-B irradiated spinach rubisco holoenzyme containing cross-linked SSU and LSU with clostripain, should result in formation of a peptide fragment ~9 kDa which is not found in fragments from unirradiated rubisco. A similar analysis for the W67S-K227L crosslink indicates an 8 kDa fragment would be formed.

Spinach rubisco which was irradiated with 300 nm radiation to produce the crosslinked heterodimer for clostripain digestion (Fig. 5.18A). The SSU and generally all the rubisco in the irradiated sample was digested more rapidly than the unirradiated sample (Fig. 5.18B). It is also clear from this gel that before digestion there is less SSU monomer in the irradiated rubisco than in the control sample. When this preparation is digested with clostripain, a small fragment (10 kDa) forms which is not observed in digests of unirradiated rubisco (Fig. 5.18B). Unfortunately, insufficient quantities of the peptide were obtained to measure the exact size of the fragment using mass spectroscopy.

### Enzymatic cleavage of Spinach LSU

A

```

1   *   10   *   20   *   30   *   40   *   50
1  MSPQTETKASVEFKAGVKDYKLTYYTPEYETLDTDILAAFRVSPQPGVPP
51  EEAGAAVAEAESSTGTWTTVWTDGLTNLDTRYKGRCYHIEPVAGEENQYICY
101 VAYPLDLFEEGSVTNMFTSIVGNVFGFKALRALRLEDLRI PVAYVKTFQG
151 PPHGIQVERDKLNKYGRPLLGCTIKPKLGLSAKNYGRAVYECLRGGLDFT
201 KDDENVNSQPFMRWRDRFLFCAEALYKAOAETGEIKGHYLNATAGTCEDM
251 MKRAVFARELGVPIVMHDYLTGGFTANTTLSHYCRDNGLLLHIHRAMHAV
301 IDRQKNHGMHFRVLAKALRLSGGDHIHSGTVVVGKLEGERDITLGFVDLLR
351 DDYTEKDRSRGIYFTQSWVSTPGVLPVASGGIHVWHMPALTEIFGDDSVL
401 QFGGGTLGHPWGNAPGAVANRVALEACVQARNEGRDLAREGNTIIREATK
451 WSPELAAACEVWKEIKFEFPAMDTV

```

### Enzymatic cleavage of Spinach SSU

B

```

1   *   10   *   20   *   30   *   40   *   50
1  MOVWPPLGLKKFETLSYLPPLTTEQLLAEVNLLVKGWIPPLEFEVKDGF
51  VYREHKSPGYDGRYWTMWKLPFMGGTDPAQVVNEVEEVKKAPPDAFVR
101 FIGFNDKREVQCISFIAYPAGY

```

C

Clostripain digestion (R/) fragment of Spinach rubisco containing cross-link between W4S-R193

					<u>kDa</u>
LSU	188	-	194	R/A...R/G	853.01
	195	-	213	R/G...R/W	2170.35
SSU	1	-	53	-/M...R/E	<u>6208.36</u>
					9231.72

**Figure 5.17.** Proteolytic cleavage of spinach rubisco photoproduct by clostripain. The fragment resulting from clostripain cleavage of rubisco photoproduct containing the proposed crosslinked arginine in LSU (R194) is underlined in (A). The SSU fragment containing W4 is underlined in (B). The resulting cross-linked fragment and its calculated molecular weight is shown in (C).

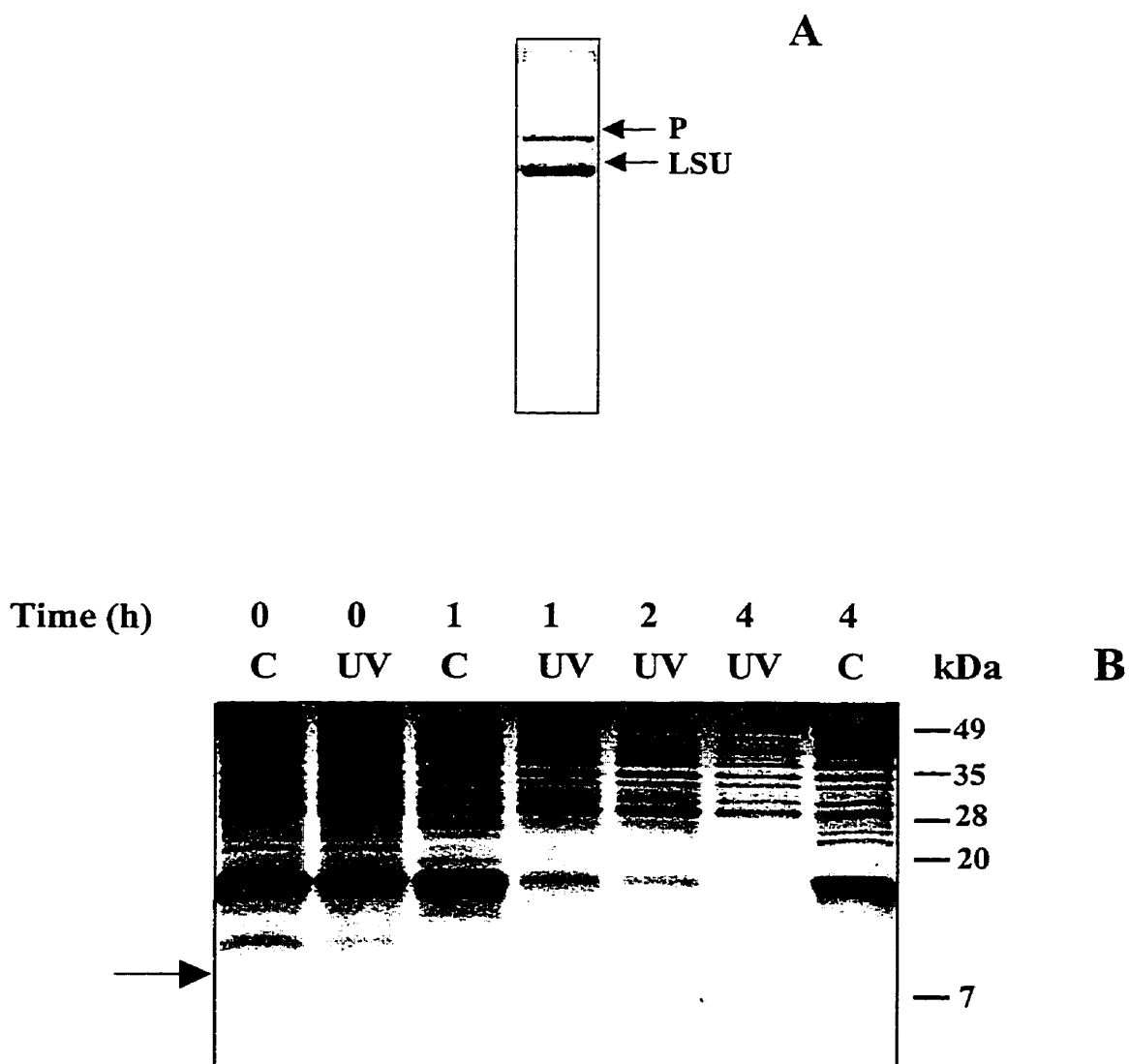


**Figure 5.18.** Partial proteolytic digest of spinach rubisco photoproduct with clostripain. A, Spinach rubisco ( $1 \text{ mg mL}^{-1}$ ) was irradiated with 300 nm radiation for 30 minutes. B, samples of unirradiated spinach rubisco (C), and UV-B-irradiated rubisco (UV), were digested over a 4 h period at  $37^\circ\text{C}$  and aliquots at each time point denatured and separated using Tricine-SDS PAGE (15% acrylamide w/w) for resolving low molecular weight proteins. Proteins were visualized using silver-staining. Molecular weight markers are shown. The arrow indicates a band that is unique to digestion of the UV-B-irradiated rubisco.



The appearance of the fragment is coincident with the disappearance of the 66 kDa heterodimer. The fragment does not appear to be stable and is digested further after 2 h under these conditions. This may be expected since clostripain also cleaves peptide bonds at lysines, albeit at a slower rate, such that after 2 h the specificity for arginines is lost. The predicted cross-linked fragment contains five lysines, hence further digestion is likely.

#### 5.4 DISCUSSION

Many proteins are susceptible to modification by UV-B due to the presence of Trp or other chromophores that absorb UV-B (Grossweiner, 1976; Pigault and Gerard, 1984; Pigault and Gerard, 1989). Other amino acids do not absorb radiation longer than 290 nm to any great extent (Fasman, 1989). Soluble leaf proteins were separated by SDS-PAGE to determine whether rubisco is modified by UV-B. Irradiation of non-acclimated canola plants, using a similar ratio of visible to UV-B as in solar radiation (100:1), resulted in no visible changes in LSU or SSU (Fig. 5.2A). However, a protein of 66 kDa accumulated during the treatment period.

The effects of UV-B on rubisco were examined by immunoblotting leaf proteins. Antisera raised against LSU bound to a ~66 kDa protein in addition to LSU (Fig. 5.2B). Further analysis of the soluble fractions using two-dimensional SDS-PAGE and immunodetection with anti-LSU antisera, showed that the 66 kDa band could be resolved into at least four isomers which migrate immediately above the predominant large subunit isomers (Fig. 5.3). Partial proteolytic digests of the LSU and the 66 kDa protein yielded very similar protein fragment patterns (Fig. 5.4). Hence, the 66 kDa protein is a high molecular weight variant of LSU formed *in vivo* during UV-B irradiation of canola. Moreover, when pea, and tomato were grown under the same conditions, a 66 kDa protein

was also observed which binds anti-LSU antisera (Fig. 5.5) although *Synechococcus* rubisco was not converted by UV-B to this 66 kDa photoproduct (Fig. 5.6).

To begin to understand the nature of the photomodification rubisco holoenzyme was purified from *B. napus* and irradiated *in vitro*. Photomodification of rubisco did not depend on the presence of other chloroplast proteins and was easily detectable *in vitro* (Fig. 5.7). Formation of the photoproduct did require that subunits were assembled into the holoenzyme, since it did not form under denaturing conditions (4M urea) (Fig. 5.8) (Voordouw et al, 1984). Given the molecular weight of the photoproduct and its formation in purified holoenzyme it was hypothesized to result from the covalent cross-linking of a LSU and SSU and this was confirmed using antisera raised against SSU (Fig. 5.9). With this realization, experiments were carried out in an effort to understand the photocross-linking process in rubisco. An attempt was made to measure kinetics of photoproduct formation *in vitro* using immunoblot detection. In general, the photoproduct appeared to accumulate over the 200 minute exposure period gradually saturating after 30 mmol m<sup>-2</sup> 290 nm radiation (Fig. 5.10). More detailed analysis was not carried out since this is not a direct method for quantifying of proteins and analysis of kinetic rate constants would be inappropriate. This sort of analysis is best done using a direct methods such as changes in tryptophan fluorescence or measurement of quantitatively-stained proteins (see Gerhardt, 1996). Ideally, this could be done using chromatographic separation of proteins. Estimation of the extinction coefficient for purified photoproduct would then allow measurement of photoproduct concentration in isolated fractions by absorbance.

In general, absorption of UV-B by Trp results in formation of an excited singlet state (Grossweiner et al, 1976, 1982; Pigault and Gerard, 1989). This excited state of Trp can either be quenched or it can initiate a number of chemical reactions. Photochemical quenching can occur

from nearby His, Tyr, Trp or Cys residues through radiationless energy transfer (Rmoso and Forster, 1975; Gonnelli and Strambini, 1995). The nature of the reactions depends on exposure of the Trp to aqueous medium or lipids (local polarity) and proximity to other reactive residues (tertiary structure) (Tallmadge and Borkman, 1990; Pigault and Gerard, 1989).

During photoexcitation Trp enters an excited singlet state which can decay to form an excited triplet state. In this state, the absorbed energy can be passed from Trp to O<sub>2</sub> forming singlet oxygen, <sup>1</sup>O<sub>2</sub>, which can then oxygenate the indole ring leading to ring lysis and formation of *N*-formylkynurenine (NFK) (Fig. 5.19) (Inoue et al, 1982; Grossweiner, 1984). This compound was originally identified as a metabolite of tryptophan catabolism (Knox and Mehler, 1950), and subsequently reported to form under a variety of oxidative conditions including exposure of proteins to sunlight (Pirie, 1971).

Alternatively, an early result of the photoexcitation of tryptophan is photoionization and ejection of an electron (Grossweiner, 1984). This results in formation of a carbon-centered tryptophan free radical ( $\bullet$ Trp), and hydrated electrons ( $e^-_{aq}$ ). Direct intramolecular transfer of electrons from Trp to adjacent residues results in their destruction (Pigault and Gerard, 1989). Similarly, UV-B irradiation of Trp residues in membrane proteins can result in lipid peroxidation (Kochevar and Yoon, 1983). In an aqueous environment, however, hydrolysis of  $\bullet$ Trp likely takes place, resulting in formation of  $\bullet$ NFKH radical which can then pass an electron to O<sub>2</sub> forming superoxide radical  $\bullet$ O<sub>2</sub><sup>-</sup> and NFK. Currently, evidence such as detection of solvated electrons and NFKH by the use of spin trapping reagents and ESR, supports the latter mechanism although elucidation of the exact details has not been reported (Andley and Clark, 1989a; Wessels et al, 1997). Such reactions also occur when Trp residues are buried inside the protein structure (Andley and Clark, 1989c).

In both of the cases above, the result of irradiation of Trp with UV-B is formation of NFK (Fig. 5.19). This product is particularly reactive chemically because of the two carbonyl groups, and it can also act as a photosensitizer (Fujimori, 1981; Andley and Clark, 1989b). In this case NFK can act as a type I or type II photosensitizer. NFK can absorb UV-B as well as UV-A, and enter an excited triplet state from which it can donate energy directly to oxygen resulting in formation of singlet oxygen which is referred to as a Type II process, whereas donation of an electron to  $O_2$  resulting in formation of  $\cdot O_2^-$  is a Type II mechanism (Foote, 1991). Hence, there are at least four possible reactive compounds that could be formed as a result of UV-B irradiation of Trp that might be involved with formation of a covalent bond; the  $\cdot$ Trp radical,  $^1O_2$ ,  $\cdot O_2^-$  radical and the carbonyl groups of NFK.

NFK could react directly with Lys residues or Arg residues forming covalent crosslinks. In the case of Lys, a Schiff base is formed with one of the NFK carbonyls (Hazell et al, 1994). The crosslink formation between NFK and Arg might proceed by a reaction similar to one commonly used to specifically modify active site arginines in enzymes (Riordan et al, 1977). This type of reaction occurs between the guanidino group of arginines and dicarbonyl reagents, mainly alpha dicarbonyl, such as methylglyoxal, phenylglyoxal and 2,3-butadione. However, acetylacetone (pentane-2,4-dione), which does not have vicinal electron-withdrawing carbonyl groups is also reactive (Pathy and Thesz, 1980; Dikler et al, 1997). In the case of UV-B-irradiated rubisco, NFK could act as the dicarbonyl reagent.

Although NFK, like acetylacetone, does not contain alpha dicarbonyls, it does have three closely spaced carbonyls, including the backbone carbonyl. Products reported from such reactions include fluorescent cyclic arrangements (pyrimidyl) (Shipanova et al, 1997; McIntosh, 1992).

To determine whether the crosslink formation involves free radicals or  $^1\text{O}_2$ , irradiation of purified *B. napus* or spinach rubisco with UV-B was carried out *in vitro* in the presence of compounds that affect these reactions. Ascorbate has been shown to specifically repair •Trp formed in lysozyme to varying degrees of efficiency (Hoey and Butler, 1984). Propylgallate has been shown to prevent modification of Trp in lysozyme by alkylperoxyl radicals (Lissi and Clavero, 1990). The flavonol aglycone quercetin has been shown to associate strongly enough with tryptophan in bovine serum albumin to quench its fluorescence (Ahmed et al, 1994).  $\beta$ -carotene is a lipophilic antioxidant that primarily quenches singlet oxygen in lipid membranes, as well as scavenging free radicals to a lesser degree (Foote et al, 1970; Tsuchihashi et al, 1995; Stratton and Liebler, 1997). Although it is highly lipophilic, beta-carotene binds to proteins and is able to effectively quench tryptophan fluorescence and hence may also have singlet oxygen quenching activity in proteins (Dufour and Haertle, 1991). The soluble tripeptide, glutathione (glutamyl-glycyl-cysteine) is also able to scavenge radicals formed in proteins (Timmins and Davies, 1993).

The effectiveness of ascorbate, quercetin, and to a lesser extent propylgallate, indicate that a formation of a radical is part of the mechanism leading to the cross-linking of subunits (Fig. 5.11). The ineffectiveness of glutathione may be a result of inaccessibility of the tryptophan involved with cross-linking.  $\beta$ -carotene acts primarily by quenching singlet oxygen, although it can also scavenging of a carbon-centered radicals.

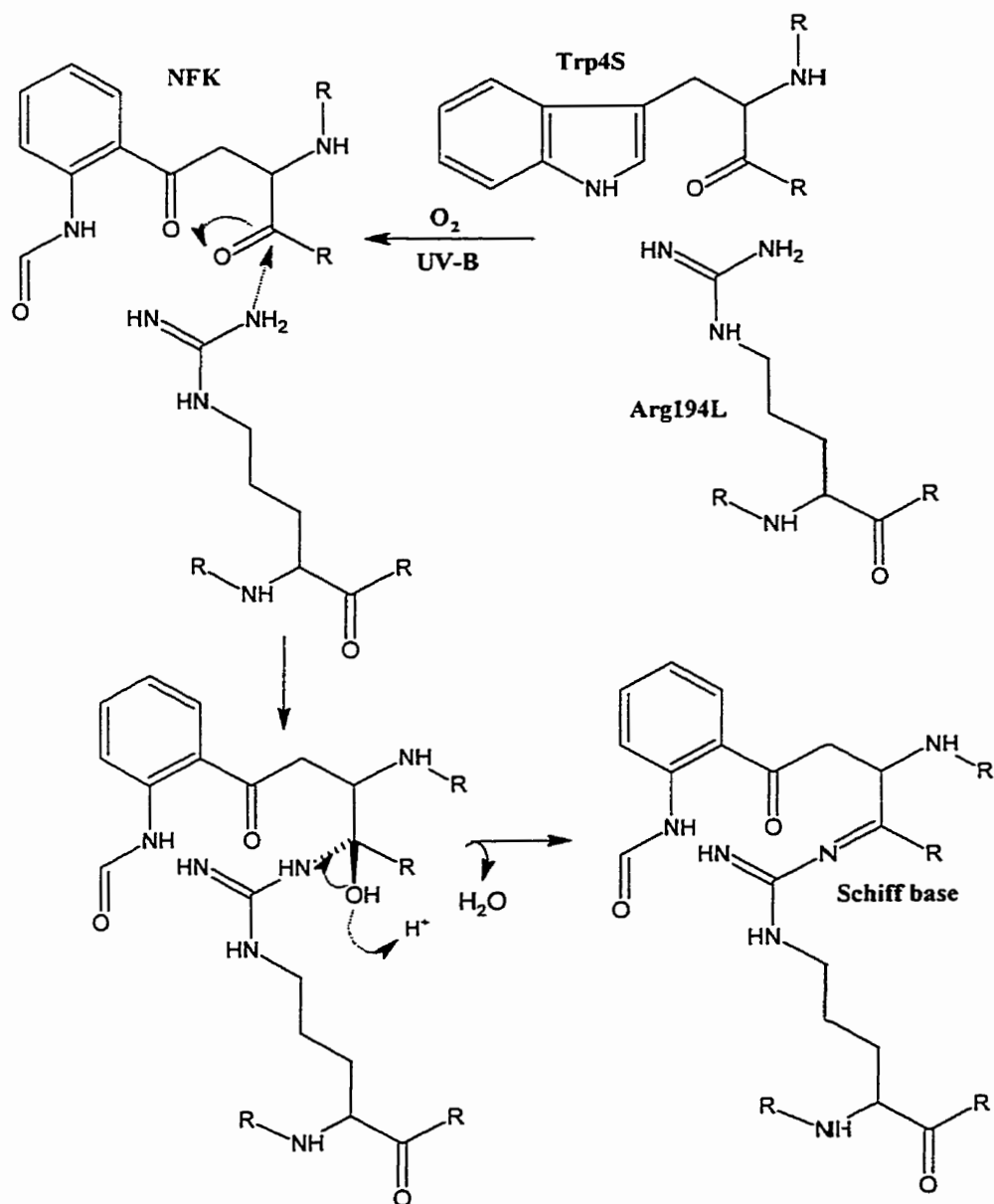


**Figure 5.19.** The proposed chemical mechanism for formation of a Schiff base crosslink between SSU and LSU of rubisco. Trp4S becomes photooxygenated forming N-formylkynurenine (NFK) which subsequently forms a Schiff base with the guanidino group of Arg194L.

result in a multifold increase in the formation of the cross-linked heterodimer (Fig. 5.12). If  $^1\text{O}_2$  was involved the yield of the reaction should be increased by the presence of  $\text{D}_2\text{O}$ . Unless there is not much water where the  $^1\text{O}_2$  is formed, or if it reacts faster with Trp than its half life. A study of the effect of UV-B irradiation on Trp fluorescence from cucumber rubisco also found mixed results regarding the involvement of singlet oxygen (Caldwell, 1993). Evidence for the involvement of  $^1\text{O}_2$  in the crosslinking reaction may be obtained more directly by isolating the crosslinked residues and determining the nature of the chemical bond between them. This approach has been used before with limited success since as yet no specific cross-linked protein fragments have been isolated from any experimental system (Tallmadge and Borkman, 1990; McDermott et al, 1991; Hott and Borkman, 1992).

Digestion of UV-B-irradiated spinach rubisco with clostripain yielded a fragment that is not present in digests of unirradiated rubisco (Fig. 5.18). However it is difficult to distinguish between the two possible crosslinks since the molecular weights are so similar (8 and 9 kDa). These two possibilities could be distinguished definitively using amino acid sequencing and determination of the mass of this fragment by mass spectroscopy. Isolation of the fragment by size exclusion chromatography could allow the exact chemical nature of the cross-linkage to be analyzed using NMR. This in turn may help elucidate the photochemical mechanism involved. Another approach that may help determine which is a more likely site for the crosslink is to analyse the amino acid sequences and crystal structures available for rubisco.

The amino acid sequences for rubisco LSU and SSU are highly conserved among higher plants (Clegg, 1993; Meagher et al, 1989). The chloroplast-encoded LSU is more conserved than the nuclear-encoded SSU. This is easily seen for the higher plant species compared in this report – canola, spinach, tobacco and pea (Fig. 13 and 14). The eight tryptophans which are highly

conserved in LSU sequences between higher and lower plants. Though generally more variable, higher plant SSU sequences contain four Trps which are present in all sequences examined (Fig. 14). In both LSU and SSU sequences, there are other Trp which are species-specific. One of the conserved Trps is a likely chromophore for the intersubunit crosslinking reaction.

The SSU sequences from cyanobacteria, red algae and brown algae, including that for *Synechococcus leopolensis* PC6301 are distinct from higher plants, especially with reference to number and position of tryptophans. The N-terminal 20 residues are quite different than higher plants, and notably, Trp4 is replaced by a lysine in *Synechococcus*. However, structures of rubisco from spinach and *Synechococcus* are very similar (Fig. 5.17).

The crystal structures of rubisco from a number of species have been solved using X-ray crystallography. These structures are among the highest resolution for very large proteins currently solved. The combination of structural and sequence conservation information can be a very powerful tool for analyzing proteins. Since Trp is the only amino acid that can absorb UV-B to any meaningful extent, the analysis can focus on the microenvironments around Trp residues that are located at the interface between SSU and LSU within the holoenzyme. Residues which were considered as potentially photoreactive with Trp are His, Lys, Arg, Tyr, and Cys (Verweij and van Stevenick, 1982; Kato et al, 1992). An examination of these sites in spinach rubisco reveals only one of the twelve highly conserved Trp residues, W4S of the SSU, lies on the surface of rubisco (Fig. 5.15), and is positioned at the interface between SSU and LSU, and within close proximity (2.6 Å) of a potentially reactive guanidino group of an arginine residue (R194L) on the adjacent LSU (Fig. 5.16). In fact, it appears to be hydrogen bonded to the backbone carbonyl of W4S. Interestingly, R194L is situated in a region of LSU (residues 170-205) which is strictly conserved between higher plants and cyanobacteria. Another pair of potentially interacting at the



LSU-SSU interface are W67S and K227L. However, these residues are not close enough to react (5 Å) in the crystal structure for spinach rubisco (Knight et al, 1990)

Examination of the SSU sequences reveals that W4S is not conserved in cyanobacteria and is replaced by a lysine residue. This may explain the earlier observation that the SSU-LSU heterodimer does not form in *Synechococcus* irradiated with UV-B. However, this result does not provide proof that the W4S residue of SSU is essential for formation of the SSU-LSU cross-link since there are many other structural differences between spinach and *Synechococcus* rubisco. For instance, one other Trp (W38S) is also not conserved, hence, *Synechococcus* SSU has two fewer Trps than the higher plant species examined. However, this result indicates the potential involvement of W4S in the photocrosslinking reaction. The hypothesis about W4S and R194L being the cross-linking partners could be tested further by investigating whether the rubisco heterodimer forms in species, such as brown or red algae which also lack W4S.

It is worth mentioning that W67S is also a possible site because of the proximity of K227L which is conserved in the species examined, and which is positioned near the indole ring (4.4 Å). The  $\epsilon$ -amino group of lysines is a good candidate to form a Schiff base with the carbonyls that may result from photooxygenation of tryptophan (Guptasarma et al, 1992) . However, in the spinach structure, K227L is partially obstructed from W67S by Y52S, Y66S, E45 and D48 and in the *Synechococcus* structure by N45S, E64S and Y66S. Since W67S and K227L are both conserved between higher plants and *Synechococcus* it is more difficult to explain this as a site for cross-linking since cross-linking does not occur in *Synechococcus*. One possible explanation is that W67S is less accessible to K227L in the *Synechococcus* rubisco than in the spinach rubisco. It is 5.7 Å from K227L in *Synechococcus* rubisco and 4.4 Å away in the spinach enzyme. In both cases, however, there must be considerable movement of these groups

towards each other for there to be a reaction between W67S and K227L which would not be the necessary for a W4S-R194L cross-link.

Another consideration is that Trp, when in an excited an electronic state, can be quenched by a His, Cys, Tyr or stabilized by negatively charged side chains, if nearby (Tallmadge and Borkman, 1990; Gonnelli and Strambini, 1995). Hence, a number of the Trps in rubisco may be quenched or stabilized after photoexcitation.

UV-B-induced photo-crosslinking of rubisco is a specific case of the more general phenomenon of oxidative modification of proteins. The way in which Trp is oxygenated to form NFK is different in each case. The large  $\pi$ -electron system of tryptophan makes it a good target for oxygenation. Rubisco itself undergoes intermolecular cross-linking *in vivo* under conditions of oxidative stress. Non-reducible dimeric forms of LSU occur after exposure to cold, O<sub>3</sub> and ethylene (Huner and Macdowall, 1979; Landry and Pell, 1993; Mehta et al, 1992). Of particular relevance, is the observation that a 65 kDa form of rubisco formed in ozone-treated poplar leaves. This effect of ozone is particularly interesting since the indole ring of tryptophan can be lysed by ozone. Although lysis of Trp by ozone proceeds by a different chemical pathway than occurs for UV-B photooxygenation, in both cases the end products, Criegee ozonide, or N-formylkynurenine, respectively, introduce new reactive carbonyl groups into the protein (Pirie, 1971; Okajima et al, 1990; Pryor and Uppu, 1993; Mudd et al, 1997). Calf-lens alpha-crystallin is also modified by both ozone and UV-B radiation resulting in formation of similar cross-links and oxidation products (Fujimori, 1982).

Of potentially broader significance is the recent isolation of 66 kDa covalently cross-linked rubisco heterodimer from microsomal membranes of the green alga *Botryococcus braunii* cultured under normal conditions (Wang and Kolattakudy, 1996). Rubisco sequences from this

group of alga are similar to higher plants and contain the putative cross-link partners W4S and R194L. What may be significant is the possibility that in some species levels of oxidative stress, which occur during normal photosynthesis may be sufficient to promote formation of the rubisco heterodimer. This could be due to endogenous levels of  $H_2O_2$  which, in the presence of  $Fe^{2+}$  can undergo Fenton reactions leading to the formation of  $\bullet OH$  which reacts readily with Trp (Gutteridge, 1994). Trp is used as a  $\bullet OH$  scavenger in some experimental systems (Henderson and Miller, 1986). It would be particularly interesting to analyse and compare the crosslinks that occur as a result of Trp modification by other chemical reactions.

Formation of a crosslinked heterodimer rubisco was not detected in *Arabidopsis* mutants (*tt5*) which do not make UV-B-absorbing compounds in response to UV-B irradiation (Rao and Ormrod, 1995a). Total rubisco activity, however, was reduced dramatically over a 5 day exposure period in these plants. The amount of rubisco activity was also reduced. Both of these results clearly indicate damage of rubisco by UV-B. One possible explanation is that there is a structural difference between rubisco from *Arabidopsis* and *B. napus* that changes the proximity of the crosslinked residues. Although highly unlikely, this explanation would imply that there is a difference in the amino acid sequence between these two species. The sequence for the *Arabidopsis* SSU is almost identical to *B. napus*. Unfortunately the sequence for the LSU of *Arabidopsis* is not available to make a comparison. Hence, the possibility that the putative crosslink partners (W4S and R194L) are no longer proximal in the *Arabidopsis* rubisco cannot be ruled out. Perhaps the turnover of rubisco is greater in plants that are exposed to UV-B for long periods of time. This remains to be determined.

As a footnote on the relationship between the structures of higher plant and cyanobacterial rubisco, it was found during the course of this study that there was a striking lack

of cross-reactivity between antibodies against rubisco from higher plants and cyanobacteria. Whether this is strictly a function of the method of antibody preparation (i.e. the use of denatured or native rubisco antigen) or a result of divergence of epitopes is not known. Certainly there are many regions of conservation in LSU between cyanobacterial and higher plant sequences and structures. However, only an antibody raised against *Euglena* had appreciable cross-reactivity.

It is very likely that photooxygenation of Trp occurs in other plant proteins. However, the photooxygenation of Trp varies depending on the surrounding environment (Pigault and Gerard, 1984, Pigault and Gerard, 1989; Tallmadge and Borkman, 1990). The W4S residue is at the surface of the SSU N-terminus and exposed to the solvent. A Trp in this type of environment is more readily modified (Tallmadge and Borkman, 1990; Pigault and Gerard, 1984). As such, it is unlikely that photooxygenation would result in any significant changes in the local environment (Berlett et al, 1996). On the other hand, if the Trp was buried, the protein structure might be disrupted by formation of additional carbonyl groups as a result of photooxygenation of the Trp. However, in this tightly packed environment an excited Trp is also more likely to be quenched by other residues such as His, Tyr or other Trp (Andley and Clark, 1989c; Hott and Borkman, 1992; Mudd et al, 1997; Finley et al, 1997). When spinach rubisco is exposed to high doses of UV-B *in vitro*, the rate of proteolytic degradation is markedly increased (Fig. 5.18B). This is an indication that the UV-B-irradiated structure is more accessible to the protease than the unexposed protein. It would be interesting to determine if this occurs at lower doses of UV-B. If so, proteolysis may be a useful assay for UV-B modification of proteins.

To summarize, an intersubunit cross-linkage between LSU and SSU during UV-B-irradiation of rubisco is reported for a number of dicot species. The cross-link also forms when purified rubisco is irradiated *in vitro*, but it is not detectable in the cyanobacteria *Synechococcus*.

Examination of amino acid sequences for rubisco indicates tryptophans are highly conserved among dicots, although cyanobacteria have are missing one tryptophan at the interface between LSU and SSU. The structure of spinach rubisco reveals that two tryptophans have potential cross-linking partner residues nearby. The more likely of the two possibilities predicts the formation of a covalent bond between W4S and R194L after photooxygenation of W4S to NFK. Crosslinked fragments were identified tentatively from proteolytic digests of UV-B-irradiated spinach rubisco.

## 7. LITERATURE CITED

- Adler V, Schaffer A, Kim J, Dolan L, Ronai Z (1995)** UV irradiation and heat shock mediate JNK activation via alternate pathways. *J Biol Chem* **270**: 26071-7
- Ahmad M, Cashmore AR (1993)** HY4 gene of *A. thaliana* encodes a protein with characteristics of a blue-light photoreceptor. *Nature* **366**: 162-6
- Ahmad M, Cashmore AR (1996)** Seeing blue: the discovery of cryptochrome. *Plant Mol Biol* **30**: 851-61
- Ahmad M, Jarillo JA, Klimczak LJ, Landry LG, Peng T, Last RL, Cashmore AR (1997)** An enzyme similar to animal type II photolyases mediates photoreactivation in *Arabidopsis*. *Plant Cell* **9**: 199-207
- Ahmad M, Jarillo JA, Smirnova O, Cashmore AR (1998)** Cryptochrome blue-light photoreceptors of *Arabidopsis* implicated in phototropism. *Nature* **392**: 720-3
- Ahmad M, Lin C, Cashmore AR (1995)** Mutations throughout an *Arabidopsis* blue-light photoreceptor impair blue-light-responsive anthocyanin accumulation and inhibition of hypocotyl elongation. *Plant J* **8**: 653-8
- Ahmed M, Ainley K, Parish J, Hadi S (1994)** Free radical-induced fragmentation of proteins by quercetin. *Carcinogenesis* **15**: 1627-1630
- Ålenius C, Vogelmann T, Bornman J (1995)** A three-dimensional representation of the relationship between penetration of UV-B radiation and UV-screening pigments in leaves of *Brassica napus*. *New Phytol* **131**: 297-302
- Allan AC, Fluhr R (1997)** Two distinct sources of elicited reactive oxygen species in tobacco epidermal cells. *Plant Cell* **9**: 1559-1572

- Allen FH, Davies JE, Galloy JJ, Johnson O, Kennard O, C.F.M, Mitchell EM, Mitchell GF, Smith JM, Watson DG (1991)** Cambridge Structural Database. *J Chem Inf Comp Sci* **31**: 187-204
- Allen J, Alexciev K, Hakansson K (1995)** Regulation by redox signaling. *Current Biology* **5**: 869-872
- Alvarez ME, Pennell RI, Meijer PJ, Ishikawa A, Dixon RA, Lamb C (1998)** Reactive oxygen intermediates mediate a systemic signal network in the establishment of plant immunity. *Cell* **92**: 773-84
- Ambler JE, Krizek DT, Semeniuk P (1975)** Influence of UV-B radiation on early seedling growth and translocation of  $^{65}\text{Zn}$  from cotyledons in cotton. *Physiologia Plantarum* **34**: 177-181
- Amici A, Levine RL, Tsai L, Stadtman ER (1989)** Conversion of amino acid residues in proteins and amino acid homopolymers to carbonyl derivatives by metal-catalyzed oxidation reactions. *J Biol Chem* **264**: 3341-6
- Andley UP, Clark BA (1989a)** The effects of near-UV radiation on human lens beta-crystallins: protein structural changes and the production of  $\text{O}_2^-$  and  $\text{H}_2\text{O}_2$ . *Photochem Photobiol* **50**: 97-105
- Andley UP, Clark BA (1989b)** Generation of oxidants in the near-UV photooxidation of human lens alpha-crystallin. *Invest Ophthalmol Vis Sci* **30**: 706-13
- Andley UP, Clark BA (1989c)** Photoreactions of human lens monomeric crystallins. *Biochim Biophys Acta* **997**: 284-91
- Andley UP, Sawardekar MA, Burris JL (1997)** Action spectrum for photocross-linking of human lens proteins. *Photochem Photobiol* **65**: 556-9

- Andrews TJ, Lorimer GH** (1987) Rubisco - structure, mechanisms, and prospects for improvement. In MD Hatch, NK Boardman, eds, *The Biochemistry of Plants A Comprehensive Treatise* **10**: 131-218
- Arami S, Hada M, Tada M** (1997) Near-UV-induced absorbance change and photochemical decomposition of ergosterol in the plasma membrane of the yeast *Saccharomyces cerevisiae*. *Microbiology* **143**: 1665-71
- Asada K** (1993) Production and action of active oxygen species in photosynthetic tissues. In *Causes of Photo-oxidative Stress and Amelioration of Defense Systems in Plants* pp 77-104. CRC Press, Boca Raton.
- Ashcroft SJ** (1997) Intracellular second messengers. *Adv Exp Med Biol* **426**: 73-80
- Assmann S** (1995) Cyclic AMP as a second messenger in higher plants. *Plant Physiol* **108**: 885-889
- Attridge TH, Black M, Gaba V** (1984) Photocontrol of hypocotyl elongation in light-grown *Cucumis sativus* L. A synergism between the blue-light photoreceptor and phytochrome. *Planta* **162**: 422-6
- Ballare CL, Barnes PW, Flint SD** (1995a) Inhibition of hypocotyl elongation by ultraviolet-B radiation in de-etiolating tomato seedlings. I. The Photoreceptor. *Physiol Plant* **93**: 584-92
- Ballare CL, Barnes PW, Flint SD, Price S** (1995b) Inhibition of hypocotyl elongation by ultraviolet-B radiation in de-etiolating tomato seedlings. II. Time-course, comparison with flavonoid responses and adaptive significance. *Physiol Plant* **93**: 593-601
- Ballare CL, Barnes PW, Kendrick RE** (1991a) Photomorphogenic effects of UV-B radiation on hypocotyl elongation in wild type and stable-phytochrome -deficient mutant seedlings of cucumber. *Physiol Plant* **83**: 652-8



- Ballare CL, Casal JJ, Kendrick RE** (1991b) Responses of light-grown wild-type and long-hypocotyl mutant cucumber seedlings to natural and simulated shade light. *Photochem Photobiol* **54**: 819-26
- Ballare CL, Scopel AL, Jordan ET, Vierstra RD** (1994) Signaling among neighboring plants and the development of size inequalities in plant populations. *Proc Natl Acad Sci U S A* **91**: 10094-8
- Ballare CL, Scopel AL, RA Sá, Radosevich** (1991c) Photomorphogenic processes in the agricultural environment. *Photochem Photobiol* **56**: 777-88
- Ballare CL, Scopel AL, Stapleton AE, Yanovsky MJ** (1996) Solar ultraviolet-B radiation affects seedling emergence, DNA integrity, plant morphology, growth rate, and attractiveness to herbivore insects in *Datura ferox*. *Plant Physiology* **112**: 161-170
- Barnes PW, Flint SD, Caldwell MM** (1990) Morphological responses of crop and weed species of different growth forms to ultraviolet-B radiation. *Amer J Bot* **77**: 1354-60
- Baskin TI, Iino M** (1987) An action spectrum in the blue and ultraviolet for phototropism in alfalfa. *Photochem Photobiol* **46**: 127-36
- Batschauer A, Ehmman B, Schafer E** (1991) Cloning and characterization of a chalcone synthase gene from mustard and its light-dependent expression. *Plant Mol Biol* **16**: 175-85
- Beerhues L, Robenek H, Wiermann R** (1988) Chalcone synthases from spinach (*Spinacia oleracea* L.) II. Immunofluorescence and immunogold localization. *Planta* **173**: 544-553
- Beggs C, Wellmann E** (1985) Analysis of light controlled anthocyanin formation in coleoptiles of *Zea mays* L.: The role of UV-B, blue, red and far red light. *Photochem Photobiol* **41**: 481-486
- Beld M, Martin C, Huits H, Stuitje A, Gerats A** (1989) Flavonoid synthesis in *Petunia hybrida*: partial characterization of dihydroflavonol-4-reductase genes. *Plant Mol Biol* **13**: 491-502

- Bender K, Blattner C, Knebel A, Iordanov M, Herrlich P, Rahmsdorf HJ** (1997) UV-induced signal transduction. *J Photochem Photobiol B* **37**: 1-17
- Blaustein AR, Kiesecker JM, Chivers DP, Anthony RG** (1997) Ambient UV-B radiation causes deformities in amphibian embryos. *Proc Natl Acad Sci U S A* **94**: 13735-7
- Boldt R, Scandalios JG** (1997) Influence of UV-light on the expression of the Cat2 and Cat3 catalase genes in maize. *Free Radic Biol Med* **23**: 505-14
- Borkman RF, McLaughlin J** (1995) The molecular chaperone function of alpha-crystallin is impaired by UV photolysis. *Photochem Photobiol* **62**: 1046-51
- Bornman JF** (1989) Target sites of UV-B radiation in photosynthesis of higher plants. *Photochem Photobiol* **4**: 145-58
- Bowler C, Chua NH** (1994) Emerging themes of plant signal transduction. *Plant Cell* **6**: 1529-41
- Brenneisen P, Wenk J, Klotz LO, Wlaschek M, Briviba K, Krieg T, Sies H, Scharffetter-Kochanek K** (1998) Central role of Ferrous/Ferric iron in the ultraviolet B irradiation-mediated signaling pathway leading to increased interstitial collagenase (matrix-degrading metalloprotease (MMP)-1) and stromelysin-1 (MMP-3) mRNA levels in cultured human dermal fibroblasts. *J Biol Chem* **273**: 5279-87
- Britt AB** (1995) Repair of DNA damage induced by ultraviolet radiation. *Plant Physiol* **108**: 891-6
- Britt AB, Chen JJ, Wykoff D, Mitchell D** (1993) A UV-sensitive mutant of Arabidopsis defective in the repair of pyrimidine-pyrimidinone(6-4) dimers. *Science* **261**: 1571-4
- Britz S** (1990) Photoregulation of root:shoot ratio in soybean seedlings. *Photochem Photobiol* **52**: 151-159
- Brodhun B, D-P Hä** (1993) UV-induced damage of photoreceptor proteins in the paraflagellar body of *Euglena gracilis*. *Photochem Photobiol* **58**: 270-4

- Caldwell CR** (1993) Ultraviolet-induced photodegradation of cucumber *Cucumis sativus* L microsomal and soluble protein tryptophanyl residues in vitro. *Plant Physiol* **101**: 947-53
- Caldwell MM** (1971) Solar UV irradiation and the growth and development of higher plants. In *Photophysiology* pp 131-177. Academic press, New York.
- Caldwell MM, Robberecht R, Billings WD** (1980a) A steep latitudinal gradient of solar ultraviolet-B radiation in the arctic-alpine life zone. *Ecology* **61**: 601-11
- Caldwell MM, Robberecht R, Nowak RS, Billings WD** (1980b) Differential photosynthetic inhibition by ultraviolet radiation in species from the Arctic-alpine life zone. *Arctic Alpine Res* **14**: 195-202
- Caldwell MM, Teramura AH, Tevini M** (1989) The changing solar ultraviolet climate and the ecological consequences for higher plants. *Trends Ecol Evol* **4**: 363-7
- Caldwell MM, Teramura AH, Tevini M, Bornman JF, Bjorn LO, Kulandaivelu G** (1995) Effects of increased solar ultraviolet radiation on terrestrial plants. *Ambio* **24**: 166-173
- Campbell AK, Trewavas AJ, Knight MR** (1996) Calcium imaging shows differential sensitivity to cooling and communication in luminous transgenic plants. *Cell Calcium* **19**: 211-8
- Castelluccio C, Paganga G, Melikian N, Bolwell GP, Pridham J, Sampson J, Riceevans C** (1995) Antioxidant potential of intermediates in phenylpropanoid metabolism in higher plants. *FEBS Letters* **368**: 188-92
- Cen YP, Bornman JF** (1993) The effect of exposure to enhanced UV-B radiation on the penetration of monochromatic and polychromatic UV-B radiation in the leaves of *Brassica napus*. *Plant Physiol* **87**: 249-55

- Chamnongpol S, Willekens H, Moeder W, Langebartels C, Sandermann H, Jr., Van Montagu M, Inze D, Van Camp W (1998)** Defense activation and enhanced pathogen tolerance induced by H<sub>2</sub>O<sub>2</sub> in transgenic tobacco. *Proc Natl Acad Sci U S A* **95**: 5818-23
- Chapple CC, Vogt T, Ellis BE, Somerville CR (1992)** An Arabidopsis mutant defective in the general phenylpropanoid pathway. *Plant Cell* **4**: 1413-24
- Chen QM, Bartholomew JC, Campisi J, Acosta M, Reagan JD, Ames BN (1998)** Molecular analysis of H<sub>2</sub>O<sub>2</sub>-induced senescent-like growth arrest in normal human fibroblasts: p53 and Rb control G1 arrest but not cell replication. *Biochem J* **332**: 43-50
- Chiesa R, McDermott MJ, Mann E, Spector A (1990)** The apparent molecular size of native alpha-crystallin B in non-lenticular tissues. *FEBS Lett* **268**: 222-6
- Chory J, Cook RK, Dixon R, Elich T, Li HM, Lopez E, Mochizuki N, Nagpal P, Pepper A, Poole D et al, (1995)** Signal-transduction pathways controlling light-regulated development in Arabidopsis. *Philos Trans R Soc Lond B Biol Sci* **350**: 59-65
- Christie JM, Jenkins GI (1996)** Distinct UV-B and UV-A/blue light signal transduction pathways induce chalcone synthase gene expression in Arabidopsis cells. *Plant Cell* **8**: 1555-67
- Cleaves H, Miller S (1998)** Oceanic protection of prebiotic organic compounds from UV radiation. *PNAS* **95**: 7260-7263
- Clegg MT (1993)** Chloroplast gene sequences and the study of plant evolution. *Proc Natl Acad Sci U S A* **90**: 363-7
- Climent I, Levine RL (1991)** Oxidation of the active site of glutamine synthetase: conversion of arginine-344 to gamma-glutamyl semialdehyde. *Arch Biochem Biophys* **289**: 371-5
- Coldiron BM (1996)** Ozone depletion update. *Dermatol Surg* **22**: 296-9

- Conconi A, Smerdon MJ, Howe GA, Ryan CA (1996)** The octadecanoid signaling pathway in plants mediates a response to ultraviolet radiation. *Nature* **383**: 826-9
- Conklin PL, Williams EH, Last RL (1996)** Environmental stress sensitivity of an ascorbic acid-deficient *Arabidopsis* mutant. *Proc Natl Acad Sci U S A* **93**: 9970-4
- Coohill TP (1989)** Ultraviolet action spectra :280-320 nm: and solar effectiveness spectra for higher plants. *Photochem Photobiol* **50**: 451-7
- Coohill TP (1992)** Action spectra revisited. *J Photochem Photobiol B* **13**: 95-8
- Curry G, Thimann K, Ray P (1956)** The base curvature response of *Avena* seedlings to the ultraviolet. *Physiol Plant* **9**: 429-40
- Dangl J, Hauffe K, Lippardt S, Hahlbrock K, Scheel D (1987)** Parsley protoplasts retain differential responsiveness to UV light and fungal elicitor. *EMBO J* **9**: 2551-2556
- Day T, Vogelmann T (1995)** Alterations in photosynthesis and pigment distributions in pea leaves following UV-B exposure. *Physiologia Plantarum* **94**: 433-440
- Day TA, Howells BW, Rice WJ (1994)** Ultraviolet absorption and epidermal-transmittance spectra in foliage. *Physiol Plant* **92**: 207-18
- Dean RT, Fu S, Stocker R, Davies MJ (1997)** Biochemistry and pathology of radical-mediated protein oxidation. *Biochem J* **324**: 1-18
- Delaye M, Tardieu A (1983)** Short-range order of crystallin proteins accounts for eye lens transparency. *Nature* **302**: 415-7
- Devary Y, Rosette C, DiDonato JA, Karin M (1993)** NF-kappa B activation by ultraviolet light not dependent on a nuclear signal. *Science* **261**: 1442-5
- Dhillon SS, Miksche JP (1983)** DNA, RNA, protein and heterochromatin changes during embryo development and germination of soybean (*Glycine max* L.). *Histochem J* **15**: 21-37

- Dietz K, Schramm M, Betz M, Busch H, Durr C, Martinoia E** (1992) Characterization of the epidermis from Barley primary leaves. I. Isolation of epidermal protoplasts. *Planta* **187**: 425-430
- Dikler S, Kelly J, Russell D** (1997) Improving mass spectrometric sequencing of arginine-containing peptides by derivatization with acetylacetone. *J Mass Spectrom* **32**: 1337-1349
- Dixon RA, Lamb CJ, Masoud S, Sewalt VJ, Paiva NL** (1996) Metabolic engineering: prospects for crop improvement through the genetic manipulation of phenylpropanoid biosynthesis and defense responses--a review. *Gene* **179**: 61-71
- Douglas C, Hoffman H, Schulz W, Hahlbrock K** (1987) Structure and UV-light stimulated expression of two 4-coumarate:CoA ligase genes in parsley. *EMBO J* **6**: 1189-1195
- Douglas CJ, Hauffe KD, Ites-Morales ME, Ellard M, Paszkowski U, Hahlbrock K, Dangl JL** (1991) Exonic sequences are required for elicitor and light activation of a plant defense gene, but promoter sequences are sufficient for tissue specific expression. *Embo J* **10**: 1767-75
- Dufour E, Haertle T** (1991) Binding of retinoids and beta-carotene to beta-lactoglobulin. Influence of protein modifications. *Biochim Biophys Acta* **1079**: 316-320
- Edwards G, Johnson E, Lai A, Krall J** (1993) Quantum yields of photosystem II and photosynthesis in an aurea mutant of tobacco (C<sub>3</sub>) and an oil yellow mutant of maize (C<sub>4</sub>) which have high capacities for photosynthesis despite low chlorophyll contents. *Plant Cell Physiol* **34**: 1205-1212
- Ensminger PA** (1993) Control of development in plants and fungi by far-UV radiation. *Physiol Plant* **88**: 501-8
- Fagerberg WR, Bornman JF** (1997) Ultraviolet-B radiation causes shade-type ultrastructural changes in *Brassica napus*. *Physiol Plant* **101**: 833-844

- Fankhauser C, Chory J** (1997) Light control of plant development. *Annu Rev Cell Dev Biol* **13**: 203-29
- Finley EL, Busman M, Dillon J, Crouch RK, Schey KL** (1997) Identification of photooxidation sites in bovine alpha-crystallin. *Photochem Photobiol* **66**: 635-41
- Fisher GJ, Datta SC, Talwar HS, Wang ZQ, Varani J, Kang S, Voorhees JJ** (1996) Molecular basis of sun-induced premature skin ageing and retinoid antagonism. *Nature* **379**: 335-9
- Foote CS** (1968) Mechanisms of photosensitized oxidation. There are several different types of photosensitized oxidation which may be important in biological systems. *Science* **162**: 963-670
- Foote CS** (1984) Mechanisms of photooxygenation. *Prog Clin Biol Res* **170**: 3-18
- Foote CS** (1991) Definition of type I and type II photosensitized oxidation. *Photochem Photobiol* **54**: 659
- Foote CS, Chang YC, Denny RW** (1970) Chemistry of singlet oxygen. XI. Cis-trans isomerization of carotenoids by singlet oxygen and a probable quenching mechanism. *J Amer Chem Soc* **92**: 5218-5219
- Foyer C, Descourvieres P, Kunert K** (1994) Protection against oxygen radicals: and important defence mechanism studied in transgenic plants. *Plant Cell Environ* **17**: 507-523
- Foyer C, Harbinson J** (1993) Oxygen metabolism and the regulation of photosynthetic transport. In *Causes of Photooxidative Stresses and Amelioration of Defense in Plants*. pp 1-42. CRC Press, Boca Raton.
- Frederick JE** (1990) Trends in atmospheric ozone and ultraviolet radiation: mechanisms and observations for the northern hemisphere. *Photochem Photobiol* **51**: 757-63
- Frederick JE, Snell HE, Haywood EK** (1989) Solar ultraviolet radiation at the Earth's surface. *Photochem Photobiol* **50**: 443-50

- Freiburghaus AU** (1994) Two-dimensional polyacrylamide gel electrophoresis of membrane proteins. *Mol Biotechnol* **2**: 281-93
- Friso G, Barbato R, Giacometti GM, Barber J** (1994) Degradation of D2 protein due to UV-B irradiation of the reaction centre of photosystem II. *FEBS Lett* **339**: 217-21
- Frohmeier H, Hahlbrock K, Schafer E** (1994) A light-responsive in vitro transcription system from evacuated parsley protoplasts. *Plant J* **5**: 437-49
- Fuglevand G, Jackson JA, Jenkins GI** (1996) UV-B, UV-A, and blue light signal transduction pathways interact synergistically to regulate chalcone synthase gene expression in *Arabidopsis*. *Plant Cell* **8**: 2347-57
- Fujimori E** (1981) Blue fluorescence and crosslinking of photooxidized proteins. *FEBS Lett* **135**: 257-260
- Fujimori E** (1982) Crosslinking and photoreaction of ozone-oxidized calf-lens alpha-crystallin. *Invest Ophthalmol Vis Sci* **22**: 402-5
- Furuya M** (1993) Phytochromes: Their molecular species, gene families, and functions. *Annu Review Plant Physiol Plant Mol Biol* **44**: 258-286
- Gaba V, Black M** (1987) Two separate photoreceptors control hypocotyl growth in green seedlings. *Nature* **278**: 51-4
- Gallo RL, Kochevar IE, Granstein RD** (1989) Ultraviolet radiation induces a change in cell membrane potential in vitro: a possible signal for ultraviolet radiation induced alteration in cell activity. *Photochem Photobiol* **49**: 655-62
- Gendreau E, Traas J, Desnos T, Grandjean O, Caboche M, Hofte H** (1997) Cellular basis of hypocotyl growth in *Arabidopsis thaliana*. *Plant Physiol* **114**: 295-305



- Ghosh S, Gepstein S, Glick B, Heikkila J, Dumbroff E** (1989) Thermal regulation of phosphoenol pyruvate carboxylase and ribulose carboxylase in C<sub>3</sub> and C<sub>4</sub> plants native to hot and temperate climates. *Plant Physiol* **90**: 1298-1304
- Ghosh S, Gepstein S, Heikkila JJ, Dumbroff EB** (1988) Use of a scanning densitometer or an ELISA plate reader for measurement of nanogram amounts of protein in crude extracts from biological tissues. *Anal Biochem* **169**: 227-33
- Girotti A** (1990) Photodynamic lipid peroxidation in biological systems. *Photochem Photobiol* **51**: 497-509
- Godar DE** (1996) Preprogrammed and programmed cell death mechanisms of apoptosis: UV-induced immediate and delayed apoptosis. *Photochem Photobiol* **63**: 825-30
- Gonnelli M, Strambini GB** (1995) Phosphorescence lifetime of tryptophan in proteins. *Biochemistry* **34**: 13847-57
- Goto N, Yamamoto KT, Watanabe M** (1993) Action spectra for inhibition of hypocotyl growth of wild-type plants and of the *hy2* long-hypocotyl mutant of *Arabidopsis thaliana* L. *Photochemistry Photobiology* **57**: 867-871
- Green R, Fluhr R** (1995) UV-B-induced PR-1 accumulation is mediated by active oxygen species. *Plant Cell* **7**: 203-212
- Greenberg B, Wilson M, Huang X-D, Duxbury C, Gerhardt K, Gensmer R** (1997) The effects of ultraviolet-B radiation on higher plants. In *Plants For Environmental Studies* pp 1-36. CRC Press, Boca Raton.
- Greenberg BM, Gaba V, Canaani O, Malkin S, Mattoo AK, Edelman M** (1989) Separate photosensitizers mediate degradation of the 32-kDa photosystem II reaction center protein in the visible and UV spectral regions. *Proc Natl Acad Sci USA* **86**: 6617-20

- Greenberg BM, Gaba V, Mattoo AK, Edelman M (1987)** Identification of a primary in vivo degradation product of the rapidly-turning-over 32 kd protein of photosystem II. *Embo J* **6**: 2865-9
- Greenberg BM, Wilson MI, Gerhardt KE, Wilson KE (1996)** Morphological and physiological responses of *Brassica napus* to ultraviolet-B radiation: Photomodification of ribulose-1,5-bisphosphate carboxylase/oxygenase and potential acclimation processes. *Journal of Plant Physiology* **148**: 78-85
- Gregersen L, Christensen AB, Sommer-Knudsen J, Collinge DB (1994)** A putative O-methyltransferase from barley is induced by fungal pathogens and UV light. *Plant Mol Biol* **26**: 1797-806
- Griggs M (1966)** Atmospheric Ozone. In *The Middle Ultraviolet: Its Science and Technology* pp 83-117. Pure and Applied Optics. John Wiley and Sons, New York.
- Grossweiner LI (1984)** Photochemistry of proteins: a review. *Curr Eye Res* **3**: 137-44
- Guptasarma P, Balasubramanian D, Matsugo S, Saito I (1992)** Hydroxyl radical mediated damage to proteins, with special reference to the crystallins. *Biochemistry* **31**: 4296-303
- Gutteridge JM (1994)** Biological origin of free radicals, and mechanisms of antioxidant protection. *Chem Biol Interact* **91**: 133-140
- Hada M, Tsurumi S, Suzuki M, Wellmann E, Hashimoto T (1996)** Involvement and non-involvement of pyrimidine dimer formation in UV-B effects on *Sorghum bicolor* Moench seedlings. *Journal of Plant Physiology* **148**: 92-99
- Hahlbrock K, Scheel D (1989)** Physiology and molecular biology of phenylpropanoid metabolism. *Annu Rev Plant Physiol Mol Biol* **40**: 347-369
- Halliwell B (1992)** The Chemistry of Free Radicals. *Toxicology and Industrial Health* **9**: 1-21

- Harter K, Frohnmeyer H, Kircher S, Kunkel T, Muhlbauer S, Schafer E (1994)** Light induces rapid changes of the phosphorylation pattern in the cytosol of evacuated parsley protoplasts. *Proc Natl Acad Sci U S A* **91**: 5038-42
- Hartmann U, Valentine WJ, Christie JM, Hays J, Jenkins GI, Weisshaar B (1998)** Identification of UV/blue light-response elements in the *Arabidopsis thaliana* chalcone synthase promoter using a homologous protoplast transient expression system. *Plant Mol Biol* **36**: 741-54
- Hashimoto T, Ito S, Yatsunami H (1984)** Ultraviolet light-induced coiling and curvature of broom sorghum first internodes. *J Photochem Photobiol B: Biol* **11**: 353-63
- Hashimoto T, Shichijo C, Yatsunami H (1991)** Ultraviolet action spectra for the induction and inhibition of anthocyanin synthesis in broom sorghum seedlings. *J Photochem Photobiol B: Biol* **11**: 353-63
- Hazell LJ, van den Berg JJ, Stocker R (1994)** Oxidation of low-density lipoprotein by hypochlorite causes aggregation that is mediated by modification of lysine residues rather than lipid oxidation. *Biochem J* **302**: 297-304
- Henderson BW, Miller AC (1986)** Effects of scavengers of reactive oxygen and radical species on cell survival following photodynamic treatment in vitro: comparison to ionizing radiation. *Radiat Res* **108**: 196-205
- Hidema J, Kumagai T, Sutherland JC, Sutherland MB (1997)** Ultraviolet-B-sensitive rice cultivar deficient in cyclobutane dimer repair. *Plant Physiol* **113**: 39-44
- Hodick D, Kutschera U (1992)** Light-Induced Inhibition of Elongation Growth in Sunflower Hypocotyls - Biophysical and Ultrastructural Investigations. *Protoplasma* **168**: 7-13
- Hoey B, Butler J (1984)** The repair of oxidized amino acids by antioxidants. *Biochim Biophys Acta* **791**: 212-218

- Horvath DM, Chua NH** (1996) Identification of an immediate-early salicylic acid-inducible tobacco gene and characterization of induction by other compounds. *Plant Mol Biol* **31**: 1061-72
- Hott JL, Borkman RF** (1992) Analysis of photo-oxidized amino acids in tryptic peptides of calf lens gamma-II crystallin. *Photochem Photobiol* **56**: 257-63
- Hsu DS, Zhao X, Zhao S, Kazantsev A, Wang RP, Todo T, Wei YF, Sancar A** (1996) Putative human blue-light photoreceptors hCRY1 and hCRY2 are flavoproteins. *Biochemistry* **35**: 13871-7
- Huang C, Ma WY, Ryan CA, Dong Z** (1997) Proteinase inhibitors I and II from potatoes specifically block UV- induced activator protein-1 activation through a pathway that is independent of extracellular signal-regulated kinases, c-Jun N-terminal kinases, and P38 kinase. *Proc Natl Acad Sci U S A* **94**: 11957-62
- Huang RP, Wu JX, Fan Y, Adamson ED** (1996) UV activates growth factor receptors via reactive oxygen intermediates. *J Cell Biol* **133**: 211-20
- Huang X-D, Dixon D, Greenberg B** (1993) Impacts of UV radiation and photomodification on the toxicity of PAHs to the higher plant *Lemna gibba* (Duckweed). *Environ Toxicol Chem* **12**: 1067-1077
- Hughes J, Lamparter T, Mittmann F, Hartmann E, Gartner W, Wilde A, Borner T** (1997) A prokaryotic phytochrome. *Nature* **386**: 663
- Huner N, Maxwell D, Gray G, Savitch L, Krol M, Ivanov A, Falk S** (1996) Sensing environmental temperature change through imbalances between energy supply and energy consumption: Redox state of photosystem II. *Plant Physiol* **98**: 358-364
- Huner N, Öquist G, Sarhan F** (1998) Energy balance and acclimation to light and cold. *Trends In Plant Sci* **3**: 224-230

- Huner NP, Macdowall FD** (1979) Changes in the net charge and subunit properties of ribulose bisphosphate carboxylase--oxygenase during cold hardening of Puma rye. *Can J Biochem* **57**: 155-64
- Huner NP, Palta JP, Li PH, Carter JV** (1981) Comparison of the structure and function of ribulosebisphosphate carboxylase--oxygenase from a cold-hardy and nonhardy potato species. *Can J Biochem* **59**: 280-9
- Hzadina G, Alscher-Hermant R, Kish VM** (1982) Subcellular localization of flavonoid synthesizing enzymes in Pisum, Phaseolus, Brassica and Spinacia cultivars. *Phytochem* **19**: 1355-9
- Ichikawa T, Suzuki Y, Czaja I, Schommer C, Lessnick A, Schell J, Walden R** (1997) Identification and role of adenylyl cyclase in auxin signalling in higher plants. *Nature* **390**: 698-701
- Imbrie CW, Murphy TM** (1984) Mechanism for inactivation of plant plasma membrane ATPase. *Photochem Photobiol* **40**: 243-8
- Inoue K, Matsuura T, Saito I** (1982) Photogeneration of superoxide and hydrogen peroxide from tryptophan and its photooxidation products: The role of 3 $\alpha$ -hydroperoxytryptophan. *Photochem Photobiol* **35**: 133-139
- Jahnen W, Hahlbrock K** (1988) Differential regulation and tissue-specific distribution of enzymes of phenylpropanoid pathways in developing parsley seedlings. *Planta* **173**: 453-458
- Jansen M, Gaba V, Greenberg B** (1998) Higher plants and UV-B radiation: balancing damage, repair and acclimation. *Trends In Plant Sci* **3**: 131-135

- Jansen MAK, Gaba V, Greenberg BM, Mattoo AK, Edelman M (1996)** Low threshold levels of ultraviolet-B in a background of photosynthetically active radiation trigger rapid degradation of the D2 protein of photosystem-II. *Plant Journal* **9**: 693-699
- Jenkins ME, Harlow GR, Liu ZR, Shotwell MA, Ma J, Mount DW (1995)** Radiation-sensitive mutants of *Arabidopsis thaliana*. *Genetics* **140**: 725-32
- Jenkins ME, Suzuki TC, Mount DW (1997)** Evidence that heat and ultraviolet radiation activate a common stress- response program in plants that is altered in the *uvh6* mutant of *Arabidopsis thaliana*. *Plant Physiol* **115**: 1351-8
- Jiang C, Yee J, Mitchell DL, Britt AB (1997)** Photorepair mutants of *Arabidopsis*. *Proc Natl Acad Sci U S A* **94**: 7441-5
- Johnson C, Morris D (1987)** Regulation of auxin transport in pea (*Pisum sativum* L.) by phenylacetic acid: inhibition of polar auxin transport in intact plants and stem segments. *Planta* **172**: 408-416
- Jordan BR, Chow WS, Strid A, Anderson JM (1991)** Reduction in *cab* and *psb A* RNA transcripts in response to supplementary ultraviolet-B radiation. *FEBS Lett* **284**: 5-8
- Jordan BR, He J, Chow WS, Anderson JM (1992)** Changes in the mRNA levels and polypeptide subunits of ribulose-1,5-bisphosphate carboxylase in response to ultraviolet-B radiation. *Plant Cell and Environment* **15**: 91-8
- Joshi PN, Biswal B, Kulandaivelu G, Biswal UC (1994)** Response of senescing wheat leaves to ultraviolet A light: changes in energy transfer efficiency and PS II photochemistry. *Radiat Environ Biophys* **33**: 167-76

- Kaiser T, Emmler K, Kretsch T, Weisshaar B, Schafer E, Batschauer A (1995)** Promoter elements of the mustard CHS1 gene are sufficient for light regulation in transgenic plants. *Plant Molecular Biology* **28**: 219-29
- Kasperbauer M (1987)** Far-red light reflection from green leaves and effects on phytochrome-mediated assimilate partitioning under field conditions. *Plant Physiol* **85**: 350-354
- Kato Y, Uchida K, Kawakishi S (1992)** Oxidative Degradation of Collagen and Its Model Peptide by Ultraviolet Irradiation. *Journal of Agricultural and Food Chemistry* **40**: 373-9
- Keller C, Van Volkenburg E (1997)** Auxin-induced epinasty of tobacco leaf tissues. A nonethylene-mediated response. *Plant Physiol* **113**: 603-610
- Kerr JB, McElroy CT (1993)** Evidence for large upward trends of ultraviolet-B radiation linked to ozone depletion. *Science* **262**: 1032-4
- Kim J, Harter K, Theologis A (1997)** Protein-protein interactions among the Aux/IAA proteins. *Proc Natl Acad Sci U S A* **94**: 11786-91
- Kim ST, Li YF, Sancar A (1992)** The third chromophore of DNA photolyase: Trp-277 of *Escherichia coli* DNA photolyase repairs thymine dimers by direct electron transfer. *Proc Natl Acad Sci U S A* **89**: 900-4
- Kircher S, Ledger S, Hayashi H, Weisshaar B, Schafer E, Frohnmeyer H (1998)** CPRF4a, a novel plant bZIP protein of the CPRF family: comparative analyses of light-dependent expression, post-transcriptional regulation, nuclear import and heterodimerisation. *Mol Gen Genet* **257**: 595-605
- Knebel A, Rahmsdorf HJ, Ullrich A, Herrlich P (1996)** Dephosphorylation of receptor tyrosine kinases as target of regulation by radiation, oxidants or alkylating agents. *Embo J* **15**: 5314-25

- Knight S, Andersson I, Brändén CI** (1990) Crystallographic analysis of ribulose-1,5-bisphosphate carboxylase from spinach at 2.4 Å. *J Mol Biol* **215**: 113-60
- Kochevar IE** (1990) UV-induced protein alterations and lipid oxidation in erythrocyte membranes. *Photochem Photobiol* **52**: 795-800
- Koes R, Spelt C, Mol J** (1989) The chalcone synthase multigene family of *Petunia hybrida* (V30): differential, light regulated expression during flower development and UV light induction. *Plant Mol Biol* **12**: 213-225
- Kramer GF, Norman HA, Krizek DT, Mirecki RM** (1991) Influence of UV-B radiation on polyamines, lipid peroxidation and membrane lipids in cucumber. *Phytochem* **30**: 2101-8
- Krinsky N** (1979) Biological roles of singlet oxygen. In *Singlet Oxygen* pp 597-641. Academic press, New York.
- Krizek D, Britz S, Mirecki R** (1998) Inhibitory effects of ambient levels of solar UV-A and UV-B radiation on growth of cv. New Red Fire lettuce. *Physiol Plant* **103**: 1-7
- Krizek D, Mirecki R, Britz S** (1997) Inhibitory effects of ambient levels of solar UV-A and UV-B radiation on growth of cucumber. *Physiol Plant* **100**: 886-891
- Kruezaier F, Ragg H, Fautz E, D NK, Hahlbrock K** (1983) UV induction of chalcone synthase mRNA in cell suspension cultures of *Petroselinium hortense*. *Proc Natl Acad Sci USA* **80**: 2591-3
- Kubasek WL, Shirley BW, McKillop A, Goodman HM, Briggs W, Ausubel FM** (1992) Regulation of Flavonoid Biosynthetic Genes in Germinating *Arabidopsis* Seedlings. *Plant Cell* **4**: 1229-36



- Kuhn DN, Chappell J, Boudet A, Hahlbrock K** (1987) Induction of phenylalanine ammonium-lyase and 4-coumarate:CoA ligase mRNAs in cultured plant cells by UV light or fungal elicitor. *Proc Natl Acad Sci USA* **81**: 1102-6
- Laemmli UK** (1970) Cleavage of structural proteins during the assembly of the head of bacteriophage T4. *Nature* **227**: 680-5
- Landry LG, Chapple CC, Last RL** (1995) Arabidopsis mutants lacking phenolic sunscreens exhibit enhanced ultraviolet-B injury and oxidative damage. *Plant Physiol* **109**: 1159-66
- Landry LG, Pell EJ** (1993) Modification of rubisco and altered proteolytic activity in O<sub>3</sub>-stressed hybrid poplar :*Populus maximowizii* x *trichocarpa*. *Plant Physiol* **101**: 1355-62
- Landry LG, Stapleton AE, Lim J, Hoffman P, Hays JB, Walbot V, Last RL** (1997) An Arabidopsis photolyase mutant is hypersensitive to ultraviolet-B radiation. *Proc Natl Acad Sci U S A* **94**: 328-32
- Lawrence ME, Possingham JV** (1986) Direct measurement of femtogram amounts of DNA in cells and chloroplasts by quantitative microspectrofluorometry. *J Histochem Cytochem* **34**: 761-8
- Learn DB, Beard J, Moloney SJ** (1993) The ultraviolet C energy emitted from FS lamps contributes significantly to the induction of human erythema and murine ear edema. *Photodermatol Photoimmunol Photomed* **9**: 147-53
- Lecari B, Sodi F, M.L. dP** (1990) Photomorphogenic responses to UV radiation: Involvement of phytochrome and UV photoreceptors in the control of hypocotyl elongation in *Lycopersicon esculentum*. *Physiologia Plantarum* **79**: 668-672
- Lee JS, Liao JH, Wu SH, Chiou SH** (1997) alpha-Crystallin acting as a molecular chaperonin against photodamage by UV irradiation. *J Protein Chem* **16**: 283-9

- Levine A, Pennell RI, Alvarez ME, Palmer R, Lamb C (1996)** Calcium-mediated apoptosis in a plant hypersensitive disease resistance response. *Curr Biol* **6**: 427-37
- Levine A, Tenhaken R, Dixon R, Lamb C (1994)** H<sub>2</sub>O<sub>2</sub> from the oxidative burst orchestrates the plant hypersensitive disease resistance response. *Cell* **79**: 583-93
- Levine RL, Garland D, Oliver CN, Amici A, Climent I, Lenz AG, Ahn BW, Shaltiel S, Stadtman ER (1990)** Determination of carbonyl content in oxidatively modified proteins. *Methods Enzymol* **186**: 464-78
- Leyser HM (1998)** Plant hormones. *Curr Biol* **8**: R5-7
- Li DY, Borkman RF, Wang RH, Dillon J (1990)** Mechanisms of photochemically produced turbidity in lens protein solutions. *Exp Eye Res* **51**: 663-9
- Li J, Nagpal P, Vitart V, McMorris TC, Chory J (1996)** A role for brassinosteroids in light-dependent development of Arabidopsis. *Science* **272**: 398-401
- Li JY, Oulee TM, Raba R, Amundson RG, Last RL (1993)** Arabidopsis flavonoid mutants are hypersensitive to UV-B irradiation. *Plant Cell* **5**: 171-9
- Lichtenthaler HK (1987)** Chlorophylls and carotenoids: pigments of photosynthetic biomembranes. *Methods Enzymol* **148**: 350-82
- Lin C, Robertson DE, Ahmad M, Raibekas AA, Jorns MS, Dutton PL, Cashmore AR (1995)** Association of flavin adenine dinucleotide with the Arabidopsis blue light receptor CRY1. *Science* **269**: 968-70
- Linscheid M, Wendisch D, Strack D (1980)** The structures of sinapic acid esters and their metabolism in cotyledons of *Raphanus sativum*. *Z Naturforsch* **35c**: 907-914
- Liochev SI, Fridovich I (1994)** The role of O<sub>2</sub><sup>-</sup> in the production of HO<sub>2</sub><sup>·</sup>: in vitro and in vivo. *Free Radic Biol Med* **16**: 29-33

- Liscum E, Young JC, Poff KL, Hangarter RP** (1992) Genetic Separation of Phototropism and Blue Light Inhibition of Stem Elongation. *Plant Physiology* **100**: 267-71
- Lissi E, Clavero N** (1990) Inactivation of lysozyme by alkylperoxyl radicals. *Free Radic Res Commun* **10**: 177-184
- Llic N, Normanly J, Cohen JD** (1996) Quantification of free plus conjugated indoleacetic acid in arabidopsis requires correction for the nonenzymatic conversion of indolic nitriles. *Plant Physiol* **111**: 781-8
- Logemann E, Wu SC, Schroder J, Schmelzer E, Somssich IE, Hahlbrock K** (1995) Gene activation by UV light, fungal elicitor or fungal infection in *Petroselinum crispum* is correlated with repression of cell cycle-related genes. *Plant J* **8**: 865-76
- Lois R** (1994) Accumulation of UV-absorbing flavonoids induced by UV-B radiation in *Arabidopsis thaliana* L.I. Mechanisms of UV-resistance in *Arabidopsis*. *Planta* **194**: 498-503
- Lorenzen M, Racicot V, Strack D, Chapple C** (1996) Sinapic acid ester metabolism in wild type and a sinapoylglucose-accumulating mutant of arabidopsis. *Plant Physiol* **112**: 1625-30
- Low P, Merida J** (1996) The oxidative burst in plant defense: function and signal transduction. *Physiol Plant* **96**: 533-542
- Madronich S, McKenzie RL, Caldwell MM, Bjorn LO** (1995) Changes in ultraviolet radiation reaching the Earth's surface. *Ambio* **24**: 143-52
- Malloy KD, Holman MA, Mitchell D, Detrich HW, 3rd** (1997) Solar UVB-induced DNA damage and photoenzymatic DNA repair in antarctic zooplankton. *Proc Natl Acad Sci U S A* **94**: 1258-63

- Margis-Pinheiro M, Martin C, Didierjean L, Burkard G** (1993) Differential expression of bean chitinase genes by virus infection, chemical treatment and UV irradiation. *Plant Mol Biol* **22**: 659-68
- Mark U, Tevini M** (1996) Combination effects of UV-B radiation and temperature on sunflower (*Helianthus annuus* L., cv. Polstar) and maize (*Zea mays* L., cv. Zenit 2000) seedlings. *J Plant Physiol* **148**: 49-56
- Martin CR** (1993) Structure, function, and regulation of the chalcone synthase. *Int Rev Cytol* **147**: 233-84
- Masaki H, Sakurai H** (1997) Increased generation of hydrogen peroxide possibly from mitochondrial respiratory chain after UVB irradiation of murine fibroblasts. *J Dermatol Sci* **14**: 207-16
- Mavandad M, Edwards R, Liang X, Lamb C, Dixon R** (1990) Effects of trans-cinnamic acid on expression of the bean phenylalanine ammonia-lyase gene family. *Plant Physiol* **94**: 671-680
- Mazza C, Battista D, Zima A, Szwarcberg M, Acevedo A, Scopel A, Ballaré C** (Year) Antioxidant and growth responses of field-grown barley crops to solar UVB radiation. Annual Meeting of the American Society of Plant Physiologists. Madison, Wisconsin. Abstract 382.
- McCormac D, Bruce D, Greenberg B** (1994) Connection between state transitions, LHCII phosphorylation and LHCII migration *in vivo* in the higher plant *Spirodela oligorrhiza*. *Biochem Biophys Acta* **1187**: 301-312
- McDermott M, Chiesa R, Roberts JE, Dillon J** (1991) Photooxidation of specific residues in alpha-crystallin polypeptides. *Biochemistry* **30**: 8653-60
- McIntosh D** (1992) Glutaraldehyde cross-links Lys-492 and Arg-678 at the active site of sarcoplasmic reticulum Ca(2+)-ATPase. *J Biol Chem* **267**: 22328-22335

- McKhann HI, Hirsch AM** (1994) Isolation of chalcone synthase and chalcone isomerase cDNAs from alfalfa (*Medicago sativa* L.): highest transcript levels occur in young roots and root tips. *Plant Mol Biol* **24**: 767-77
- Meagher RB, Berry-Lowe S, Rice K** (1989) Molecular evolution of the small subunit of ribulose biphosphate carboxylase: nucleotide substitution and gene conversion. *Genetics* **123**: 845-63
- Mehta RA, Fawcett TW, Porath D, Mattoo AK** (1992) Oxidative stress causes rapid membrane translocation and in vivo degradation of ribulose-1,5-biphosphate carboxylase/oxygenase. *J Biol Chem* **267**: 2810-6
- Melaragno JE, Mehrotra B, Coleman AW** (1993) Relationship between endopolyploidy and cell size in epidermal tissue of *Arabidopsis*. *Plant Cell* **5**: 1661-1668
- Mendez F, Penner R** (1998) Near-visible ultraviolet light induces a novel ubiquitous calcium-permeable cation current in mammalian cell lines. *J Physiol (Lond)* **507**: 365-77
- Millner PA** (1995) The auxin signal. *Curr Opin Cell Biol* **7**: 224-31
- Millner PA, White IR, Groarke DA, Theil G, Blatt MR** (1994) Novel strategies to an auxin-evoked transport control. *Symp Soc Exp Biol* **48**: 203-13
- Miyamoto Y, Sancar A** (1998) Vitamin B2-based blue-light photoreceptors in the retinohypothalamic tract as the photoactive pigments for setting the circadian clock in mammals. *Proc Natl Acad Sci U S A* **95**: 6097-102
- Mons N, Decorte L, Jaffard R, Cooper DM** (1998) Ca<sup>2+</sup>-sensitive adenylyl cyclases, key integrators of cellular signalling. *Life Sci* **62**: 1647-52
- Moseley H, Mackie RM** (1997) Ultraviolet B radiation was increased at ground level in scotland during a period of ozone depletion. *Br J Dermatol* **137**: 101-2

- Mudd JB, Dawson PJ, Tseng S, Liu FP (1997)** Reaction of ozone with protein tryptophans: band III, serum albumin, and cytochrome C. *Arch Biochem Biophys* **338**: 143-9
- Nakajima S, Sugiyama M, Iwai S, Hitomi K, Otoshi E, Kim ST, Jiang CZ, Todo T, Britt AB, Yamamoto K (1998)** Cloning and characterization of a gene (UVR3) required for photorepair of 6-4 photoproducts in *Arabidopsis thaliana*. *Nucleic Acids Res* **26**: 638-44
- Nogues S, Allen D, Morison J, Baker N (1998)** Ultraviolet-B radiation effects on water relations, leaf development, and photosynthesis in droughted pea plants. *Plant Physiol* **117**: 173-181
- Nogues S, Baker NR (1995)** Evaluation of the role of damage to photosystem II in the inhibition of CO<sub>2</sub> assimilation in pea leaves on exposure to UV-B radiation. *Plant Cell and Environment* **18**: 781-7
- Okajima T, Kawata Y, Hamaguchi K (1990)** Chemical modification of tryptophan residues and stability changes in proteins. *Biochemistry* **29**: 9168-75
- Patthy L, Thesz J (1980)** Origin of the selectivity of alpha-dicarbonyl reagents for arginyl residues of anion-binding sites. *Eur J Biochem* **105**: 387-93
- Pepper AE (1998)** Molecular evolution: old branches on the phytochrome family tree. *Curr Biol* **8**: R117-20
- Pfundel EE, Pan RS, Dilley RA (1992)** Inhibition of violaxanthin deepoxidation by ultraviolet-B radiation in isolated chloroplasts and intact leaves. *Plant Physiology* **98**: 1372-1380
- Pigault C, Gerard D (1984)** Influence of the location of tryptophanyl residues in proteins on their photosensitivity. *Photochem Photobiol* **40**: 291-6
- Pigault C, Gerard D (1989)** Selective degradation of amino acids photosensitized by tryptophan in polypeptidic structures. *Photochem Photobiol* **50**: 23-8

- Pirie A** (1971) Formation of N-formylkynurenine in proteins from lens and other sources by exposure to sunlight. *Biochem. J.* **125**: 203-208
- Polidoros AN, Scandalios JG** (1997) Response of the maize catalases to light. *Free Radic Biol Med* **23**: 497-504
- Pryor WA, Uppu RM** (1993) A kinetic model for the competitive reactions of ozone with amino acid residues in proteins in reverse micelles. *J Biol Chem* **268**: 3120-6
- Pyke K** (1994) *Arabidopsis* - Its use in the genetic and molecular analysis of plant morphogenesis. *New Phytologist* **128**: 19-37
- Quail PH** (1997) The phytochromes: a biochemical mechanism of signaling in sight? *Bioessays* **19**: 571-9
- Quaite FE, Sutherland BM, Sutherland JC** (1992) Action spectrum for DNA damage in alfalfa lowers predicted impact of ozone depletion. *Nature* **358**: 576-8
- Quillet-Mary A, Jaffrezou JP, Mansat V, Bordier C, Naval J, Laurent G** (1997) Implication of mitochondrial hydrogen peroxide generation in ceramide- induced apoptosis. *J Biol Chem* **272**: 21388-95
- Rabilloud T, Carpentier G, Tarroux P** (1988) Improvement and simplification of low-background silver staining of proteins by using sodium dithionite. *Electrophoresis* **9**: 288-91
- Rambler MB, Margulis L** (1980) Bacterial resistance to ultraviolet irradiation under anaerobiosis: implications for pre-phanerozoic evolution. *Science* **210**: 638-40
- Rao MV, Ormrod DP** (1995a) Differential response of photosynthetic pigments, rubisco activity and rubisco protein of *Arabidopsis thaliana* exposed to UVB and ozone. *Photochemistry and Photobiology* **62**: 727-735

- Rao MV, Ormrod DP (1995b)** Impact of UVB and O<sub>3</sub> on the oxygen free radical scavenging system in *Arabidopsis thaliana* genotypes differing in flavonoid biosynthesis. *Photochemistry and Photobiology* **62**: 719-726
- Rao MV, Ormrod DP (1995c)** Ozone exposure decreases UVB sensitivity in a UVB-sensitive flavonoid mutant of *Arabidopsis*. *Photochem Photobiol* **61**: 71-8
- Rao MV, Paliyath G, Ormrod DP (1996)** Ultraviolet-B- and ozone-induced biochemical changes in antioxidant enzymes of *Arabidopsis thaliana*. *Plant Physiol* **110**: 125-36
- Rao PV, Huang QL, Horwitz J, Zigler JS, Jr. (1995)** Evidence that alpha-crystallin prevents non-specific protein aggregation in the intact eye lens. *Biochim Biophys Acta* **1245**: 439-47
- Ray PM, Curry GM (1958)** Intermediates and competing reactions in the photodestruction of indoleacetic acid. *Nature* **181**: 896-7
- Rayle DL, Cleland RE (1992)** The Acid Growth Theory of Auxin-Induced Cell Elongation is Alive and Well. *Plant Physiology* **99**: 1271-4
- Reuber S, Bornman JF, Weissenbock G (1996)** A flavonoid mutant of barley (*Hordeum vulgare* L.) exhibits increased sensitivity to UV-B radiation in the primary leaf. *Plant Cell Environ* **19**: 593-601
- Riordan JF, McElvany KD, Borders CL, Jr. (1977)** Arginyl residues: anion recognition sites in enzymes. *Science* **195**: 884-6
- Rmoso C, Forster LS (1975)** Tryptophan fluorescence lifetimes in lysozyme. *J Biol Chem* **250**: 3738-45
- Ros J, Tevini M (1995)** Interaction of UV-radiation and IAA during growth of seedlings and hypocotyl segments of sunflower. *Journal of Plant Physiology* **146**: 295-302



- Rose RJ, Cran DG, Possingham JV** (1975) Changes in DNA synthesis during cell growth and chloroplast replication in greening spinach leaf disks. *J Cell Sci* **17**: 27-41
- Rother T, Acker G, Scheibe R** (1988) Immunogold localization of chloroplast protein in spinach leaf mesophyll, epidermis and guard cells. *Bot Acta* **101**: 311-320
- Rowland S** (1991) Stratospheric Ozone Depletion. *Annu Rev Phys Chem* **42**: 731-768
- Sancar A** (1994) Structure and function of DNA photolyase. *Biochemistry* **33**: 2-9
- Sancar A** (1996) No "End of History" for photolyases. *Science* **272**: 48-9
- Schagger H, von Jagow G** (1987) Tricine-sodium dodecyl sulfate-polyacrylamide gel electrophoresis for the separation of proteins in the range from 1 to 100 kDa. *Anal Biochem* **166**: 368-79
- Scharffetter-Kochanek K, Wlaschek M, Brenneisen P, Schauen M, Blandschun R, Wenk J** (1997) UV-induced reactive oxygen species in photocarcinogenesis and photoaging. *Biol Chem* **378**: 1247-57
- Schauerte JA, Gafni A** (1995) Photodegradation of tryptophan residues and attenuation of molecular chaperone activity in alpha-crystallin are correlated. *Biochem Biophys Res Commun* **212**: 900-5
- Schieven GL, Mittler RS, Nadler SG, Kirihara JM, Bolen JB, Kanner SB, Ledbetter JA** (1994) ZAP-70 tyrosine kinase, CD45, and T cell receptor involvement in UV- and H<sub>2</sub>O<sub>2</sub>-induced T cell signal transduction. *J Biol Chem* **269**: 20718-26
- Schmelzer E, Jahnen W, Hahlbrock K** (1988) In situ localization of light-induced chalcone synthase mRNA, chalcone synthase, and flavonoid end products in the epidermal cells of parsley leaves. *Proc Natl Acad Sci USA* **85**: 2989-93

- Schreiber U** (1983) Chlorophyll fluorescence yield changes as a tool in plant physiology. *Photosynth Res* **4**: 361-373
- Schulz M, Weissenbock G** (1986) Isolation and separation of epidermal and mesophyll protoplasts from rye primary leaves - tissue-specific characteristics of secondary phenolic product accumulation. *Z Naturforsch* **41c** p22 **7**: 22-7
- Schulze-Lefert P, Dangl JL, Becker-Andre M, Hahlbrock K, Schulz W** (1989) Inducible in vivo DNA footprints define sequences necessary for UV light activation of the parsley chalcone synthase gene. *Embo J* **8**: 651-6
- Seckmeyer G, Mayer B, Erb R, Bernhard G** (1994) UV-B in Germany Higher in 1993 Than in 1992. *Geophysical Research Letters* **21**: 577-80
- Sembdner G, Atzorn R, Schneider G** (1994) Plant hormone conjugation. *Plant Mol Biol* **26**: 1459-81
- Sharma V, Strack D** (1985) Vacuolar localization of l-sinapoylglucose: L-malate sinapoyltransferase in protoplasts from cotyledons of *Raphanus sativus*. *Planta* **163**: 563-568
- Sheahan JJ** (1996) Sinapate esters provide greater UV-B attenuation than flavonoids in *Arabidopsis thaliana* (Brassicaceae). *Amer J Bot* **83**: 679-686
- Shimmura S, Suematsu M, Shimoyama M, Tsubota K, Oguchi Y, Ishimura Y** (1996) Subthreshold UV radiation-induced peroxide formation in cultured corneal epithelial cells: the protective effects of lactoferrin. *Exp Eye Res* **63**: 519-26
- Shipanova IN, Glomb MA, Nagaraj RH** (1997) Protein modification by methylglyoxal: chemical nature and sythetic mechanism of a major fluorescent adduct. *Arch Biochem Biophys* **344**: 29-36
- Shirasu K, Dixon RA, Lamb C** (1996) Signal transduction in plant immunity. *Curr Opin Immunol* **8**: 3-7

- Smith H, Xu Y, Quail PH** (1997a) Antagonistic but complementary actions of phytochromes A and B allow seedling de-etiolation. *Plant Physiol* **114**: 637-41
- Smith JB, Jiang X, Abraham EC** (1997b) Identification of hydrogen peroxide oxidation sites of alpha A- and alpha B-crystallins. *Free Radic Res* **26**: 103-11
- Staelin L, Arntzen C** (1983) Regulation of chloroplast membrane function: Protein phosphorylation changes the spatial organization of membrane components. *J Cell Biol* **97**: 1327-1337
- Staiger D, Kaulen H, Schell J** (1989) A CACGTG motif of the *Antirrhinum majus* chalcone synthase promoter is recognized by an evolutionarily conserved nuclear protein. *PNAS* **89**: 6930-6934
- Stapleton AE, Walbot V** (1994) Flavonoids can protect maize DNA from the induction of ultraviolet radiation damage. *Plant Physiol* **105**: 881-9
- Staxen I, Bergounioux C, Bornman JF** (1993) Effect of ultraviolet radiation on cell division and microtubule organization in *Petunia hybrida* protoplasts. *Protoplasma* **173**: 70-6
- Steinmetz V, Wellmann E** (1986) The role of solar UV-B in growth regulation of cress (*Lepidium sativum* L.) seedlings. *Photochem Photobiol* **43**: 189-93
- Steinmuller D, Tevini M** (1985) Action of ultraviolet radiation (UV-B) upon cuticular waxes in some crops. *Planta* **164**: 557-564
- Stewart A, Bewley J** (1990) The participation of *cis*-4-cyclohexene-1,2-dicarboximide in the inhibition of light-controlled growth processes. *Plant Sci* **67**: 141-149
- Strack D** (1977) Sinapic acid ester fluctuations in cotyledons of *Raphanus sativus*. *Z. Pflanzanphysiol* **84**: 139-145

- Strack D** (1982) Development of 1-O-sinapoyl-beta-D-glucose: l-malate sinapoyltransferase activity in cotyledons of red radish (*Raphanus sativus* L. var. *sativus*). *Planta* **155**: 31-36
- Strack D** (1997) Phenolic metabolism. In *Plant Biochemistry* pp 387-416. Academic Press, New York.
- Strack D, Tkotz N, Klug M** (1978) Phenylpropanoid metabolism in cotyledons of *Raphanus sativus* and the effect of competitive *in vivo* inhibition of L-phenylalanine ammonia-lyase (PAL) by hydroxylamine derivatives. *Z Pflanzenphysiol.* **89**: 343-353
- Stratton SP, Liebler DC** (1997) Determination of singlet oxygen-specific versus radical-mediated lipidperoxidation in photosensitized oxidation of lipid bilayers: effect of beta-carotene and alpha-tocopherol. *Biochemistry* **36**: 12911-12920
- Sullivan JH, Teramura AH** (1989) Field study of the interaction between solar UV-B radiation and drought on photosynthesis and growth in soybean. *Plant Physiol* **92**: 141-6
- Sullivan JH, Teramura AH, Ziska LH** (1990) Variation in UV-B sensitivity in plants from a 3000-m elevational gradient in Hawaii. *Am J Bot* **79**: 737-43
- Szwarcberg-Bracchitta M, Giordano C, Rousseaux M, Zima A, Mazza C, Scopel A, Caldwell M, Ballaré C** (Year) UVB- and UVA-induced DNA damage in field grown plants. Annual Meeting of the American Society of Plant Physiologists. Madison, Wisconsin. Abstract 401.
- Takahama U, Oniki O** (1997) A peroxidase/phenolics/ascorbate system can scavenge hydrogen peroxide in plant cells. *Physiol Plant* **101**: 845-852
- Takayanagi S, Trunk JG, Sutherland JC, Sutherland BM** (1994) Alfalfa seedlings grown outdoors are more resistant to UV-induced DNA damage than plants grown in a UV-free environmental chamber. *Photochem Photobiol* **60**: 363-7

- Takeuchi Y, Akizuki M, Shimizu H, Kondo N, Sugahara K (1989)** Effect of UV-B (290-320 nm) irradiation on growth and metabolism of cucumber cotyledons. *Physiol Plant* **76**: 425-30
- Tako M, Kobayashi T, Oikawa A, Yasui A (1989)** Tandem arrangement of photolyase and superoxide dismutase genes in *Halobacterium halobium*. *J Bacteriol* **171**: 6323-9
- Tallmadge DH, Borkman RF (1990)** The rates of photolysis of the four individual tryptophan residues in UV exposed calf gamma-II crystallin. *Photochem Photobiol* **51**: 363-8
- Taylor HR (1994)** Ocular effects of UV-B exposure. *Doc Ophthalmol* **88**: 285-93
- Tevini M, Steinmuller D (1987)** Influence of light, UV-B radiation, and herbicides on wax biosynthesis of cucumber seedlings. *J Plant Physiol* **3**: 111-121
- Tevini M, Teramura AH (1989)** UV-B effects on terrestrial plants. *Photochem Photobiol* **50**: 479-87
- Tevini M, Thoma U, Iwanzik W (1983)** Effects of enhanced UV-B radiation on germination, seedling growth, anatomy and pigments of some crop plants. *Z. Pflanzenphysiol.* **109**: 435-448
- Thompson J (1984)** Physical changes in membranes of senescing and environmentally stressed plant tissues. In *Physiology of Membrane Fluidity*. pp 85-108. CRC Preass, Boca Raton, FL.
- Thompson JD, Higgins DG, Gibson TJ (1994)** CLUSTAL W: improving the sensitivity of progressive multiple sequence alignment through sequence weighting, position-specific gap penalties and weight matrix choice. *Nucleic Acids Res* **22**: 4673-80
- Timmins GS, Davies MJ (1993)** An EPR spin trapping study of albumin protein radicals formed by photodynamic action of haematoporphyrin. *J Photochem Photobiol B* **21**: 167-173
- Todo T, Ryo H, Yamamoto K, Toh H, Inui T, Ayaki H, Nomura T, Ikenaga M (1996)** Similarity among the *Drosophila* (6-4)photolyase, a human photolyase homolog, and the DNA photolyase-blue-light photoreceptor family. *Science* **272**: 109-12

- Tousey R** (1966) The Radiation from the Sun. In *The Middle Ultraviolet: Its Science and Technology* pp 1-40. Pure and Applied Optics. John Wiley and Sons, New York.
- Tretyn A, Kendrick RE, Wagner G** (1992) The roles of calcium ions in phytochrome action. *Photochem Photobiol* **54**: 1135-55
- Trewavas A, Read N, Campbell AK, Knight M** (1996) Transduction of Ca<sup>2+</sup> signals in plant cells and compartmentalization of the Ca<sup>2+</sup> signal. *Biochem Soc Trans* **24**: 971-4
- Tsuchihashi H, Kigoshi M, Iwatsuki M, Niki E** (1995) Action of beta-carotene as an antioxidant against lipid peroxidation. *Arch Biochem Biophys* **323**: 137-147
- Ulmasov T, Hagen G, Guilfoyle TJ** (1997) ARF1, a transcription factor that binds to auxin response elements. *Science* **276**: 1865-8
- van Tunen A, Koes R, Spelt C, van der Krol A, Stuitje A, Mol J** (1988) Cloning of the two chalcone flavanone isomerase genes from *Petunia hybrida*: coordinate, light-regulated and differential expression of flavonoid genes. *EMBO J* **7**: 1257-1263
- Vass I, Sass L, Spetea C, Bakou A, Ghanotakis DF, Petrouleas V** (1996) UV-B-induced inhibition of photosystem II electron transport studied by EPR and chlorophyll fluorescence. Impairment of donor and acceptor side components. *Biochemistry* **35**: 8964-73
- Verweij H, van Stevenick J** (1982) Model studies on photodynamic cross-linking. *Photochem Photobiol* **35**: 265-267
- Vierstra R, Poff K** (1981) Mechanism of specific inhibition of phototropism by phenylacetic acid in corn seedling. *Plant physiol* **67**: 1011-1015
- Vile GF, Tanew-Ilitschew A, Tyrrell RM** (1995) Activation of NF-kappa B in human skin fibroblasts by the oxidative stress generated by UVA radiation. *Photochem Photobiol* **62**: 463-8

- Vogt T, Aebershold R, Ellis B** (1993) Purification and characterization of sinapine synthase from seeds of *Brassica napus*. *Arch Biochem Biophys* **300**: 622-8
- Voordouw G, van der Vies SM, Bouwmeister PP** (1984) Dissociation of ribulose-1,5-bisphosphate carboxylase/oxygenase from spinach by urea. *Eur J Biochem* **141**: 313-8
- Vorst O, van Dam F, Weisbeek P, Smeekens S** (1993) Light-regulated expression of the *Arabidopsis thaliana* ferredoxin A gene involves both transcriptional and post-transcriptional processes. *Plant J* **3**: 793-803
- Walker JC** (1980) Atmospheric constraints on the evolution of metabolism. *Orig Life* **10**: 93-104
- Wei N, Kwok SF, von Arnim AG, Lee A, McNellis TW, Piekos B, Deng XW** (1994) *Arabidopsis* COP8, COP10, and COP11 genes are involved in repression of photomorphogenic development in darkness. *Plant Cell* **6**: 629-43
- Weissenbock G, Hedrich R, Sachs G** (1986) Secondary phenolic products in isolated guard cell, epidermal cell and mesophyll cell protoplasts from pea (*Pisum sativum* L.) leaves: Distribution and determination. *Protoplasma* **134**: 141-148
- Weisshaar B, Block A, Armstrong GA, Herrmann A, Schulze-Lefert P, Hahlbrock K** (1991) Regulatory elements required for light-mediated expression of the *Petroselinum crispum* chalcone synthase gene. *Symp Soc Exp Biol* **45**: 191-210
- Wellmann E, Schneider-Ziebert U, Beggs CJ** (1984) UV-B inhibition of phytochrome-mediated anthocyanin formation in *Sinapis alba* L. cotyledons. Action spectrum and the role of photoreactivation. *Plant Physiol* **75**: 997-1000
- Wessels JM, Foote CS, Ford WE, Rodgers MA** (1997) Photooxidation of tryptophan: O<sub>2</sub>(1 delta g) versus electron-transfer pathway. *Photochem Photobiol* **65**: 96-102

- Wheeler S, Barnes P, Shinkle J** (1997) Separate short-term growth responses of dicot seedlings to different regions within the UV-B spectrum. *Plant Physiol Abstract* 424
- Wightman F, Lighty D** (1982) Identification of phenylacetic acid as a natural auxin in the shoots of higher plants. *Physiol Plant.* **55**: 17-24
- Wilson K, Wilson M, Greenberg B** (1998) Identification of the flavonoid glycosides that accumulate in *Brassica napus* L. cv Topas specifically in response to ultraviolet-B radiation. *Photochem Photobiol* **67**: 547-553
- Wilson MI, Ghosh S, Gerhardt KE, Holland N, Babu TS, Edelman M, Dumbroff EB, Greenberg BM** (1995) Photomodification of ribulose-1,5-bisphosphate carboxylase oxygenase holoenzyme by ultraviolet-B radiation: formation of a 66 kD variant of the large subunit. *Plant Physiol* **109**: 221-229
- Wilson MI, Greenberg BM** (1993a) Protection of the D1 photosystem II reaction center protein from degradation in ultraviolet radiation following adaptation of *Brassica napus* L to growth in ultraviolet-B. *Photochem Photobiol* **57**: 556-63
- Wilson MI, Greenberg BM** (1993b) Specificity and photomorphogenic nature of ultraviolet-B-induced cotyledon curling in *Brassica napus* L. *Plant Physiol* **102**: 671-7
- Wingender R, Rohrig H, Horicke C, Schell J** (1990) cis-regulatory elements involved in ultraviolet light regulation and plant defense. *Plant Cell* **2**: 1019-26
- Wingender R, Rohrig H, Horicke C, Wing D, Schell J** (1989) Differential regulation of soybean chalcone synthase genes in plant defence, symbiosis and upon environmental stimuli. *Mol Gen Genet* **218**: 315-22
- Wojtaszek P** (1997) Oxidative burst: an early plant response to pathogen infection. *Biochem J* **322**: 681-92



- Yamamoto E, Towers GHN (1985)** Cell wall bound ferulic acid in barley seedlings during development and its photoisomerization. *Plant Physiol* **87**: 441-9
- Yamasaki H, Sakihama Y, Ikehara N (1997)** Flavonoid-peroxidase reaction as a detoxification mechanism of plant cells against H<sub>2</sub>O<sub>2</sub>. *Plant Physiol* **115**: 1405-1412
- Yanovsky MJ, Casal JJ, Whitelam GC (1995)** Phytochrome A, phytochrome B and HY4 are involved in hypocotyl growth responses to natural radiation in Arabidopsis: Weak de-etiolation of the phyA mutant under dense canopies. *Plant Cell and Environment* **18**: 788-94
- Yasui A, Eker AP, Yasuhira S, Yajima H, Kobayashi T, Takao M, Oikawa A (1994)** A new class of DNA photolyases present in various organisms including aplacental mammals. *Embo J* **13**: 6143-51
- Yeh KC, Wu SH, Murphy JT, Lagarias JC (1997)** A cyanobacterial phytochrome two-component light sensory system. *Science* **277**: 1505-8
- Zamansky GB, Perrino BA, Chou IN (1991)** Disruption of cytoplasmic microtubules by ultraviolet radiation. *Exp Cell Res* **195**: 269-73
- Zaremba TG, LeBon TR, Millar DB, Smejkal RM, Hawley RJ (1984)** Effects of ultraviolet light on the in vitro assembly of microtubules. *Biochemistry* **23**: 1073-80
- Zhang J, Hu X, Henkow L, Jordan BR, Strid A (1991)** The effects of ultraviolet-B radiation on the CF<sub>0</sub>F<sub>1</sub>-ATPase. *Biochim Biophys Acta* **1185**: 295-302
- Zhao S, Sancar A (1997)** Human blue-light photoreceptor hCRY2 specifically interacts with protein serine/threonine phosphatase 5 and modulates its activity. *Photochem Photobiol* **66**: 727-